
Doctoral Dissertations

Student Theses and Dissertations

Spring 2014

Degradable nanocomposite preformed particle gel for chemical enhanced oil recovery applications

Paul Tongwa

Follow this and additional works at: https://scholarsmine.mst.edu/doctoral_dissertations

 Part of the [Oil, Gas, and Energy Commons](#), and the [Petroleum Engineering Commons](#)

Department: Geosciences and Geological and Petroleum Engineering

Recommended Citation

Tongwa, Paul, "Degradable nanocomposite preformed particle gel for chemical enhanced oil recovery applications" (2014). *Doctoral Dissertations*. 3114.

https://scholarsmine.mst.edu/doctoral_dissertations/3114

This thesis is brought to you by Scholars' Mine, a service of the Missouri S&T Library and Learning Resources. This work is protected by U. S. Copyright Law. Unauthorized use including reproduction for redistribution requires the permission of the copyright holder. For more information, please contact scholarsmine@mst.edu.

DEGRADABLE NANOCOMPOSITE PREFORMED PARTICLE GEL FOR
CHEMICAL ENHANCED OIL RECOVERY APPLICATIONS

by

PAUL TONGWA

A DISSERTATION

Presented to the Faculty of the Graduate School of the
MISSOURI UNIVERSITY OF SCIENCE AND TECHNOLOGY

In Partial Fulfillment of the Requirements for the Degree

DOCTOR OF PHILOSOPHY

in

PETROLEUM ENGINEERING

2014

Approved
Baojun Bai, Advisor
Runar Nygaard
Ralph Flori
Shari Dunn-Norman
Parthasakha Neogi

© 2014

Paul Tongwa

All Rights Reserved

ABSTRACT

This work presents two new materials that can be potentially used in conformance control to increase ultimate oil recovery from mature oilfields.

The first product is a degradable nanocomposite preformed particle gel for enhanced in-depth mobility control. Three different types of degradable nanocomposite preformed particle gels were synthesized. These three nanocomposite hydrogels were made using Laponite XLG, Calcium Montmorillonite, and Sodium Montmorillonite nanomaterials. It was observed that after degradation, Laponite XLG nanocomposite hydrogels had the highest post-degradation viscosity (4437 cp), followed by sodium nanocomposite hydrogels (129 cp), and lastly calcium nanocomposite hydrogels (75.5 cp). Thus, degradable Laponite XLG nanocomposite hydrogels are recommended for secondary polymer flooding, since they have the highest post-degradation viscosity under anaerobic conditions.

The second product is an elastomeric rubber gel as a potential fracture-sealing agent. An elastomeric rubber gel has been synthesized from degraded preformed particle gel crosslinked with Poly (ethylene glycol) diacrylate and bentonite clay. Elastomeric rubber gel formed using 0.5% degraded preformed particle gel crosslinked with Poly(ethylene glycol) Diacrylate-200 is the most promising since it contains the least amount of degraded preformed particle gel (0.5%), requires the least amount of clay (50%), and has the highest gel strength (93520 Pa). Thus they are potential fracture-sealing materials.

ACKNOWLEDGMENTS

I would first of all like to thank the God of Jesus Christ, the Most High God, for the gift of life, and for all his many provisions while here at Missouri S&T Rolla.

I would like to sincerely thank my advisor, Dr Baojun Bai, for accepting me as a PhD student in his research group. For his continued supervision and for funding, and for the exposure I have had since I was his student. I have learned and acquired many research skills working under him. Thank you sir.

My deepest gratitude also goes to the members of my committee, Dr Runar Nygaard, Dr Ralph Flori, Dr Shari Dunn-Norman, and Dr Neogi Parthasakha for accepting to be on my committee, and for the valuable time, and effort they have put in supervising my work.

Special thanks also go to my colleagues and labmates; Pu Jingyang, Abdulmohsin Imqam, Farag Muhammed, Hilary Elue, Ayman Almohsin, Zun Chen for the time spent working together, and for the exchange of knowledge.

Lastly, I would like to thank my family for their constant support and encouragement.

TABLE OF CONTENTS

| | Page |
|---|------|
| ABSTRACT..... | iii |
| ACKNOWLEDGMENTS | iv |
| LIST OF ILLUSTRATIONS..... | x |
| LIST OF TABLES..... | xv |
| SECTION | |
| 1. INTRODUCTION..... | 1 |
| 2. LITERATURE REVIEW | 7 |
| 2.1. THE NECESSITY OF ENHANCED RECOVERY TECHNOLOGY | 7 |
| 2.1.1. Enhanced Oil Recovery | 8 |
| 2.1.2. Justification For Enhanced Oil Recovery..... | 8 |
| 2.1.3. Overview of Enhanced Oil Recovery Methods..... | 8 |
| 2.2. THE USE OF GEL TREATMENT TO INCREASE OIL AND GAS PRODUCTION | 10 |
| 2.3. PROGRESS IN GEL DEVELOPMENT FOR CONFORMANCE CONTROL | 11 |
| 2.3.1. In-situ Gel Technology..... | 12 |
| 2.3.1.1 Limitations of in-situ gelation..... | 12 |
| 2.3.1.2 Types of in-situ gel systems..... | 15 |
| 2.3.2. Preformed Gel Technology | 21 |
| 2.3.2.1 Partially preformed gels | 23 |
| 2.3.2.2 Microgels | 25 |
| 2.3.2.3 pH-sensitive crosslinked polymers | 27 |

| | |
|---|----|
| 2.3.2.4 Bright water | 29 |
| 2.3.2.5 Colloidal dispersion gels..... | 31 |
| 2.3.2.6 Preformed particle gels | 32 |
| 2.3.3. Nanocomposite Preformed Particle Gel | 37 |
| 2.4. SUMMARY OF LITERATURE REVIEW..... | 47 |
| 3. EXPERIMENTAL DESCRIPTION AND METHODOLOGY..... | 48 |
| 3.1. MATERIALS..... | 48 |
| 3.2. GEL SYNTHESIS AND FABRICATION..... | 51 |
| 3.3. METHODS OF NANOCOMPOSITE PREFORMED PARTICLE GEL EVALUATION | 53 |
| 3.3.1. Evaluation of Nanocomposite Preformed Particle Gel Before Degradation..... | 53 |
| 3.3.1.1 Swelling kinetics..... | 53 |
| 3.3.1.2 Gel rheology test | 53 |
| 3.3.1.3 Thermostability test | 55 |
| 3.3.1.4 Environmental scanning electron microscopy evaluation. | 57 |
| 3.3.2. Evaluation of Nanocomposite Preformed Particle Gel After Degradation..... | 58 |
| 3.3.2.1 Viscosity measurements..... | 58 |
| 3.3.2.2 Gel rheology test | 59 |
| 3.3.2.3 Environmental scanning electron microscopy and optical microscopy measurements | 59 |
| 4. FACTORS AFFECTING NANOCOMPOSITE PREFORMED PARTICLE GEL PROPERTIES..... | 60 |
| 4.1. EFFECT OF TEMPERATURE ON GEL PROPERTIES..... | 63 |
| 4.2. EFFECT OF CROSSLINKER ON GEL PROPERTIES..... | 66 |

| | |
|---|-----|
| 4.3. EFFECT OF INITIATOR ON GEL PROPERTIES..... | 70 |
| 4.4. EFFECT OF MONOMER ON GEL PROPERTIES | 73 |
| 5. RESULTS AND DISCUSSION: DEGRADABLE NANOCOMPOSITE PREFORMED PARTICLE GEL AS MOBILITY CONTROL AGENT | 76 |
| 5.1. EVALUATION OF DEGRADABLE NANOCOMPOSITE PREFORMED PARTICLE GEL WITH LAPONITE XLG AS NANOMATERIAL (LXLG NANOCOMPOSITE PPG) | 78 |
| 5.1.1. Improvement in LXLG Nanocomposite PPG Properties with Incorporation of Nanomaterials | 78 |
| 5.1.1.1 Increased mechanical strength | 78 |
| 5.1.1.2 Increased swelling and thermal resistance | 79 |
| 5.1.1.3 Increased post-degradation viscosity of LXLG nanocomposite PPG. | 86 |
| 5.1.2. Evaluation of LXLG Nanocomposite PPG Microstructure and Morphology, Before and After Degradation..... | 88 |
| 5.1.2.1 Environmental scanning electron microscopy imaging of LXLG nanocomposite PPG before its degradation | 88 |
| 5.1.2.2 Environmental scanning electron microscopy (ESEM) imaging of LXLG nanocomposite PPG after its degradation | 92 |
| 5.1.2.3 Optical microscopy imaging of LXLG nanocomposite PPG after degradation | 94 |
| 5.2. EVALUATION OF DEGRADABLE NANOCOMPOSITE PREFORMED PARTICLE GEL WITH CALCIUM MONTMORILLONITE AS NANOMATERIAL (Ca ²⁺ NANOCOMPOSITE PPG)..... | 95 |
| 5.2.1. Improvement in Ca ²⁺ Nanocomposite PPG Properties with Incorporation of Nanomaterials | 95 |
| 5.2.1.1 Increased mechanical strength | 95 |
| 5.2.1.2 Increased swelling and thermal resistance | 96 |
| 5.2.1.3 Increased post-degradation viscosity of Ca ²⁺ nanocomposite PPG | 103 |

| | |
|--|-----|
| 5.2.2. Evaluation of Ca^{2+} Nanocomposite PPG Microstructure and Morphology, Before and After Degradation..... | 104 |
| 5.2.2.1 Environmental scanning electron microscopy imaging of Ca^{2+} nanocomposite PPG before its degradation | 104 |
| 5.2.2.2 Environmental scanning electron microscopy imaging of Ca^{2+} nanocomposite PPG after its degradation | 108 |
| 5.2.2.3 Optical microscopy imaging of Ca^{2+} nanocomposite PPG after degradation | 110 |
| 5.3. EVALUATION OF DEGRADABLE NANOCOMPOSITE PREFORMED PARTICLE GEL WITH SODIUM MONTMORILLONITE AS NANOMATERIAL (Na^+ NANOCOMPOSITE PPG)..... | 111 |
| 5.3.1. Improvement in Na^+ Nanocomposite PPG Properties with Incorporation of Nanomaterials | 111 |
| 5.3.1.1 Increased mechanical strength | 111 |
| 5.3.1.2 Increased swelling and thermal resistance | 112 |
| 5.3.1.3 Increased post-degradation viscosity of Na^+ nanocomposite PPG. | 118 |
| 5.3.2. Evaluation of Na^+ Nanocomposite PPG Microstructure and Morphology, Before and After Degradation..... | 119 |
| 5.3.2.1 Environmental scanning electron microscopy imaging of Na^+ nanocomposite PPG before its degradation | 119 |
| 5.3.2.2 Environmental scanning electron microscopy imaging of Na^+ nanocomposite PPG after its degradation..... | 123 |
| 5.3.2.3 Optical microscopy imaging of Na^+ nanocomposite PPG after degradation | 124 |
| 5.4. SUMMARY OF THREE TYPES OF DEGRADABLE NANOCOMPOSITE PPGs STUDIED | 125 |
| 6. RESULTS AND DISCUSSION: ELASTOMERIC RUBBER GEL AS PERMANENT FRATURE-SEALING AGENT | 127 |
| 6.1. ELASTOMERIC RUBBER GEL MADE FROM DEGRADED PPG AND NANOMATERIAL..... | 127 |

| | |
|--|-----|
| 6.1.1. Synthesis of Elastomeric Rubber Gel..... | 128 |
| 6.1.2. Evaluation of Rubber Gel Properties..... | 130 |
| 6.1.2.1 Rule out other monomer possibilities | 130 |
| 6.1.2.2 Determine if elastomeric rubber gel can be formed with directly prepared polymer, without going through degraded PPG | 130 |
| 6.1.2.3 Effect of PEG-DA molecular weight on rubber gel properties | 132 |
| 6.1.2.3.1 Using PEG-200-DA | 132 |
| 6.1.2.3.2 Using PEG-400-DA | 133 |
| 6.1.2.3.3 Using PEG-600-DA | 135 |
| 6.1.2.3.4 Summary of the different PEG-DA molecular weights studied..... | 137 |
| 6.1.2.4 Longterm thermal stability of rubber gel made using 0.5% degraded PPG..... | 137 |
| 6.1.2.5 Characterization of elastomeric rubber gel made from 0.5% degraded PPG using PEG-200-DA | 138 |
| 6.1.3. Summary of Elastomeric Rubber Gel Discussion | 141 |
| 7. CONCLUSIONS | 143 |
| 8. SUGGESTED FUTURE WORK..... | 145 |
| BIBLIOGRAPHY | 146 |
| VITA..... | 158 |

LIST OF ILLUSTRATIONS

| | Page |
|---|------|
| Figure 1.1. Degradable Nanocomposite Preformed Particle Gel for Improved Mobility Control and Effective Volumetric Sweep Efficiencies in Heterogeneous Reservoirs..... | 4 |
| Figure 1.2. Novel Elastomeric Rubber Gel as a Fracture-Sealing Material. | 6 |
| Figure 2.1. EOR Methods. | 9 |
| Figure 2.2. An Overview of Focused Area of Research: Gel Treatment..... | 10 |
| Figure 2.3. Chromium Cation | 17 |
| Figure 2.4. Aluminium Cation | 18 |
| Figure 2.5. Difference between Precipitates and Gels..... | 21 |
| Figure 2.6. Effect of Rate on Residual Resistance Factor (F_{rr}) in a 2-mm-wide Fracture. | 24 |
| Figure 2.7. Polymer and Fully Water-Soluble Microgel Species | 26 |
| Figure 2.8. Schematic Representation of the Behavior of a Hydrogel with a pH-Sensitive Release. | 27 |
| Figure 2.9. Mechanism Leading to Increase in Polymer Viscosity Due to Side Chain Ionization (a) Swelling and Viscosity Increase of Polyacrylic Acid upon Ionization (b) Molecular Structure of (a) Polyacrylic Acid, (b) Crosslinked Poly-acrylate Hydrogel. | 28 |
| Figure 2.10. Brightwater® is Injected as a One-time Batch Together with Injection Water at Concentrations of about 1.5%. | 30 |
| Figure 2.11. How Brightwater Technology Works. | 30 |
| Figure 2.12. Comparison of Colloidal Dispersion Gels and Bulk Gels..... | 31 |
| Figure 2.13. Production Curve for 24 Connected Wells..... | 35 |
| Figure 2.14. The Different Mechanisms of How Particle Gels Pass Through a Pore Throat | 36 |

| | |
|---|----|
| Figure 2.15. Free Radical Polymerization of Nanocomposite Gels..... | 38 |
| Figure 2.16. Schematic Illustration of Formation of Hydrogen Bonds in Nylon-6/montmorillonite Nanocomposite Gel..... | 39 |
| Figure 2.17. Nanocomposite Clay Classification. | 43 |
| Figure 2.18. Stepwise Mechanism of Clay Platelets Exfoliation during Melt Compounding..... | 44 |
| Figure 2.19. XRD Patterns for XLG Clay and Dried Gels (XLG1-10)..... | 45 |
| Figure 2.20. Progress in Gel Development for Conformance Control. | 46 |
| Figure 3.1. Unit Cell Structures of The Different Nanomaterials Studied (a). Single Laponite Crystal and Unit Cell Structure of Laponite Layered Silicate (available online at www.scprod.com). (b) Unit Cell Structure of Sodium and Calcium Montmorillonite..... | 49 |
| Figure 3.2. Molecular Structures of Compounds Used in Study | 50 |
| Figure 3.3. Nanocomposite Preformed Particle Gel Synthesis and Fabrication..... | 52 |
| Figure 3.4. Haake Rheoscope Setup Used to Measure Rheology of Gel. | 55 |
| Figure 3.5. Manifold Used to Seal Ampoule during Thermostability Measurement. | 56 |
| Figure 3.6. Different Ovens Used to Evaluate Longterm Thermal Stability of Gel at 45°C, 60 °C, and 80 °C | 57 |
| Figure 3.7. Brookfield Viscometer Model DV II+ for Measuring Post-degradation Gel Viscosity..... | 58 |
| Figure 4.1. Synthesis of Nanocomposite Preformed Particle Gel | 60 |
| Figure 4.2. Mechanism of Acrylamide Polymerization Using Ammonium Persulfate.... | 61 |
| Figure 4.3. Effect of Temperature on Gel Formation Time..... | 64 |
| Figure 4.4. Elastic Modulus Increases with Increasing Temperature | 65 |
| Figure 4.5. Variation of Gel's Elastic Strength with Time | 65 |
| Figure 4.6. Variation of Elastic and Viscous Modulus with Angular Frequency for Sample Synthesized at 45 °C..... | 66 |

| | |
|---|----|
| Figure 4.7. Effect of Crosslinker Concentration on Gel Formation Time | 67 |
| Figure 4.8. Variation of Crosslinker Concentration with Gel's Elastic (G') and Viscous Modulus (G''), and When Combined Respectively | 68 |
| Figure 4.9. Effect of Initiator on Gel Formation Time. | 71 |
| Figure 4.10. Variation of Gel's Elastic Modulus with Time for Samples Prepared with Initiator Concentrations Ranging from 50 ppm to 1000 ppm shown in (a) and (b) | 72 |
| Figure 4.11. Effect of Monomer Concentration on Gel Formation Time | 74 |
| Figure 4.12. Effect of Monomer Concentration on Gel's Elastic Modulus, G' | 74 |
| Figure 4.13. Variation of Gel's Elastic and Viscous Moduli with Time for Samples Prepared with Monomer Concentrations Ranging from 5% to 40%, Shown in (a) and (b) Respectively | 75 |
| Figure 5.1. Degradable Nanocomposite Preformed Particle Gel for Improved Mobility Control and Effective Volumetric Sweep Efficiencies in Heterogeneous Reservoirs | 77 |
| Figure 5.2. An Obvious Improvement in Hydrogel Mechanical Strength is Observed between Gels with LXLG Nanomaterials and Those without Nanomaterials | 79 |
| Figure 5.3. (a-f): Longterm Thermal Stability of LXLG Nanocomposite Hydrogels Under Aerobic Conditions and in 1% Brine Solution and Formation Water. . | 81 |
| Figure 5.4. (a-f): Longterm Thermal Stability of LXLG Nanocomposite Hydrogels Under Anaerobic Conditions and In 1% Brine Solution and Formation Water | 84 |
| Figure 5.5. Aerobic and Anaerobic Environment of LXLG Samples Tested Showing both Before and After Sample Degrades Into Polymer Solution | 86 |
| Figure 5.6. Before-degradation Environmental Scanning Electron Microscopy (ESEM) Micrographs | 89 |
| Figure 5.7. After-degradation Environmental Scanning Electron Microscopy (ESEM) Micrographs | 93 |
| Figure 5.8. Optical Micrographs of Degraded 0.2% LXLG Nanocomposite PPG | 95 |

| | |
|--|-----|
| Figure 5.9. An Obvious Improvement in Hydrogel Mechanical Strength is Observed Between Dry Gels With Nanomaterials and Those Without Nanomaterials | 96 |
| Figure 5.10. a-f: Longterm Thermal Stability of Ca^{2+} Nanocomposite PPG Under Aerobic Conditions and In 1% Brine Solution and Formation Water. | 98 |
| Figure 5.11. a-f: Longterm Thermal Stability of Ca^{2+} Nanocomposite PPG Under Anaerobic Conditions and In 1% Brine Solution and Formation Water. | 101 |
| Figure 5.12. Aerobic and Anaerobic Environment of Ca^{2+} Nanocomposite PPG Samples Tested Showing both Before and After Sample Degrades Into Polymer Solution..... | 103 |
| Figure 5.13. Before-degradation Environmental Scanning Electron Microscopy (ESEM) Micrographs | 106 |
| Figure 5.14. After-degradation Environmental Scanning Electron Microscopy (ESEM) Micrographs | 109 |
| Figure 5.15. Optical Microscopy Micrograph of Degraded 0.2% Ca^{2+} Nanocomposite PPG. | 110 |
| Figure 5.16. An Obvious Improvement in Hydrogel Mechanical Strength is Observed Between Na^{+} Nanocomposite PPGs and Those Without Nanomaterials | 111 |
| Figure 5.17. a-f: Longterm Thermal Stability of Na^{+} Nanocomposite PPG Under Aerobic Conditions and in 1% Brine Solution and Formation Water. | 113 |
| Figure 5.18. a-f: Longterm Thermal Stability of Na^{+} Nanocomposite Hydrogels Under Anaerobic Conditions and in 1% Brine Solution and Formation Water | 116 |
| Figure 5.19. Aerobic and Anaerobic Environment of Na^{+} Nanocomposite PPG Samples Tested Showing both Before and After Sample Degrades Into Polymer Solution..... | 118 |
| Figure 5.20. Before-degradation Environmental Scanning Electron Microscopy (ESEM) Micrographs | 121 |
| Figure 5.21. After-degradation Environmental Scanning Electron Microscopy (ESEM) Micrographs | 123 |
| Figure 5.22. Optical Micrograph of Degraded 0.2% Na^{+} Nanocomposite PPG..... | 124 |

| | |
|--|-----|
| Figure 6.1. Novel Elastomeric Rubber Gel As a Fracture-Sealing Material. | 127 |
| Figure 6.2. Pictorial Illustration of Elastomeric Rubber Gel | 129 |
| Figure 6.3. A Block Flow Diagram Illustrating the Process of Elastomeric Rubber Gel Formation. | 129 |
| Figure 6.4. Phase Diagram Showing the Amount of Clay and Degraded PPG Required to Form Elastomeric Rubber Gel when PEG-200-DA Was Used. | 132 |
| Figure 6.5. Variation of Rubber Gel's Strength (G') with Amount of Clay Used For Different Degraded PPG Concentrations | 133 |
| Figure 6.6. Phase Diagram Showing the Amount of Clay and Degraded PPG Required to Form Elastomeric Rubber Gel When PEG-400-DA Was Used. | 134 |
| Figure 6.7. Variation of Rubber Gel's Strength (G') With Amount of Clay Used For Different Degraded PPG Concentrations | 135 |
| Figure 6.8. Phase Diagram Showing the Amount of Clay and Degraded PPG Required to Form Elastomeric Rubber Gel When PEG-600-DA Was Used. | 136 |
| Figure 6.9. Variation of Rubber Gel's Elastic Strength (G') With Amount of Clay Used. | 136 |
| Figure 6.10. Schematic of Longterm Thermal Testing of Elastomeric Rubber Gel | 138 |
| Figure 6.11. Longterm Thermal Testing of Elastomeric Rubber Gel Simulating Different Reservoir Environments of 45°C, 60 °C, and 80 °C | 138 |
| Figure 6.12. Controlled Stress Creep Measurements of 0.5% Degraded PPG Elastomeric Rubber Gel | 139 |
| Figure 6.13. Controlled Stress (CS) Recovery Measurements of 0.5% Degraded PPG Elastomeric Rubber Gel | 140 |
| Figure 6.14. Oscillation Stress Sweep Measurements of 0.5% Degraded PPG Elastomeric Rubber Gel | 141 |

LIST OF TABLES

| | Page |
|--|------|
| Table 3.1. Cost of Nanomaterials Studied | 50 |
| Table 3.2. Formation Water Formula for Simulating Daqing Oilfield Water. | 51 |
| Table 4.1. Effect of Temperature on Gelation Time and Gel Strength of Synthesized Gel | 64 |
| Table 4.2. Effect of Crosslinker on Gelation Time and Gel Strength of Synthesized Gels. | 67 |
| Table 4.3. Calculation of the Molecular Weight of the Polymer Chain from Polyacrylamide Gel Crosslinked with PEG-200-DA..... | 70 |
| Table 4.4. Effect of Initiator on Gelation Time and Gel Strength of Synthesized Gels ... | 71 |
| Table 4.5. Effect of Monomer Concentration on Gelation Time and Gel Strength of Synthesized Gels | 73 |
| Table 5.1. Viscosity Measurements for Pure Polymer, Pure LXLG Nanomaterial, and Degraded LXLG Nanocomposite PPG | 87 |
| Table 5.2. Viscosity Measurements For Pure PAM Polymer, Pure Ca^{2+} MMT Nanomaterial, and Degraded Ca^{2+} Nanocomposite PPG..... | 104 |
| Table 5.3. Viscosity Measurements For Pure Polymer, Pure Na^{+} MMT Nanomaterial, and Degraded Na^{+} Nanocomposite PPG..... | 119 |
| Table 5.4. Summary Results of All Three Degradable Nanocomposite Hydrogels Studied. | 126 |
| Table 6.1. Confirming That Rubber Gel Can Only Be Formed With Acrylamide Monomer | 130 |
| Table 6.2. Confirming That Rubber Gel Can Only Be Formed With Degraded PPG Solution and Not With Directly Prepared Polymers | 131 |
| Table 6.3. Summary of The Different PEG-DA Molecular Weights Studied | 137 |

1. INTRODUCTION

The fact that the oil and gas industry is spending a lot of money and using every available cutting-edge technology to find oil in risky and unfavorable terrains such as the deep seas and polar regions of the earth suggests that primary and secondary oil production from existing fields is reaching peak production. The existing mature fields still contain significant and unrecoverable quantities of hydrocarbons which cannot be recovered economically by current available technologies.

Rather than explore for oil in such risky terrains, why not optimize oil production from already existing, mature fields which have a well-known production history and performance? Such enormous and untapped amount of hydrocarbons in already existing, mature, left-behind fields is the goal of Enhanced Oil Recovery (EOR, also called tertiary production). EOR methods are crucial to a continuous world supply of oil.

As reservoirs mature, oil production declines while water production rises. Excess and unwanted water production from mature fields is one major problem that has plagued the oil industry for decades. Excess water production usually results in increased environmental concerns, increased levels of corrosion and scale and ultimately leads to early shut-in of wells that still contain significant volumes of hydrocarbons (Liu et al. 2006; Bai et al. 2007a).

One fundamental reason for excess water production is the existence of fractures and permeability variations between the different layers of a reservoir. Fractures present a water-thief zone through which injected water channels through, from the injector to the producer, thereby leaving hydrocarbons in the low permeability (non-fractured) zones untouched. The injected water follows the path of least resistance (high permeability zones), bypassing large amounts of oil in low permeability matrix. This leads to increased, unwanted water production and poor oil recovery.

Therefore, plugging reservoir fractures and thus correcting reservoir heterogeneity (that is conformance control), is key to an increased oil production, and hence the reason for this work.

In an attempt to mitigate excess water production and hence increase hydrocarbon production, hydrogels are often injected near-wellbore or far-wellbore to preferentially

seal fractures or higher permeability zones (Tongwa et al. (2013a; 2013b), Bai et al. (2007b; 1999; 2008), Liu et al. (1999). These hydrogels as fracture-plugging and fluid diverting materials have been employed in conformance control (profile modification) and in the control of excess water production during EOR applications, (Bai et al. 1999, 2007a, 2007b, 2008; Zhang et al. 2011; Vossoughi, S. 2000; Wang et al. 2001; 2003).

Mechanistically, hydrogel is injected into high permeability and fracture zones. Afterwards, subsequent injection of driving fluids are forced or redirected to the low permeability, unswept oil-rich zones, sweeping out oil from them, leading to additional oil production. This, in summary, is the goal of any gel treatment work. This process is called profile modification or permeability modification. As the term implies, the process seeks to even out or correct the sharp difference in permeabilities that exist in the different formation layers, creating a homogeneous reservoir.

Over the years, different types of gel treatments have been utilized in an attempt to solve conformance control problems. Initially, industry started using in-situ gels in which gelling solution is injected into reservoir and crosslinking of gelling solution to form 3-D bulk gel occurs downhole. This technology was dropped due to its inherent disadvantages such as selective injectivity, possible damage to low permeability zones, dispersion and dilution of gelant, syneresis, dehydration, and inadequate control of gelation time (Seright, 1990; Young et al., 1988; Asghari, 1999; Bryant et al. 1996; Willhite et al., 1986).

In an attempt to overcome the various limitations of in-situ gel technology, industry experts and researchers developed a novel technology to address conformance control problems called preformed gel technology. Preformed gels are three-dimensional, hydrophilic crosslinked polymers, which in contact with water, swell but do not dissolve as a result of a chemical or physical crosslinking and often than not will undergo a volume phase change when surrounding conditions such as temperature, salinity or pH change (Wen-Fu et al., 2006; Kytai and Jennifer, 2002). The novelty and main difference between this technology and in-situ gel technology is that with preformed gel, gel formation takes place at the surface, well ahead before injection, whereas with in-situ gelation, crosslinking and gel formation occurs downhole in the reservoir (Bai et al., 2013; Frampton et al., 2004). This technology was revolutionary in that it addressed some

of the problems posed by in-situ gelation such as dilution and dispersion of gelant, chromatographic separation of gelant solution, dehydration, syneresis, and most importantly damage of low permeability zones.

However, despite some of the tremendous advantages of preformed gels over in-situ gels, preformed gels have not as yet provided an all-encompassing solution to the problem of conformance control and reservoir heterogeneity. Some of the limitations of preformed gels include: (a) Mechanical: inadequate strength and toughness, (b) thermal: inadequate thermal resistance to withstand very extreme reservoir conditions, shorter degradation time, (c) swelling: inadequate swelling ability, (d) elasticity: inadequate gel elasticity.

Thus, there is a present need to provide a product that surpasses the performance of current preformed gels. Two new products are presented in this work. These two products will serve as a mobility control agent and as a permanent fluid-diverting agent respectively.

The first product presented is an extension of existing preformed gels by the incorporation of nanomaterials in gel design for improved mobility control.

Prior research by Jia, 2011 involved degradable preformed particle gels for improved mobility control. However, he obtained post-degradation viscosities that were negligible. Thus there was a need to improve on this.

The current dissertation is an extension and a continuation of the work of Jia, 2011. We propose a degradable nanocomposite Preformed Particle Gel, called nanocomposite PPG, which incorporates nanoclay in the gel. The incorporation of nanomaterials not only has the potentiality to overcome prior limitations of conventional preformed gels such as poor longterm thermal stability and inadequate mechanical strength, but results in improvement in gel performance and properties to withstand adverse and extreme reservoir conditions, and also in improvement in post-degradation gel viscosity after the gel degrades under reservoir conditions. The novelty of this work involves a dramatic increase in post-degradation gel viscosity compared to currently existing gels without nanomaterials.

This product, when injected into the reservoir, will initially act as a conformance control agent by plugging water-thief zones and channels, thereby directing injected

water to sweep out oil from low permeability oil-rich zones. After an extended time period, this product degrades into a highly viscous polymer solution (Figure 1.1) which then moves deeper into the reservoir, mixes with flood water and increases its viscosity, and by so doing improves water and polymer flooding processes by increasing water sweep efficiency, thereby enhancing oil production. Therefore, the viscosity of the gel after it degrades is of key concern.

(a) Initially, excess water production exists from fractures or high permeability zones of reservoir.

(b) On initial injection into reservoir, nanocomposite PPG serves to plug high permeability near well-bore zones, diverting injected water to sweep out oil from low permeability region.

(c) After an extended time period, nanocomposite PPG degrades into highly viscous polymer solution that moves into deeper regions of reservoir to increase the viscosity of flood water and hence boost polymer flooding. Oil production is thus increased.

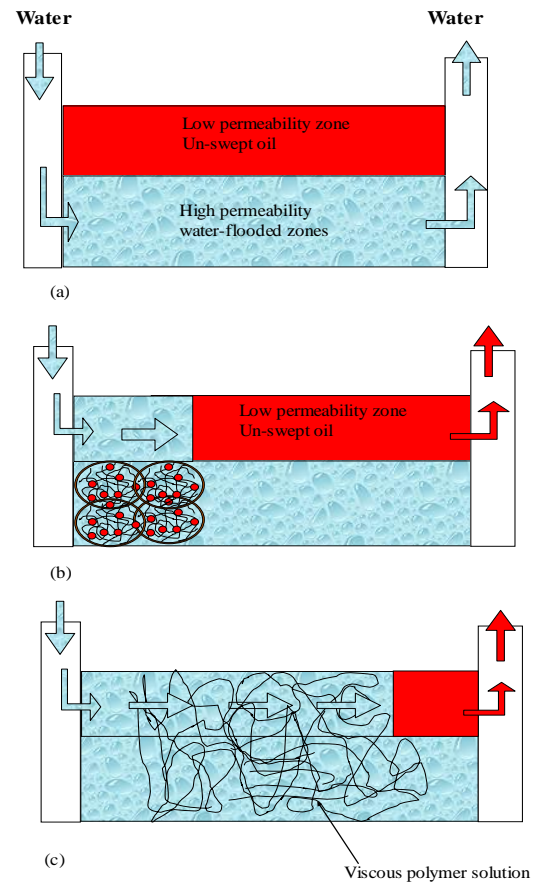


Figure 1.1. Degradable Nanocomposite Preformed Particle Gel for Improved Mobility Control and Effective Volumetric Sweep Efficiencies in Heterogeneous Reservoirs.

The general scheme of this first technology includes the following processes: 1) preparing crosslinked nanocomposite PPGs with a predetermined size, 2) dispersing the nanocomposite PPGs into a brine solution to form swelled PPGs, 3) injecting the swelled nanocomposite PPGs into the target reservoir, 4) the following treatment after PPGs injection such as water flooding, polymer flooding or Surfactant Polymer flooding etc. can be performed to improve the oil recovery by reducing the excess water production, and 5) after certain period of time, the decomposition of the injected nanocomposite PPGs eventually through the hydrolysis induced by heat or pH into high viscosity linear polymer solution for the secondary polymer flooding to further enhance the oil recovery.

The second product presents a novel Preformed Particle Gel as a permanent fluid-diverting agent. In some conformance control cases, very long-term fracture-plugging is needed.

Preformed Particle Gels are not very effective in completely sealing reservoir fractures. This is because, at higher pressures, channeling or fingering could occur through the gel plug (Figure 1.2). Thus, there is a need to develop a product which overcomes this problem. This chapter presents an elastomeric rubber-like material which does not easily cause channeling. This product, rubber-like in nature, will not degrade easily under reservoir conditions, and will serve as a plug for reservoir fractures.

To author's best knowledge, such a product has not been developed by industry.

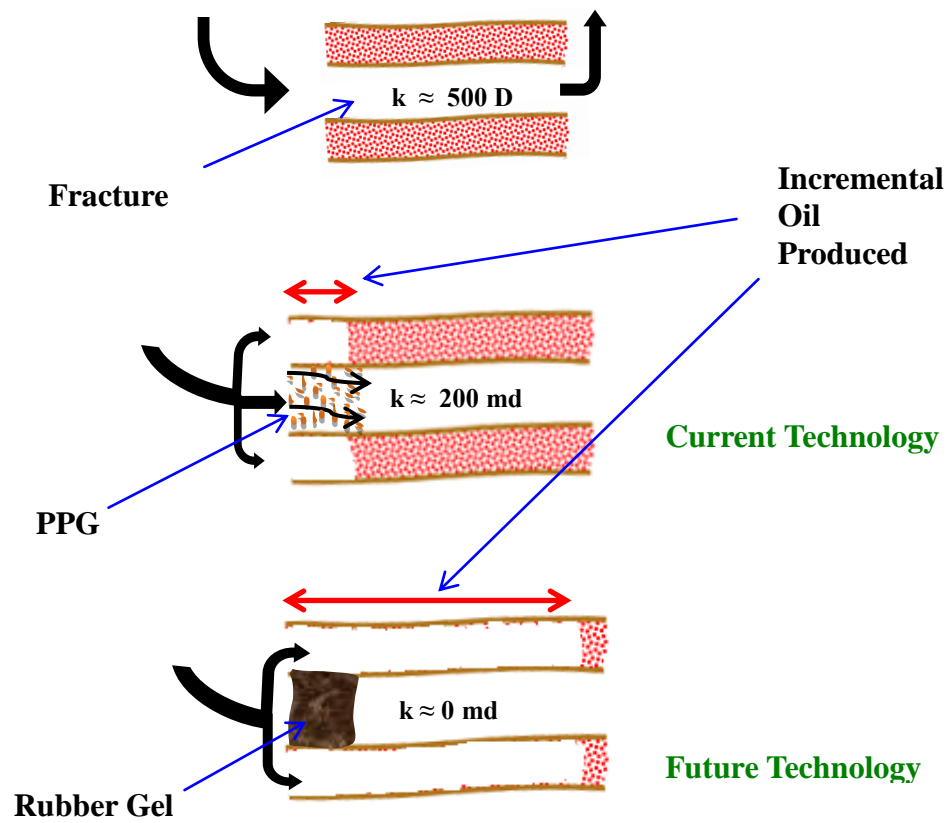


Figure 1.2. Novel Elastomeric Rubber Gel as a Fracture-Sealing Material.

The above two products constitute the basis for this PhD dissertation.

2. LITERATURE REVIEW

2.1. THE NECESSITY OF ENHANCED RECOVERY TECHNOLOGY

Why do individuals study what they study, and why must they continue to study what they study? This is the question that every research student or research engineer must answer correctly before attempting to begin any research endeavor. The necessity and relevance of one's work must be clearly obvious to all. Otherwise, research becomes rudimentary, repetitive, and non-beneficial.

Crude oil has been in existence for many centuries. This is due to the overwhelming necessity for a continuous oil and gas production to satisfy the growing world energy demand. Planet earth has such a huge dependence on crude oil, that at present, life on Earth is practically impossible without it. Thus, by every stretch of the intellect, by the application of one's creative mind power, and by any and every means possible, researchers must come up with new and better ways to produce crude oil.

The process of oil and gas extraction is a 3-stage process, namely: primary production, secondary production, and tertiary (or enhanced oil recovery) production. From primary recovery, which involves oil production by natural reservoir pressure or artificial methods, about 12-15% of the Original Oil-in-place (OOIP) is usually obtained. The mechanisms for primary oil recovery include: depletion drive-solution gas drive, gas cap drive, water drive, gravity drainage, and combination drive. However, over time, reservoir pressure declines and becomes insufficient to push out economic quantities of oil. Thus secondary recovery is needed.

Secondary recovery mechanisms are used to augment primary recovery. Secondary recovery involves the injection of water or gas to maintain pressure and to aid in displacing oil. From secondary recovery, we obtain an additional 15-20% of the OOIP.

Thus, from primary and secondary recovery combined, we only obtain about 35% of the OOIP (Green & Wilhite, 1998). Thus about 45% of the OOIP remain unrecovered and are targets for tertiary oil production (Department of Energy, 2005).

Tertiary oil recovery, also called Enhanced Oil Recovery (EOR) refers to oil production by the injection of substances (such as steam, chemicals etc.) that were not originally present in the reservoir, with the ultimate goal of increasing reservoir energy,

mobilizing residual/remaining oil, and improving microscopic and macroscopic sweep efficiencies. It provides an opportunity to significantly recover additional quantities of oil from abandoned and producing oil reservoirs.

2.1.1. Enhanced Oil Recovery. Enhanced Oil Recovery (EOR) methods are crucial to a continuous world supply of oil. For instance, in the United States alone, 377 billion barrels of oil are unrecoverable by current technologies and are targets for EOR applications. Worldwide, Thomas, S. (2008) estimates this value to be 7.0×10^{12} barrels. That is 7.0×10^{12} barrels of oil will remain in reservoirs worldwide after primary and secondary recovery methods have been exhausted. Furthermore, when unfavorable reservoir conditions exist such as low matrix permeability, high Interfacial tension (IFT), oil wet matrix, low matrix porosity and high oil viscosity, the need for EOR technology is even more urgent. And interestingly, this is the case with most reservoirs. So then it is asked, is it more profitable to drill new wells or should we rather optimize production from already existing wells?

2.1.2. Justification For Enhanced Oil Recovery. Enhanced Oil Recovery (EOR) is indispensable today because of the following reasons:

- 65% of oil remains in the reservoir after primary and secondary recovery. This is too huge to be ignored.
- By 2030, 688 billion barrels of oil will be recovered from EOR versus 732 billion barrels from new discoveries. (Steidtmann, 2008).
- EOR applies to existing reservoirs. Hence it does not require exorbitant costs of exploring and drilling new wells.
- Already existing infrastructures in place. No need for new infrastructures to be put in place before commencing EOR work. As opposed to the huge infrastructural costs accrued during drilling and completion of new wells.

2.1.3. Overview of Enhanced Oil Recovery Methods. EOR methods are classified under two main categories: thermal and non-thermal (Figure 2.1.). The ultimate goal of each EOR method is to create a set of favorable downhole conditions to mobilize remaining oil. Thus each EOR method is only applicable to unique reservoirs with particular rock and fluid properties.

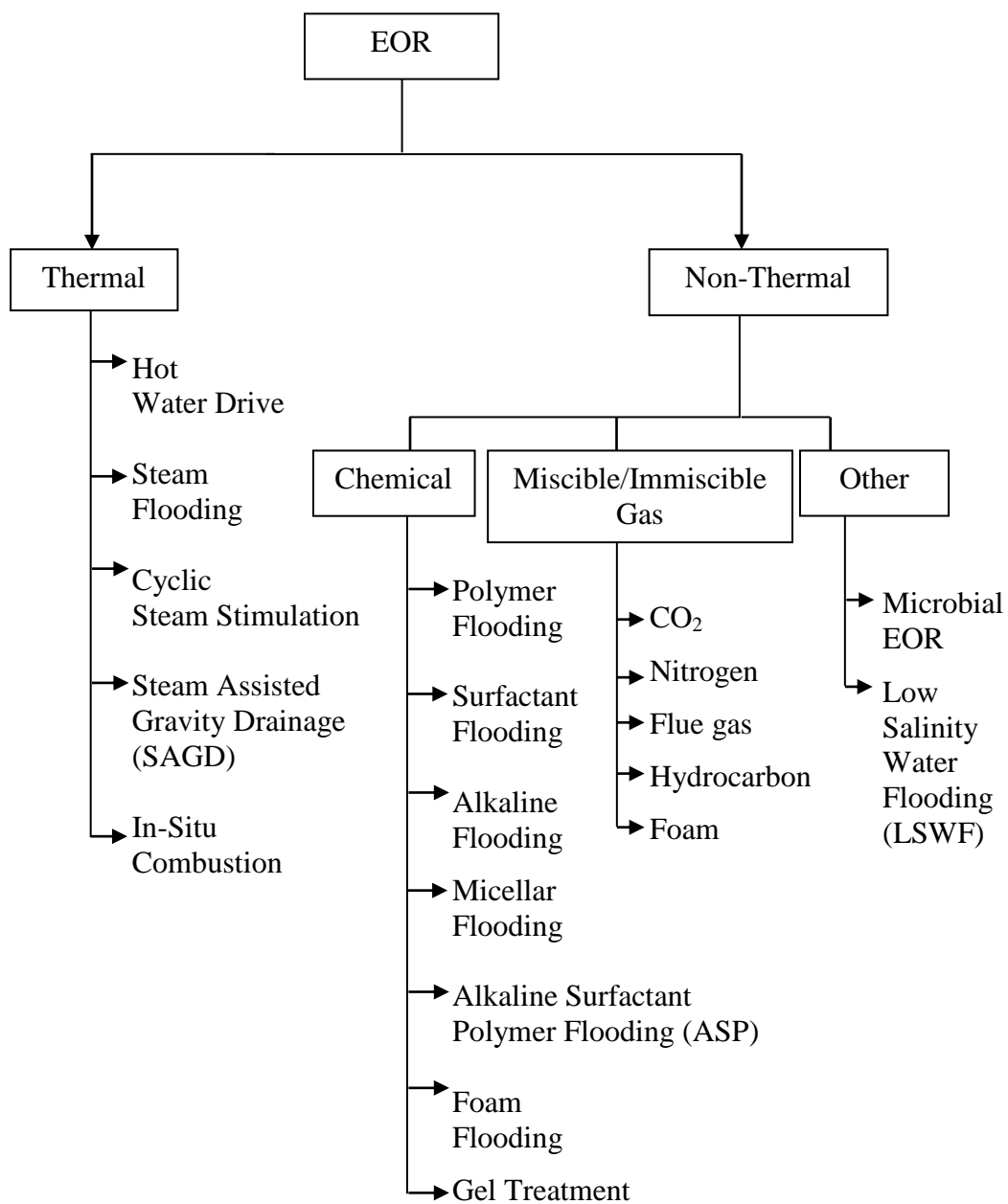


Figure 2.1. EOR Methods.

Having given an overview of EOR, lets now move into our focused area of research: Gel treatment (Figure 2.2.).

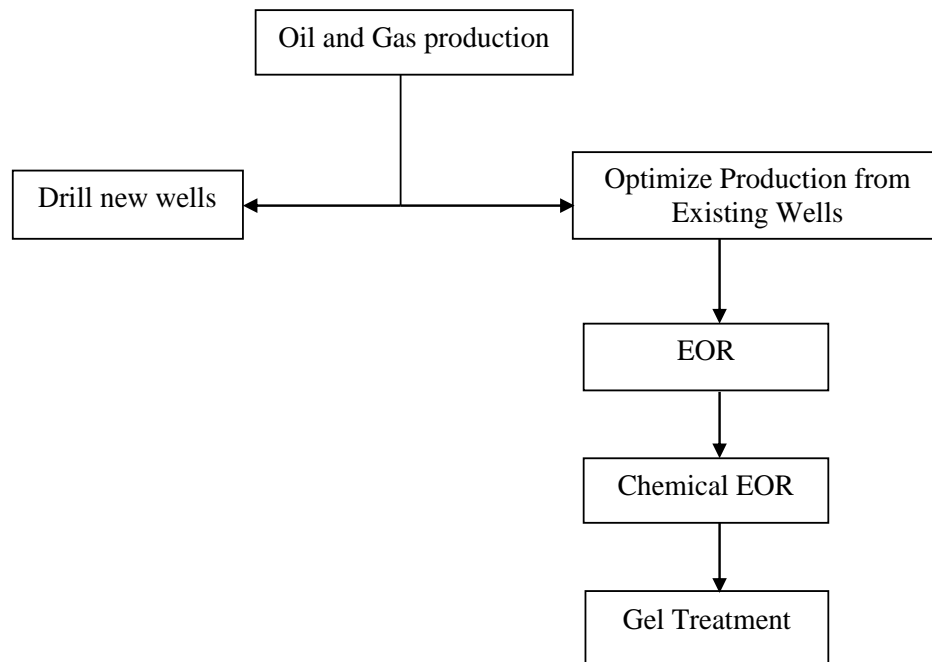


Figure 2.2. An Overview of Focused Area of Research: Gel Treatment.

2.2. THE USE OF GEL TREATMENT TO INCREASE OIL AND GAS PRODUCTION

One pivotal reason why oil recovery is never a hundred percent is because of reservoir heterogeneity and fractures. Fractures present a water-thief zone through which injected flood water channels through, from the injector to the producer, thereby leaving hydrocarbons in the low permeability (non-fractured) zones untouched. This leads to increased, unwanted water production and poor oil recovery. Thus plugging reservoir fractures and correcting reservoir heterogeneity (that is conformance control), is key to an increased oil production.

For a reservoir produced by some external fluid drive, Borling et al., (1994) defined conformance control as that process by which the fluid drive gets closer and closer to the ideal conforming condition. That is, it refers to any process that enables the driving phase to uniformly sweep hydrocarbons across the entire reservoir to the producing well. A perfectly conforming drive will uniformly sweep across the reservoir, leaving no isolated oil pockets while an imperfectly conforming drive will only sweep parts of the reservoir and omit regions containing producible hydrocarbons. In a wider sense, it refers to any technique that strives to correct reservoir heterogeneity, reduce water production and redistribute injected water, either near the wellbore or deep in the reservoir.

Excess water production is a frequent problem that occurs in mature reservoirs as a result of longterm water-flooding. Such excess water production usually results in increased environmental concerns, increased levels of corrosion and scale and ultimately leads to early shut-in of wells that still contain significant volumes of hydrocarbons (Liu et al., 2006; Bai et al., 2007a).

In an attempt to mitigate excess water production and hence increase hydrocarbon production, gels are often injected near wellbore or far-wellbore to preferentially seal fractures or higher permeability zones, thus diverting injected flood-water into low permeability unswept hydrocarbon-rich zones (Bai et al., 2007a; Bai et al., 1999; Bai et al., 2008; Liu et al., 1999). Gels as fracture-plugging and fluid diverting materials have been employed in conformance control (profile modification) and in the control of excess water production during EOR applications (Zhang et al., 2011; Vossoughi, S., 2000; Wang et al., 2001; Wang et al., 2003). However, over the years, there have been considerable developments in gel technology as it relates to conformance control.

2.3. PROGRESS IN GEL DEVELOPMENT FOR CONFORMANCE CONTROL

As earlier mentioned, oil production during secondary recovery (that is water flooding) is never 100% because of the existence of permeability variations in the

different layers of the reservoir. Such reservoir heterogeneity often leads to very poor volumetric sweep efficiencies. The injected flood water follows the path of least resistance (high permeability zones), bypassing large amount of oil in low permeability matrix. A plausible solution to this problem is to inject a plugging material and seal the high permeability zones, such that when injected fluids are injected, they will be forced or redirected to the low permeability, unswept oil-rich zones, sweeping out oil from them, leading to additional oil production. This, in summary, is the goal of any gel treatment.

Over the years, different types of gel treatments have been utilized in an attempt to solve conformance control problems. These include:

- i. In-situ gel technology
- ii. Preformed Gel Technology (PPG)

2.3.1. In-situ Gel Technology. As the term implies, in-situ gelation refers to the injection of a gelling solution (called a gelant) into the reservoir, and crosslinking of gelant solution to form a 3-D bulk gel takes place downhole (Vossoughi, S. 2000; Abdel et al., 2008). Ideally, the gelant solution, being highly liquid, is supposed to preferentially flow into the high permeability zone, then crosslinks inside this zone at elevated reservoir temperatures, and form a 3-D gel which acts as a plugging material, reducing the permeability of the high permeability zone. As such, injected fluid is redirected to low permeability, unswept oil-rich regions of the reservoir.

So, we observe that the success of any in-situ gelation job is based on the premise that the gelant solution will selectively flow into the high permeability zones and not enter the low permeability regions. However, Todd et al., (1991) found this assumption to be non-plausible. Seright, (1988; 1989) also found this assumption doubtful.

2.3.1.1 Limitations of in-situ gelation. (i) Selective injectivity and possible damage to low permeability zones: During gel injection, the ideal scenario is for gel to flow into high permeability strata. While much of the gel flows into high permeability regions, some however, enter low-permeability, oil-rich regions and damage them (Liang et al., 1990; Seright, 1990). Several solutions have been attempted to restrict the flow of gelant solution to just high permeability strata. Seright, (1991) suggested that zonal isolation will prove promising in addressing the problem of low permeability zone damage during gel injection. However, he observed that the technique of zonal isolation

will be more needed in unfractured reservoirs than in fractured reservoirs, in which very sharp contrasts in permeability variations exist between the different reservoir layers. In fractured formations, zonal isolation is not needed since there already exists a remarkable difference in permeability between the fractures and matrix. As such, gelant will easily flow into fractures.

However, in formations where fractures do not exist, but there exists a large difference between high and low permeability regions in the matrix, then zonal isolation is highly recommended. Further support for utilizing zonal isolation has been provided by Avery et al., (1986). Todd et al., (1991) has shown that selective injection of gelant using the method of zonal isolation was successful for a reservoir which had three separate layers with different permeabilities, in which a chromium-redox based gelant solution was used. Additionally, Hoefner et al., (1991) presented laboratory-based data supporting the idea that zonal isolation (also called selective penetration) was possible with chromium xanthan gels. They observed that selective penetration was mainly a function of permeability and injection rates. Nevertheless, the technique of zonal isolation does not entirely solve the problem of low-permeability zone damage. In formations where cross-flows exist in far-wellbore, employing zonal isolation is of little benefit, since injected gelant will flow across reservoir layers into low permeability strata, and hence plug and damage them.

(ii) Dispersion and Dilution of Gelant Solution: A crucial concern with in-situ gel technology is the alteration of the original gelant composition before the gelant ever gets to the fractures or high permeability regions. Dilution and dispersion of gelant solution by formation water is one major limitation in the utilization of in-situ gel technology. Dilution refers to the mixing of gelant solution with formation water, leading to a decrease in its concentration. Dispersion, however, refers to mixing caused by variations in the velocity within each flow channel and from one channel to another (Arya et al., 1988).

Dilution and dispersion could reduce gelant to such low concentrations that crosslinking and gelation become impossible (Young et al., 1988). They advanced that the ability of the chemical bank to be sufficiently diluted enough to make gelation

impossible would depend on: the size of the chemical bank, the diffusion coefficient, the gelation time, and the extent of dilution required to prevent gelation.

The larger the size of the chemical bank, the more dilution is necessary to prevent gelation and vice versa. Typical diffusion coefficients are normally in the order of $1.5 \times 10^{-6} \text{ in}^2/\text{sec}$ ($10^{-5} \text{ cm}^2/\text{s}$) for low molecular weight chemicals such as acrylamide monomer, phenol, and formaldehyde (Erdey-Gruz, 1974). High molecular weight gelling agents such as Polyacrylamide or Xanthan typically have diffusion coefficients in the order of $1.5 \times 10^{-9} \text{ in}^2/\text{sec}$ ($10^{-8} \text{ cm}^2/\text{s}$) (Southwick et al., 1982).

Normally, gel formation times usually range from a few minutes to a few days for most gelant compositions. In principle, the gelation time decreases with increasing concentration of gelling agents and vice versa (Prud'homme et al., 1984; Southard et al., 1984).

Seright (1991) concluded that gel formation will be hampered if more than 10% of the original gelant concentration is diluted. They observed that generally, if the minimum concentration for gelation is greater than 50% of the original concentration, then the size of gelant solution will be reduced by dilution and dispersion. However, if the minimum concentration for gelation is less than 50% of the original concentration, then dilution and dispersion will instead increase the size of the gelant solution.

(iii) Dehydration: Another limitation of in-situ gelation is the loss of water from the gelant solution as it flows from the well surface into the reservoir. Water can either seep out into nearby formation, or travel ahead of the gelant, leaving the polymeric components of the gelant behind, due to the high pressure gradient that exists between the gelant and the formation (Asghari, 1999). Such loss of water leads to dehydration of gels and hence formation of a gel of lesser size than was initially anticipated, that is, gel shrinkage. The same phenomenon is observed when cement is squeezed inside the formation because of pressure application. It loses water and becomes harder than was initially anticipated when it sets (Seright 1998, 1999).

(iv) Syneresis: Conversion of gelant solution to bulk gel is made possible by the presence of crosslinker. As crosslinker concentration increases, more crosslink junction points are formed, leading to bulk 3-D gel network. As crosslinker concentration continues to increase, so does the strength of the gel. However, above a particular

threshold concentration, too much crosslinker is present and excessive crosslinking takes place. This causes the gel to contract in volume, releasing water in the process. This phenomenon is called syneresis. Bryant et al. (1996) reported that depending on the composition of the gelant, a syneresed gel may shrink and occupy as small as 5% of the original volume of the gelant solution.

Thus, the effectiveness of a shrunked gel in plugging a highly porous and permeable formation would be seriously compromised. Because the gel shrinks (syneresed), it cannot fully seal the pores it was initially meant to seal. This leaves open pore spaces through which injected fluid can pass through. Thus the efficacy of the gel as a fracture-sealing or pore-sealing material becomes diminished (Kvanvik et al., 1995).

(v) Inadequate Control of Gelation Time: Another setback with in-situ gelation is the lack of gelation time control. Since gel formation time depends on the compositions of the gelant, it becomes difficult to ascertain at what time gel formation actually takes place downhole, since the original gelant composition at the surface is usually altered downhole because of dilution by formation water, dispersion of gelant, syneresis, dehydration, or chromatographic separation of the chemicals that constituted the original gelant composition.

Furthermore, since it is experimentally impossible to mimic downhole reservoir conditions, it thus becomes almost impossible to exactly predict when gelant forms 3-D bulk gel downhole. The issue of concern here is the fact that we cannot tell where and when gel forms in the reservoir. Near well-bore?, far well-bore?, or perhaps if the gel formation ever took place at all (Aslam et al., 1986; Willhite et al., 1986).

Additionally, it was also observed that gel formation time was affected by shear rate. As the gelant solution flows from the surface equipment down to the wellbore, and from the wellbore into the formation, shearing of the gelant solution distorts its original composition and affects gel formation time (Vossoughi, 2000).

2.3.1.2 Types of in-situ gel systems. All in-situ gel systems usually involve the crosslinking of a polymeric system using either organic or metallic crosslinkers. Over the course of three decades, much research has been done to optimize the best polymer and crosslinker system respectively. Initially, it was observed that partially hydrolyzed polyacrylamide would form gel when crosslinked with chromium or aluminum ions. It

was also observed that xanthan gum (a biopolymer), would also form gel when crosslinked with chromium.

In general, two main types of polymer systems have been studied: synthetic and natural polymers. Synthetic polymers include: polyethyleneimine (PEI), polyvinyl alcohol (PVA) and partially hydrolyzed polyacrylamide (the most commonly utilized synthetic polymer because of its relatively low cost and quick dissolution in water).

Different types of natural polymers have been utilized. The most common are polysaccharides such as xanthan gum, guar, and cellulose.

Two main types of crosslinkers have been utilized: metallic or organic crosslinkers. Common examples of metallic crosslinkers include: aluminum, chromium, boron, and titanium. Common examples of organic crosslinkers include: resorcinol, polyethylene glycol diacrylate, polyvinyl alcohol, N',N'-methylene bisacrylamide, polyethylene glycol dimethacrylate, polypropylene glycol diacrylate, ethylene glycol diacrylate, trimethylol propane trimethacrylate, ethoxylated trimethylol triacrylate, ethoxylated pentaerythritol tetra acrylate, diallylamine, triallylamine, divinyl sulfone, and diethyleneglycol diallyl ether (Marrocco, 1987; Chang et al., 1987; Mumallah, 1987, Sydansk, 1988).

However, cost and environmental concerns are usually a deciding factor in which gel system to use. Some of the crosslinkers are toxic and pose environmental and health concerns. Depending on the gelation time, some are more suited for near-wellbore applications in which shorter gel formation times are required. Others, because of their chemical structure can withstand higher temperatures. As such, they are used for very high temperature applications, such as N',N'-methylene bisacrylamide which can withstand higher temperatures for a longer time.

(I) Chromium systems: By far the most commonly employed gel system in the oil industry, gel systems with chromium as the crosslinker have been utilized for more than three decades (Figure 2.3).

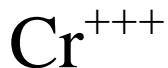


Figure 2.3. Chromium Cation.

Rouston (1972) observed that partially hydrolyzed Polyacrylamide (HPAM) can be crosslinked with chromium (III) hydroxide to form a 3-D bulk gel. He observed that a gelant solution comprising of a mixture of HPAM and chromium (III) hydroxide, when injected into porous and permeable formations, reduced their permeability. This composition was first marketed and commercialized by the chemical firm, Dow Chemicals under the trade name “ChannelB-lock”. Clampitt and Hessert (1974) observed that chromium based gel systems gel within minutes to hours of injection, and that gelation time depends on chromium concentration and other reservoir factors such as temperature, pH, and salinity.

Chromium gels by forming a trivalent complex with the three lone pairs of electrons on the carboxylate moiety of the polymer backbone. This process is called reduction or gain of electrons. Common reducing agents employed in chromium gelation include sodium bisulfite and thiourea. Sodium bisulfite enables gel formation to occur faster while thiourea affords longer gelation time. Additionally, Aslam et al. (1986) have also reported gel formation from a Chromium (III)/HPAM system.

Besides polyacrylamide based systems, biopolymers have also been crosslinked with chromium to form gel. Abdo et al., (1984) have reported obtaining a reduction in permeability with xanthan-Cr(III) based systems. Similarly, guar/Cr(III), and carboxymethylcellulose (CMC)/Cr(III) based gel systems have also been reported. The main difference between a synthetic polymer-based gel system such as HPAM, and a natural polymer-based system such as xanthan is the relatively shear-sensitive nature of synthetic-based polymer systems. It is well reported that polyacrylamide will easily undergo shear degradation during downhole injection. Such prolonged shearing shortens

the polymer chain, alters its chemical structure, and makes crosslinking and hence gel formation impossible. Whereas, natural biopolymers such as xanthan are not easily susceptible to shear degradation (Vossoughi, 2000).

It has also been observed that in reservoirs with very high hydrogen sulfite content, gelation usually occurs extremely fast. This is because hydrogen sulfite is a strong reducing agent. As such, chromium in the presence of hydrogen sulfite usually crosslinks faster and forms gel before the gelant ever gets to its designated location in the high permeability streaks. This is disadvantageous in that there is the possibility of near-wellbore damage from premature gel formation. Mumallah (1987) and Sydansk (1988) were able to circumvent this problem by complexing the chromium. Mumallah showed that forming a chromium propionate complex delays its release in solution, thus prolonging crosslinking and hence gelation. In solution, propionate slowly dissociates from chromium, releasing the chromium and making it available for crosslinking with the polymer. Sydansk (1988) also showed that forming a chromium acetate complex also functions in like manner. Substitution of acetate groups by carboxyl groups of polymer delays gel formation and enables an HPAM/Cr(III) gel system to gel much longer and at a higher pH than it would normally have without forming the chromium-acetate complex.

(II) Aluminum Systems: Aluminum, just like Cr (III), has the ability to form trivalent complexes (Figure 2.4). This is due to its ability to accept three lone pairs of electrons and form a trivalent metal complex with electron donor groups like carboxylates.

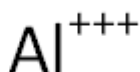


Figure 2.4. Aluminium Cation.

Conversely to Cr (III), aluminum is often preferred because it is relatively less toxic than Cr (III). As such, it is environmentally friendly and does not pose a serious

threat to the environment and to ground water contamination and pollution. Hydrolyzed polyacrylamide/Cr (III) gel systems were first studied by Needham et al. (1974). They observed that an HPAM/Cr (III) gel system reduced the permeability of a permeable rock by a factor of 10. However, Parmeswar and Willhite, (1988) showed that the gel formed just within a few centimeters into the entrance of the core. However, Fletcher et al. (1991) observed that in-depth gelation of HPAM/Cr (III) is possible by regulating the temperature. They conducted a slim tube experiment at 25 °C and 70 °C. They found that gel formation occurred in-depth in the sample kept at 75 °C, whereas no in-depth gelation occurred in the sample kept at 25°C. Dovan and Hutchins (1987) further observed that an HPAM/Cr (III) gel system is only possible at a very narrow pH range of 6-7 and that gelation is best observed in fresh water. This is because in formation water, calcium and magnesium, being divalent ions, compete with aluminum for citrate ions. This therefore makes HPAM/Cr (III) gelation in formation water very slow, if at all possible.

(III) Organic Gel Systems: Besides metallic crosslinkers, organic crosslinkers have also been used to form in-situ gels in which the crosslinker forms covalent bonds with the polymer functional group. Organic gel systems are usually stronger than metallic gel systems. This is for the obvious fact that covalent bonds formed by organic crosslinkers are stronger than ionic bonds formed by metallic crosslinking. Seright and Martin (1991) designed an organically crosslinked sulfomethylated resorcinol gel system which produced a permeability reduction of 99% and tolerates high salinity environments. Its ability to achieve such high permeability reduction and act as a good plugging agent was attributed to the strong covalent bonds formed during gel formation (Raje et al., 1999). Moradi-Araghi et al. (1989) have also presented a gel system formed through covalent bonding of a terpolymer (such as N-vinyl-2-pyrrolidone, acrylamide, sodium 2-acrylamide-2-methylpropane sulfonate) with phenol and formaldehyde as crosslinker. Such gels can withstand temperatures as high as 149 °C (300°F) and seawater salinity (Hsieh and Moradi-Araghi, 1991). Paul and Strom, (1987) also designed a non-xanthan anionic heteropolysaccharide S-130 which gels either by itself or with a metallic crosslinker (such as Cr (III)) and organic crosslinkers (such as ethylene diamine or piperazine). The following organic gel systems have been studied:

(III.1) Polyvinyl Alcohol Gel Systems: A fairly common organic gel system, polyvinyl alcohol (PVA) with aldehyde as crosslinker, has been utilized. It is formed by the reaction between two solutions, one consisting of polyvinyl alcohol and a polyvinyl alcohol copolymer, and the other containing an aldehyde and water (Marrocco, 1987). Usually an acidic catalyst is required and a common aldehyde utilized is glutaraldehyde. This gel system is marketed by Pfizer company under the trade name Flowperm 465.

(III.2) Phenolic Gel Systems: Phenolic gels are formed by the reaction of a phenol, such as resorcinol, and an aldehyde, such as formaldehyde (Chang et al., 1985, 1987). They are usually made to be used in reservoirs with very harsh conditions such as very high temperatures, high salinity, and high pH. Chang et al., (1985; 1988) reported a phenolic gel system which gelled at pH of more than 9 and was used in a reservoir with temperatures as high as 92 °C (197 F).

(III.3) Colloidal Silica Gel. Jurinak et al. (1989) reported a colloidal silica gel system developed for oilfield applications. Colloidal silica concentrations of 6 to 15 weight percent are usually required to form gels with sufficient strength and durability for oilfield applications. They have been used for temperature ranges from 90°F to 210°F (32.2 °C to 98.9 °C).

The ability of colloidal grouts as sodium silicate to self-polymerize and form plugs has been exploited (Lakatos et al, 2001; Heaven et al, 1999). In the presence of an activator such as nitric acid or sulfuric acid, and at room temperature, these silicates precipitate to form hard, solid but porous and permeable temporary plugs (Bauer et al., 2005) as shown in Figure 2.5. At reservoir conditions, however, these plugs physically break down, lose their mechanical and tensile properties and become porous, permitting fluid flow through them. Impermeability of a plugging agent is a fundamental requirement in the design of permeability reduction material. Furthermore, the activators used, nitric and sulfuric acids are all strong acids, which require special handling and storage and are very costly.

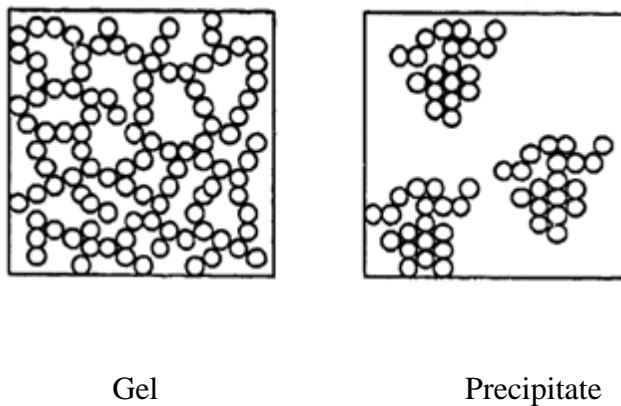


Figure 2.5. Difference between Precipitates and Gels.

Thus, in the history of conformance control, in-situ gels were the first kind of materials utilized in an attempt to plug fractures or high permeability streaks. However, as discussed, the possibility of damaging low permeability formations and several other limitations outlined above have prevented industry from widely embracing this technique as a solution to solving permeability variation problems in reservoirs. On the contrary, these limitations compelled industry to find new and better solutions to address conformance control problems. This search of a better performance product led industry experts and researchers to develop a novel technology in addressing conformance control problems in reservoirs. This technology is called Preformed Gel Technology.

2.3.2. Preformed Gel Technology. In an attempt to overcome the limitations of In-situ gel technology, industry experts and researchers developed a novel technology to address conformance control problems called preformed gel technology. The novelty and main difference between this technology and in-situ gel technology is that with preformed gel, gel formation takes place at the surface, well ahead before injection, whereas with in-situ gelation, crosslinking and gel formation occur downhole in the reservoir. The technology was revolutionary in that it solved the problems posed by in-

situ gelation such as dilution and dispersion of gelant, chromatographic separation of gelant solution, dehydration, syneresis, and most importantly damage of low permeability zones.

Preformed gels are three-dimensional, hydrophilic crosslinked polymers, which in contact with water, swell but do not dissolve as a result of a chemical or physical crosslinking and most often, will undergo a volume phase change when surrounding conditions such as temperature, salinity or pH change (Wen-Fu and Sung-Chuan, 2006).

Materials that swell in water are the most ideal candidates for sealing fractures or fissure systems. In contact with water, these materials swell to many times their original size and occupy the fractures in which they are present, thus creating a restriction to fluid flow through the fractures. In fact, Imran et al. (2008) and Bai et al. (2007a; 2007b) have reported some polymeric materials swelling up to 400 times their original weight.

Usually, these materials are bullheaded into the well to shut off fractures. Imran et al., (2008) advanced several benefits for using swellable materials for conformance control:

- They provide an effective seal to avoid direct communication from injectors to producers in a matter of hours.
- No requirement for specialized mixing equipment (they are added on-the-fly).
- They are economical. A small amount swells and yields a large volume.
- Rapid and controlled water absorption.
- They have the ability to withstand influxes of water, which can help prevent dilution of cement or other remediation products.

Water swellable materials have found applicability in the following cases (Imran et al., 2008):

- Fractures and fissures in communication.
- High permeability strata or zones.
- Deteriorated layers of formation rock with friable or karsted aspects.
- Near-wellbore repairs (because of its ability to absorb water to help counter the influx of water).
- Loss circulation problems for horizontal drilling and primary cementing.

- Remedial workovers where the presence of a highly communicated crossflow behind casing can cause dilution of any sealant or cement.
- Production wells, (when the system is combined with a tail-in of cement or conformance porosity sealants).

Preformed Gels are usually formed by a free radical, multi-component, polymerization reaction that involves monomer and initiator in the presence of a crosslinker and other additives. Several types of preformed gels exist: (1), partially preformed gels, (2), microgels, (3) pH-sensitive crosslinked polymers (4) bright water, (5) colloidal dispersion gels and (6) preformed particle gels (PPG).

Various types of preformed gels have been studied over the years. These include:

2.3.2.1 Partially preformed gels. Seright (2004) has studied a partially preformed gel for disproportionate permeability reduction during gel placement. Partially preformed gels are those in which the gel is injected downhole in a partially formed state, that is, shortly after the first sign of gel structure is detected. In partially formed gelation technology, care is taken to ensure that enough gel structure is formed before injection so as to avoid gelant-solution leak off and possible formation damage of low permeability strata. However, care is also taken to avoid complete gel formation prior to injection. This is because much higher injection pressures are usually needed for injecting fully formed gels. Such partially formed gels have better placement than in-situ gels and will eventually gel into strong gels that function as water shut-off agents. The advantage of partially formed gels is that they exhibit very low pressure gradients during placement in reservoir fractures.

The essence of this technology is to develop gels that will readily flow into fractures and then effectively plug the fractures during brine flow after placement, especially in wide fractures with widths of 2mm to 4mm. Seright (2004) has studied a Cr (III)-acetate-HPAM partially formed gel used to reduce the flow capacity of fractures at 41oC. In their experimental work, they observed that after gel placement, water residual resistance factor values, (residual resistance factor of water, F_{rrw}) decreased from 100,000 to 39,000. Thus partially formed gels provided effective permeability reductions in reservoir fractures. However, they also observed that the gel reduced the flow capacity

toward oil (residual resistance factor of oil, F_{rro}) by a factor of 1500. Nevertheless, the gel still showed a significant disproportionate permeability reduction.

This is because at any given rate, F_{rrw} values were 3 to 9 times greater than F_{rro} values (Figure 2.6). Furthermore, Sydansk et al. (2005) observed in a laboratory study that a partially formed chromium (II)-carboxylate/acrylamide-polymer (CC/AP) gel showed much lower effective viscosities during placement than comparably fully formed gels. Partially formed gels (less than 8 hours old) showed up to 100 times lower effective viscosities (17 to 35 cp) during flow through a 1-mm wide fracture than fully formed gels (older than 15 hours) with the same chemical composition. This observation led them to conclude that partially formed gels exhibit higher injectivities and lower placement pressures than fully formed gels. Sydansk et al. (2004) also observed a similar effective viscosity reduction using a mixture of high and low molecular weight CC/AP partially formed gel. They also observed that gelant solution leak-off was very low for these partially formed gels.

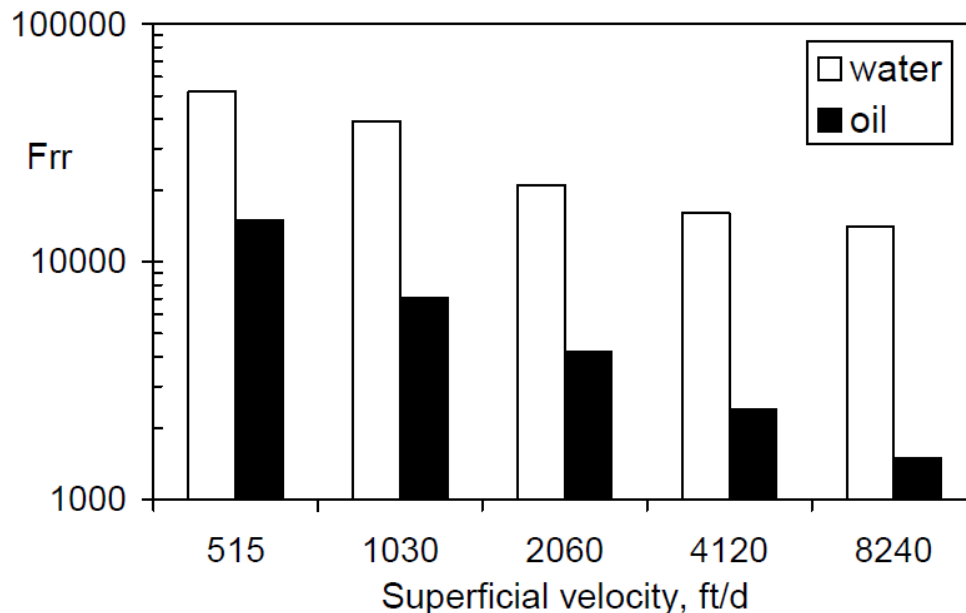


Figure 2.6. Effect of Rate on Residual Resistance Factor (F_{rr}) in a 2-mm-wide Fracture.

2.3.2.2 Microgels. Microgels are preformed gels formed by ionically or covalently crosslinking a polymer. They usually range in size from 0.3 to 2 μm (Zaitoun et al., 2007). To obtain smaller microgels (about 0.3 μm), higher crosslinker concentration and hence high crosslink density are needed. This makes the gels hard and less deformable. To obtain larger microgels (2 μm), less crosslinker concentration and hence less crosslink density is needed. This makes the gels soft and easily deformable (Figure 2.7). Microgels reduce water permeability by adsorbing onto formation surface on pore walls by capillary forces in the presence of oil so that oil permeability remains unaffected. Thus, controlling the adsorbed layer thickness and hence water permeability reduction is by the selection of microgel size and by increasing the concentration of injection and flow-induced over-adsorption (Rousseau et al., 2005).

Microgels are formed by gelling a polymer and crosslinker solution mixture under shear flow. The process of microgel formation involves four stages (Chauveteau et al., 1999; Chauveteau et al., 2000; Chauveteau et al., 2001): (1) the induction period, during which the microgels are few and small and remain isolated. (2) the pregel period, during which there is a rapid increase in viscosity. (3) the microgel size limitation period, during which viscosity is at its peak and cannot increase anymore, and lastly (4) the microgel consolidation period, during which the crosslinking continues and is characterized by an increase in both intra and intermolecular crosslinks inside the microgels.

The technology of microgels was developed in an attempt to overcome some of the inherent limitations associated with in-situ gel application and polymer flooding. Since in-situ gelation kinetics are highly dependent on reservoir environment and physico-chemical conditions, there was a need to develop a stable and size-controlled product whose gelation kinetics are least affected by reservoir environmental physico-chemical conditions. Microgels are prepared onsite at surface facilities prior to injection and their sizes are controlled by shearing. An ideal microgel should comprise the following (Chauveteau et al., 2003): (1) should be insensitive to shear and reservoir physico-chemical conditions. (2) should be size-controlled to prevent face plugging. (3) should be small enough to ensure an in-depth treatment and large enough to reduce water permeability significantly, (4) should be soft enough to be collapsed onto pore walls by capillary pressure in the presence of oil flow in order to be disproportionate relative

modifiers, (5) should be strongly adsorbing onto pore surface and stable over time, and lastly, (6) should be non-toxic to the environment.

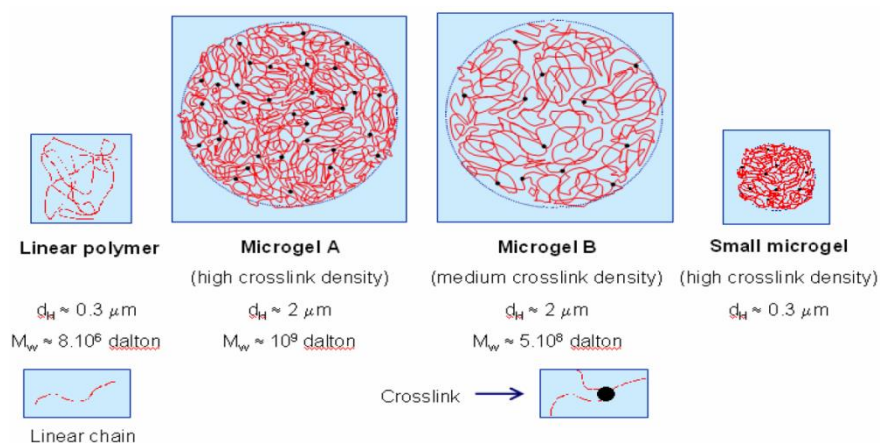


Figure 2.7. Polymer and Fully Water-Soluble Microgel Species.

Microgels have been proven to be good relative permeability modifiers, and to have excellent shear, and also thermal and chemical stability (Chauveteau et al., 2001). Additionally, since they have larger sizes than polymers used in polymer floods, they are better suited to avoid low permeability formation zone damage, which is a commonly reported problem with polymer floods or in-situ gel application. In their first field application, Zaitoun et al. (2007) showed that microgels of $2\mu\text{m}$ sizes were easily placed in high-permeability, near-wellbore strata, whereas very minimal penetration of microgels was observed in low and medium permeability zones.

Lastly, Rousseau et al. (2005) observed that due to the remarkable ability of microgels to reduce permeability at long distances without any face plugging, they are hence good candidates, not only for water shutoff operations, but also for conformance control of heterogeneous reservoirs. Additionally, they further suggested that microgels could also be used as mobility control fluids when reservoir conditions are too severe for linear polymers to be used.

2.3.2.3 pH-sensitive crosslinked polymers. pH-sensitive gels refer to those hydrogels whose swelling ability is dependent on the pH of the environment. Thus they are very applicable in controlled release systems (Figure 2.8). Mechanistically, their pH-dependent swelling response is due to the presence of ionizable side groups on the side chain of the polymer or hydrogel backbone. For hydrogels with acidic side groups, swelling ability increases in basic environment while for gels with basic side groups, swelling increases in acidic environment (Peppas et al., 2000; Saez et al., 2003).

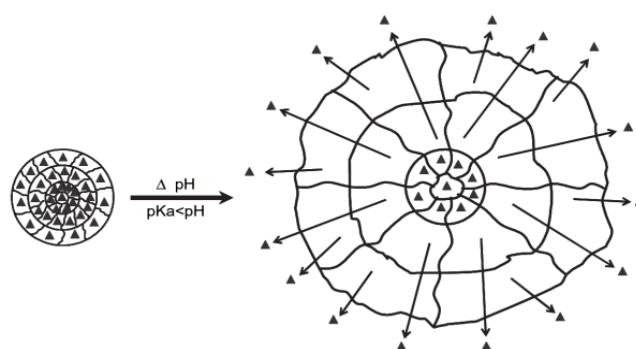


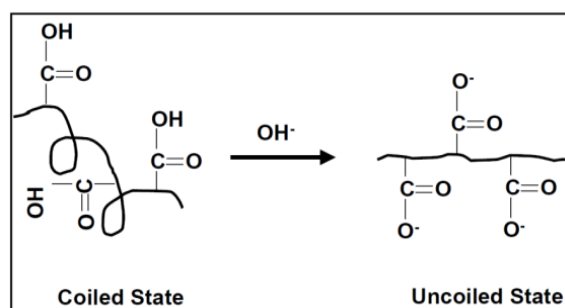
Figure 2.8. Schematic Representation of the Behavior of a Hydrogel with a pH-Sensitive Release.

As a result of this behavior, pH-sensitive hydrogels have found application in several sectors, including conformance control, agriculture, and in medicine for controlled drug release applications. The rate and time of release of pH-sensitive hydrogels is determined by the polymer ratio, or by the crosslink density in the gel (Dinh et al., 1999).

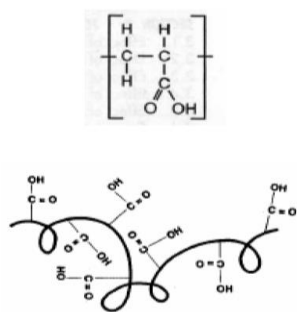
In the area of conformance control, Al-Anazi and Sharma (2002) have proposed a new strategy for utilizing pH-sensitive polymers. They observed that anionic polyacrylic acid polymer is very pH-sensitive. At a pH of 2.5, it has a viscosity of 5 cp. However, at pH above 6, polymer viscosity increases tremendously to 20,000 cp. Thus they can be easily injected at low pH since their viscosity is near water (an acid pre-flush is required before injection in order to create initial low pH environment downhole). They easily propagate deep into the reservoir formation and in contact with higher pH reservoir

fluids, they swell and gel, and plug water thief channels or high permeability streaks. Additionally, they observed that the gelled polymer was stable even at pressure gradients of 4000 psi/ft.

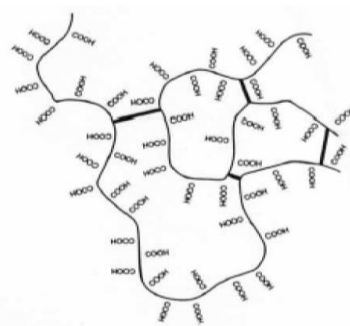
Mechanistically, polyacrylic acid, being a polyelectrolyte, exists naturally in a coiled, low viscosity state. However, as the pH of its environment increases, its carboxylic acid side groups are ionized by the excess hydroxyl (OH^-) groups in solution. Electrostatic repulsive forces of now formed carboxylate side groups cause the polymer chain to uncoil and expand. This behavior thus increases the viscosity of the polymer as it is ionized in an alkaline environment (Figure 2.9) (Huh et al., 2005).



(a)



(a) poly(acrylic acid)



(b) crosslinked poly-acrylate hydrogel

(b)

Figure 2.9. Mechanism Leading to Increase in Polymer Viscosity Due to Side Chain Ionization (a) Swelling and Viscosity Increase of Polyacrylic Acid upon Ionization (b) Molecular Structure of (a) Polyacrylic Acid, (b) Crosslinked Poly-acrylate Hydrogel.

Furthermore, polyelectrolytes such as polyacrylic acid have been used as scale inhibitors to prevent scale formation near-wellbore and in-depth of well (McTeir et al., 1993).

2.3.2.4 Bright water. Bright Water, first commercialized in 2009 by Tiorco (Nalco Company) as Brightwater®, refers to a novel technology developed for in-depth waterflood conformance control. This technology was developed by an industry consortium of BP, Chevron, and Nalco. It was first tested in Indonesia in 2001 (Pritchett et al., 2003). Brightwater® is a sub-micron particulate chemistry (suspension of crosslinked polymer particles) that is injected into reservoir together with injection water. Because of its very small sizes (about 0.5 μm), the particles can move deep into the formation. Under elevated downhole temperatures, the particles slowly expand to several times their original size (due to the temperature-triggered hydrolysis of the crosslinking bonds) and plug pore throats, thus diverting injected flood water to low permeability, oil-bearing strata as shown in (Figures 2.10 and 2.11) (Bruno et al., 2010).

Some of the advantages of this technology include: (1) simple injection system. It is injected together with injection water using already existing chemical injection infrastructures in place. (2) Particles can swell up to four to ten times their original size depending on reservoir salinity. The applicability and effectiveness of Brightwater technology depends on the following conditions (Ghaddab et al., 2010):

- Absence of fractures in the formation.
- Water cut less than 98%.
- Water injection running.
- Reservoir temperatures above 35 °C.
- Evidence of water thief zones.
- Porosity of highest permeability zones greater than 17%.
- Permeability of thief zone greater than 100 mD.
- Injection water salinity under 70,000 ppm.

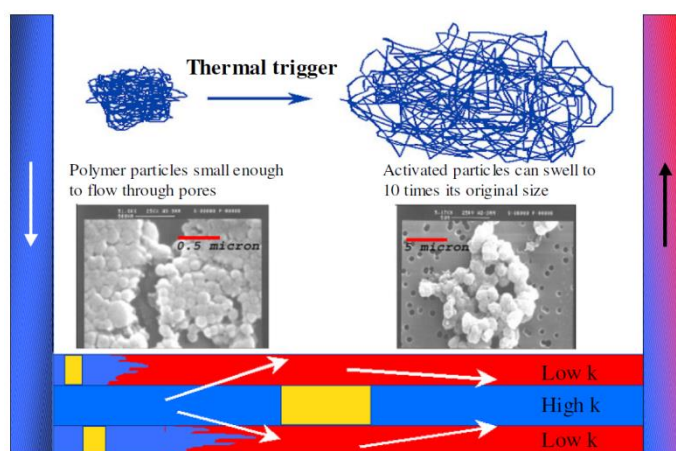


Figure 2.10. Brightwater® is Injected as a One-time Batch Together with Injection Water at Concentrations of about 1.5%.

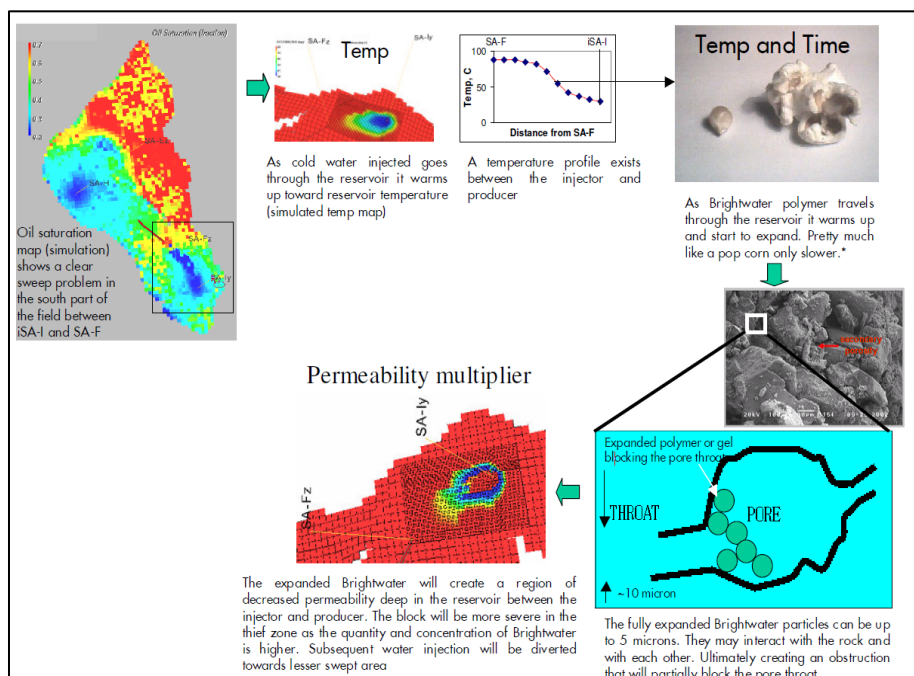


Figure 2.11. How Brightwater Technology Works.

Several field trials of this technology have been carried out in several areas including the North Sea (Lugo, 2010), Argentina (Yanez et al., 2007), and Alaska (Ohms et al., 2009). The Argentina field trials reported no incremental oil production using this technology. However, the field trials in Alaska and the North Sea reported a 60,000 bbl and 130,000 bbl respectively incremental oil production over a four year and one year period respectively.

2.3.2.5 Colloidal dispersion gels. Prior to the development of Colloidal Dispersion Gels (CDGs), existing gels could only be applied near-wellbore. In-depth permeability modification at the time was impossible. Thus, there was a necessity to develop a technology that could address in-depth water channeling and crossflow problems in the reservoir. This was the essence of Colloidal Dispersion Gels (CDGs). CDGs are homogenous bulk gels made from a low concentration of polymer and crosslinker and are meant specifically for use in in-depth reservoirs (Mack and Smith, 1994). The requirement of a low polymer and crosslinker concentration allows for large volumes of CDGs to be injected economically. Commonly utilized polymer is partially hydrolyzed Polyacrylamide. Crosslinker employed is aluminum citrate.

CDGs are so-called because the gels consist of isolated bundles of crosslinked polymer molecules which are suspended in solution. They are also called aggregates. Mechanistically, since low polymer concentrations (100 – 1200 ppm) are used, the polymer chain is not long enough to form a continuous gel network. Rather, distinct gel bundles form in solution, with different bundles having little intermolecular interactions amongst each other (Figure 2.12).

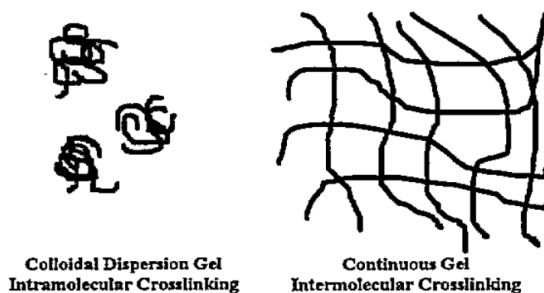


Figure 2.12. Comparison of Colloidal Dispersion Gels and Bulk Gels.

An advantage of CDGs over other gels is that with CDGs, a relatively small amount of crosslinker is needed for crosslinking to occur. Typical polymer: aluminum ratios used are in the range of 20:1 to 100:1. It was also observed that CDGs have better performance in fresher waters. In solution with total dissolved solids (TDS) of about 30,000 ppm and above, gels lose strength and become weaker. Furthermore, it is a cost effective process, since less polymer and crosslinker concentrations are needed.

2.3.2.6 Preformed particle gels. Preformed Particle Gels (PPGs) belong to a family of hydrogels called Super Absorbent Polymers (SAP). SAPs are a special kind of materials that can absorb up to several times their original weight in solution and will not easily release the absorbed fluid when pressure or stress is applied to it. SAPs have found several applications in industry, ranging from cosmetics (diapers, feminine hygiene products), agriculture, and in medicine for drug-release applications. However, for water shutoff and conformance control-related applications, traditional SAPs have proved ineffective due to their fast swelling times, low strength under applied pressures, and poor thermal stability under elevated temperatures (Bai et al., 2008).

Thus, there existed a need to develop new SAPs for conformance control-related applications. A novel SAP for conformance control with improved performance, called Preformed Particle Gel (PPG) have been developed (Li et al., 1999; Bai et al., 2004, 2007b). PPGs are three-dimensional, hydrophilic crosslinked polymers, which in contact with water, swell but do not dissolve as a result of a chemical or physical crosslink and often than not will undergo a volume phase change when surrounding conditions such as temperature, salinity or pH change (Wen-Fu and Sung-Chuan, 2006). Preformed Particle Gels are usually formed by a free radical, multi-component polymerization reaction that involves monomer and initiator in the presence of a crosslinker and other additives. They can be designed/made either into millimeter-sized, micrometer-sized, or nano-sized particles, depending on field application and matrix permeability. PPG offers the following advantages (Bai et al., 2004):

- Since crosslinking and gel formation occurs at the surface facilities, PPG can overcome some inherent drawbacks in in-situ gelation systems such as lack of gelation time control, gelant solution dilution, degradation, chromatographic separation, and dehydration.

- PPG is strength-and size-controlled, environmentally friendly, thermally stable over long periods of time and is not sensitive to reservoir minerals and formation water salinity.
- PPG can resist temperatures as high as 120 °C and salinity as high as 300,000 mg/L.
- Additionally, PPG can be carried downhole into reservoir by produced water. This saves the usage of fresh water and helps in produced water disposal.
- Also, it requires very simple on-site facilities. Cost of operation is minimized.

The process of PPG involves the following:

- Crosslinking of gelant solution prior to injection to form 3-dimensional bulk gel.
- Drying, grinding, and sieving of bulk gel to micro size particles, called Preformed Particle Gel.
- Soaking and injection of micro sized particles into fractures or high permeability zones of reservoir to act as plugging agents.

PPG technology was first used in China in 1999, in the Zhongyuan oilfield, SINOPEC (Bai et al., 2004). Ever since then, PPG treatments for mature oil fields have been widely and extensively applied throughout China and beyond. This, in part, is due to the fact that most of the oilfields in China were discovered in continental sedimentary basins and are comprised of reservoirs with sharp permeability variations and complex geologic conditions (Li and Zhou, 1986). In an attempt to maintain rapidly declining reservoir pressures, water floods were employed at a relatively early stage of the reservoir. This resulted in increased water production in wells that were relatively new and still contained large volumes of oil. Thus the need for a technology to curb water production and correct reservoir heterogeneity was imperative.

However, the study of Preformed Particle Gel gained interest, not only in mature oilfields in China, but also in the United States. Seright (1997; 2000; 2003) has studied the extrusion behavior of PPG through fractures and ascertained that they have better placement and better permeability reduction than in-situ gels.

How then can we identify the types of reservoirs that require PPG treatment? In order for a particular reservoir to be an ideal candidate for PPG treatment, several conditions have to be met. A comprehensive in-depth knowledge of factors such as wellbore and near wellbore conditions, reservoir geology, static and dynamic reservoir information are all important information in determining the appropriateness of a particular well for PPG treatment. Generally speaking, in order for a well to be a suitable candidate for PPG treatment, the following conditions are necessary (Bai et al., 2008):

- Excellent interconnectivity between neighboring injectors and producers must exist. A low water injection pressure must exist.
- Well must have an excellent and wide oil pay zone located in the main sand body of the fluvial depositional reservoir.
- The well should have a relatively high average water cut.
- Well must have both a sharp vertical or areal heterogeneity and a large inner-layer permeability contrast. Additionally, the injection and production profiles of the connected wells should not be homogenous.
- The well should have been flooded to different degrees. That is, low, middle and none-flushed zones should exist in the reservoir.

From experimental and field studies, Bai, (2001) observed that a low concentration, large volume PPG injection is key to any successful PPG treatment. They observed that where PPG treatments were unsuccessful (Bai et al., 2007b), the PPG volume used was low or the PPG concentration was high. They advanced that a high concentration PPG injection may induce new fractures near wellbore as a result of vigorous vibrating bottomhole pressure. Low injection rates are usually employed during PPG injection. This is to decrease gel damage on low-permeability oil regions. Additionally, during injection, smaller PPG sizes are usually injected first in order to ensure that PPG propagates into deep regions of the formation, then gradually larger sizes are injected depending on real-time injection pressure responses. So then, how can we determine the effectiveness of PPG as a conformance control agent?

In order to determine the performance of a well both before and after gel injection, two different methods are utilized. One way is to measure the well injection profile. This shows the plugging effect of PPG on different zones near wellbore. The

second method is to perform a well test analysis. This includes obtaining starting pressures, injection pressures (as those before treatment), and pressure drawdown test for pressure index PI (90). These parameters give us an indication of PPG plugging in the in-depth of the reservoir.

In a Daqing oilfield study, Bai et al., (2008) observed that for 26 wells treated, PPG treatment decreased water production and increased oil production by almost 15,000 tons (Figure 2.13). That is for every ton of PPG injected, 113 tons of incremental oil was produced. For these 26 wells, the following input and output costs were realized:

PPG costs: 132 tons \times (1.46 \times 10⁴) RMB/ton = 192.72 \times 10⁴ RMB

PPG injection costs: 4 wells \times (18 \times 10⁴) RMB/well = 72 \times 10⁴ RMB

Injection profile measurement: 8 times \times (1.1 \times 10⁴) RMB/time = 9.9 \times 10⁴ RMB

Pressure drawdown test: 12 times \times (0.8 \times 10⁴) RMB/time = 9.6 \times 10⁴ RMB

Total input: 284.22 \times 10⁴ RMB

Oil price: 2,100 RMB/ton (about 40 \$/bbl)

Output from oil sales: 15,000 tons \times (0.21 \times 10⁴) RMB/ton = 3150 \times 10⁴ RMB

Output-Input ratio: 11.08

These results prove that PPG treatment is productive and profitable.

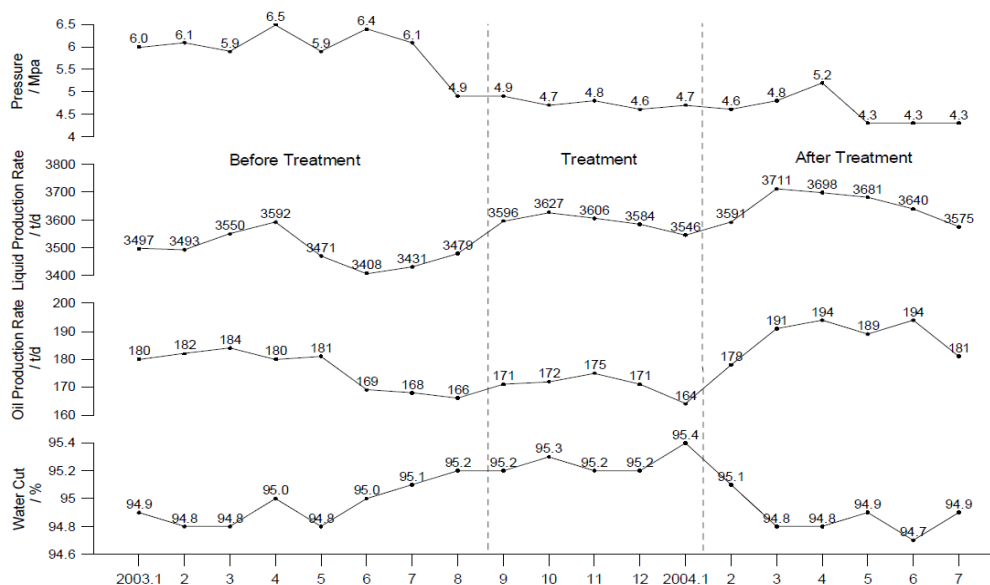


Figure 2.13. Production Curve for 24 Connected Wells.

How then can PPG be transported through porous media? In studying the transport of PPG through porous media, Coste et al., (2000) observed that transport of PPG through porous formation occurs by three main types of mechanism:

- Deformation of the particle.
- Shrinking of the particle by expulsion of water.
- Breaking of the particle.

The essence of this study was to ascertain the fact that, if and when PPG encounters a small pore throat, would it still propagate through it and continue its movement into the deeper regions of the formation? They concluded that when PPG comes in contact with a small pore throat, the particle will either deform and slide through the pore throat, shrink to a smaller size and go through the pore throat, or break into small pieces and move through the pore throat (Figure 2.14).

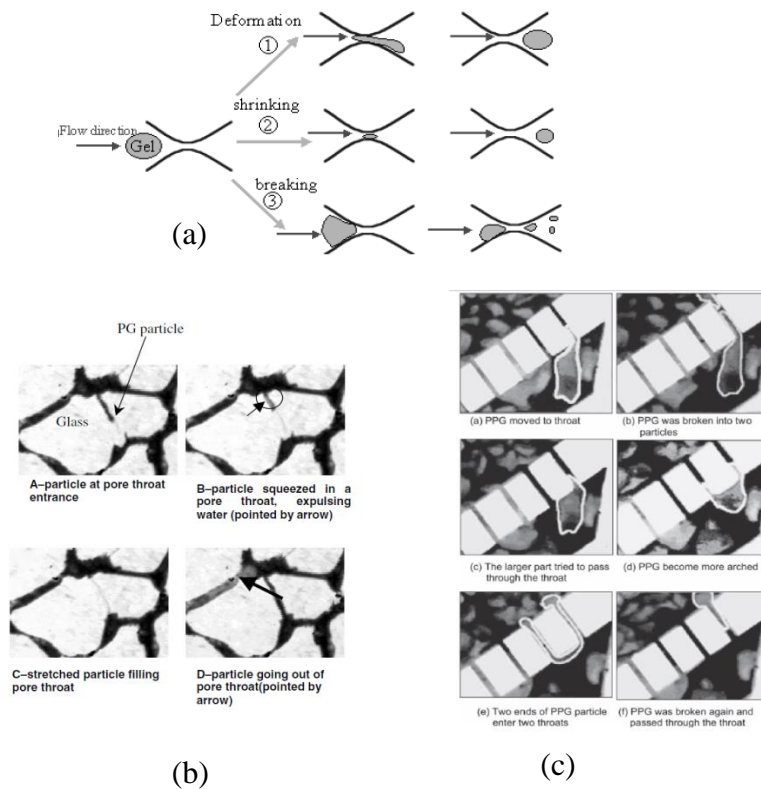


Figure 2.14. The Different Mechanisms of How Particle Gels Pass Through a Pore Throat.

Several factors affect the behavior and properties of PPG. Bai et al. (2007a) showed that monomer concentration, crosslinker concentration, initiator concentration, clay concentration, and temperature all play crucial roles in the properties of PPG. They observed that gel strength increases with monomer concentration and becomes stable at monomer concentrations above 15 weight percent. They also observed that gel strength increases as crosslinker concentration increases. This is because increasing crosslinker concentration leads to a higher crosslink density. Additionally, the swelling ability of the gel decreased with increasing crosslinker concentration. This is because increasing crosslinker concentration leads to a more dense gel with less available spaces for water intake. They also showed that increasing the initiator concentration leads to a faster gel formation time. More initiators in solution mean more free radicals are produced, which means a faster polymerization reaction. However, excess initiators in solution could result in the formation of shorter polymer chains leading to gels with less dense crosslink network.

In summary, despite the tremendous advantages of preformed gels over in-situ gels, preformed gels did not provide an all-encompassing solution to the problem of conformance control and reservoir heterogeneity. Some of the limitations of preformed gels include:

- Mechanical: Inadequate modulus, inadequate toughness.
- Thermal: Inadequate thermal resistance to withstand very extreme reservoir conditions, shorter degradation time.
- Swelling: Inadequate swelling ability.
- Elasticity: Inadequate gel elasticity

Thus, there is a continuous need to provide a technology that surpasses the performance of current conformance control gel products.

2.3.3. Nanocomposite Preformed Particle Gel. Nanocomposite preformed particle gels (nanocomposite PPG), are a newer trend in gel design for profile modification and conformance control applications (Bai et al., 2007a). Nanocomposite PPG is an extension of existing PPG technology. It refers to preformed gels synthesized by incorporating nanomaterials in the gel design. Nanocomposite PPGs are prepared by

an in-situ free radical polymerization reaction that involves monomer, crosslinker, initiator, additives, and nano material (Figure 2.15).

The incorporation of nanomaterials in gel design is an effective way to improve gel properties and boost performance. The technique of nanotechnology refers to the creation of uniquely designed materials, devices, and/or systems through control on the nanometer-length scale. It refers to the exploitation of novel properties and phenomena developed at this scale (Roco et al., 2000).

Common nanomaterials that have been studied include montmorillonite clays, carbon nanofibers, polyhedral oligomeric silsesquioxanes (POSS), carbon nanotubes, silicon dioxide, aluminum dioxide, titanium dioxide, laponite clays, kaolinite clays, etc. Price and structure are key factors in the selection of a nanomaterial.

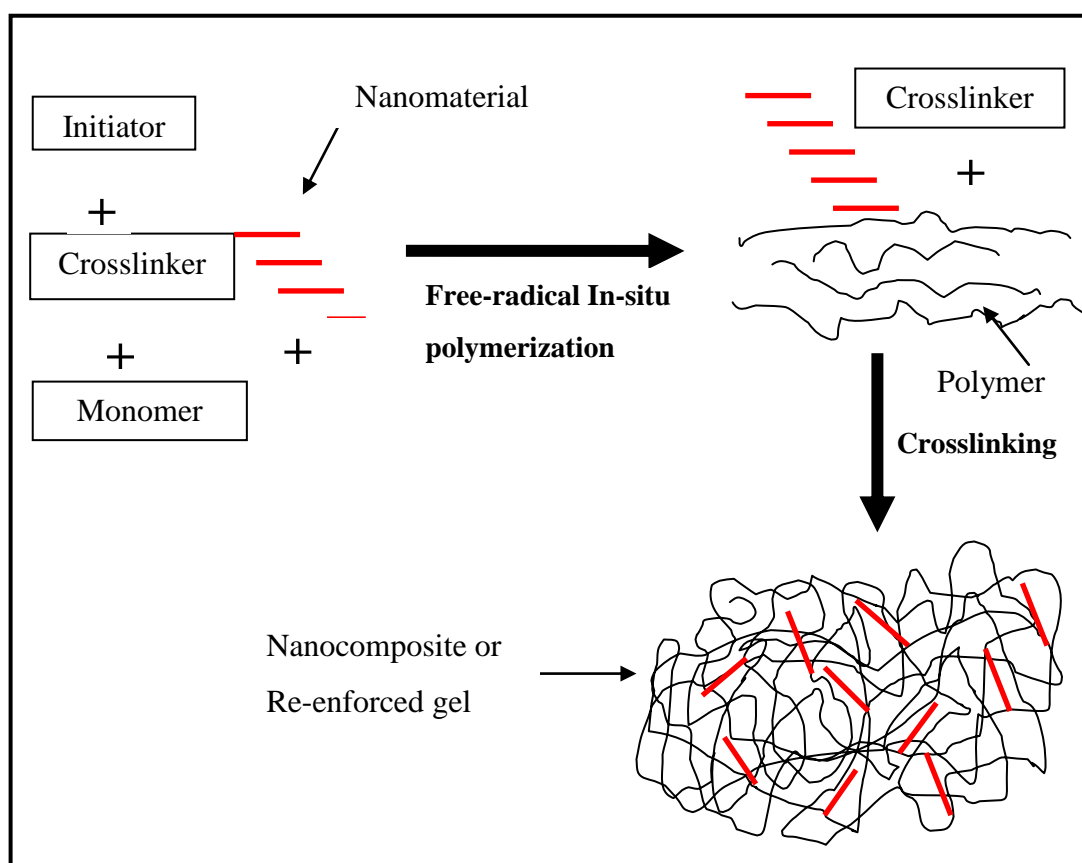


Figure 2.15. Free Radical Polymerization of Nanocomposite Gels.

The reason nanocomposite gels perform better than gels without nanomaterials is because of the strong interactions that exist between the nanomaterial surface and the polymer matrix. For instance, when nanoclays are used, stronger interfacial interactions are formed between the polymer matrix and the clay silicates (Figure 2.16) (Ray and Okamoto, 2003). This is because, as a result of the complex nature of clays, chemical reactivity is usually high at the clay surface (Shibayama et al., 2004; Olphen V.H., 1977; Pinnavaia et al., 2000).

Nelson and Cosgrove (2004) also showed that the ability of polymer chains to bond or adsorb on clay surface is a strong function of polymer molecular weight. Larger polymer chains can wrap from one face of the clay particle to the other or extend over the edge of the clay particle, whereas shorter polymer chains cannot. Additionally, clays have a large aspect ratio, such as thin plates or narrow rods. As such, they are suitable for use as reinforcing filler materials in a polymer network.

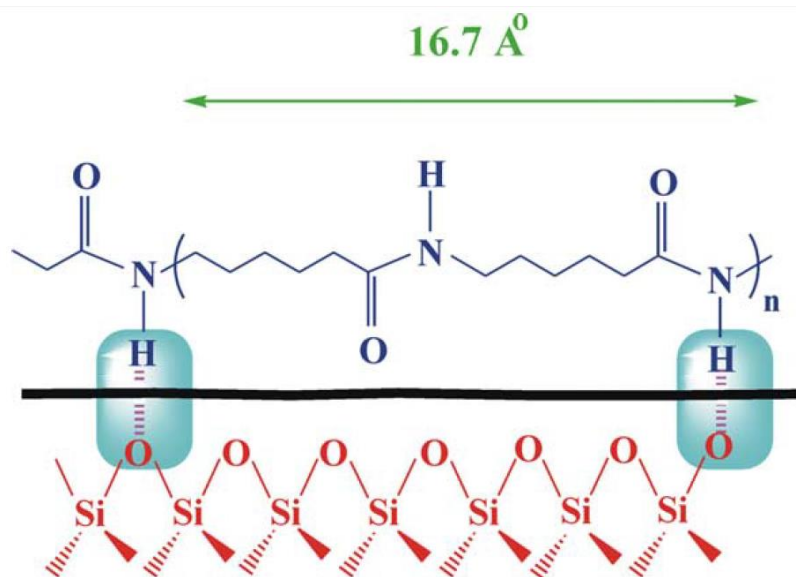


Figure 2.16. Schematic Illustration of Formation of Hydrogen Bonds in Nylon-6/montmorillonite Nanocomposite Gel.

Some of the advantages of nanocomposite gels over conventional gels without nanomaterial include:

- Mechanical: Increased gel strength, increased modulus strength, inadequate toughness.
- Thermal: Increased thermal resistance to withstand extreme reservoir conditions, longer degradation time, longer thermal stability.
- Swelling: Increased swelling ability; nano material provides a large surface area for increased water absorption.
- Elasticity: Increased gel elasticity.
- Viscosity: Increased post-degradation viscosity

As previously stated, nanocomposite preformed gels (Pavlidou and Papaspyrides, 2008; Chung and Lai, 2010; Okay and Oppermann, 2007; Darder et al. (2005; 2006); Phang et al., 2005) have attracted great interests, both in industry and academia due mainly to the improvement in materials properties brought about by the incorporation of nanomaterials in gel design. Shibayama et al. (2004), Haraguchi and Takehisa (2002a), and Haraguchi et al. (2002b) have reported an increase in nanocomposite gel properties such as increased mechanical toughness and deformability and high heat resistance. They showed that nanocomposite gels have distinct and superior properties over non nanocomposite gels, which make them highly applicable in areas such as biomedical tissue-engineering, sensors, drug delivery systems, and mechanical devices such as artificial muscles and micro-actuators (Haraguchi and Takehisa, 2002a). Other improvements in product performance include higher modulus, increased heat resistance, decreased gas permeability and flammability, and increased biodegradability of biodegradable polymers (Ray and Okamoto, 2003).

Li et al. (2004) have reported a polyacrylic acid/Attapulgate nanocomposite gel with excellent water absorbency (1000 g H₂O/g) with potential applications in agricultural and horticultural industry. Monomer and crosslinker used were acrylic acid and N'N'-Methylenebisacrylamide respectively.

A similar study was conducted by Weian et al. (2005) using polyacrylamide/attapulgate nanocomposite. Again, excellent swelling abilities in saline

solution was observed. Monomer and crosslinker used were acrylamide and N'N'-Methylenebisacrylamide. These gels had potential application in agriculture.

Lee and Chen (2004) conducted a study whereby a poly [acrylic acid-co-poly (ethylene glycol)] methyl ether acrylate/ hydrotalcite nano composite gel was tested as a successful bio adhesive for drug-carrier applications. Bio adhesive drug carriers adhere to the mucosal surfaces of the buccal cavity and skin and increase therapeutic efficiency. Monomers used in this study were acrylic acid and polyethylene glycol methyl ether acrylate. Crosslinker used was N'N'-Methylenebisacrylamide.

Weian et al. (2005) published a work in 2005 which involved a nanocomposite hydrogel designed from acrylic acid and sodium-montmorillonite. Such nanocomposite gel exhibited higher thermal stability and higher swelling ratio than conventional hydrogel.

In their study, Xia et al. (2003) observed that a poly N-isopropylacrylamide/sodium-montmorillonite nanocomposite hydrogel showed improved performance. They observed that incorporating sodium-montmorillonite clay into the N-isopropylacrylamide (PNIPAM) polymer network improved gel mechanical property. However, they also observed that increasing the clay concentration led to a decrease in the swelling ability of the gel. They argued that this decreasing swelling phenomenon is because the clay is physically entrapped inside the gel matrix rather than bond chemically to the gel. They also observed that PNIPAM is temperature sensitive and undergoes a volume phase transition. Above 34 °C, the gel shrinks and below this temperature, it swells. Such temperature sensitivity affords PNIPAM nanocomposite gels and their derivatives potential applications in controlled drug delivery, chemical separation, sensors, and actuators.

Additionally, Liu et al. (2006) have observed that improving the mechanical strength of PNIPAM hydrogels can be achieved by incorporating Laponite XLS clay instead of sodium-montmorillonite. Laponite XLS allowed easier dispersibility of higher amounts of clay compared to sodium-montmorillonite. Tensile strengths of 1 MPa and elongation at break of 1400% were obtained. Such values have never been reported by any PNIPAM gels before.

Additional corroborations substantiating the improvement in material properties with nanoclays were presented by the Toyota research group (Okada et al., 1990). They observed that Nylon-6 (N6)/montmorillonite nano composite gel resulted in pronounced improvements in thermal and mechanical properties when very small amounts of clay loadings were used.

Clays are attracting increased interests in polymer science research because of their high cation exchange capacities, surface area, surface reactivity, and adsorptive properties. Hectorite and montmorillonite are the most commonly smectite-type layered silicates employed in the preparation of nanocomposites. However, in their original state, these clays are very hydrophilic and will readily disperse in water but not in a polymer solution. Nevertheless, most monomers are highly hydrophilic and readily dissolve in water. So, the design of most nano composite hydrogels usually begin monomer and then convert the monomer to polymer by in-situ free radical polymerization. By so doing, the clay is able to properly disperse in the aqueous solution before polymerization takes place.

If utilizing monomers is not desired, another solution to this problem is to alter the surface property of the clay to make it hydrophobic, enabling its dispersion in a polymer medium. The most commonly reported means of achieving this is by replacing the interlayer cations in the clay with quaternary ammonium or phosphonium salts (Liu et al., 2006). This enables the clay to dissolve in an organophilic polymer solution.

Another issue worth mentioning in the preparation of clay nanocomposites is dispersibility. Clays naturally exist as tactoids, making dispersion by simple mixing very difficult. Without adequate clay dispersion, sandwiching of polymer chains between clay layers is practically impossible. This leads to the formation of a non-homogenous and incoherent gel. Thus, the success of any nanocomposite gel formation depends on proper clay dispersion. Figure 2.17 and Figure 2.18 (Koo and Pilato, 2003) depicts three scenarios that occur during clay mixing. Either the clays remain unmixed, are slightly separated (intercalated), or are completely separated (exfoliated). As shown in Figure 2.17, during intercalation, polymer chains are inserted in the clay layers in a regular fashion. During clay exfoliation, the individual clay layers are separated far apart.

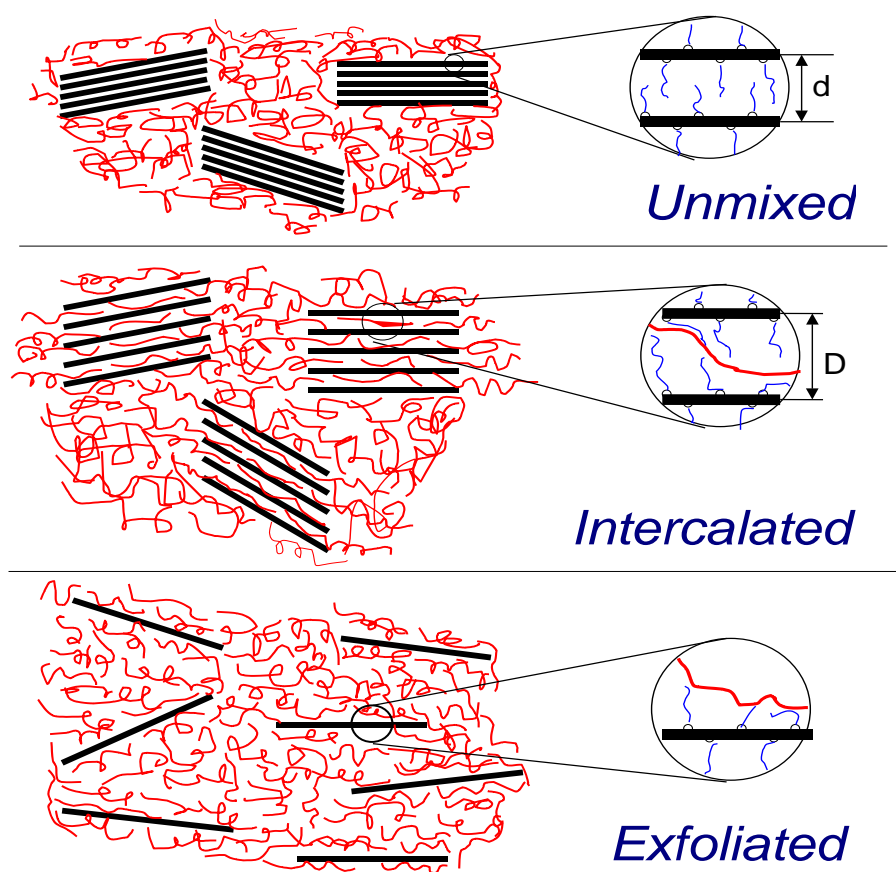


Figure 2.17. Nanocomposite Clay Classification.

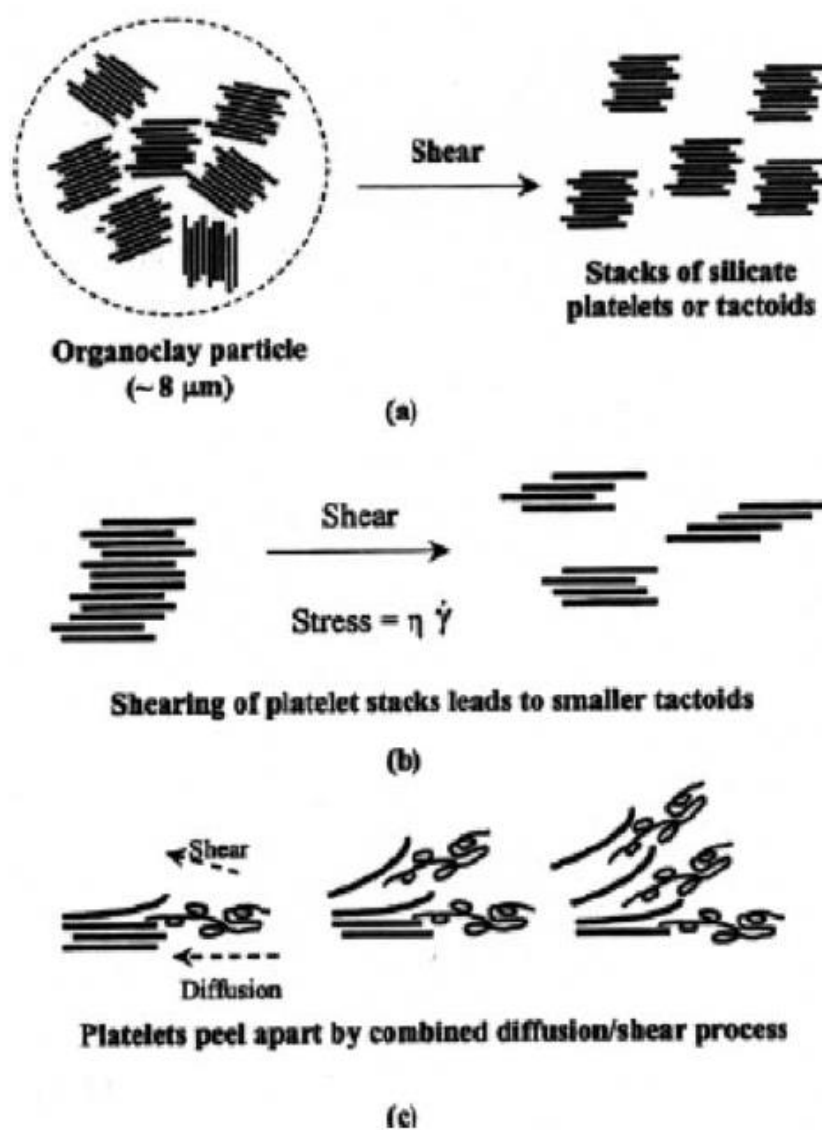


Figure 2.18. Stepwise Mechanism of Clay Platelets Exfoliation during Melt Compounding.

In an earlier work, Tongwa et al. (2013a) published a partially hydrolyzed polyacrylamide (HPAM)/ Laponite XLG clay nano composite gel that illustrates this. Small angle X-ray diffraction (XRD) was employed to determine the degree of clay exfoliation and determine polymer intercalation between clay layers (Figure 2.19).

Intercalated or exfoliated clay morphologies are usually identified by monitoring the position of the basal reflection in the clay nanomaterial. In an exfoliated nanocomposite, an extensive separation of layers occurs such that the basal reflection disappears. However in intercalated nanocomposites, a limited separation of layers occurs which results in a shift in basal reflection to a lower value. A d001 interplanar distance in Laponite XLG clay at $2\theta = 7.4^\circ$ was observed. After incorporation of polymer, intercalated morphologies were observed in nano composite gels XLG3-10, as is evidenced by the shift of 2θ to lower angles, which implies an increase in d spacing of clay (from Bragg's equation; $n\lambda = 2d\sin\theta$). Complete exfoliation was observed for XLG1 as evidenced by the absence of the basal peak. This is due perhaps to the lower clay concentration. Similar results have been published by Zolfaghari et al., 2006.

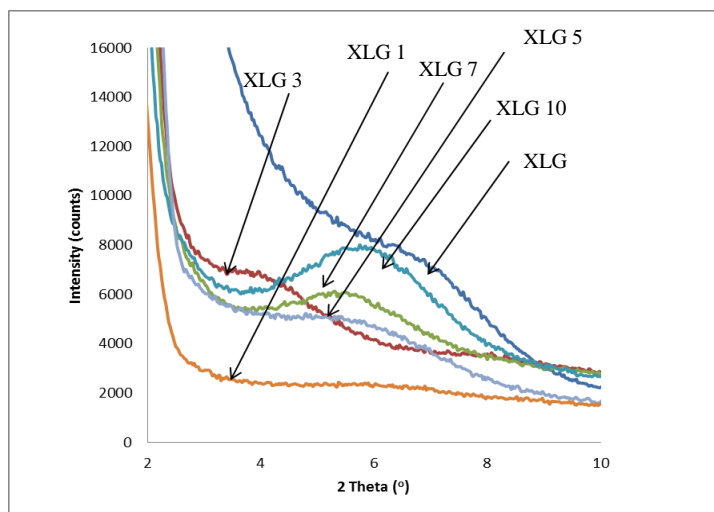


Figure 2.19. XRD Patterns for XLG Clay and Dried Gels (XLG1-10).

In conclusion, nanocomposite hydrogels have superior performances over hydrogels without nanomaterials. As such, they are being studied for various applications, including agriculture, medicine, and cosmetics.

Also, it is observed from the above review that the synthesis of nanocomposite hydrogels employing a monomer/polymer, crosslinker, and nanoclay system is not a novelty.

Therefore, we are quick to mention that the emphasis in the current dissertation is not in the synthesis of a novel nanocomposite gel, but in its application after nanocomposite gel degradation (Figure 2.20).

Prior research with nanocomposite hydrogels focused on their applications/properties prior to gel degradation. This dissertation, however, focuses on the application/properties of nano composite gels after degradation. Thus the novelty in this dissertation is in product application after degradation, and not in product design.

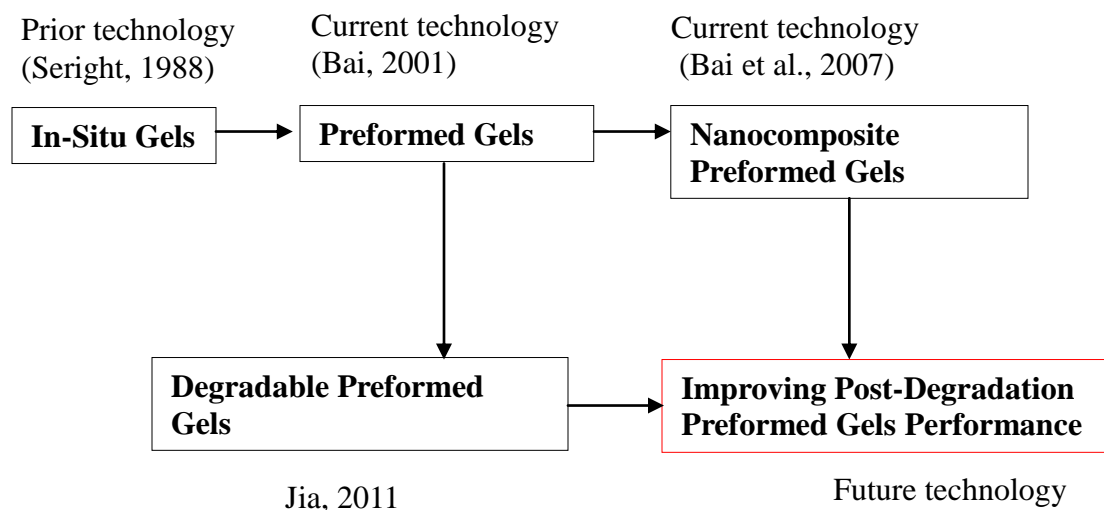


Figure 2.20. Progress in Gel Development for Conformance Control.

2.4. SUMMARY OF LITERATURE REVIEW

In summary, the various gel treatments that have been used for addressing water shut-off and conformance control problems in mature reservoirs have been reviewed. Firstly, the different types of in-situ gel systems were studied at length and reasons why this technology was inadequate were also given. Problems such as dehydration, lack of gelation time control, and possible damage to low permeability zones were advanced as reasons why in-situ gelation was unsatisfactory.

Next preformed gels were also reviewed. Several of these were studied, including; partially preformed gels, colloidal dispersion gels, microgel, Bright Water, and preformed particle gels (PPG). Their synthesis, application conditions, and their limitations were thoroughly reviewed.

Lastly, progress was made by looking at nanocomposite gels, which have superior properties and performance than preformed gels. It was emphasized that these nanocomposite gels have been used in many industry sectors, such as agriculture, medicine, cosmetics, and even enhanced oil recovery (Bai et al., 2004).

However, in all these applications, pre-degradation properties of nanocomposite gel were of concern. Prior research with nanocomposite hydrogels focused on their applications/properties before gel degradation, such as their water retention, swelling ability, and other properties.

The current dissertation, however, focuses on the application/properties of nanocomposite gels after degradation, such as post-degradation gel viscosity. Thus, the novelty in this dissertation is in product application after degradation, and not in product design, which to the best of our knowledge, has not been explored before.

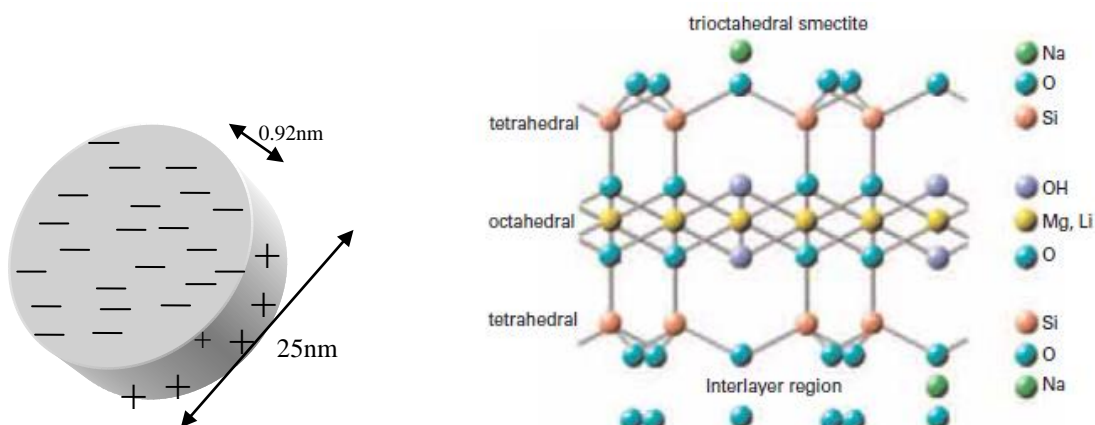
3. EXPERIMENTAL DESCRIPTION AND METHODOLOGY

3.1. MATERIALS

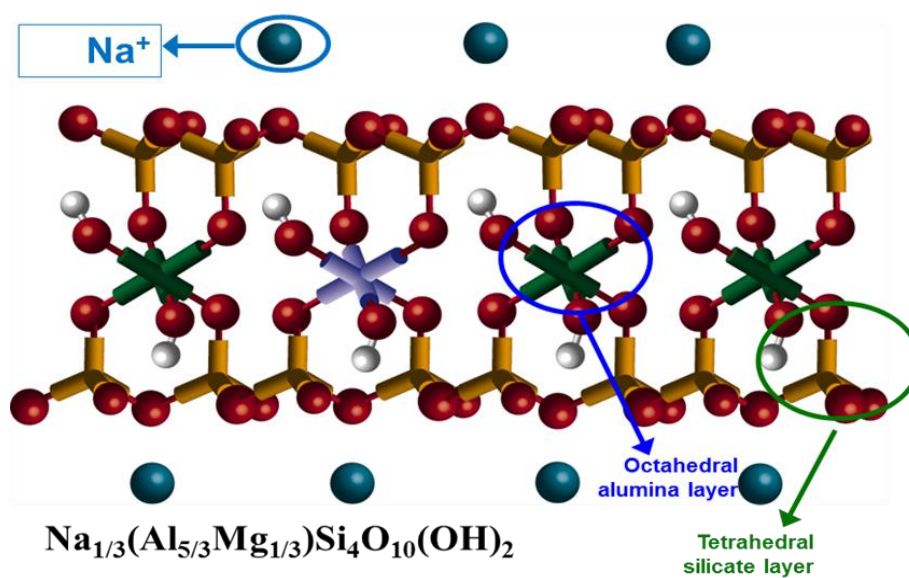
Three types of clay nanomaterials were employed in this study: Laponite XLG (LXLG), Calcium Montmorillonite (Ca^{2+} MMT), and Sodium Montmorillonite (Na^{+} MMT). All three clay types were received with courtesy from Southern Clay Products (SCP) Inc. Laponite XLG was received as white granular powder. Na^{+} MMT and Ca^{2+} MMT were received as light brown and dark brown granular powder respectively. Figure 3.1 shows the unit cell structures of these three clay nanomaterials and Table 3.1 shows their cost.

Monomers utilized in this study are acrylamide (AM), acrylic acid (AA), and 2-acrylamido-2-methylpropane sulfonic acid sodium salt (AMPS). Acrylamide (98.5+%) was purchased from Alfa Aesar Company (Ward Hill, MA) as a white granular solid and is completely water soluble. It was used as received. Acrylic acid (anhydrous) was purchased from Sigma Aldrich Company, 99% and contained 180-200 ppm MEHQ as inhibitor. AMPS was received with courtesy from Lubrizol Company as a white crystalline solid with 90 – 100 % by weight. Figure 3.2 shows the chemical structure of the monomers.

Initiator used in this study is Ammonium persulfate (APS) obtained from Sigma-Aldrich. Crosslinkers utilized in study include; polyethylene glycol diacrylate (molecular weights 200 – 3400), polyethylene glycol dimethacrylate (molecular weights 200 -600) and was purchased from commercial companies and used as received. NaCl (99.8%) was purchased from Fisher Scientific Inc. and used as received. Distilled water was used for the synthesis and swelling experiments. Formation water was prepared for the swelling experiments as explained in the formula listed in Table 3.2.



(a)



(b)

Figure 3.1. Unit Cell Structures of The Different Nanomaterials Studied (a). Single Laponite Crystal and Unit Cell Structure of Laponite Layered Silicate (available online at www.scprod.com). (b) Unit Cell Structure of Sodium and Calcium Montmorillonite.

Table 3.1. Cost of Nanomaterials Studied.

| Type of Nanomaterial | Cost |
|-------------------------|-----------------------------|
| Laponite XLG | \$19.0/Kilogram (\$8.64/lb) |
| Calcium Montmorillonite | \$0.32/lb |
| Sodium Montmorillonite | \$4.0/lb |

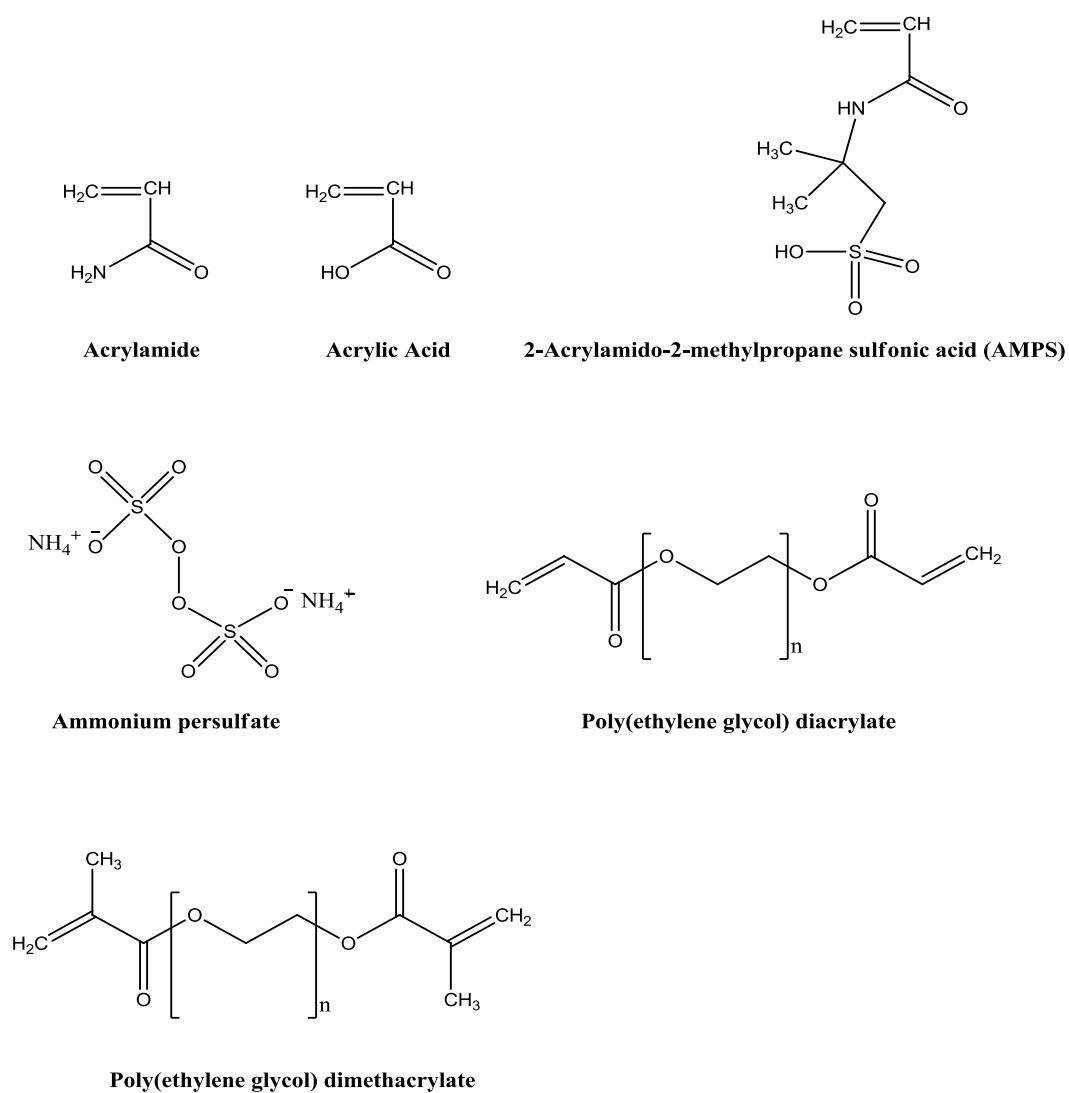


Figure 3.2. Molecular Structures of Compounds Used in Study.

Table 3.2. Formation Water Formula for Simulating Daqing Oilfield Water.

| Salt Name | Formula | Grams |
|--------------------------------|--------------------------------------|--------|
| Sodium Chloride | NaCl | 13.200 |
| Sodium Bicarbonate | NaHCO ₃ | 2.670 |
| Sodium Sulfate | Na ₂ SO ₄ | 0.690 |
| Potassium Chloride | KCl | 0.282 |
| Calcium Chloride Dihydrate | CaCl ₂ •2H ₂ O | 1.053 |
| Magnesium Chloride Hexahydrate | MgCl ₂ •6H ₂ O | 1.005 |
| Distilled Water | H ₂ O | 2981.1 |
| Total Solids Dissolved | TDS | 18.900 |
| Adjust the brine pH to 7.30 | | |

3.2. GEL SYNTHESIS AND FABRICATION

Nanocomposite gels were synthesized via free-radical crosslinking polymerization. The nanomaterial concentration is in the range of 0.2% to 5%. Nanomaterials used were nanoclays; Laponite XLG, Calcium montmorillonite, and Sodium montmorillonite. In general, the monomer concentration is in the range of 23-30% with the crosslinker concentration from redox initiation system, ammonium persulfate ((NH₄)₂S₂O₈, APS) was employed to polymerize the monomer solutions of AM and AMPS. The pH of the solution was kept at neutral pH 7.

The following is one example to illustrate the synthesis process for nanocomposite gels. First, 30 g of acrylamide was dissolved in 100 g of distilled water in a double-necked flat-bottomed reactor equipped with inlet and outlet tubes for nitrogen gas. The mixture was stirred at room temperature for 10 minutes. Then 3% (3.9g) of Laponite XLG was added to the solution and stirred vigorously overnight to ensure complete exfoliation of clay nanomaterial. Then, 10,000 ppm of the labile crosslinker

PEG-200 was added to the mixture and stirred for 10 minutes. The mixed solution was then purged with nitrogen gas for 30 minutes before 100 ppm of APS ($(\text{NH}_4)_2\text{S}_2\text{O}_8$) was added to the solution. This resulting solution was kept for 10 hours at 55°C in a water bath to ensure complete polymerization.

A strong and elastic bulk gel was formed and cut into small pieces (Figure 3.3). It was then purified by soaking in a large amount of distilled water for three days to remove any unreacted monomers and additives, followed by being put in an oven at 60°C until the weight could not change any more. The dried gel solids were crushed into very small particle sizes, called preformed particle gels (nano PPGs), by blending in a blender machine (Black & Decker). Nano PPGs with the particle size between 80-100 mesh ($180\mu\text{m}$ - $250\mu\text{m}$) were selected through the standard testing sieves (Fisher Scientific Company) for further characterization and evaluation.

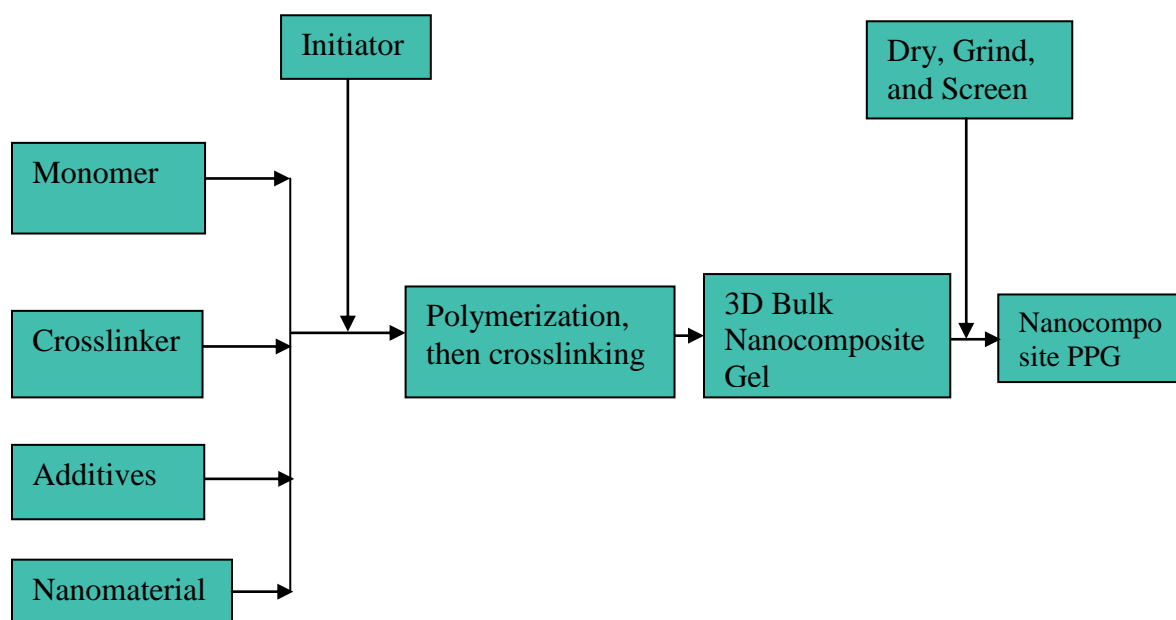


Figure 3.3. Nanocomposite Preformed Particle Gel Synthesis and Fabrication.

3.3. METHODS OF NANOCOMPOSITE PREFORMED PARTICLE GEL EVALUATION

3.3.1. Evaluation of Nanocomposite Preformed Particle Gel Before Degradation. After nanocomposite PPG was synthesized, several properties of the gel were evaluated before it underwent degradation at elevated temperatures.

3.3.1.1 Swelling kinetics. The essence of swelling measurements is to ascertain the maximum swelling capacity of nanocomposite PPG in order to determine its ability to swell and plug reservoir fractures and high permeability matrices. Also, measuring swelling kinetics at room temperature enables us to establish the mixing time before pumping the gel solution into the formation at room temperature. Such information is also needed to aid in the selection of the PPG product best suited for a specific field application in regard to its formation temperature. Swelling studies were carried out with dried and ground PPGs by immersing 0.5 grams of the dry particles in 1% NaCl brine and formation water respectively. This was to study the effects of different salinity concentrations on gel swelling behavior. Furthermore, swelling was also carried out at 45°C, 60°C, and 80°C to study the effects of temperature on swelling behavior. The swelling ratio of the gels was calculated from the following equation:

$$\text{Swelling Ratio} = V_s/V_i$$

Where, V_i is the volume of dry gel and V_s is the volume of swollen gel.

3.3.1.2 Gel rheology test. The rheological properties of hydrogels were measured using a Haake RheoScope RO1 version 3.61.0000 from Thermo Scientific (Figure 3.4). The sensor used for all measurements was PP20 with a gap of 2 mm. The samples were cut into dimensions of 20 mm (L) x 20 mm (W) x 2.5 mm (D). The measurements were set as an oscillation model and frequency experiments were first performed in the range of 1-15 Hz in order to establish the extent of the linear viscoelastic region. Based on the data, all subsequent oscillation time-dependent experiments were performed at a fixed frequency of 1 Hz and controlled stress (CS) of 1.0 Pa to obtain the values of G' and G'' as a function of time. All runs were repeated at least three times.

It is very important to know how far the gel can be stretched or deformed before it breaks; if the gel's elastic character dominates over its viscous nature; and how the gel's

properties vary with composition, temperature, and strain. Therefore, several tests were carried out to determine these rheological properties, including the gel's elastic (G') and viscous (G'') moduli over time and strain. The measurements of the elastic (G') and viscous (G'') moduli over strain were tested with a fixed frequency at 1 Hz and the strain varied from 0.1% to 2000%.

A gel-strength code was also used to access the gel both as it was synthesized and after swelling (Sydansk and Argabright 1987; Sydansk 1988):

- A. No detectable gel formed: The gel appears as a polymer solution and no gel is visually detectable.
- B. Highly flowing gel: The gel appears to be only viscous.
- C. Flowing gel: Most of the obviously detectable gel flows to the top of the vial upon inversion.
- D. Moderately flowing gel: Only a small portion (about 5 to 15%) of the gel does not readily flow to the top of the vial upon inversion—usually characterized as a tonguing gel (i.e., after hanging out of the jar, the gel can be made to flow back into the bottle by slowly turning the bottle upright).
- E. Barely flowing gel: The gel can barely flow to the top of the vial and/or a significant portion ($> 15\%$) of the gel does not flow upon inversion.
- F. Highly deformable nonflowing gel: The gel flows about halfway down the vial upon inversion.
- G. Moderately deformable nonflowing gel: The gel does not flow to the top of the vial upon inversion.
- H. Slightly deformable nonflowing gel: The gel surface only slightly deforms upon inversion.
- I. Rigid gel: There is no gel-surface deformation upon inversion.
- J. Ringing rigid gel: A tuning-fork-like mechanical vibration can be felt after tapping the bottle.

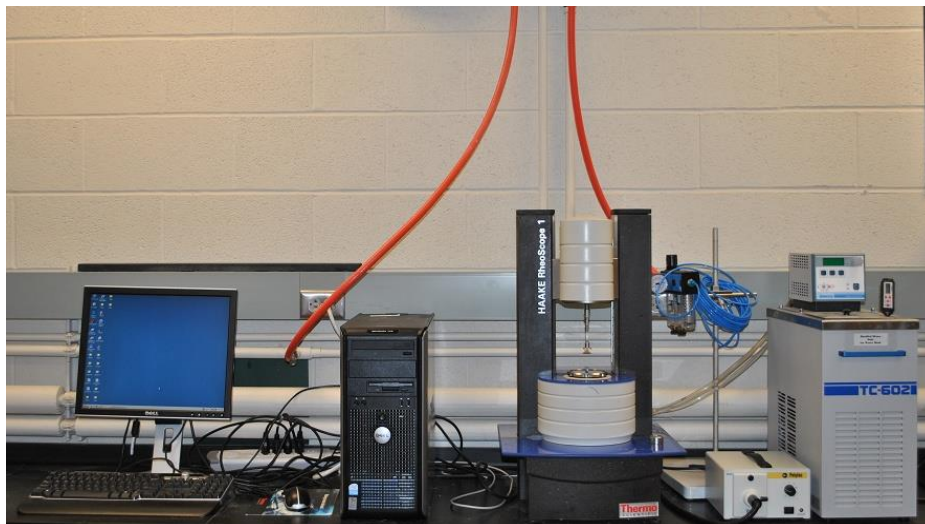


Figure 3.4. Haake Rheoscope Setup Used to Measure Rheology of Gel.

3.3.1.3 Thermostability test. The reason for the thermostability test is to determine how long nanocomposite PPG takes to degrade under simulated reservoir conditions. Knowing the duration of thermal degradation indicates how long nanocomposite PPG will function as a plugging material, after which it will degrade into viscous polymer solution which will then move deeper into reservoir and augment polymer flooding.

Thermostability tests were carried out in the key apparatus shown in Figure 3.5. 10,000 ppm; 5,000 ppm, and 1,000 ppm gel concentrations were prepared. For 10,000ppm gel concentration, 11.88 grams brine (1.0 weight percent NaCl) solution was added into an ampoule containing 0.12 grams of dry particle gels. Likewise, for 5000 ppm gel concentration, 11.94 grams of 1% brine were added into an ampoule containing 0.06 grams of gel. For 1,000 ppm gel concentration, 0.012 grams of gel and 11.988 grams of 1% brine were used. Therefore, the total solution volume was set at 12 grams total for each ampoule.

The ampoules were placed one at a time into the manifold. The valves were closed and a vacuum pump was started. After the ampoules have been attached to the manifold, each valve was slowly opened one at a time. This was to minimize any rush of

liquid or gas out of the ampoule into the manifold. The vacuum pump continued to run at -25 psi for about half an hour to remove the dissolved gases in the liquid sample, including any trace of dissolved oxygen that might have remained in the sample. Next, the ampoules were flame sealed in place. The sealed ampoules were weighed using an analytical balance with an accuracy of 0.0001 grams, and then were placed in an oven and aged at 45°C, 60°C and 80°C (Figure 3.6).

After the specified aging times, one ampoule was taken out of the oven and cooled to room temperature. This ampoule was reweighed to confirm that there had been no leakage of any solution. If the weight loss was about 0.001 grams or more, there was possible leakage with this ampoule. In that case another ampoule would be used for a post-aging measurement.



Figure 3.5. Manifold Used to Seal Ampoule during Thermostability Measurement.



Figure 3.6. Different Ovens Used to Evaluate Longterm Thermal Stability of Gel at 45°C, 60 °C, and 80 °C.

3.3.1.4 Environmental scanning electron microscopy evaluation.

Environmental Scanning Electron Microscopy (ESEM) studies were employed to study the porous network structure of the gel. This gives information about pore-interconnectivity and swelling propensity. After the particle gels were completely swollen in brine, ESEM was used to examine the surface morphology of the swollen particle gel. Swollen nanocomposite PPG samples were mounted on metal stubs at a low vacuum degree (4.6 Torr), and a relatively low temperature (near 0°C). The samples first underwent a freeze process in the chamber of an FEI Quanta 600 FEG extended vacuum scanning electron microscope. To emphasize the gel microstructure, the following ESEM imaging protocol was followed: the temperature and pressure were decreased simultaneously from 0°C and 4.6 Torr to -5°C and 2-3 Torr, thereby freezing the sample; the temperature was then allowed to rise to 20°C with a rate of 2°C/minute at 2-3 Torr pressure to sublimate water from the sample at a relative humidity of 12.5%.

3.3.2. Evaluation of Nanocomposite Preformed Particle Gel After Degradation. After the nanocomposite PPGs degraded under simulated reservoir conditions, several properties of the degraded gels were evaluated.

3.3.2.1 Viscosity measurements. The viscosity of nanocomposite PPG after thermal degradation was measured. After an extended time period, gel degrades into a viscous polymer solution. This viscous polymer solution will then move into deeper regions of the reservoir to increase the viscosity of the flood water and boost polymer flooding process. Thus the higher the post-degradation gel viscosity, the better its ability to improve polymer flooding process. The viscosity of the solution was measured at 45°C, 60°C, and 80°C with the Brookfield viscometer with a shear rate of 6 RPM using an #18 or #34 spindle as shown in Figure 3.7. The viscosity measured at 6 RPM was recorded as the reported value.



Figure 3.7. Brookfield Viscometer Model DV II+ for Measuring Post-degradation Gel Viscosity.

3.3.2.2 Gel rheology test. Gel strength measurements after degradation were done to determine the post-degraded gel strength. The same procedure described in prior section (for pre-degraded gel) was employed.

3.3.2.3 Environmental scanning electron microscopy and optical microscopy measurements. Optical microscopy and ESEM studies were used to determine the sizes of the post-degraded gel solution. The essence of this study is to evaluate the porous network structure of the gel after degradation. This gives information about pore-interconnectivity and swelling tendencies. Author postulates that the gels degrade from their original large millimeter sizes to a viscous polymer solution.

4. FACTORS AFFECTING NANOCOMPOSITE PREFORMED PARTICLE GEL PROPERTIES

Nanocomposite preformed particle gels were synthesized by a multi-component reaction that involves monomer, initiator, crosslinker, and nano material all in a single reaction flask. The reaction starts with a stepwise process that involves conversion of monomer to polymer, and thereafter crosslinking of polymer to obtain bulk nano gels (Figure 4.1). The nano particle serves as a filler material, to re-enforce the properties (strength) of the gel, thus, the name nanocomposite gel or re-enforced particle gel.

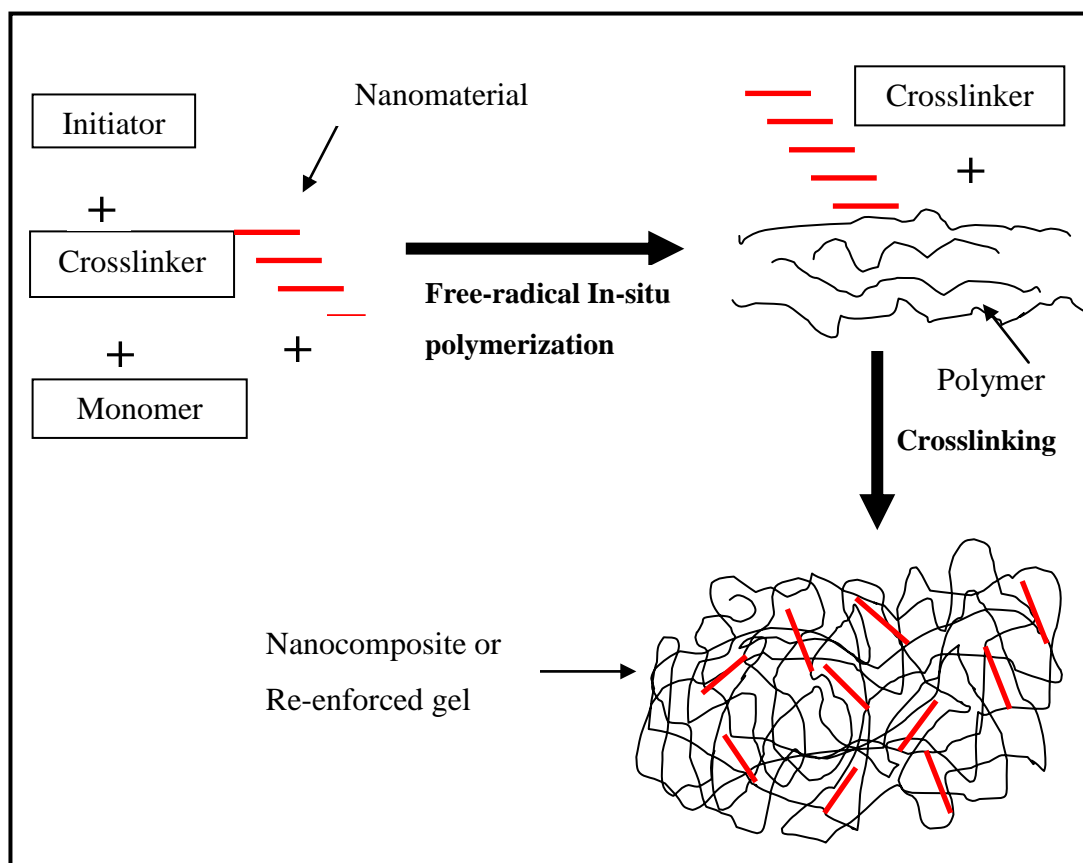


Figure 4.1. Synthesis of Nanocomposite Preformed Particle Gel.

Conversion of monomer to polymer is by a free-radical, redox-initiated and redox-propagated reaction. Free radicals are induced by the action of heat. At elevated temperatures, initiator π - π single bond dissociates and release free-radicals which attack neutral monomer molecules, leading to a polymerization (extension) of the polymer chain. Chain termination is by reaction of two free radicals (Figure 4.2). Crosslinking of formed polymer chains is by the formation of junction points between two or more polymer chains at different points along polymer chain length, leading to a 3-dimensional gel structure.

i. Initiation Stage

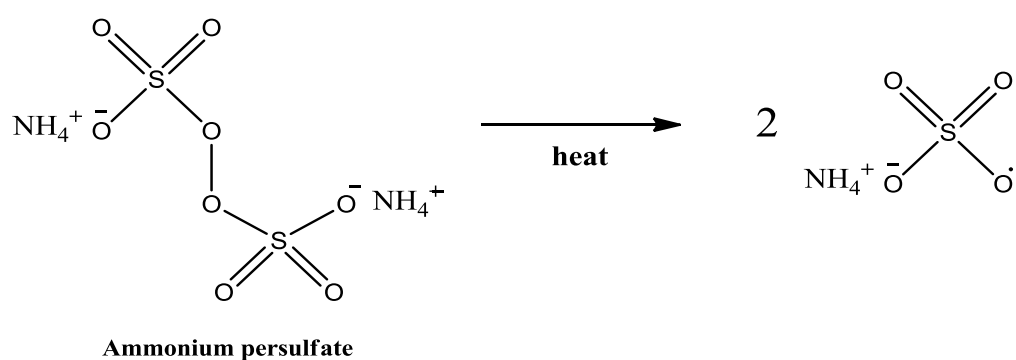


Figure 4.2. Mechanism of Acrylamide Polymerization Using Ammonium Persulfate.

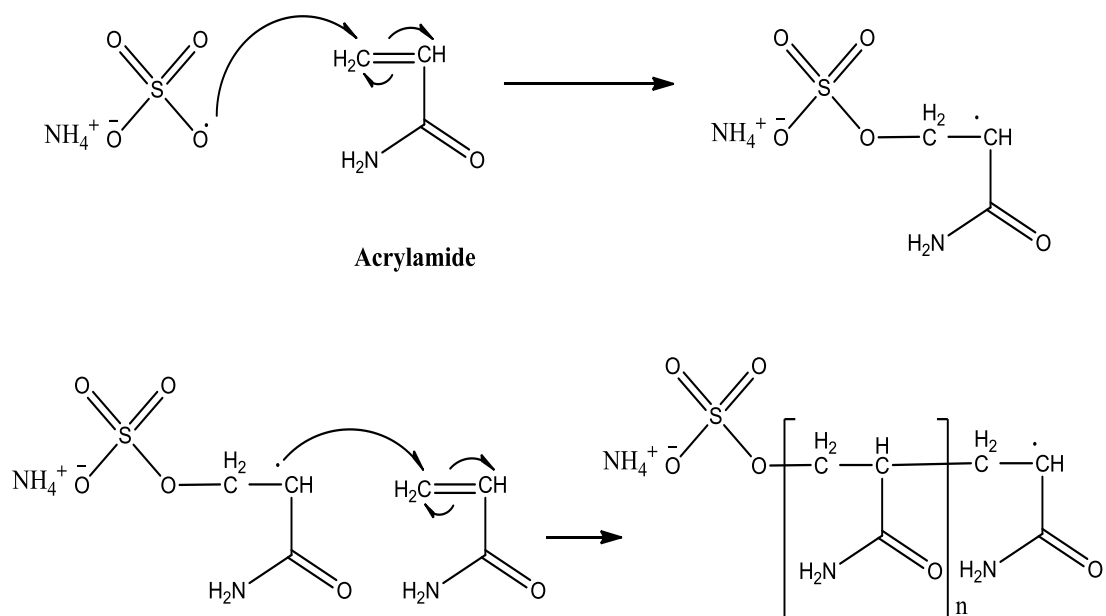
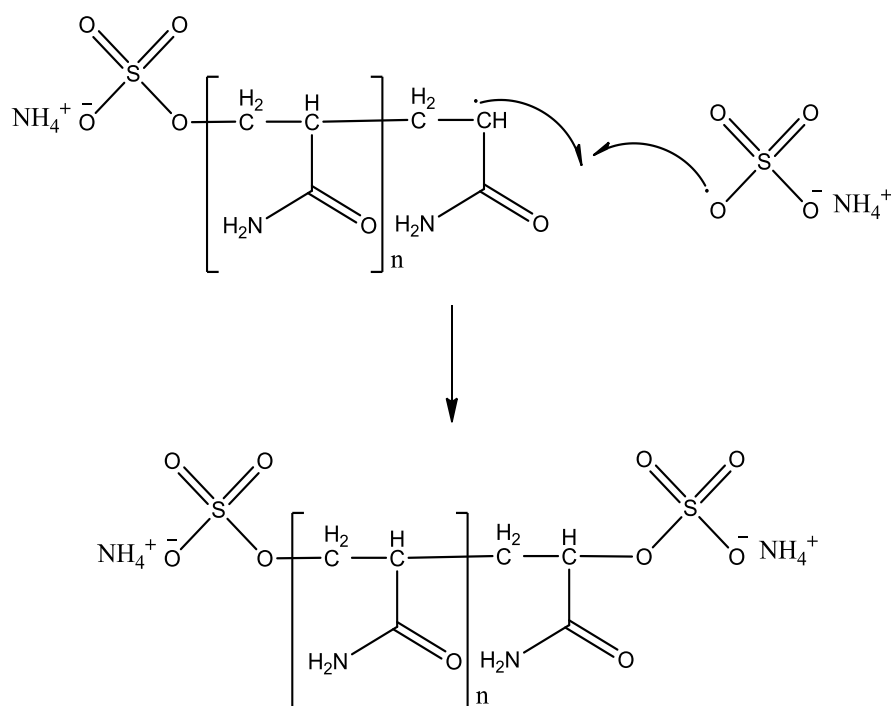
ii. Propagation Stage**iii. Termination Stage**

Figure 4.2. Mechanism of Acrylamide Polymerization Using Ammonium Persulfate.
(Cont.)

Several factors affect the processes of polymerization and crosslinking, and therefore the properties of the synthesized nano-composite gel. Temperature, monomer, crosslinker, and initiator concentrations all play significant roles in gel formation and hence gel properties. Therefore, it is necessary to study these.

4.1. EFFECT OF TEMPERATURE ON GEL PROPERTIES

Temperature has a significant effect on the rate of polymerization, and hence the rate of gel formation. In studying the effect of temperature on gelation, all other reactants were kept constant. Synthesis temperature was the only variable. Synthesis temperature was varied between 25°C and 65°C in 10 degrees increment. Monomer (acrylamide) concentration was kept constant at 23%. Nanoclay (Laponite XLG) concentration was kept constant at 2%. The initiator (ammonium persulfate) and crosslinker (PEG-200-DA) concentrations were fixed at 100 ppm and 250 ppm respectively.

Gel formation time and gel strengths are presented in Table 4.1 and Figure 4.3. It is clearly observed from these that the higher the temperature, the faster the gel formation, and the stronger the gels. The rate of initiator dissociation is dependent chiefly on solution temperature. As temperature increases, more initiators dissociate into free radicals and react with monomers, leading to an increase in polymer chain propagation and crosslinking. Thus stronger gels are formed.

However, at lower temperatures (almost ambient conditions of 25°C and 35°C), initiator dissociation rate is very slow and polymerization and crosslinking takes several months. Gels formed are very weak and easily deformable (Figure 4.4 and Figure 4.5). This result is further corroborated by Figure 4.6 in which the difference between G' and G'' increases progressively, signifying an increase in gel strength with increasing temperature.

Table 4.1. Effect of Temperature on Gelation Time and Gel Strength of Synthesized Gel.

| Sample # | Crossli nker (ppm) | Mon omer (%) | Initiator (ppm) | Temp. (°C) | Gelation time (hrs) | G', Pa | G'', Pa | Sydansk's gel strength code |
|----------|--------------------------|--------------------|--------------------|---------------|------------------------|-----------|------------|--------------------------------------|
| PPG-25 | 250 | 23 | 100 | 25 | 2232 | 200 | 20 | D |
| PPG-35 | 250 | 23 | 100 | 35 | 80 | 240 | 26 | F |
| PPG-45 | 250 | 23 | 100 | 45 | 15 | 3250 | 400 | I |
| PPG-55 | 250 | 23 | 100 | 55 | 5 | 4500 | 710 | I |
| PPG-65 | 250 | 23 | 100 | 65 | 4 | 7065 | 1150 | I |

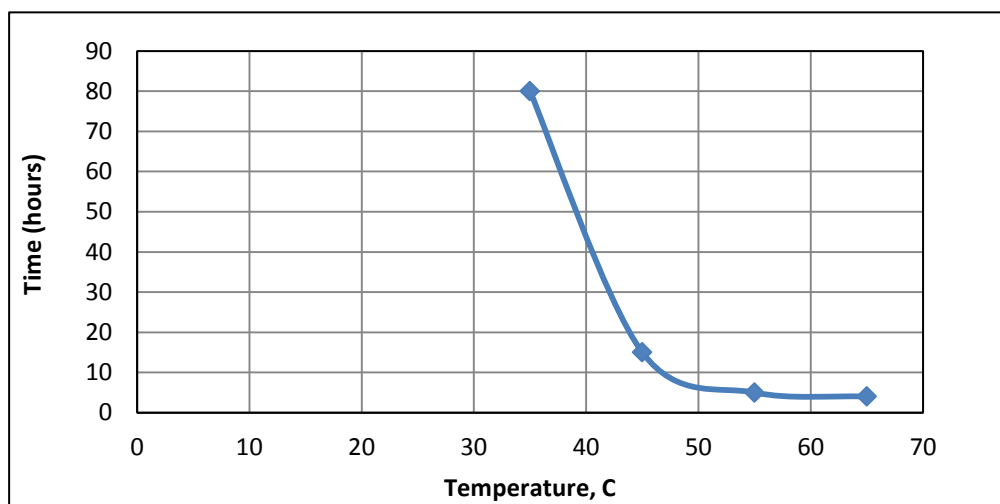


Figure 4.3. Effect of Temperature on Gel Formation Time.

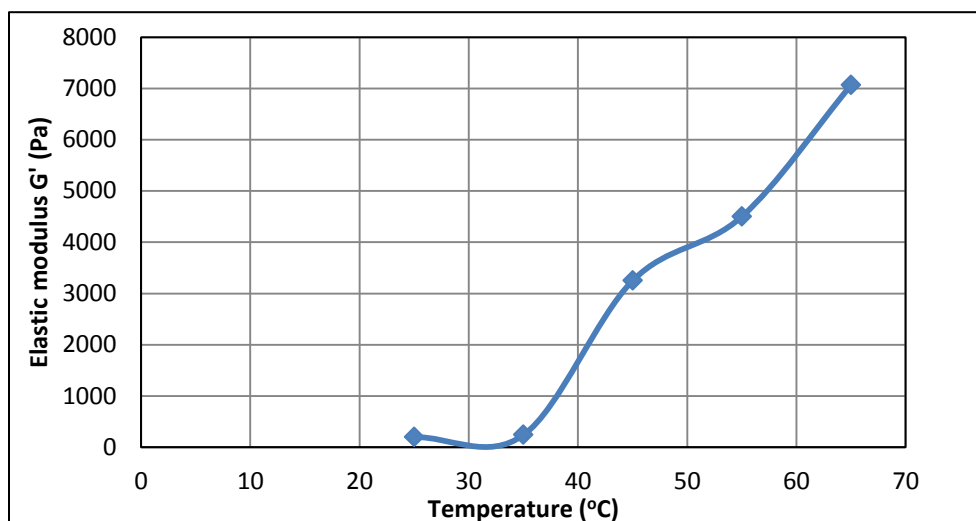


Figure 4.4. Elastic Modulus Increases with Increasing Temperature.

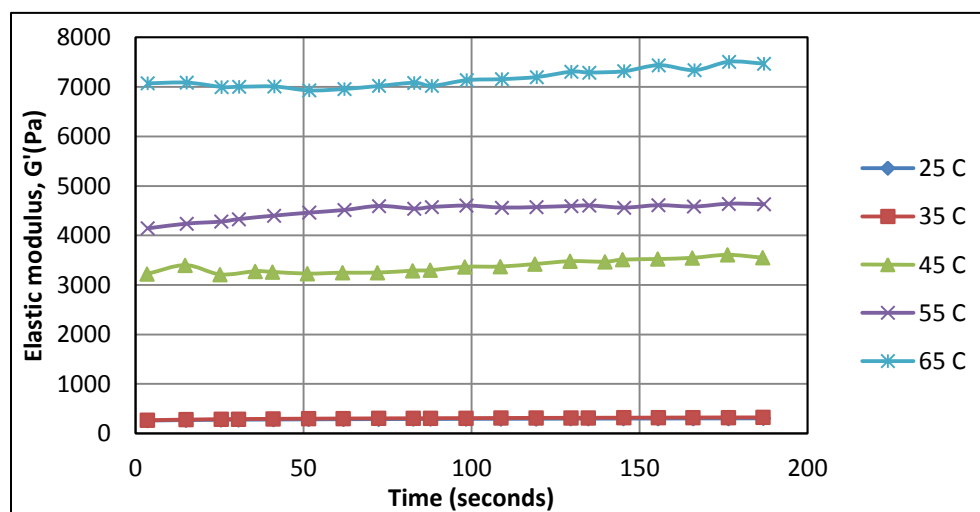


Figure 4.5. Variation of Gel's Elastic Strength with Time.

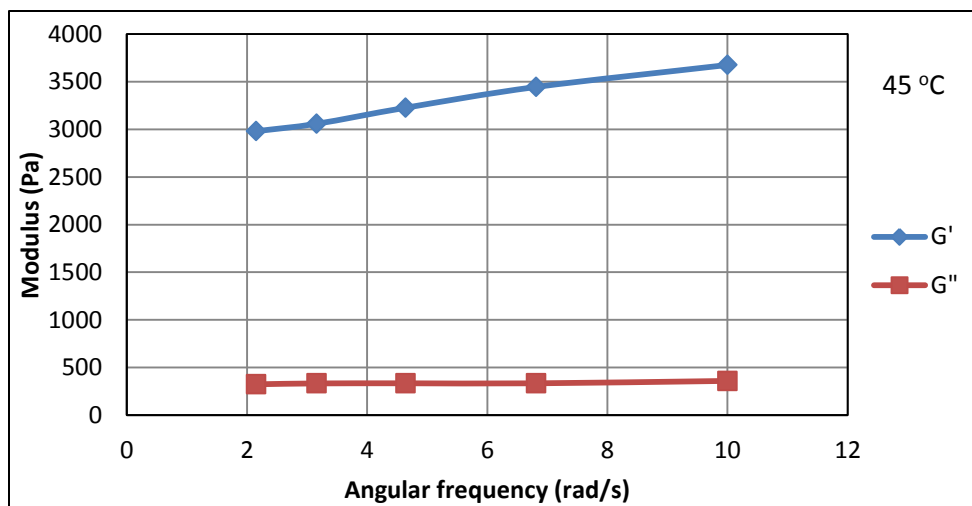


Figure 4.6. Variation of Elastic and Viscous Modulus with Angular Frequency for Sample Synthesized at 45 °C.

4.2. EFFECT OF CROSSLINKER ON GEL PROPERTIES

In studying the effect of crosslinker on gel properties, all other reactants were held constant and only crosslinker (PEG-200-DA) concentrations were varied. Monomer (acrylamide) concentration was constant throughout at 23%. Synthesis temperature was fixed at 45°C while initiator (ammonium persulfate) concentration was kept constant at 100 ppm (Table 4.2).

Up till 1000 ppm crosslinker concentration, gel formation time is observed to decrease with increase in crosslinker concentration. However, above a crosslinker concentration of 1000 ppm, gelation time starts to increase (Figure 4.7). Similarly, up till 1000 ppm of crosslinker concentration, gel strength increases with crosslinker concentration. However, above a crosslinker concentration of 1000 ppm, gel strength starts to decrease (Figure 4.8).

The increase in gel strength with increasing crosslinker concentration is due to an increase in active crosslink points along the polymer chain. As crosslinker concentration increases, more and more junction points are formed leading to an increase in gel network density and hence higher gel strength. However, above the threshold crosslinker

concentration of 1000 ppm, excessive crosslinker presence in solution causes spontaneous and sporadic crosslinking of shorter or incompletely formed polymer chains, leading to a less dense network structure and hence a decrease in gel strength. Therefore, under current synthetic conditions, the range of crosslinker concentration is recommended to be below 1000 ppm.

Table 4.2. Effect of Crosslinker on Gelation Time and Gel Strength of Synthesized Gels.

| Sample # | Crosslinker (ppm) | Monomer (%) | Initiator (ppm) | Temp. (°C) | Gelation time (mins) | G' (Pa) | G'' (Pa) | Sydansk's Gel strength code |
|----------|-------------------|-------------|-----------------|------------|----------------------|---------|----------|-----------------------------|
| PPG-250 | 250 | 23 | 100 | 45 | 170 | 1400 | 350 | I |
| PPG-500 | 500 | 23 | 100 | 45 | 125 | 1430 | 210 | I |
| PPG-1000 | 1000 | 23 | 100 | 45 | 125 | 3400 | 700 | I |
| PPG-1500 | 1500 | 23 | 100 | 45 | 125 | 2550 | 380 | I |
| PPG-3000 | 3000 | 23 | 100 | 45 | 145 | 1500 | 200 | I |

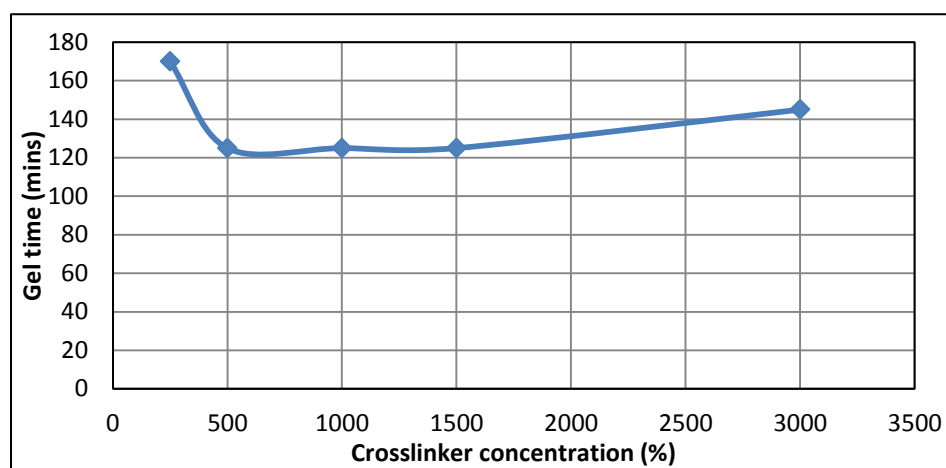
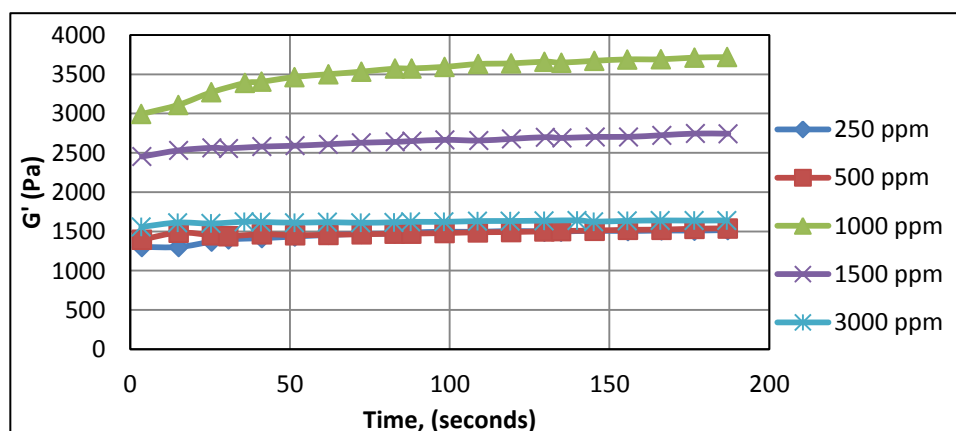
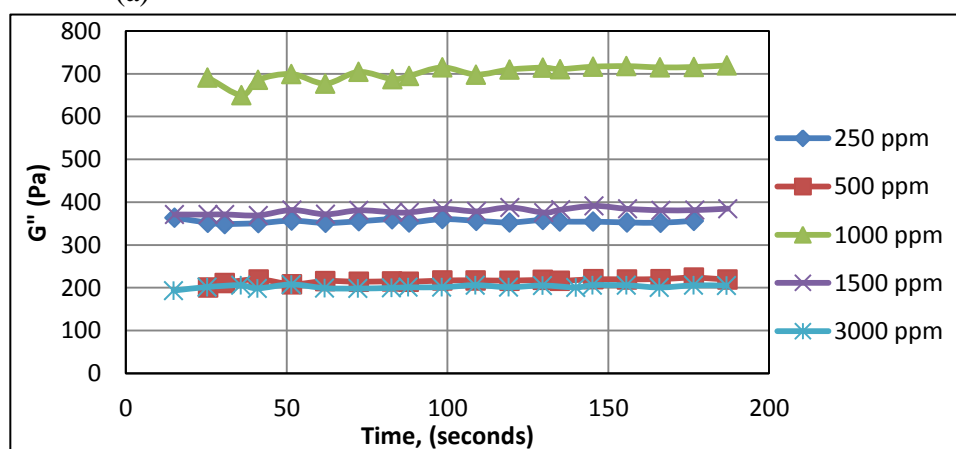


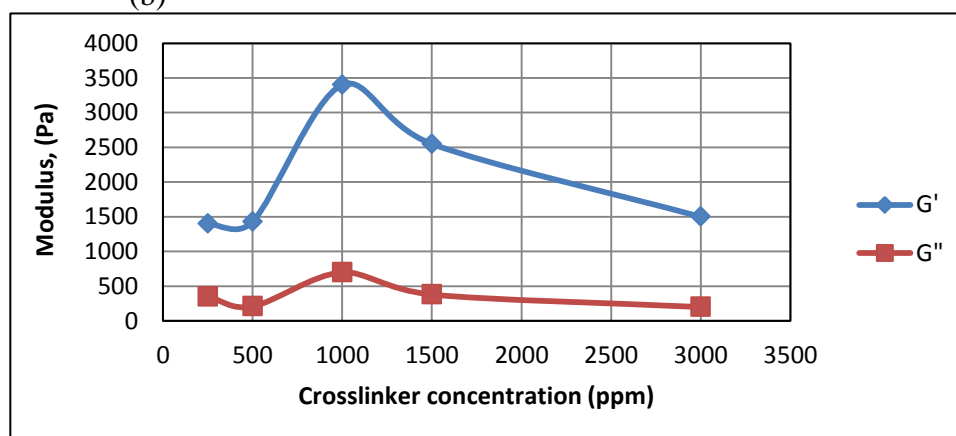
Figure 4.7. Effect of Crosslinker Concentration on Gel Formation Time.



(a)



(b)



(c)

Figure 4.8. Variation of Crosslinker Concentration with Gel's Elastic (G') and Viscous Modulus (G''), and When Combined Respectively.

Equations 1 and 2 below, postulated by Wang, 2008 was used to calculate the theoretical estimate of the molecular weight of the polymer chain and the number of acrylamide units between crosslink junction points. Table 4.3 presents the calculated molecular weight of an average polymer chain (M) linking two crosslink junction points, and also the number of acrylamide units (# AM) that exist between each crosslink junction in the gel. It is observed from Table 4.3 that increase in crosslinker concentration up to an amount of 1000 ppm leads to a decrease in average molecular weight of polymer chain between crosslink points and a corresponding increase in gel strength, G' . However, above 1000 ppm crosslinker concentration, the molecular weight of the polymer chain between two crosslink points increases and gel strength starts to decrease.

$$G' = nRT \quad \dots\dots\dots 1$$

$$M = [AM]/n \quad \dots\dots\dots 2$$

Where;

n = the number of active polymer chain per unit volume (mol/m^3)

R = the gas constant ($8.31 \text{ J}/(\text{mol K})$)

G' = the plateau value of the elastic modulus G'

n = number of active junctions

$[AM]$ = acrylamide concentration

Table 4.3. Calculation of the Molecular Weight of the Polymer Chain from Polyacrylamide Gel Crosslinked with PEG-200-DA.

| Sample # | Crosslinker (ppm) | G' (Pa) | T (°C) | T (K) | AM conc. (g/ml) | n (mol/ml) | M (g/mol) |
|----------|-------------------|---------|--------|-------|-----------------|------------|-----------|
| PPG-250 | 250 | 1400 | 45 | 318 | 0.3 | 0.5297 | 0.566 |
| PPG-500 | 500 | 1430 | 45 | 318 | 0.3 | 0.5411 | 0.554 |
| PPG-1000 | 1000 | 3400 | 45 | 318 | 0.3 | 1.2866 | 0.233 |
| PPG-1500 | 1500 | 2550 | 45 | 318 | 0.3 | 0.9649 | 0.311 |
| PPG-3000 | 3000 | 1500 | 45 | 318 | 0.3 | 0.5676 | 0.529 |

A plausible explanation for this is that as crosslinker concentration increases, more crosslink points are formed along the polymer chain, accounting for the decrease in inter-crosslink junction distance and a higher strength of the gel. However, above the threshold crosslinker concentration of 1000 ppm, the inter-crosslink junction distance increases, and gel strength starts to decrease. A possible explanation for the decrease in gel strength above 1000 ppm is the occurrence of chain transfer reactions, leading to impromptu termination of polymerization reaction.

4.3. EFFECT OF INITIATOR ON GEL PROPERTIES

In order to evaluate the effect of initiator concentration on gelation kinetics, several experiments were run in which the temperature, monomer, and crosslinker concentrations were constant. Only initiator concentrations were varied. Temperature was constant at 60 °C, while monomer and crosslinker concentrations were fixed at 23% and 250 ppm respectively. Initiator concentration was varied between 50 ppm and 1000 ppm.

An obvious relationship between initiator concentration and gelation time is observed in Table 4.4 and Figure 4.9. As clearly seen, gel formation time decreases

exponentially with increasing initiator concentration. This is easily explained. More initiators mean more free radicals. As concentration of initiators increase, more initiators are cleaved into free radicals, leading to a higher presence of free radicals in solution, thereby facilitating polymerization of monomers and subsequent crosslinking to form gel.

Table 4.4. Effect of Initiator on Gelation Time and Gel Strength of Synthesized Gels.

| Sample # | Crosslinker (ppm) | Monomer (%) | Initiator (ppm) | Temp (°C) | Gelation time (hours) | G', Pa | G'', Pa | Sydansk's gel strength code |
|----------|-------------------|-------------|-----------------|-----------|-----------------------|--------|---------|-----------------------------|
| PPG-50 | 250 | 23 | 50 | 60 | 24.5 | 2000 | 250 | J |
| PPG-100 | 250 | 23 | 100 | 60 | 10.5 | 18000 | 2700 | I |
| PPG-200 | 250 | 23 | 200 | 60 | 5.17 | 12000 | 2000 | I |
| PPG-400 | 250 | 23 | 400 | 60 | 2.5 | 6000 | 1000 | I |
| PPG-1000 | 250 | 23 | 1000 | 60 | 1.5 | 4000 | 650 | I |

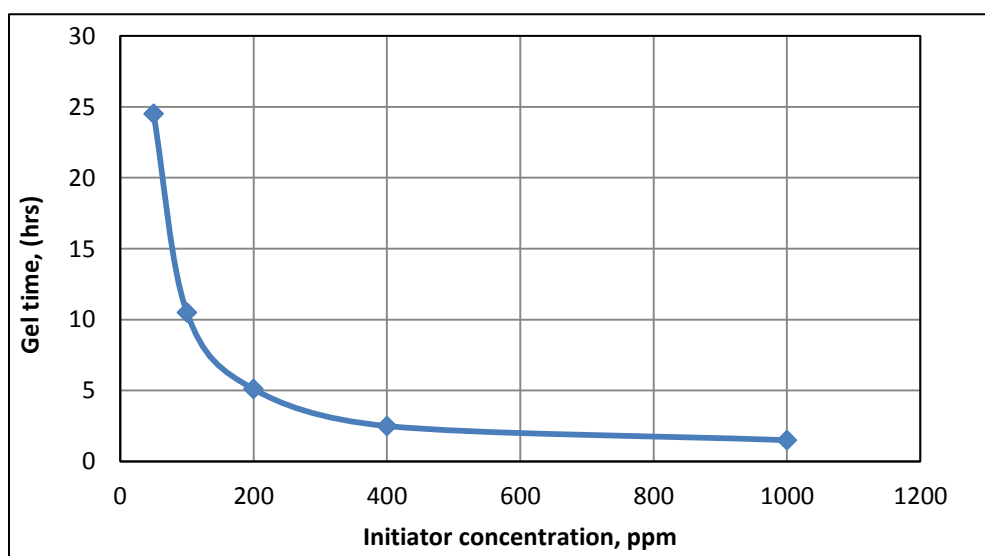


Figure 4.9. Effect of Initiator on Gel Formation Time.

However, a slightly different trend is observed between initiator concentration and gel strength. From 50 ppm to 100 ppm initiator concentration, gel strength increased dramatically from 2000 Pa to 18000 Pa (Figure 4.10). However, above 100 ppm, gel strength starts to decrease. A plausible explanation for this observation is that as initiator concentration increased from 50 ppm to 100 ppm, the right amount of free radicals are released which attack monomer units and form long polymer chains. Subsequent crosslinking of polymer chains along several junction points forms a dense network structure with a high gel strength. However, above 100 ppm initiator concentration, excess amount of free radicals released leads to the formation of progressively shorter polymer chains with increasing initiator concentration. Crosslinking of such shorter polymer chains leads to a progressive decline in gel strength. Thus to obtain optimal gel strength, initiator concentration is recommended to be below 100 ppm.

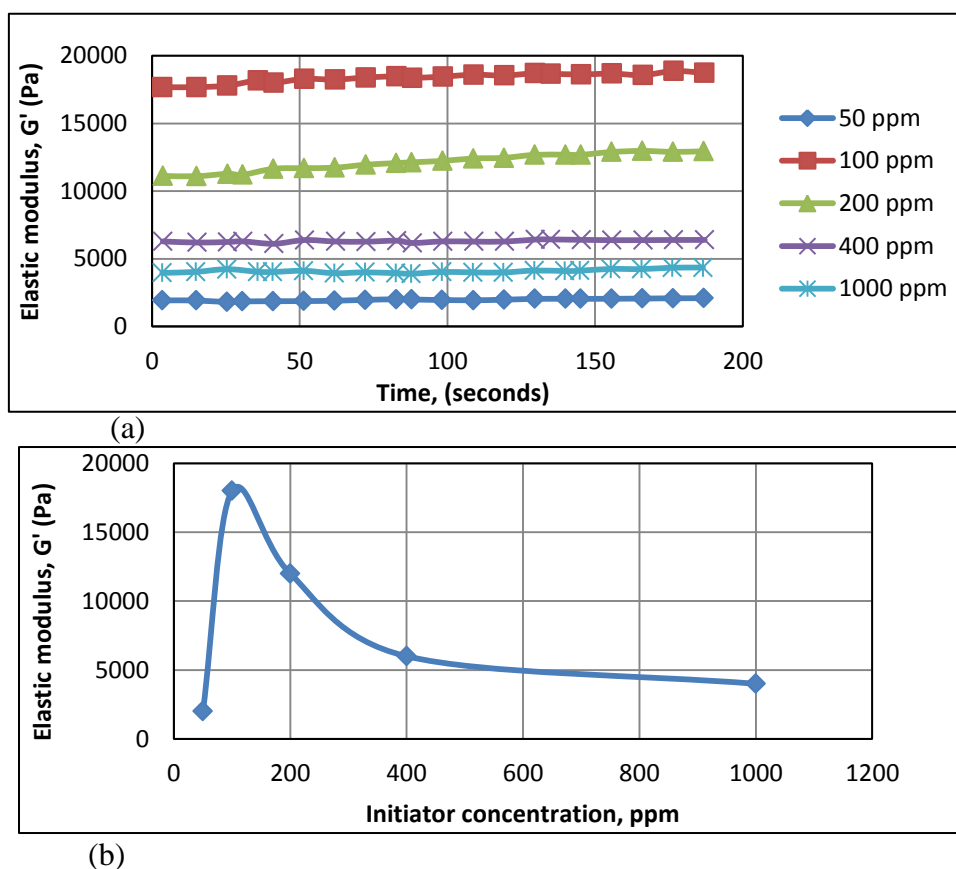


Figure 4.10. Variation of Gel's Elastic Modulus with Time for Samples Prepared with Initiator Concentrations Ranging from 50 ppm to 1000 ppm shown in (a) and (b).

4.4. EFFECT OF MONOMER ON GEL PROPERTIES

The amount of monomer in solution has a significant role to play in the process of polymerization and subsequently crosslinking. In order to study the effect of monomer concentration on polymerization and subsequently gel formation, all other reactants were kept constant. Monomer concentration was the only variable. Monomer concentration was varied between 5% and 40%. Synthesis temperature was kept constant at 60 °C. Nanoclay (Laponite XLG) concentration was kept constant at 2%. The initiator (ammonium persulfate) and crosslinker (PEG-200) concentrations were fixed at 100 ppm and 250 ppm, respectively.

Table 4.5 presents a summary of the parameters employed in the experimental setup, while Figure 4.11 presents the variation of monomer concentration and gelation time. It is observed from Figure 4.11 that gel formation time decreases as monomer concentration increases. This is logical because as monomer concentration in solution increases, free radicals can easily attack readily available monomer molecules, speeding up the chain propagation stage. The contrary is equally true. When monomer concentration is low, the frequency of free radical - monomer reaction decreases, since monomer molecules are not readily available in solution. Thus polymerization and subsequently gel formation time is increased.

Table 4.5. Effect of Monomer Concentration on Gelation Time and Gel Strength of Synthesized Gels.

| Sample # | Crosslinker (ppm) | Monomer (%) | Initiator (ppm) | Temp. (°C) | Gelation time (hours) | G' (Pa) | G'' (Pa) | Sydank's Gel strength code |
|----------|-------------------|-------------|-----------------|------------|-----------------------|---------|----------|----------------------------|
| PPG-5 | 250 | 5 | 100 | 60 | 6.92 | 850 | 125 | H |
| PPG-10 | 250 | 10 | 100 | 60 | 6.67 | 700 | 100 | H |
| PPG-15 | 250 | 15 | 100 | 60 | 6.25 | 480 | 80 | I |
| PPG-23 | 250 | 23 | 100 | 60 | 3.75 | 1600 | 210 | I |
| PPG-30 | 250 | 30 | 100 | 60 | 3.75 | 1550 | 180 | I |
| PPG-40 | 250 | 40 | 100 | 60 | 3.75 | 5500 | 480 | I |

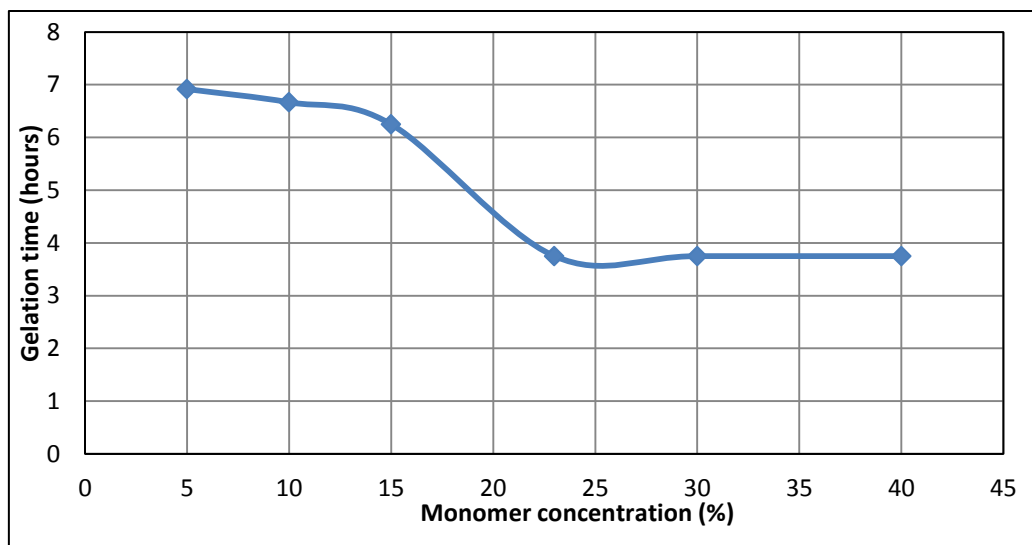


Figure 4.11. Effect of Monomer Concentration on Gel Formation Time.

Figure 4.12 presents the variation of gel strength with monomer concentration. It is observed that below 15% monomer concentration, a highly flowable gel is formed. This is due to the insufficient monomer molecules available to form the polymer backbone. The weak and liquid-like nature of gels formed below 15% monomer concentration is what accounts for the inconsistent values in elastic modulus. However, above 15% monomer concentration, because of sufficient availability of monomer molecules, a longer polymer chain backbone is formed, leading to the formation of stronger gels and a progressive increase in elastic moduli with monomer concentration.

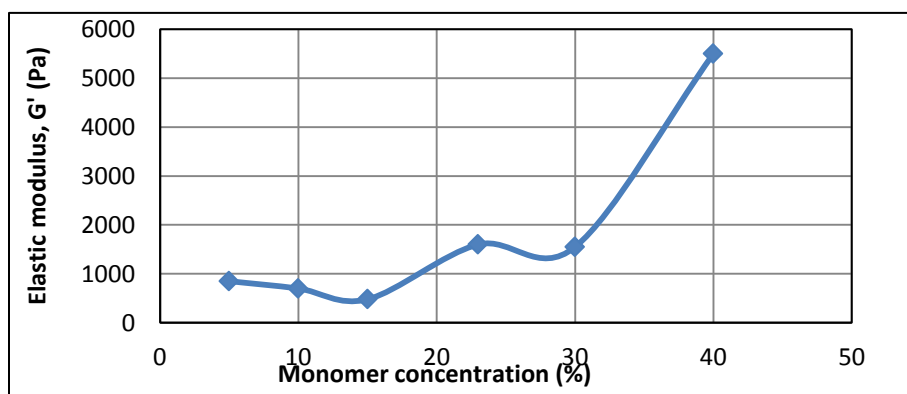
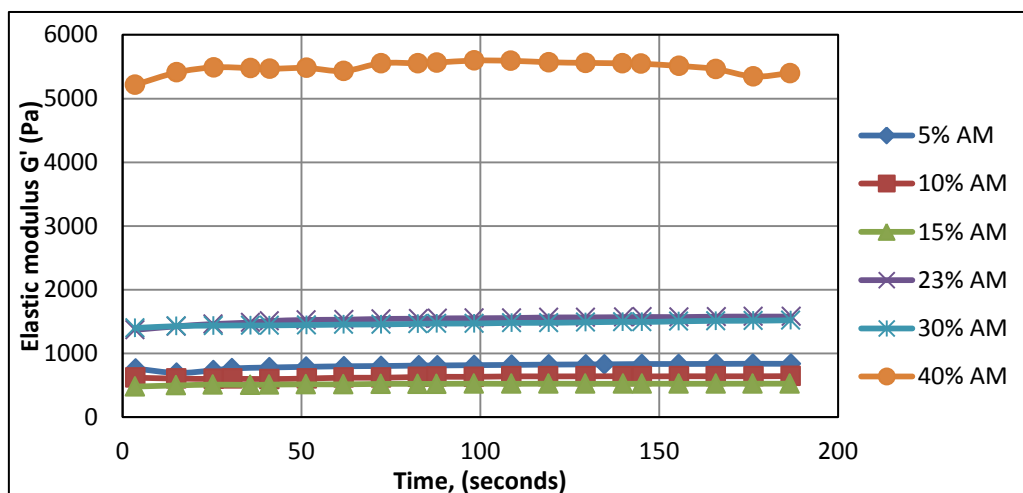
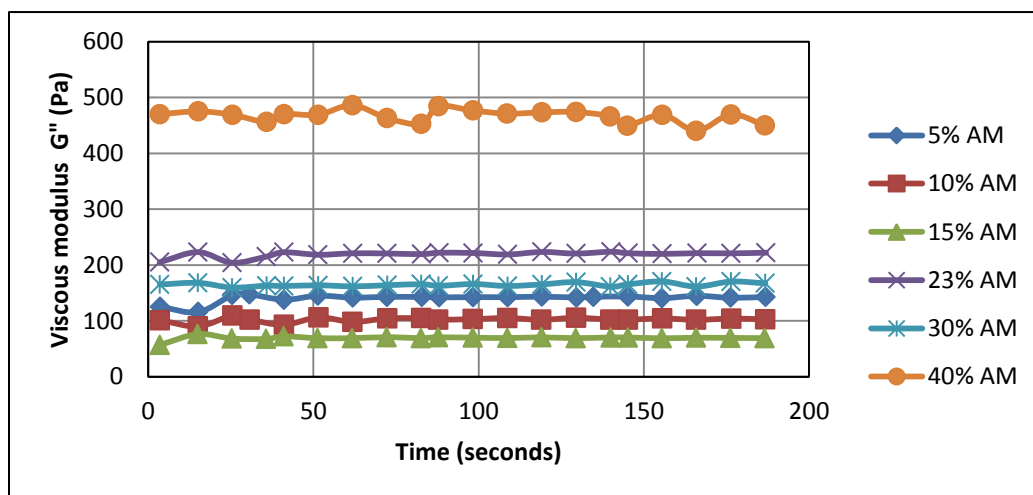


Figure 4.12. Effect of Monomer Concentration on Gel's Elastic Modulus, G' .

Figure 4.13 present the elastic (G') and viscous (G'') modulus of gels prepared with 5% - 40% monomer concentration. All samples were freshly prepared and immediately loaded onto the rheoscope for the testing of gel strength.



(a)



(b)

Figure 4.13. Variation of Gel's Elastic and Viscous Moduli with Time for Samples Prepared with Monomer Concentrations Ranging from 5% to 40%, Shown in (a) and (b) Respectively.

5. RESULTS AND DISCUSSION: DEGRADABLE NANOCOMPOSITE PREFORMED PARTICLE GEL AS MOBILITY CONTROL AGENT

This section presents results on the first product: Degradable Nanocomposite Preformed Particle Gels for enhanced in-depth mobility control. In Section six, the results of the second product, preformed gels as permanent fluid-diverting agents will be presented.

This first product presented is an extension of existing preformed gel technology by the incorporation of nanomaterials in gel design for improved mobility control. A degradable nanocomposite Preformed Particle Gel is proposed, called nanocomposite PPG, which involves the incorporation of nanoclay in it. The incorporation of nanomaterials not only overcomes prior limitations of conventional preformed gels such as poor long-term thermal stability and inadequate mechanical strength, but results in improvement in gel performance and properties to withstand adverse and extreme reservoir conditions, and also in improvement in post-degradation gel viscosity after the gel degrades under reservoir conditions. The novelty of this work involves a dramatic increase in post-degradation gel viscosity compared to currently existing gels without nanomaterials (Jia, 2011).

This product, when injected into the reservoir, will initially act as a conformance control agent by plugging water-thief zones and channels, thereby directing injected water to sweep out oil from low permeability oil-rich zones. After an extended time period, this product degrades into a highly viscous polymer solution which then moves deeper into the reservoir, mixes with flood water, and increases its viscosity. By so doing, the water and polymer flooding processes is enhanced since water sweep efficiency increases, increasing oil production. Therefore, the viscosity of the gel after it degrades is of key concern (Figure 5.1).

The general scheme of this first product includes the following processes: 1) preparing crosslinked nanocomposite PPGs with a predetermined size, 2) dispersing the nanocomposite PPGs into a brine solution to form swelled PPGs, 3) injecting the swelled nanocomposite PPGs into the target reservoir, 4) the usual treatment after PPGs injection such as water flooding, polymer flooding or SP flooding etc is performed to improve oil

recovery by reducing excess water production, and 5) after a certain time period, the injected nanocomposite PPG decomposes through hydrolysis induced by heat into a high viscosity linear polymer solution for the secondary polymer flooding to further enhance oil recovery.

(a) Initially, excess water production exists from fractures or high permeability zones of reservoir.

(b) On initial injection into reservoir, nanocomposite PPG serves to plug high permeability near well-bore zones, diverting injected water to sweep out oil from low permeability region.

(c) After an extended time period, nanocomposite PPG degrades into highly viscous polymer solution that moves into deeper regions of reservoir to increase the viscosity of flood water and hence boost polymer flooding. Oil production is thus increased.

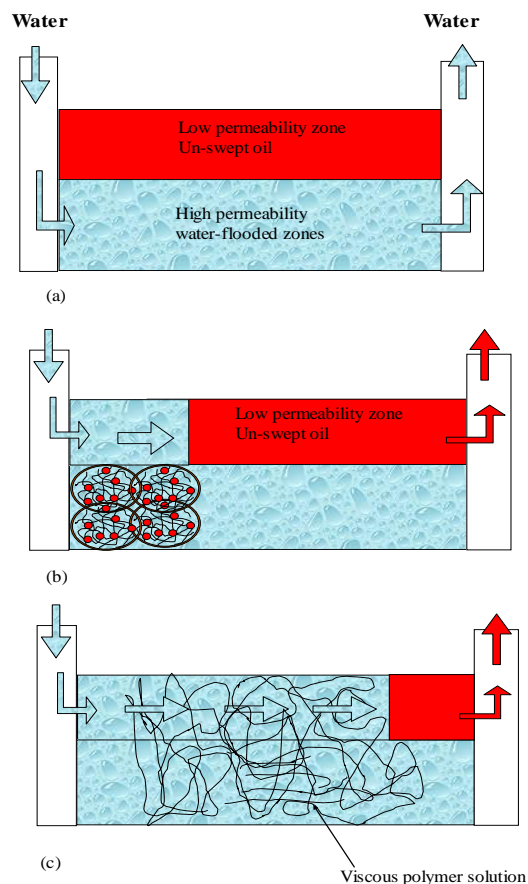


Figure 5.1. Degradable Nanocomposite Preformed Particle Gel for Improved Mobility Control and Effective Volumetric Sweep Efficiencies in Heterogeneous Reservoirs.

Three different types of nanocomposite gels were made using three different types of nanomaterials. The nanomaterials used in this study include: Laponite XLG, Calcium Montmorillonite, and Sodium Montmorillonite. The reason for trying out different nanomaterials was so that we could choose that which has the best performance.

A detailed side-by-side comparison of currently existing and novel nanocomposite hydrogels reveals that the latter far supercedes existing hydrogels in terms of product performance and usefulness. A summary of the results obtained for the three different studies is presented below.

5.1. EVALUATION OF DEGRADABLE NANOCOMPOSITE PREFORMED PARTICLE GEL WITH LAPONITE XLG AS NANOMATERIAL (LXLG NANOCOMPOSITE PPG)

5.1.1. Improvement in LXLG Nanocomposite PPG Properties with Incorporation of Nanomaterials. The following properties were studied:

5.1.1.1 Increased mechanical strength. The rheology behavior of LXLG nanocomposite hydrogels and hydrogels with no nanomaterial were studied. The mechanical strength of a gel often can be estimated by its viscoelastic properties such as elastic modulus (G'). The variation in elastic modulus (G') with time for LXLG nanocomposite hydrogel with 0.2%, 0.6%, and 3% nanomaterial is presented in Figure 5.2 and is compared against hydrogel without nanomaterial. It is observed from Figure 5.2 that the elastic modulus significantly increases with increasing nanomaterial concentration. The elastic modulus of hydrogel with no nanomaterial is at lowest value of 800 Pa. Clearly, an increase in gel strength is observed as LXLG nanomaterial is introduced.

Additionally, measurements were done for both dry gels and for gels swollen in 1% NaCl solution (hydrogels were swollen until they could rise no further). The reason for this measurement was to ascertain by how much gel strength decreased after gel swelled. Results indicate that after swelling, gel strength decreased by 1.8% for gels containing 0.2% LXLG nanomaterial, by 11.1% for gels containing 0.6% LXLG nanomaterial, and by 5.6% for gels containing 3% LXLG nanomaterial. For gels with no nanomaterial, gel strength decreased by 11.8% after swelling. As gels absorb water, their crosslink density decreases, hence they swell. Hydrogel without nanomaterial swelled the most, since it has no re-enforcing crosslink network provided by the addition of nanomaterial. As expected, 3% LXLG hydrogel with the most amount of nanomaterial

swelled the least. The additional crosslink networks provided by the higher nanomaterial concentration resisted excessive swelling.

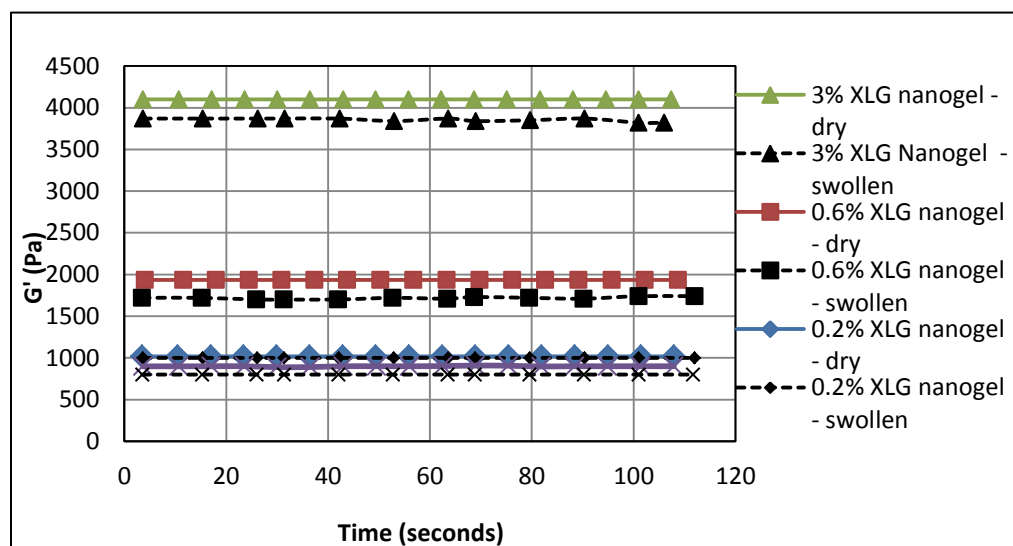


Figure 5.2. An Obvious Improvement in Hydrogel Mechanical Strength is Observed between Gels with LXLG Nanomaterials and Those without Nanomaterials.

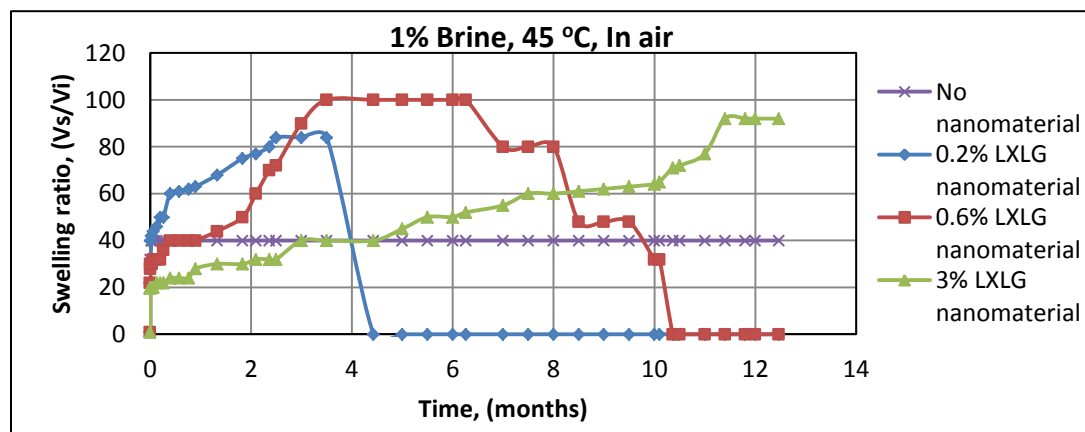
5.1.1.2 Increased swelling and thermal resistance. (I) Swelling kinetics and thermal resistance in presence of air: Once injected downhole into fractures or high permeability streaks, the longterm thermal stability of hydrogels to continuously seal fractures under adverse reservoir conditions is important. Without longterm endurance, gels rapidly degrade, leading to a re-opening of an already sealed fracture, thus re-creating a water-thief channel.

Therefore, ensuring hydrogels can adequately seal fractures over a prolonged period of time is paramount. Longterm thermal testing was done both under aerobic (in presence of oxygen) and anaerobic (under vacuum, in absence of oxygen) conditions. Aerobic oxidation in presence of oxygen causes gel to degrade much faster. Therefore, it was necessary to remove oxygen in the sample in order to avoid premature gel breakdown. This practice also simulates downhole reservoir environment where oxygen concentration is minimal. Furthermore, testing was done using both brine and formation

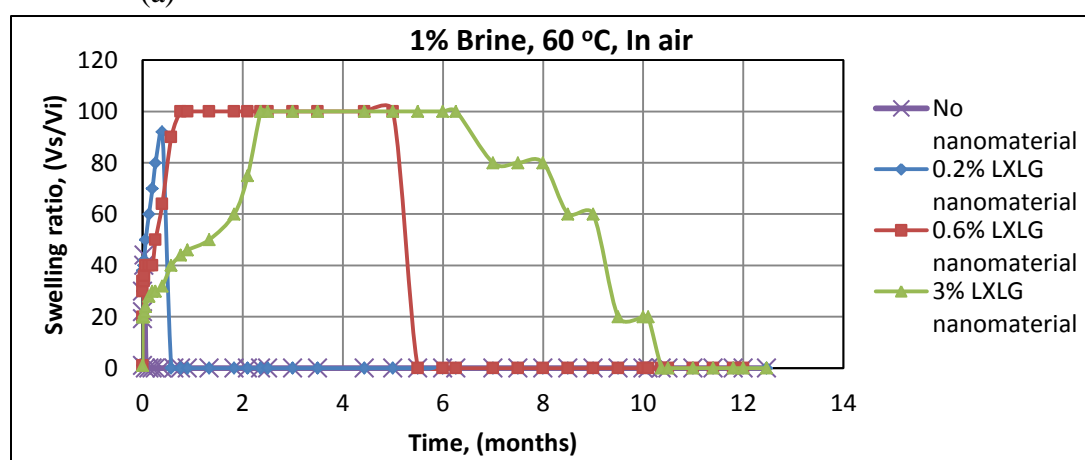
water respectively as the solvent. Additionally, testing was done at three different temperatures: 45°C, 60 °C, and 85 °C so as to mimic different reservoir temperatures.

Figures 5.3a-f present longterm testing in aerobic conditions using both 1% brine and formation water. All Samples were synthesized using 23% acrylamide monomer, 100 ppm ammonium persulfate initiator, and 250 ppm to 10000 ppm of polyethylene glycol diacrylate crosslinker depending on nanomaterial concentration. As nanomaterial concentration increases, crosslinker concentration was increased. This is because, when nanomaterial concentration was increased, gel did not form, implying that the crosslinker was absorbed or adsorbed by nanomaterial. Thus as we increased nanomaterial amount, we likewise increased crosslinker amount to ensure sufficient crosslinkers existed in solution to afford crosslinking and gel formation. As is clearly seen from Figure 5.3a-f, hydrogels with no nanomaterial rapidly degraded within days whereas for hydrogels with 0.2% XLG, 0.6% XLG, and 3% XLG nanomaterial, degradation occurred over several months in some cases and in others hydrogels have not degraded yet.

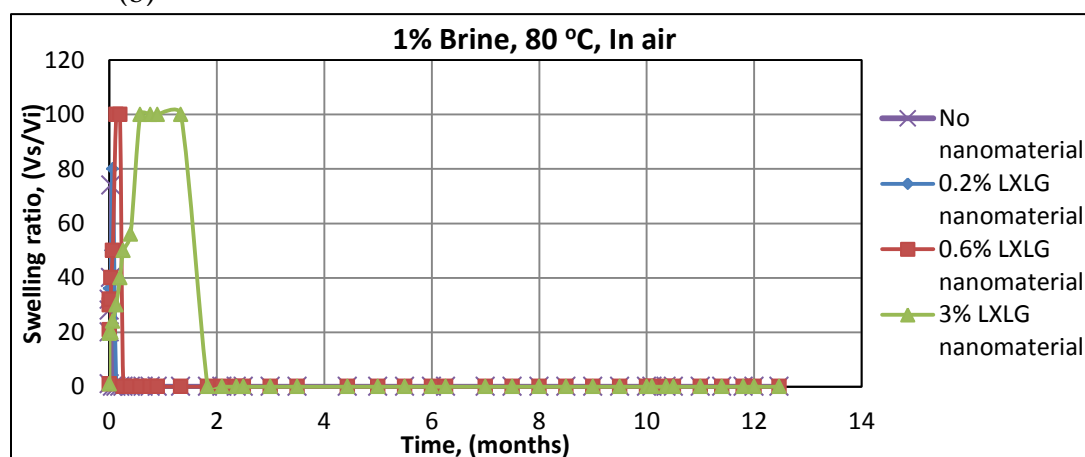
Additionally, we observed that an increase in nanomaterial concentration led to an increase in longterm thermal resistance of hydrogels. This is as expected because increasing nanomaterial concentration leads to an increased participation of nanomaterial in the gelation process, affording a stronger gel. Such dramatic improvement in longterm thermal stability of nanocomposite hydrogels is one key reason we believe they are potentially valuable in conformance control applications. Additionally, the time required to breakdown depends on reservoir conditions, such as temperature, pH, etc.



(a)

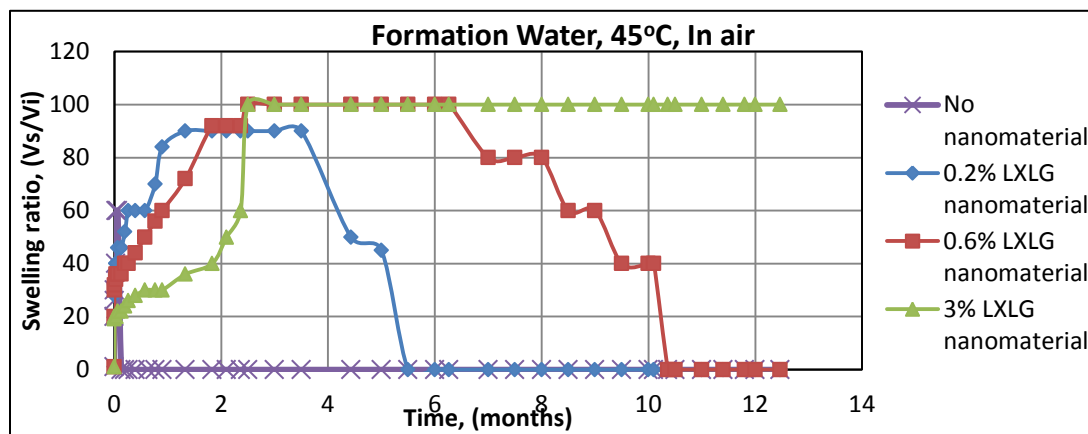


(b)

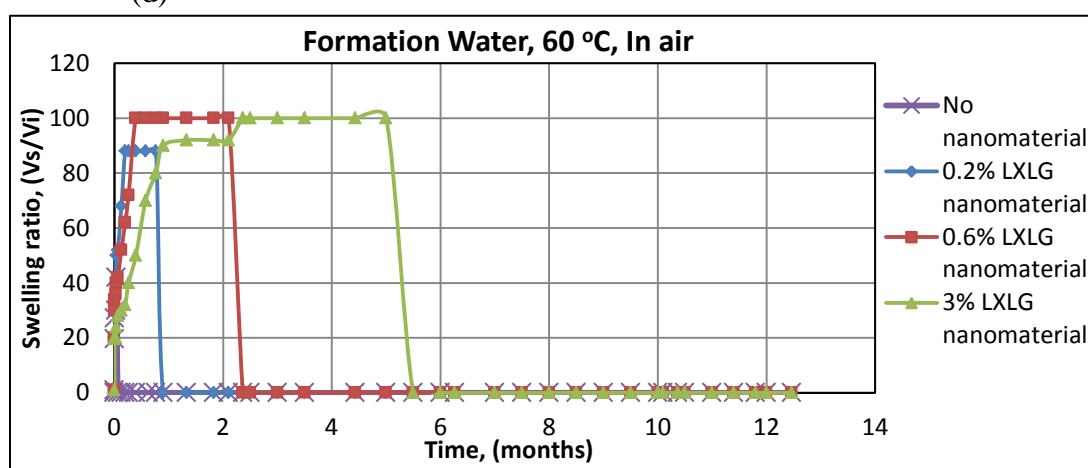


(c)

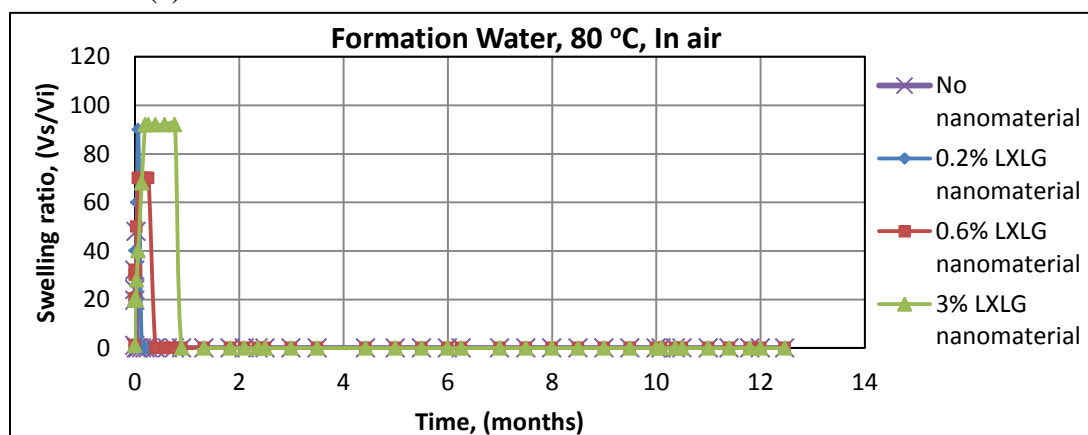
Figure 5.3. (a-f): Longterm Thermal Stability of LXLG Nanocomposite Hydrogels Under Aerobic Conditions and in 1% Brine Solution and Formation Water.



(d)



(e)

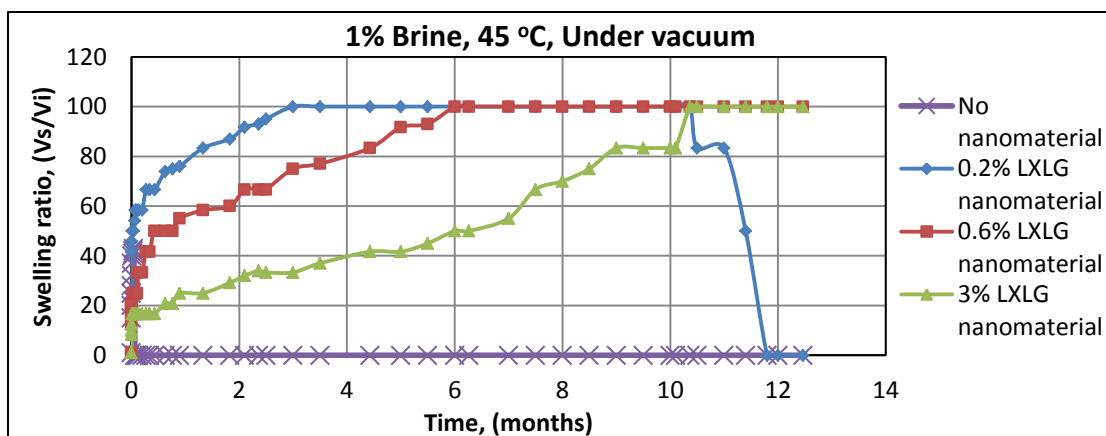


(f)

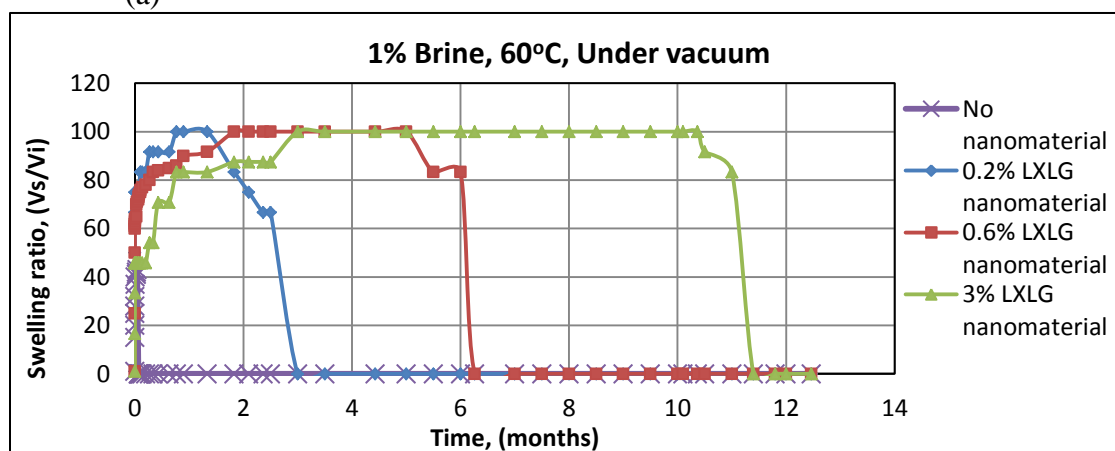
Figure 5.3. (a-f): Longterm Thermal Stability of LXLG Nanocomposite Hydrogels Under Aerobic Conditions and in 1% Brine Solution and Formation Water. (Cont).

(II) Swelling kinetics and thermal resistance under vacuum: Figures 5.4a to Figures 5.4f present longterm testing in anaerobic conditions using both 1% brine and formation water. The reason for testing gel degradation under anaerobic conditions was to simulate reservoir environment where oxygen amounts are minimal. Oxidation in presence of oxygen causes gel to degrade much faster. Therefore, it was necessary to remove every trace of oxygen in order to avoid premature gel breakdown.

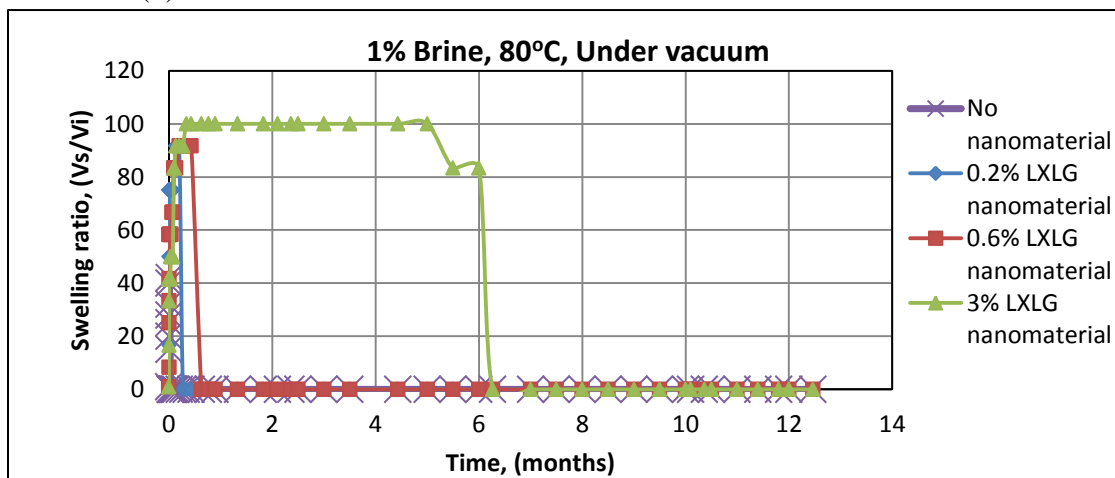
Comparing Figure 5.4 and 5.3, we observe that on average, it takes a much longer time for gels to degrade in anaerobic conditions than in aerobic conditions. For example, comparing Figure 5.3c and Figure 5.4c, in Figure 5.3c (under aerobic conditions), nanocomposite gel with 3% XLG nanomaterial degraded under about two months. However in Figure 5.4c (under anaerobic conditions) gel degradation occurred in about six months. It took an additional 4 months to degrade when oxygen was removed.



(a)

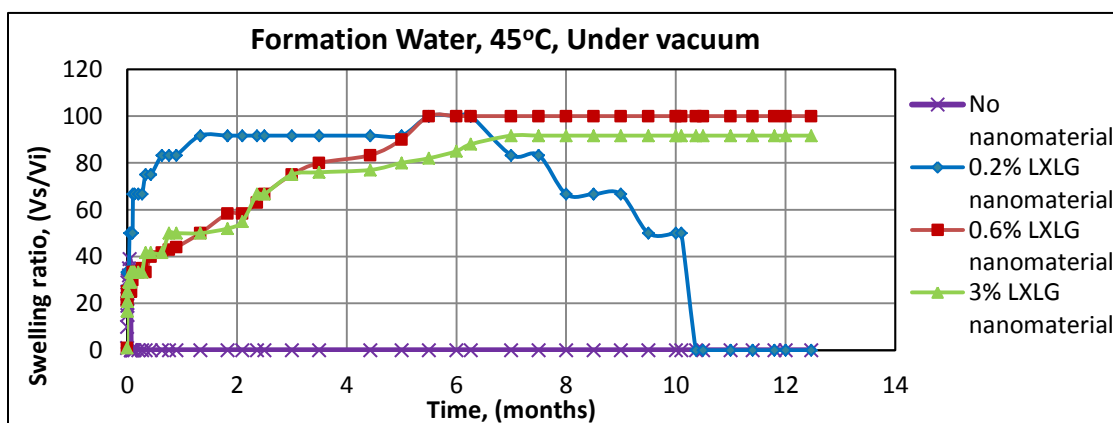


(b)

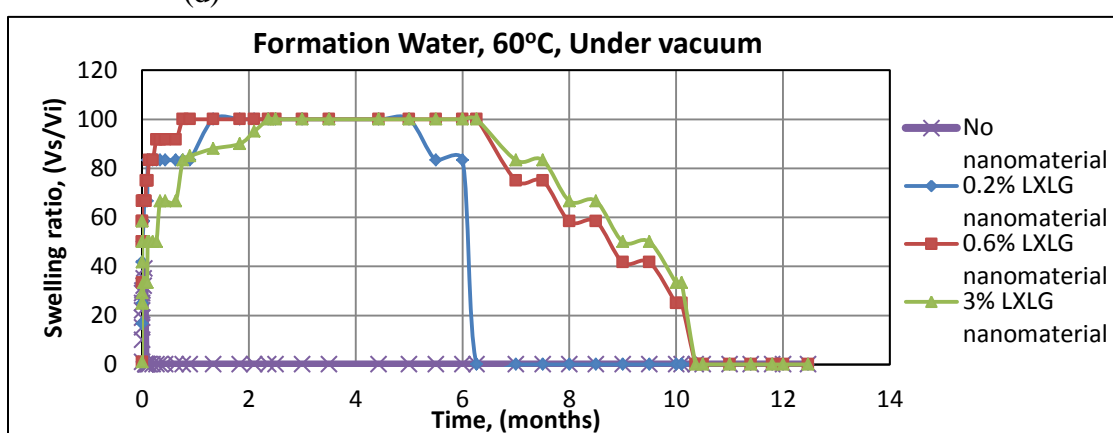


(c)

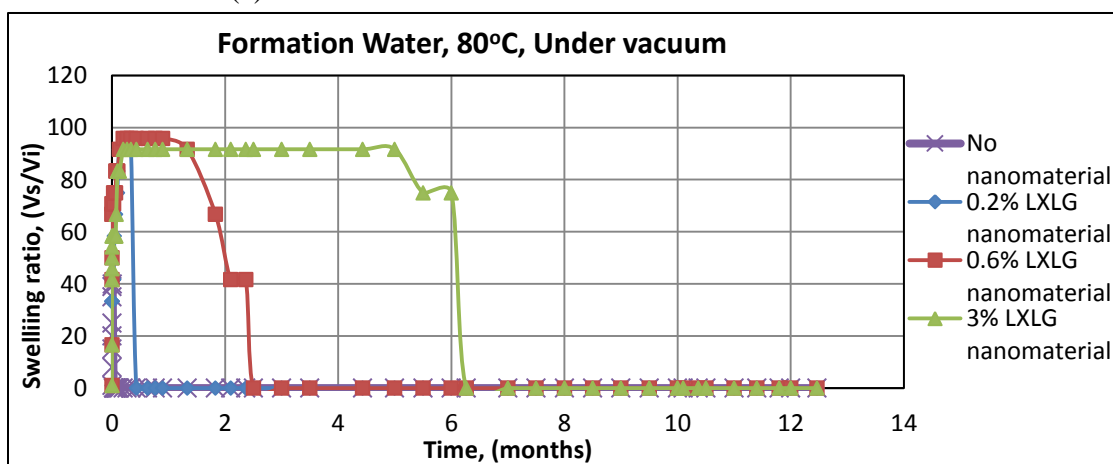
Figure 5.4. (a-f): Longterm Thermal Stability of LXLG Nanocomposite Hydrogels Under Anaerobic Conditions and In 1% Brine Solution and Formation Water.



(d)



(e)



(f)

Figure 5.4. (a-f): Longterm Thermal Stability of LXLG Nanocomposite Hydrogels Under Anaerobic Conditions and In 1% Brine Solution and Formation Water. (Cont).

5.1.1.3 Increased post-degradation viscosity of LXLG nanocomposite PPG.

The present invention provides a new and improved method combining gel treatment and polymer flooding processes during an oil recovery operation. In one hand, the inventive LXLG nanocomposite PPG can serve as a plugging agent for a designed and controlled period to improve conformance control so that more oil may be swept out of the low permeability formation pores to the production well.

On the other hand, depending on the reservoir temperature, pH value, and/or formation water salinity, the LXLG nanocomposite PPG eventually and completely decompose through hydrolysis into linear polymer chain solutions. This resulting polymer solution can then move into the reservoir formation to perform the polymer flooding. Figure 5.5 presents a picture of LXLG nanocomposite hydrogels both before and after their degradation in both aerobic and anaerobic environment.

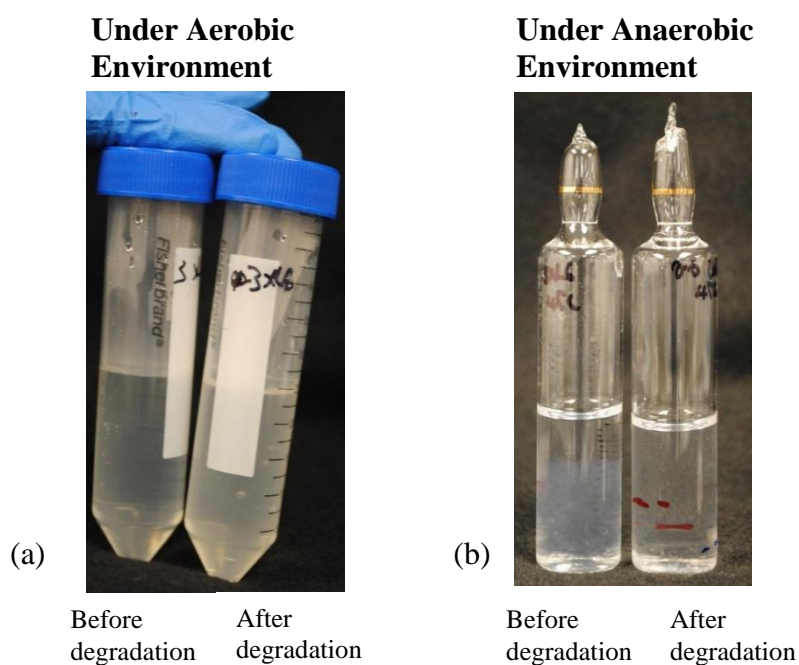


Figure 5.5. Aerobic and Anaerobic Environment of LXLG Samples Tested Showing both Before and After Sample Degrades Into Polymer Solution.

The novelty of the work involves the dramatic increase of the viscosity of the post-degradation linear polymer solution from 170 cp (for 0.3% PPG without nanomaterial) to a viscosity of 4437 cp (in 1% brine solution) for 0.6% LXLG Nanocomposite PPG. This represents a 2510% viscosity increase (Table 5.1). Such tremendous viscosity increase was brought about by the incorporation of LXLG nanomaterial during PPG synthesis.

On thermal degradation/hydrolysis, LXLG nanocomposite PPG degrades, releasing a low molecular weight polymer solution and clay particles. These re-associate by a physical interaction after degradation, increasing the polymer solution viscosity massively. Thus, the invention provides a unique process integrating together the two sub-processes, nanocomposite PPG-based conformance control/gel treatment and polymer flooding, during an oil recovery operation with improved efficiency and operability.

Table 5.1. Viscosity Measurements for Pure Polymer, Pure LXLG Nanomaterial, and Degraded LXLG Nanocomposite PPG.

| Conc. (%) | Pure Polyacrylamide Polymer (PAM) | Pure LXLG Nanomaterial | Degraded LXLG Nanocomposite PPG | | Degraded PPG with No Nanomaterial |
|--------------|-----------------------------------|------------------------|---------------------------------|-----------------------------|-----------------------------------|
| | Viscosity, (cp) | Viscosity, (cp) | Viscosity, (cp) - Aerobic | Viscosity, (cp) - Anaerobic | Viscosity, (cp) (0.3%) |
| 0.2% | 30.6 | 2 | 20 | 1113 | 170 |
| 0.6% | 107.2 | 3 | 39.7 | 4437 | |
| 1% | 353.5 | 3.7 | 612.5 | -- | |
| 3% | 6303 | 4.5 | 3069 | 7563 | |
| 5% | 48340 | 10 | 6982 | -- | |

5.1.2. Evaluation of LXLG Nanocomposite PPG Microstructure and Morphology, Before and After Degradation. Firstly, before degradation results are presented.

5.1.2.1 Environmental scanning electron microscopy imaging of LXLG nanocomposite PPG before its degradation. A detailed microscopic study of LXLG nanocomposite hydrogel was done using an Environmental Scanning Electron Microscope (ESEM), and was compared against hydrogels with no nanomaterial. Studying the network structure of hydrogel is important because it gives us information about pore-interconnectivity. This information is useful in understanding the mechanisms of gel swelling behavior, gel strength after it swells, and perhaps even its thermal resistance ability. Figure 5.6a presents an ESEM micrograph of pure LXLG nanomaterial. Figure 5.6b presents an ESEM micrograph of pure polyacrylamide (PAM) polymer. Figure 5.6c presents a 3-D micrograph of bulk LXLG nanocomposite hydrogel. Figure 5.6d presents a micrograph of hydrogel with no nanomaterial. The micrographs of LXLG nanocomposite hydrogel are presented in Figures 5.6e to Figures 5.6g. The reason we present different micrographs of the nanocomposite gels is to show different sections of the material.

Comparing the pure Laponite XLG and pure polymer solution with the degraded nanocomposite gels, we infer that the thick network structure of the nanocomposite gel is as a result of the network structure observed in the pure polymer superimposed with the pure nanomaterial.

Contrasting the hydrogel with no nanomaterial versus the hydrogel with nanomaterial, (that is Figures 5.6d versus Figures 5.6e – g), it is observed that although a porous interconnected network structure is seen in both nanocomposite and non-nanocomposite hydrogels, in LXLG nanocomposite hydrogels however (Figures 5.6e-g), the network structure is thicker, denser, and corrugated whereas in hydrogels with no nanomaterial, the network structure is finer, less dense, and smooth. Obviously, we say that the presence of nanomaterial in nanocomposite hydrogel affords this difference.

Author is also quick to point out that when brine was used as the solvent, the network structure was extremely dense (Figure 5.6e) such that the pores in the network are almost closed up. However, this phenomenon was not observed when distilled water

was used as the solvent. In an attempt to explain this phenomenon, we could only ascribe the presence of salt ions in the brine as a reason for this occurrence. A similar phenomenon was observed by Nelea et al., 2007.

Lastly, Figures 5.6g show to us that when this nanocomposite gels are stretched thin, a thinner network structure will be likewise observed.

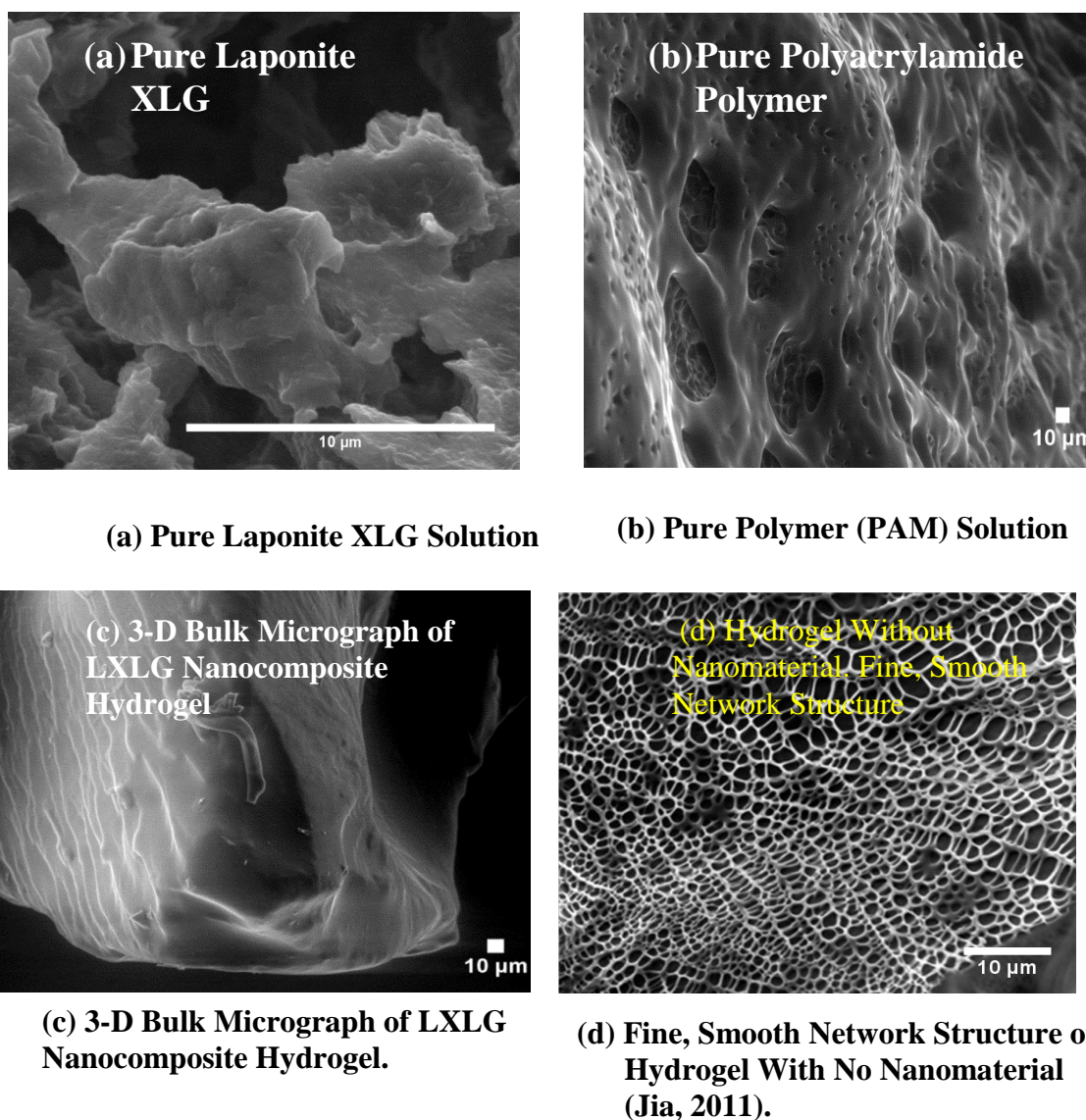
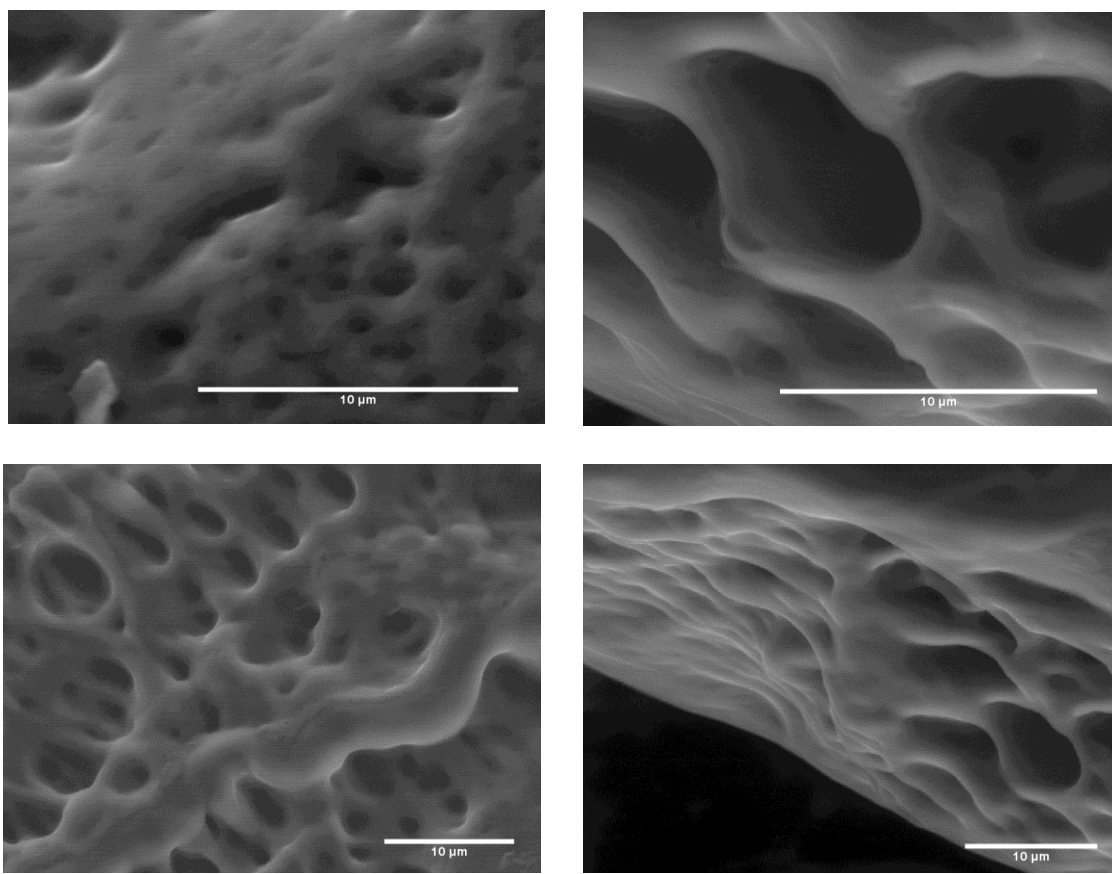
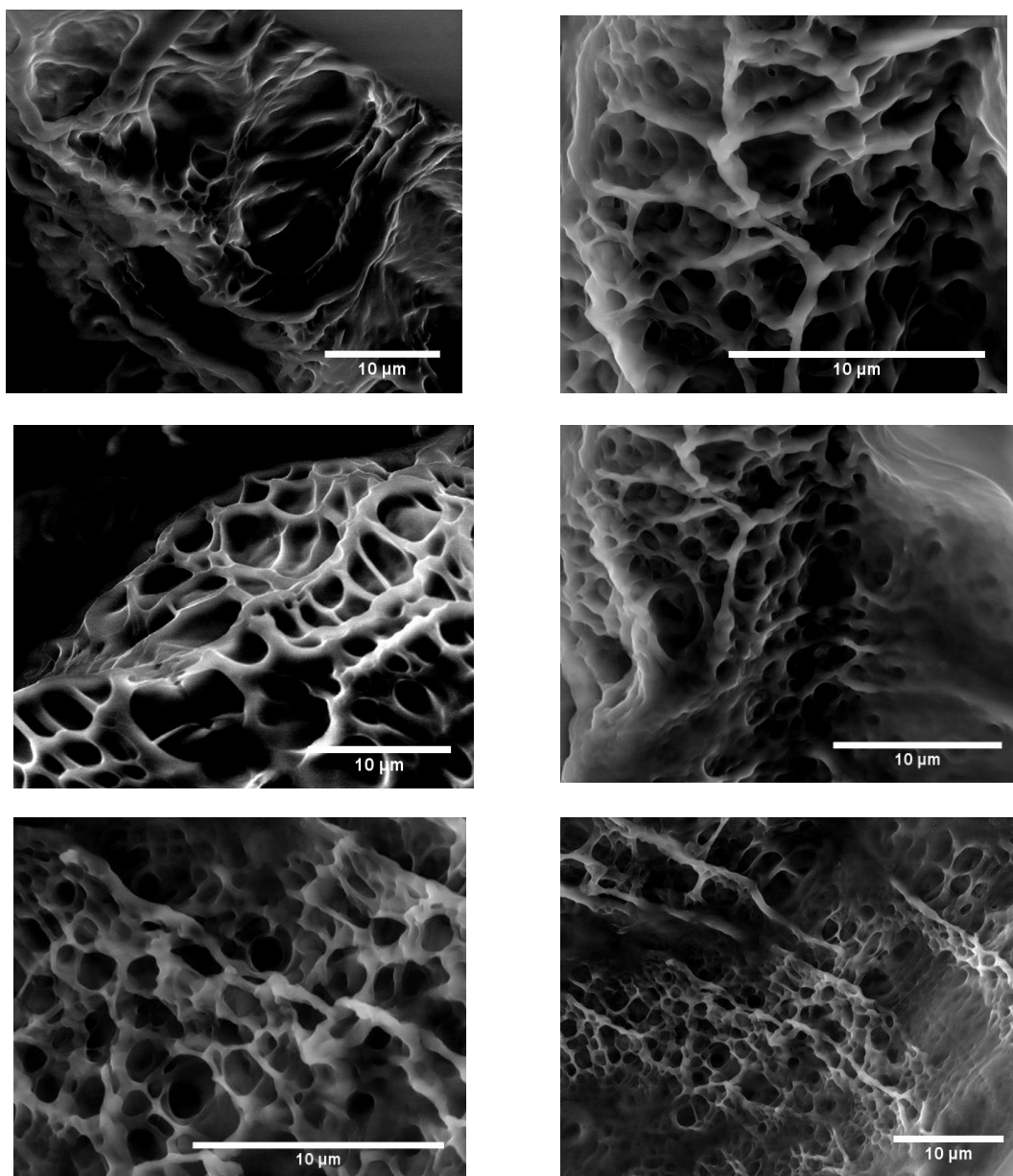


Figure 5.6. Before-degradation Environmental Scanning Electron Microscopy (ESEM) Micrographs.



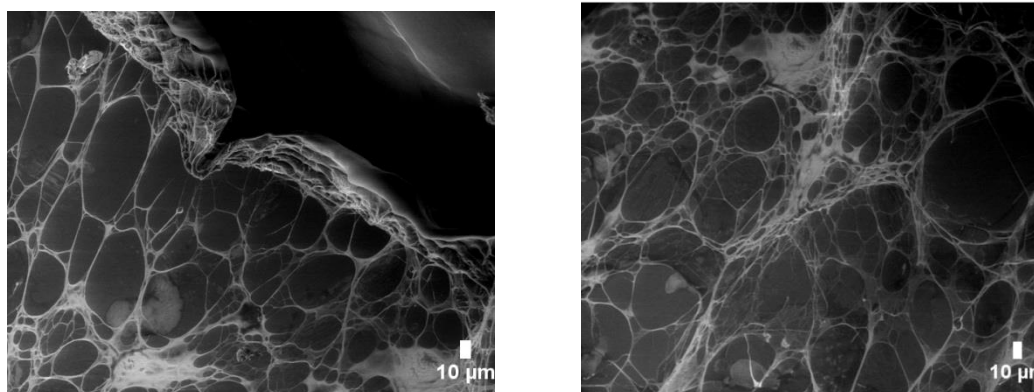
(e) Very Thick and Dense Network Structure of LXLG Nanocomposite Gel Swelled in 1% Brine as Solvent.

Figure 5.6. Before-degradation Environmental Scanning Electron Microscopy (ESEM) Micrographs. (Cont).



(f) Corrugated and Very Thick Network Structure of LXLG Nanocomposite Gel Swelled in Distilled Water as Solvent.

Figure 5.6. Before-degradation Environmental Scanning Electron Microscopy (ESEM) Micrographs. (Cont).



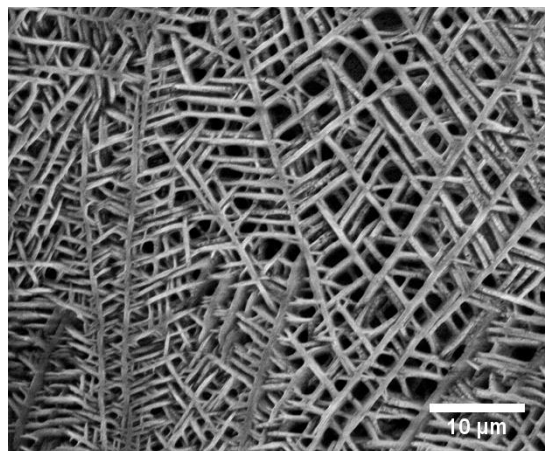
(g) Network Structure of an Extremely Stretched, Thin Section of LXLG Nanocomposite Hydrogel Swelled in Distilled Water.

Figure 5.6. Before-degradation Environmental Scanning Electron Microscopy (ESEM) Micrographs. (Cont).

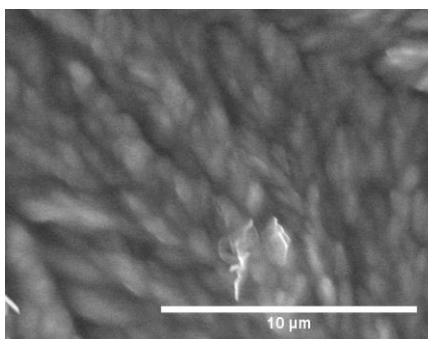
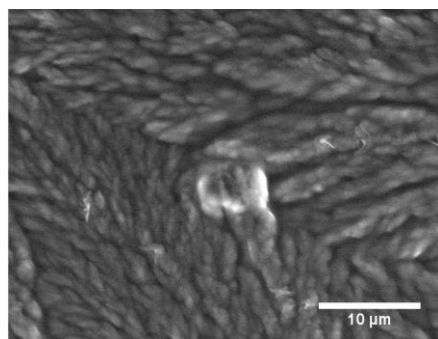
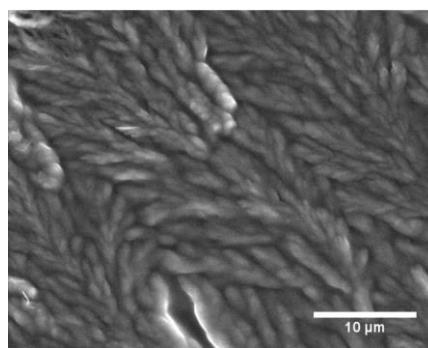
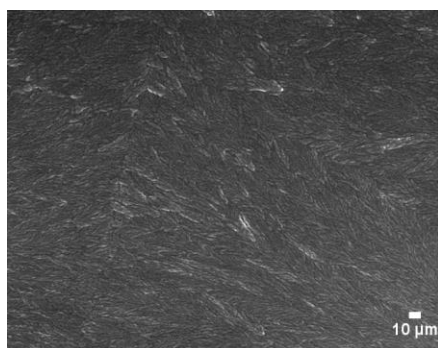
5.1.2.2 Environmental scanning electron microscopy (ESEM) imaging of LXLG nanocomposite PPG after its degradation. After the hydrogels degraded, ESEM micrographs were again taken of the degraded sample. Figure 5.7a shows the micrograph of the degraded hydrogel with no nanomaterial. Figures 5.7b and Figure 5.7c show the micrographs of a 1% degraded LXLG nanocomposite gel. As is clearly seen in both non-nanocomposite (Figure 5.7a) and nanocomposite gel (Figures 5.7b-c), the homogenous porous network structure that was initially observed before degradation disappears (collapses), signifying the degradation of the gel material into a polymer solution. In degraded gel without nanomaterial, the observed solution is less dense than in degraded gel with nanomaterial. This is ascribed to the presence of nanomaterial in gel design.

Worthy of mention is a significant difference between Figures 5.7b and Figures 5.7c. In Figure 5.7b, the initial network structure collapses into a ridge-like structure, whereas in Figures 5.7c, a block-like micrograph is observed. We lack sufficient knowledge to explain this occurrence. Characterization of hydrogel network is a complex

process given its 3-dimensional complex nature and its frequent, dynamic changes to outside stimuli such as solvent, temperature, salinity, pH etc.

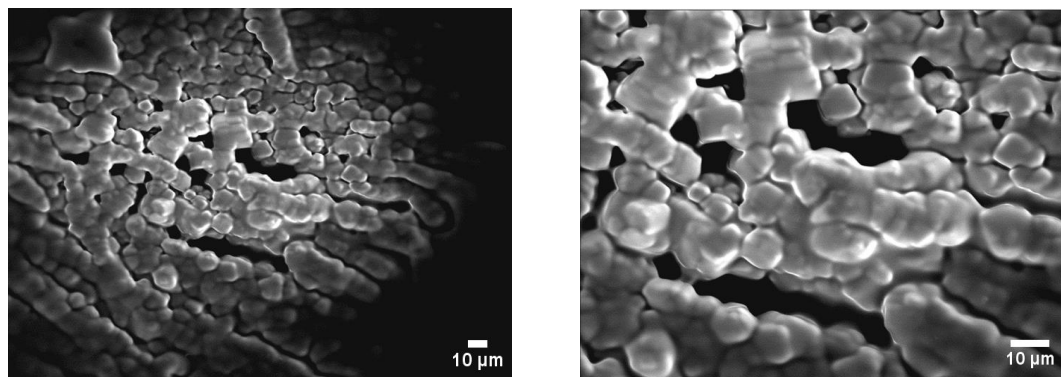


(a) Degraded Hydrogel With No Nanomaterial (Jia, 2011)



(b) Degraded 1% LXLG Nanocomposite Hydrogel: Ridge-like Structure is Observed

Figure 5.7. After-degradation Environmental Scanning Electron Microscopy (ESEM) Micrographs.



(c) Degraded 1% LXLG Nanocomposite Hydrogel: Block-like Structure is Observed

Figure 5.7. After-degradation Environmental Scanning Electron Microscopy (ESEM) Micrographs. (Cont).

5.1.2.3 Optical microscopy imaging of LXLG nanocomposite PPG after degradation. After the LXLG nanocomposite PPG degraded, we utilized an optical microscope to help us understand the nature of the degraded nanocomposite material. Figure 5.8 presents an optical micrograph of a 0.2% LXLG Nanocomposite gel after degradation. Gel composition is 23% acrylamide, 100 ppm ammonium persulfate initiator and 625 ppm PEG crosslinker. We observed very small particles which were uniformly distributed across the entire sample and had an approximate size of about 1.5 microns. These smaller particles can travel deeper into the formation to mobilize additional oil.

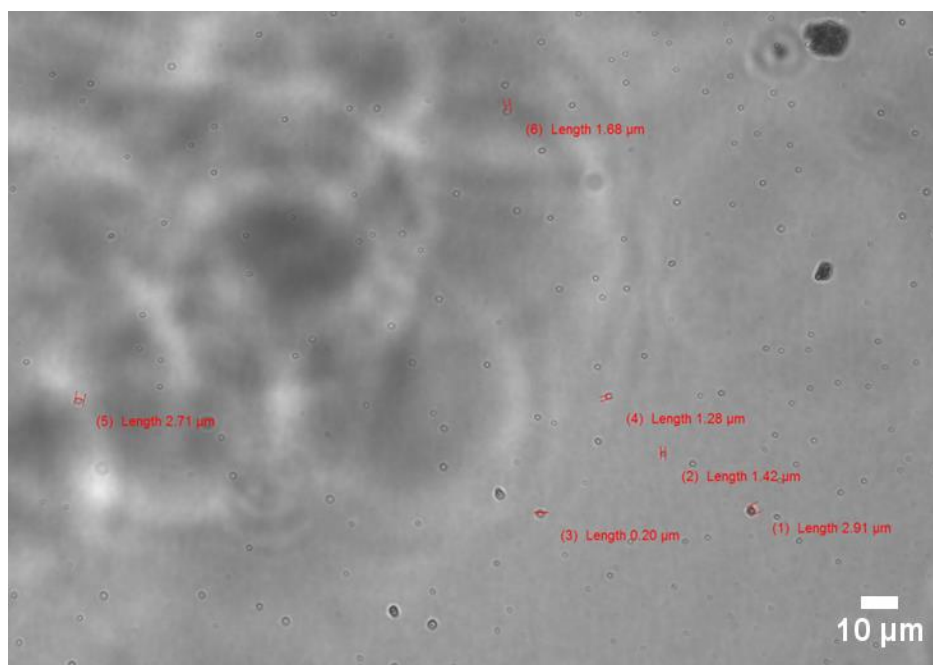


Figure 5.8. Optical Micrographs of Degraded 0.2% LXLG Nanocomposite PPG.

5.2. EVALUATION OF DEGRADABLE NANOCOMPOSITE PREFORMED PARTICLE GEL WITH CALCIUM MONTMORILLONITE AS NANOMATERIAL (Ca^{2+} NANOCOMPOSITE PPG)

5.2.1. Improvement in Ca^{2+} Nanocomposite PPG Properties with Incorporation of Nanomaterials. The following properties were studied:

5.2.1.1 Increased mechanical strength. The second type of nanocomposite hydrogel studied was that made using Calcium Montmorillonite as the Nanomaterial (Ca^{2+} Nanocomposite PPG). The rheology behavior of Ca^{2+} Nanocomposite PPGs and PPGs with no nanomaterial were studied. The variation in elastic modulus (G') with time for Ca^{2+} Nanocomposite PPG with 0.2%, 0.6%, and 3% calcium nanomaterial is presented in Figure 5.9 and is compared against hydrogel with no nanomaterial. It is observed from Figure 5.9 that the elastic modulus significantly increases with increasing nanomaterial concentration. The elastic modulus of hydrogel with no nanomaterial is at

lowest value of 800 Pa, while hydrogel with 3% calcium nanomaterial has an elastic modulus of about 18000 Pa. Clearly, an increase in gel strength is observed as nanomaterial is introduced.

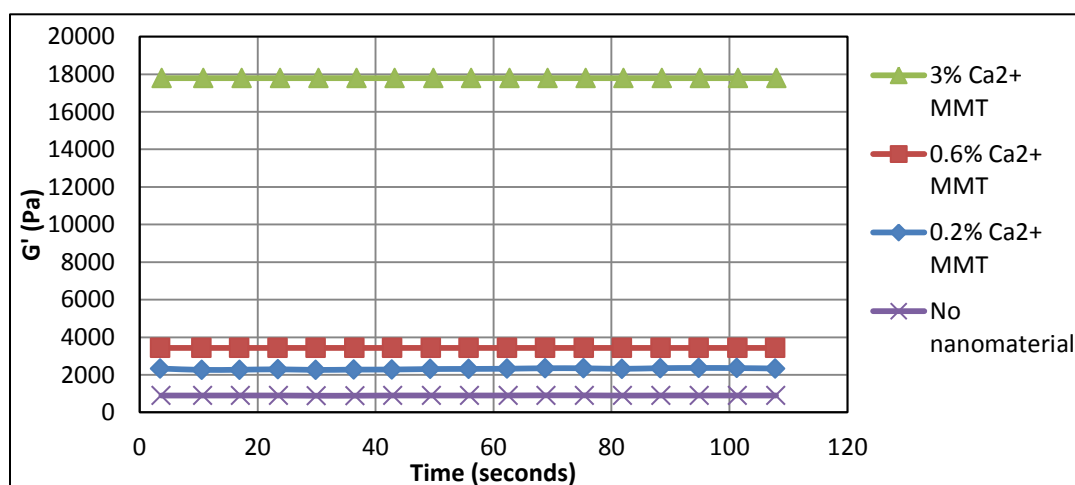


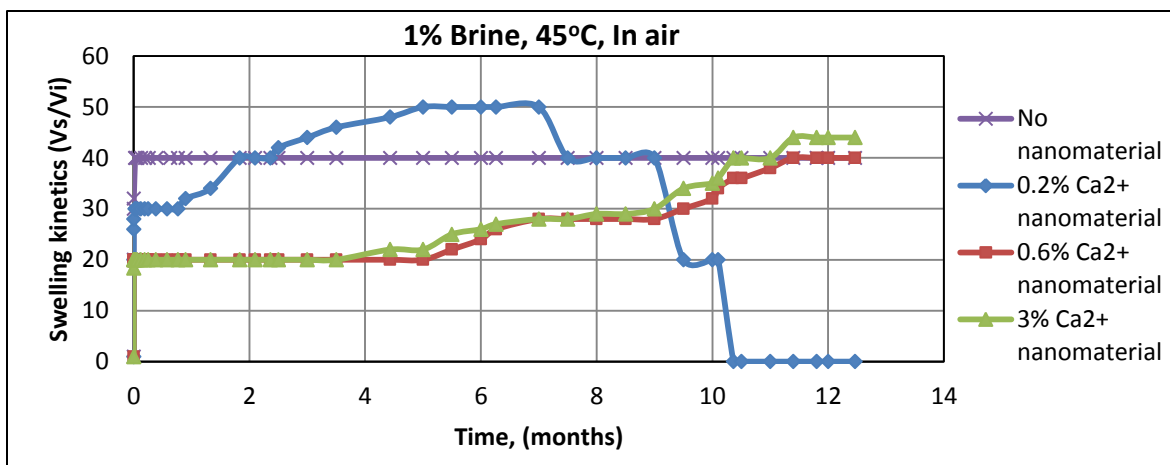
Figure 5.9. An Obvious Improvement in Hydrogel Mechanical Strength is Observed Between Dry Gels With Nanomaterials and Those Without Nanomaterials.

5.2.1.2 Increased swelling and thermal resistance. (I) Swelling kinetics and thermal resistance in presence of air: Similar to the swelling kinetics and thermal resiliency of LXLG nanocomposite PPGs studied in Section 5.1 above, a similar study was conducted for Ca²⁺ nanocomposite PPG. Once injected downhole into fractures or high permeability streaks, the longterm thermal resiliency of hydrogels to continuously seal fractures under adverse reservoir conditions is important. Without longterm endurance, gels rapidly degrade, leading to a re-opening of an already sealed fracture, thus re-creating a water-thief channel.

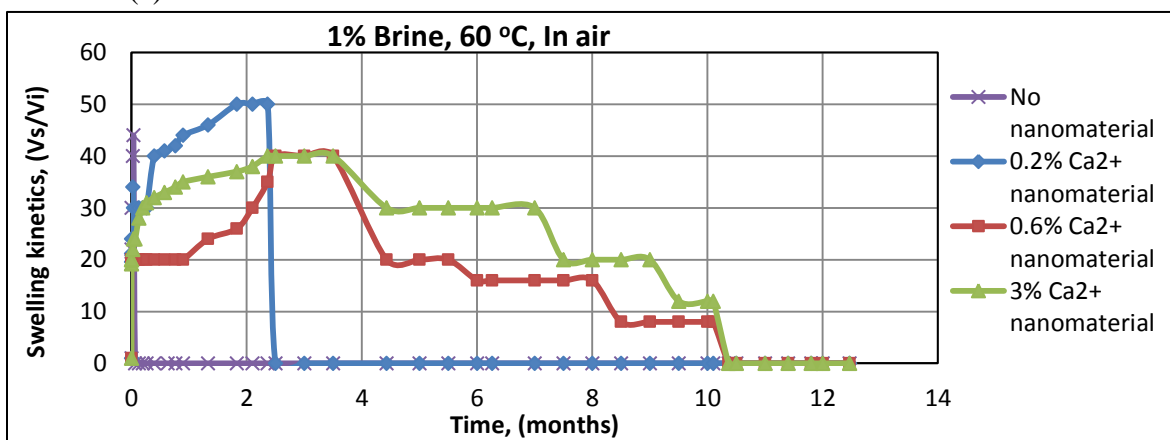
Therefore, ensuring hydrogels can adequately seal fractures over a prolonged period of time is paramount. Longterm thermal testing was done both under aerobic (in presence of oxygen) and anaerobic (under vacuum, in absence of oxygen) conditions. Aerobic oxidation in presence of oxygen causes gel to degrade much faster. Therefore, it

was necessary to remove every trace of oxygen in order to avoid premature gel breakdown. This also simulates downhole reservoir environment where oxygen concentration is minimal. Furthermore, testing was done using both brine and formation water respectively as the solvent. Additionally, testing was done under three different temperatures: 45°C, 60 °C, and 85 °C so as to mimic different reservoir temperatures.

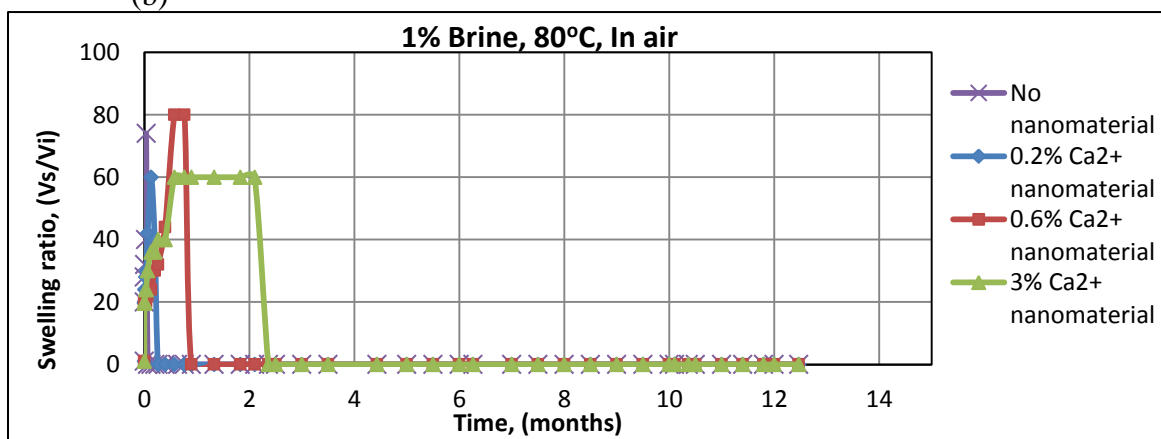
Figures 5.10a-f present longterm testing in aerobic conditions using both 1% brine and formation water. As is clearly seen from Figures 5.10a-f, hydrogels with no nanomaterial rapidly degraded within days whereas for hydrogels with 0.2% Ca^{2+} , 0.6% Ca^{2+} , and 3% Ca^{2+} nanomaterial, degradation occurred over several months in some cases and in others, Ca^{2+} nanocomposite PPGs have not yet degraded. Additionally, it was observed that an increase in nanomaterial concentration led to an increase in longterm thermal resistance of hydrogels. This is as expected because increasing nanomaterial concentration leads to an increased participation of nanomaterial in the gelation process, affording a stronger gel. Such dramatic improvement in longterm thermal stability of nanocomposite hydrogels is one key reason we believe they are potentially valuable in conformance control applications.



(a)

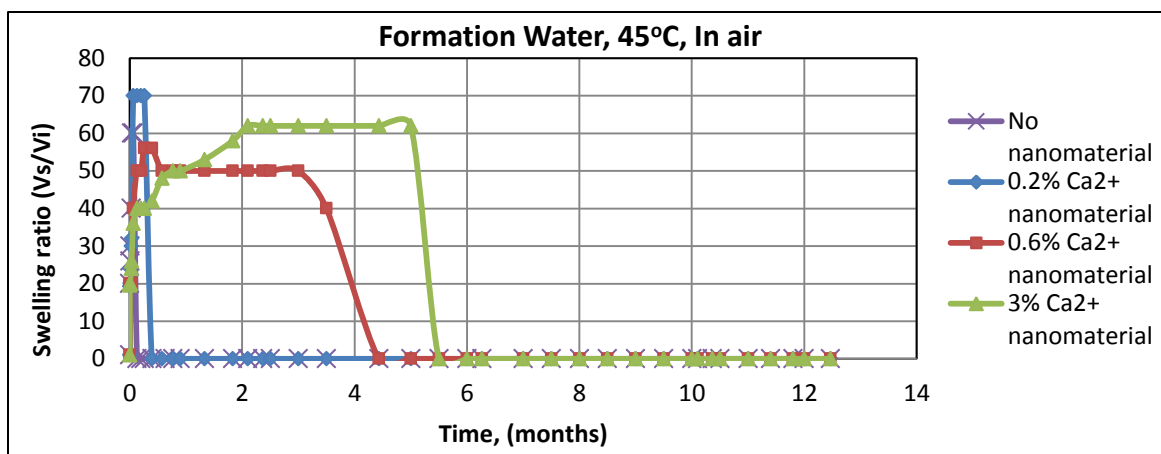


(b)

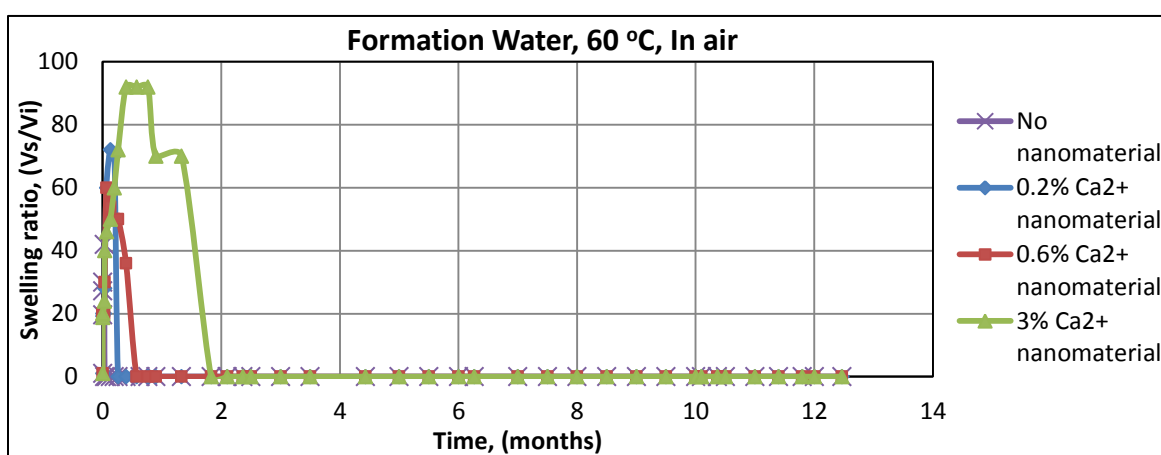


(c)

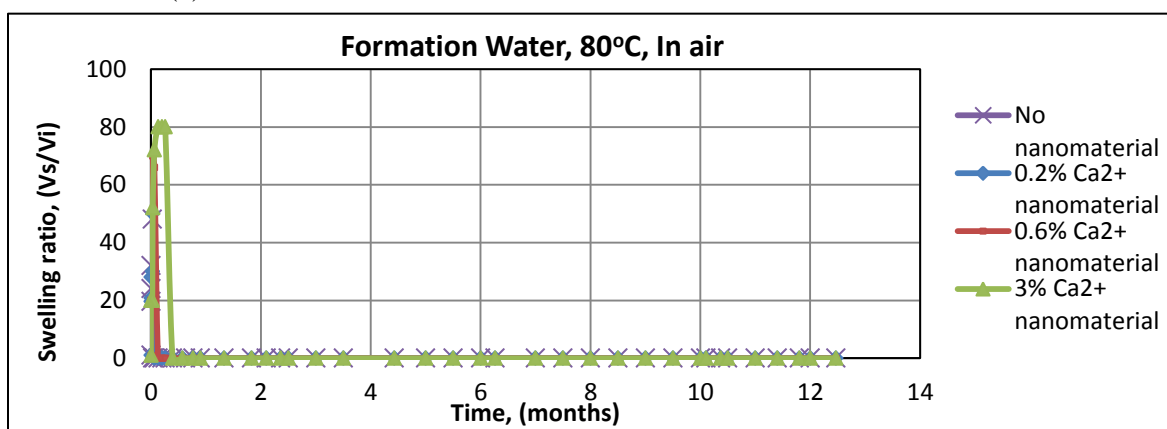
Figure 5.10. a-f: Longterm Thermal Stability of Ca^{2+} Nanocomposite PPG Under Aerobic Conditions and In 1% Brine Solution and Formation Water.



(d)



(e)

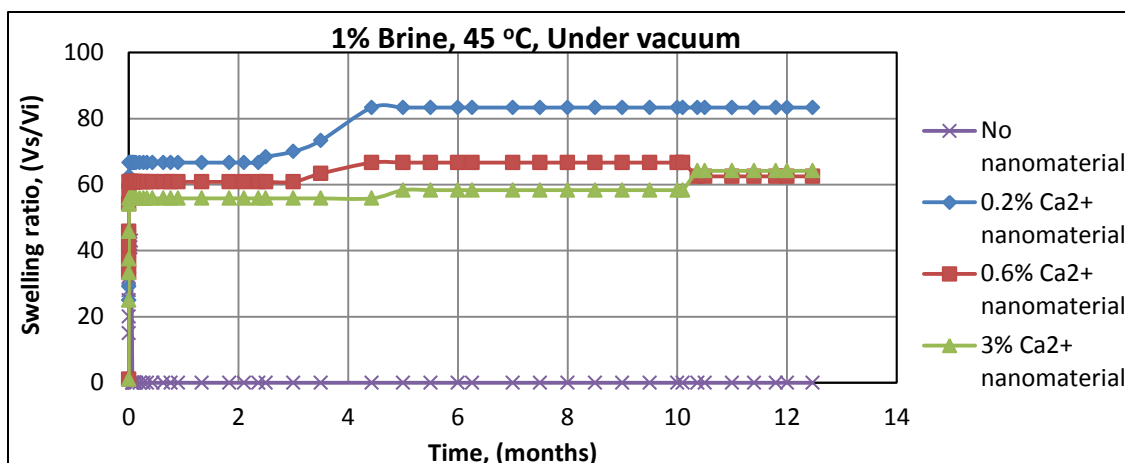


(f)

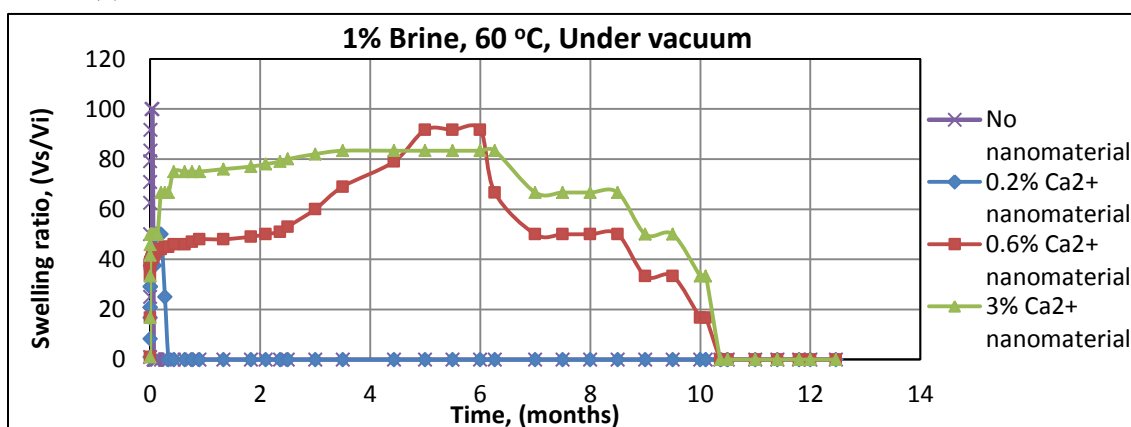
Figure 5.10. a-f: Longterm Thermal Stability of Ca²⁺ Nanocomposite PPG Under Aerobic Conditions and In 1% Brine Solution and Formation Water. (Cont).

(II) Swelling kinetics and thermal resistance under vacuum: Figures 5.11a-f present longterm testing in anaerobic conditions using both 1% brine and formation water. The reason for testing gel degradation under anaerobic conditions was to simulate reservoir environment where oxygen amounts are minimal. Oxidation in presence of oxygen causes gel to degrade much faster. Therefore, it was necessary to remove every trace of oxygen in order to avoid premature gel breakdown.

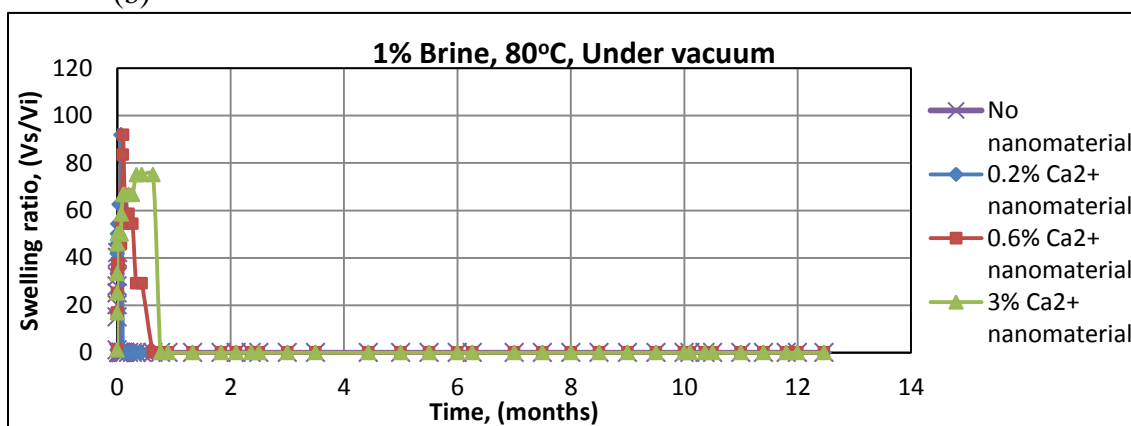
Comparing Figure 5.10 and 5.11, it is observed that on average, it takes a much longer time for gels to degrade in anaerobic conditions than in aerobic conditions. For example, comparing Figure 5.10d and Figure 5.11d, in Figure 5.10d (under aerobic conditions), nanocomposite gel with 3% calcium nanomaterial degraded under about 5.7 months. However in Figure 5.11d (under anaerobic conditions) gel degradation occurred in about 10 months. It took about 4.3 more months for PPGs to degrade when oxygen was removed.



(a)

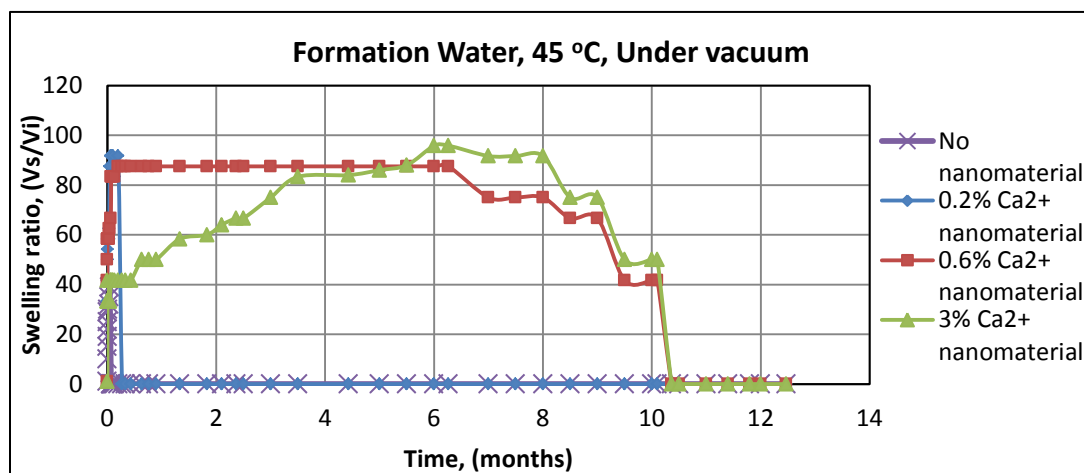


(b)

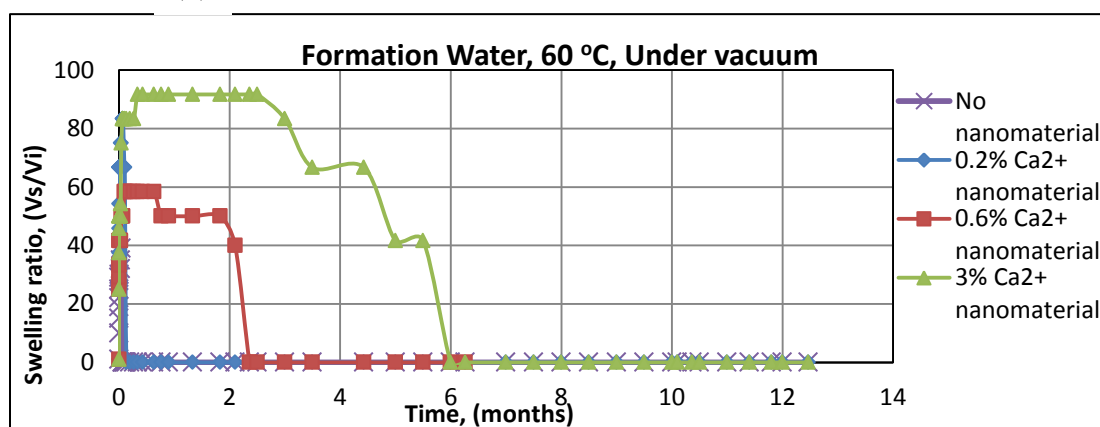


(c)

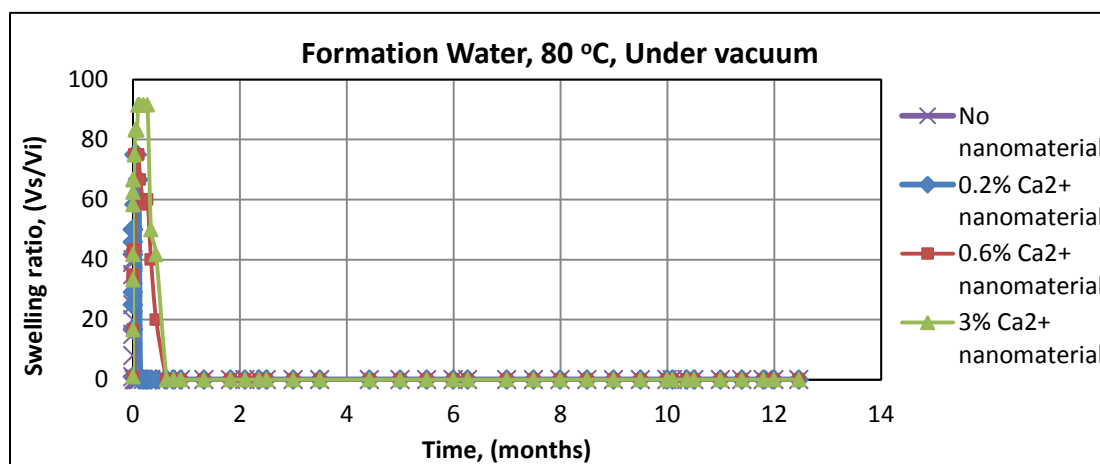
Figure 5.11. a-f: Longterm Thermal Stability of Ca²⁺ Nanocomposite PPG Under Anaerobic Conditions and In 1% Brine Solution and Formation Water.



(d)



(e)



(f)

Figure 5.11. a-f: Longterm Thermal Stability of Ca²⁺ Nanocomposite PPG Under Anaerobic Conditions and In 1% Brine Solution and Formation Water. (Cont).

5.2.1.3 Increased post-degradation viscosity of Ca^{2+} nanocomposite PPG. As with LXLG Nanocomposite PPG, the viscosity of the degraded Ca^{2+} Nanocomposite PPG was also measured. Figure 5.12 presents a picture of Ca^{2+} Nanocomposite PPG both before and after their degradation in both aerobic and anaerobic environment.

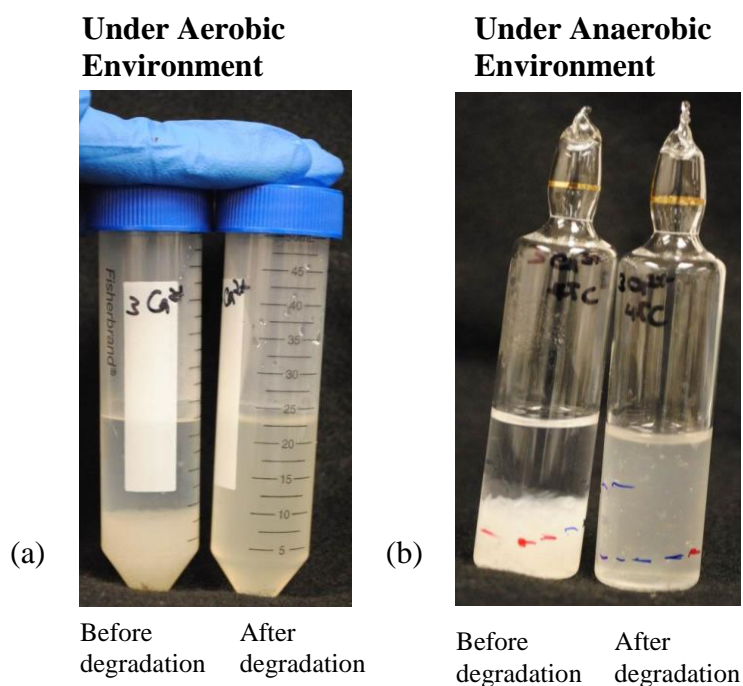


Figure 5.12. Aerobic and Anaerobic Environment of Ca^{2+} Nanocomposite PPG Samples Tested Showing both Before and After Sample Degrades Into Polymer Solution.

The results of viscosity measurements are presented in Table 5.2. As earlier explained in Sections 5.1.1.3, the nanocomposite PPG initially serves in conformance control by plugging water-thief streaks. After an extended time period however, nanocomposite PPG degrades into linear polymer solution which moves deeper into formation to enhance secondary polymer flooding.

However, it was observed that the highest viscosity of the degraded Ca^{2+} Nanocomposite PPG (75.5 cp) does not even equate the viscosity of the degraded hydrogel with no nanomaterial (170 cp). Therefore we suggest that Ca^{2+} Nanocomposite PPG can only be used in plugging water-thief channels, and not in enhancing secondary polymer flooding, since its degraded viscosity is negligible.

Table 5.2. Viscosity Measurements For Pure PAM Polymer, Pure Ca^{2+} MMT Nanomaterial, and Degraded Ca^{2+} Nanocomposite PPG.

| Concentration (%) | Pure Polyacrylamide Polymer (PAM) | Pure Ca^{2+} MMT Nanomaterial | Degraded Ca^{2+} Nanocomposite PPG | | Degraded Hydrogel with No Nanomaterial |
|-------------------|-----------------------------------|--|---|-----------------------------|--|
| | Viscosity, (cp) | Viscosity, (cp) | Viscosity, (cp) - Aerobic | Viscosity, (cp) - Anaerobic | Viscosity, (cp) |
| 0.20% | 30.6 | 2 | 3 | 18.15 | 170 |
| 0.60% | 107.2 | 3.5 | 5 | 30 | |
| 1% | 353.5 | 4.5 | 11 | -- | |
| 3% | 6303 | 6 | 13 | 75.5 | |
| 5% | 48340 | 12 | 17 | -- | |

5.2.2. Evaluation of Ca^{2+} Nanocomposite PPG Microstructure and Morphology, Before and After Degradation. Firstly, before degradation results are presented.

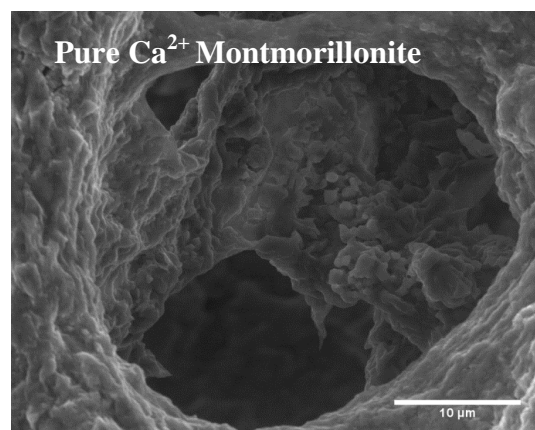
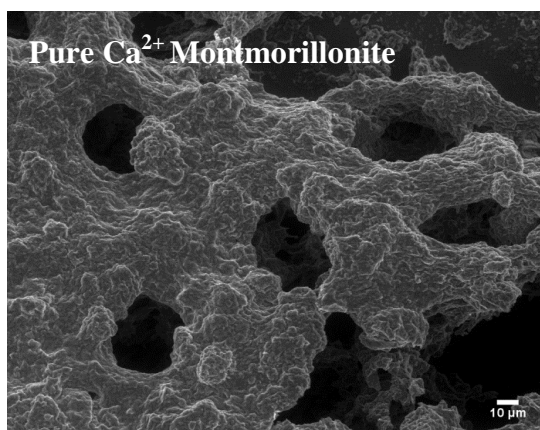
5.2.2.1 Environmental scanning electron microscopy imaging of Ca^{2+} nanocomposite PPG before its degradation. Similar to the ESEM studies conducted in Section 5.1.2.1 above for LXLG Nanocomposite PPG, a detailed microscopic study of Ca^{2+} Nanocomposite PPG was likewise done using an Environmental Scanning Electron Microscope (ESEM), and was compared against hydrogels with no nanomaterial. Studying the network structure of hydrogel is important because it gives us information about pore-interconnectivity. This information is useful in

understanding the mechanisms of gel swelling behavior, gel strength after it swells, and perhaps even its thermal resistance ability.

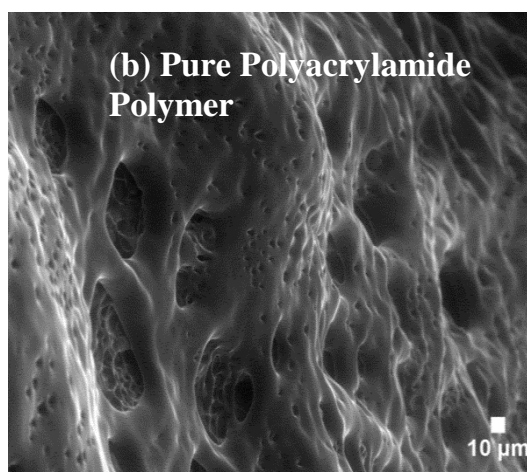
Figure 5.13a presents an ESEM micrograph of pure Calcium Montmorillonite nanomaterial. Figure 5.13b presents an ESEM micrograph of pure polyacrylamide (PAM) polymer. Figure 5.13c presents a micrograph of hydrogel with no nanomaterial. The micrographs of Ca^{2+} Nanocomposite PPG swelled in 1% Brine is presented in Figure 5.13d. A very conspicuous porous network structure is seen. Figure 5.13e presents the ESEM micrographs of Ca^{2+} nanocomposite PPG swelled in distilled water. In distilled water, the conspicuous porous network structure diminishes.

Contrasting the hydrogel with no nanomaterial versus the hydrogel with nanomaterial, (that is Figures 5.13c versus Figures 5.13d –e), we observe that although a porous interconnected network structure is seen in both nanocomposite and non-nanocomposite hydrogels, in Ca^{2+} Nanocomposite PPG however (Figures 5.13d-e), the network structure is more conspicuous, thicker, denser, and corrugated whereas in hydrogels with no nanomaterial, the network structure is finer, less dense, and smooth. Obviously, we say that the presence of Calcium Montmorillonite nanomaterial in nanocomposite hydrogel affords this difference.

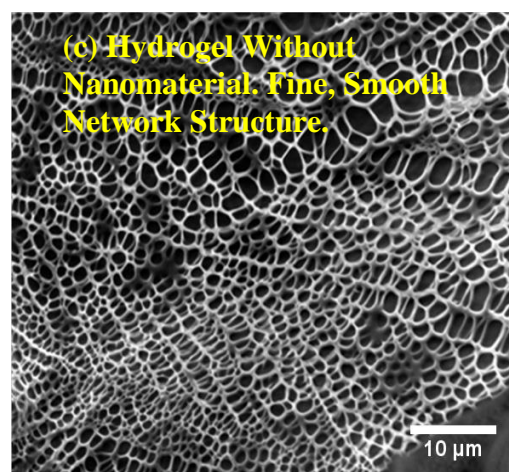
Author herein mentions that when brine was used as the solvent, the network structure is extremely conspicuous (Figure 5.13d) such that the pores are very clearly visible. However, when distilled water was used as the solvent, the conspicuousness of the network structure diminishes. The reason for this occurrence is not fully understood. An opposite phenomenon was observed by Nelea et al., 2007. In their work, they instead observed that the network structure was very conspicuous when distilled water was used, and when brine was used, the network was less visible.



(a) Pure Ca^{2+} Montmorillonite

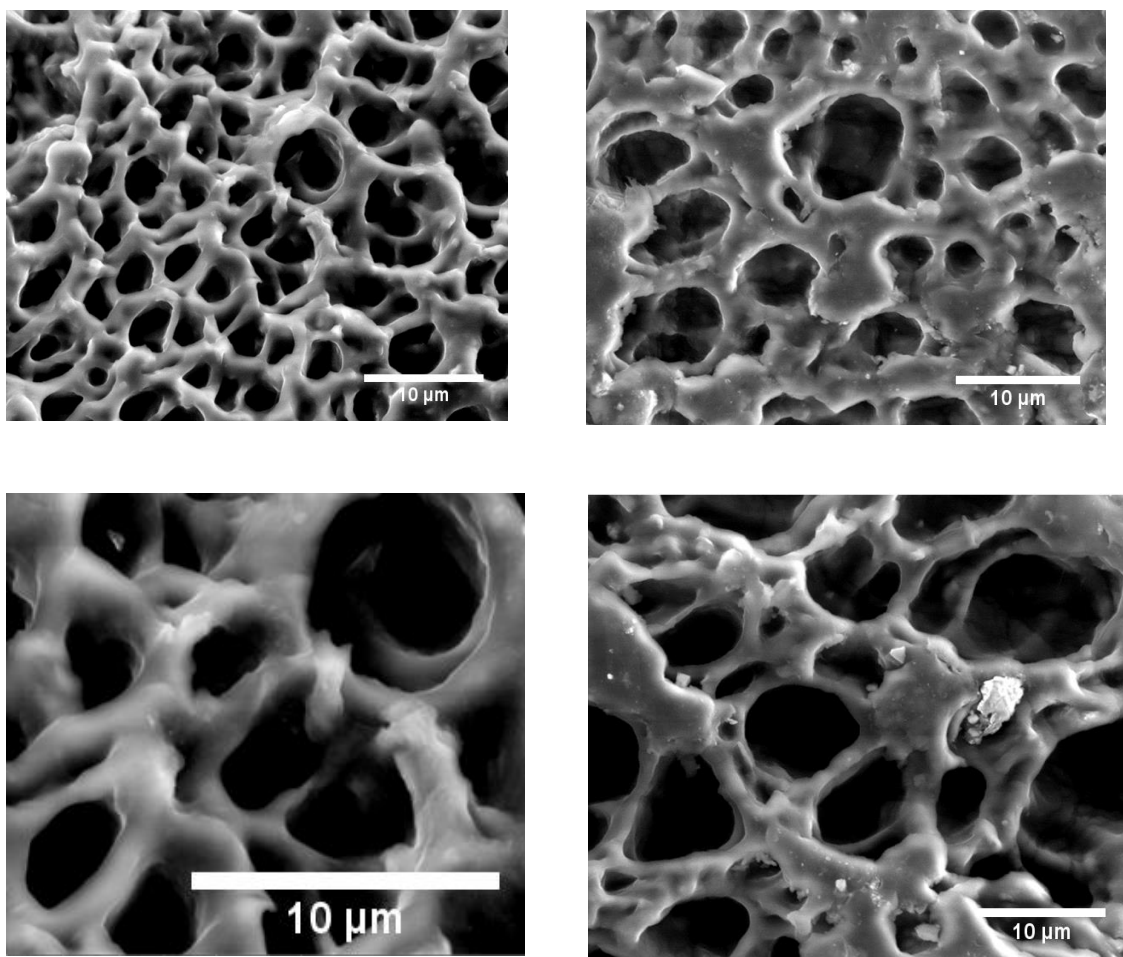


**(b) Pure Polymer (PAM)
Solution**



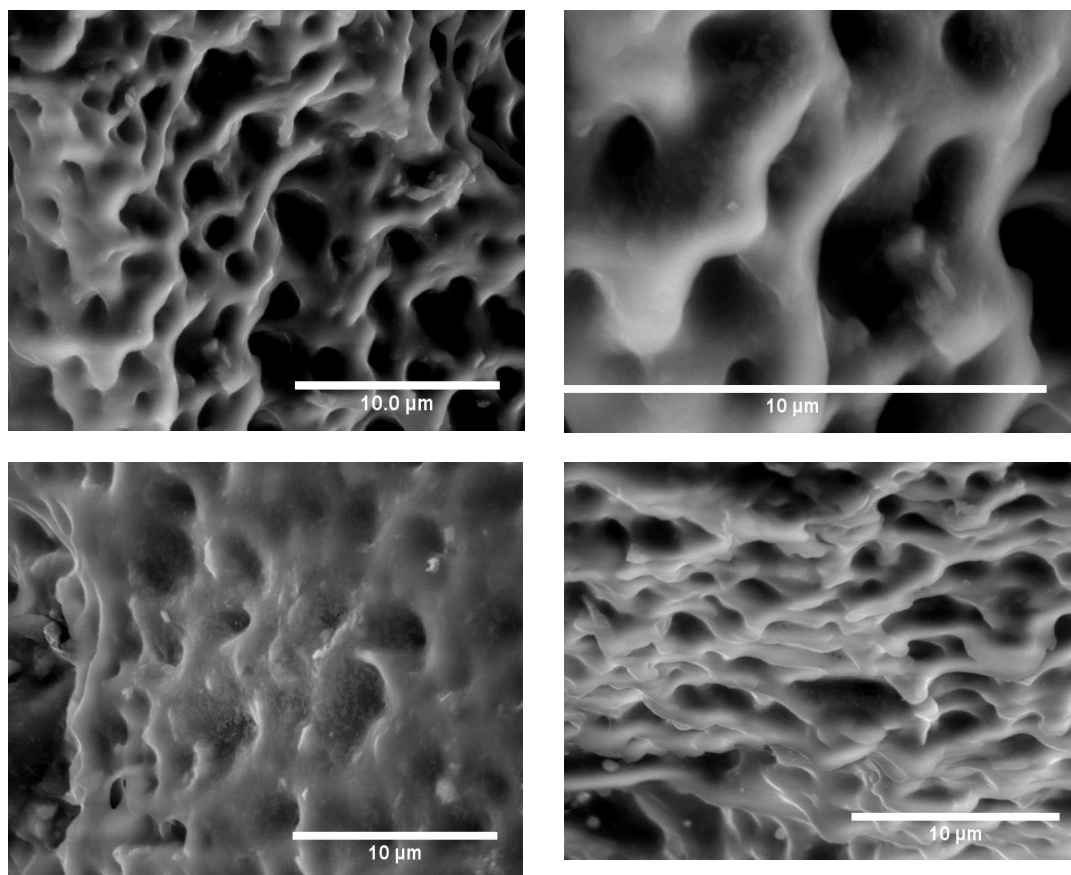
**(c) Fine, Smooth Network Structure
of Hydrogel With No
Nanomaterial (Jia, 2011)**

Figure 5.13. Before-degradation Environmental Scanning Electron Microscopy (ESEM) Micrographs.



(d) ESEM Micrographs of Ca²⁺ Nanocomposite PPG Swelled in 1% Brine.

Figure 5.13. Before-degradation Environmental Scanning Electron Microscopy (ESEM).
(Cont).

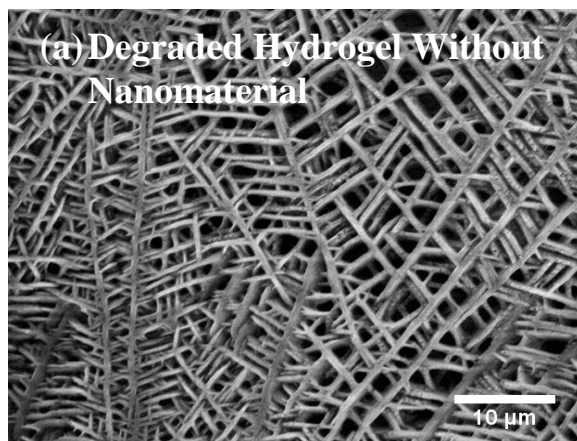


(e) ESEM Micrographs of Ca^{2+} Nanocomposite PPG Swelled in Distilled Water.

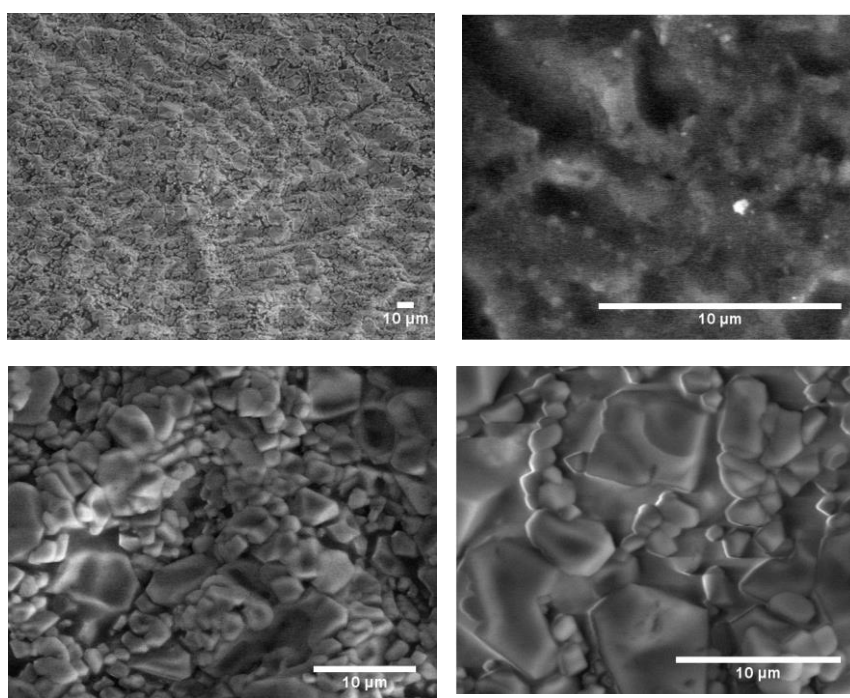
Figure 5.13. Before-degradation Environmental Scanning Electron Microscopy (ESEM) Micrographs. (Cont).

5.2.2.2 Environmental scanning electron microscopy imaging of Ca^{2+} nanocomposite PPG after its degradation. After the Ca^{2+} Nanocomposite PPG degraded, ESEM micrographs were again taken of the degraded sample. Figure 5.14a shows the micrograph of the degraded hydrogel with no nanomaterial. Figures 5.14b show the micrographs of a 3% degraded Ca^{2+} Nanocomposite PPG. As is clearly seen in both non-nanocomposite (Figure 5.14a) and nanocomposite gel (Figures 5.14b), the homogenous porous network structure that was initially observed before degradation disappears (collapses) into block-like structures in degraded Ca^{2+} Nanocomposite PPG

and into ridge-like structures in degraded gel without nanomaterial. This signifies the degradation of the gel material into a polymer solution.



(a) Degraded Hydrogel with No Nanomaterial (Jia, 2011).



(b) Degraded 3% Ca^{2+} Nanocomposite PPG: Tiny Block-like Particles are Observed

Figure 5.14. After-degradation Environmental Scanning Electron Microscopy (ESEM) Micrographs.

5.2.2.3 Optical microscopy imaging of Ca^{2+} nanocomposite PPG after degradation. After the Ca^{2+} Nanocomposite PPG degraded, we utilized an optical microscope to help us understand the nature of the degraded nanocomposite material. Figure 5.15 presents an optical micrograph of a 0.2% Ca^{2+} Nanocomposite gel after degradation. Gel composition is 23% acrylamide, 100 ppm ammonium persulfate initiator and 1500 ppm PEG crosslinker. We observed very few and tiny particles which were sparsely scattered across the entire sample and had an approximate size of about 3 microns (Figure 5.15). These smaller particles can travel deeper into the formation to mobilize additional oil.

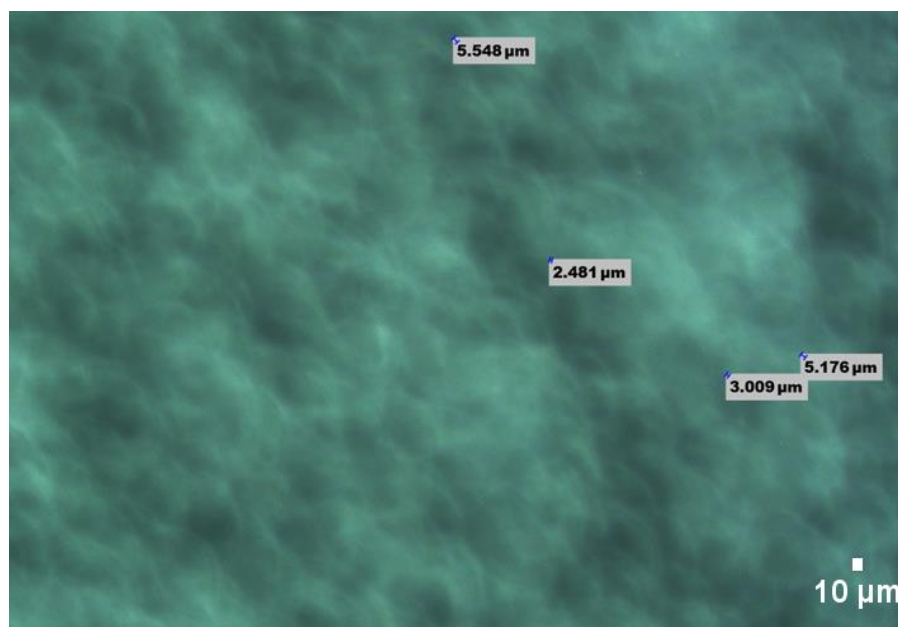


Figure 5.15. Optical Microscopy Micrograph of Degraded 0.2% Ca^{2+} Nanocomposite PPG.

5.3. EVALUATION OF DEGRADABLE NANOCOMPOSITE PREFORMED PARTICLE GEL WITH SODIUM MONTMORILLONITE AS NANOMATERIAL (Na^+ NANOCOMPOSITE PPG)

5.3.1. Improvement in Na^+ Nanocomposite PPG Properties with Incorporation of Nanomaterials. The following properties were studied:

5.3.1.1 Increased mechanical strength. The third and last type of nanocomposite hydrogel that was studied was that made using Sodium Montmorillonite as the nanomaterial (Na^+ Nanocomposite PPG). The rheology behavior of dry Na^+ Nanocomposite PPG and hydrogels with no nanomaterial were studied. The variation in elastic modulus (G') with time for Na^+ Nanocomposite PPG with 0.2%, 0.6%, and 3% Na^+ nanomaterial is presented in Figure 5.16 and is compared against hydrogel with no nanomaterial. It is observed from Figure 5.16 that the elastic modulus significantly increases with increasing nanomaterial concentration. The elastic modulus of hydrogel with no nanomaterial is at lowest value of 800 Pa, while hydrogel with 3% Na^+ nanomaterial has an elastic modulus of about 6300 Pa. Clearly, an increase in gel strength is observed as nanomaterial is introduced.

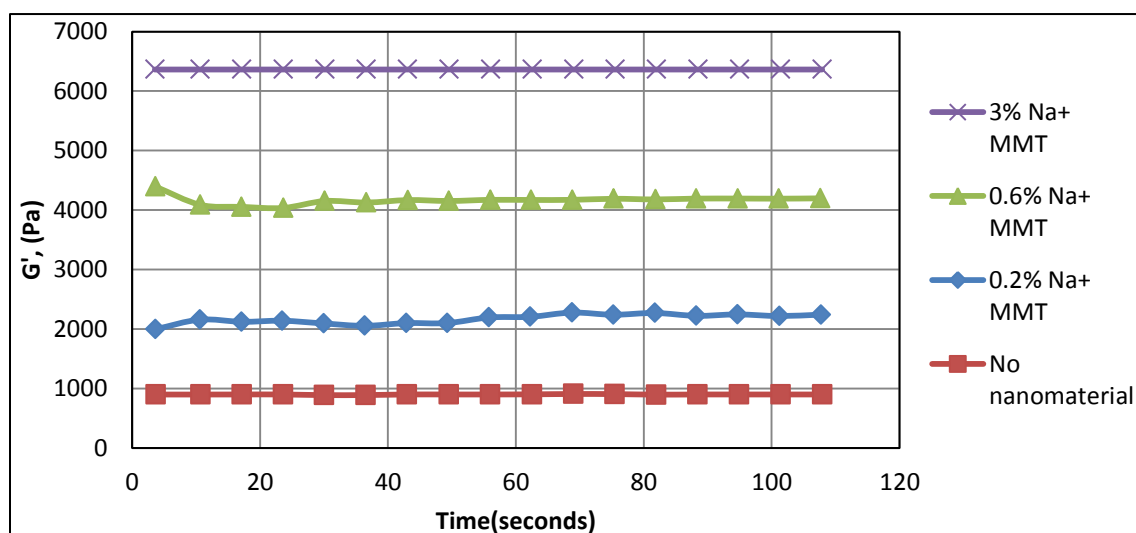


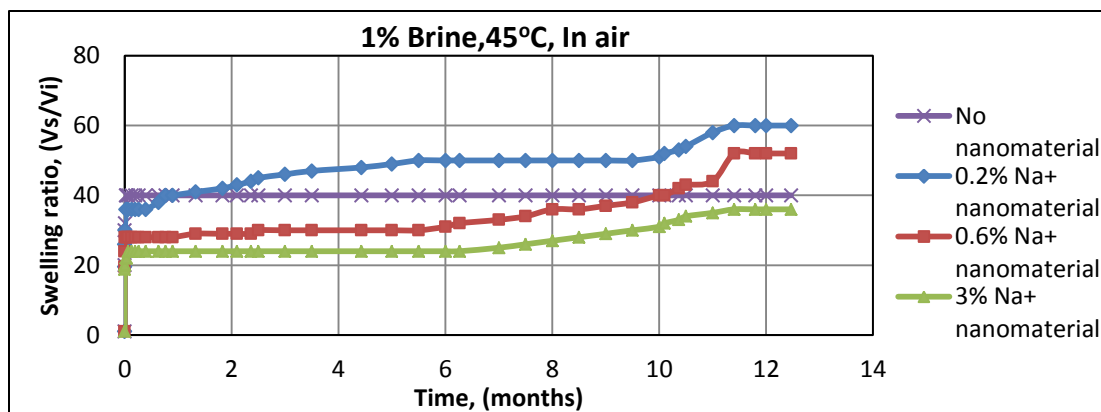
Figure 5.16. An Obvious Improvement in Hydrogel Mechanical Strength is Observed Between Na^+ Nanocomposite PPGs and Those Without Nanomaterials.

5.3.1.2 Increased swelling and thermal resistance. (I) Swelling kinetics and thermal resistance in presence of air: Similar to the swelling kinetics and thermal resiliency for LXLG and Ca^{2+} nanocomposite PPG studied in Sections 5.1.1.2 and 5.2.1.2 above, a similar study was conducted for Na^+ Nanocomposite PPG. Once injected downhole into fractures or high permeability streaks, the longterm thermal resiliency of hydrogels to continuously seal fractures under adverse reservoir conditions is important. Without longterm endurance, gels rapidly degrade, leading to a re-opening of an already sealed fracture, thus re-creating a water-thief channel.

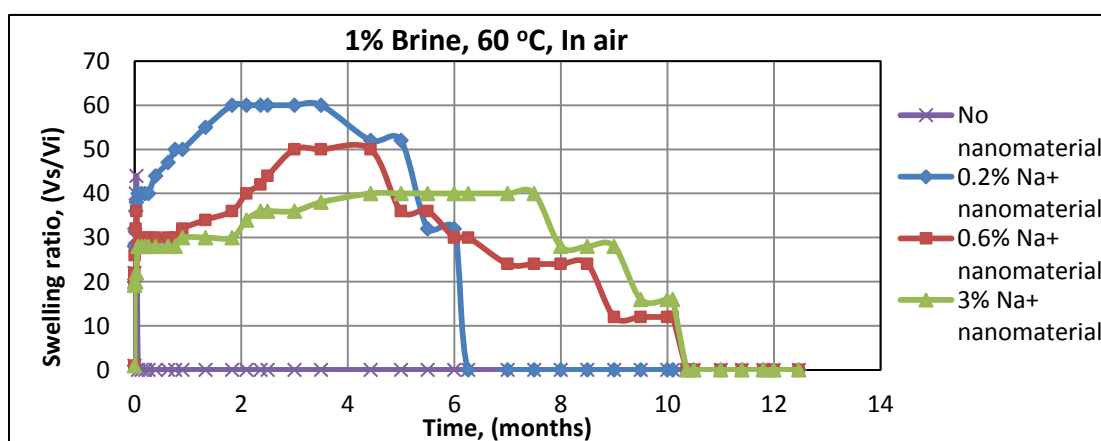
Therefore, ensuring hydrogels can adequately seal fractures over a prolonged period of time is paramount. Longterm thermal testing was done both under aerobic (in presence of oxygen) and anaerobic (under vacuum, in absence of oxygen) conditions. Aerobic oxidation in presence of oxygen causes gel to degrade much faster. Therefore, it was necessary to remove every trace of oxygen in order to avoid premature gel breakdown. This also simulates downhole reservoir environment where oxygen concentration is minimal. Furthermore, testing was done using both brine and formation water respectively as the solvent. Additionally, testing was done under three different temperatures: 45°C, 60 °C, and 85 °C so as to mimic different reservoir temperatures.

Figures 5.17a-f present longterm testing in aerobic conditions using both 1% brine and formation water. As is clearly seen from Figure 5.17a-f, hydrogels with no nanomaterial rapidly degraded within days whereas for hydrogels with 0.2% Na^+ , 0.6% Na^+ , and 3% Na^+ nanomaterial, degradation occurred over several months in some cases and in others, Na^+ Nanocomposite PPGs have not yet degraded.

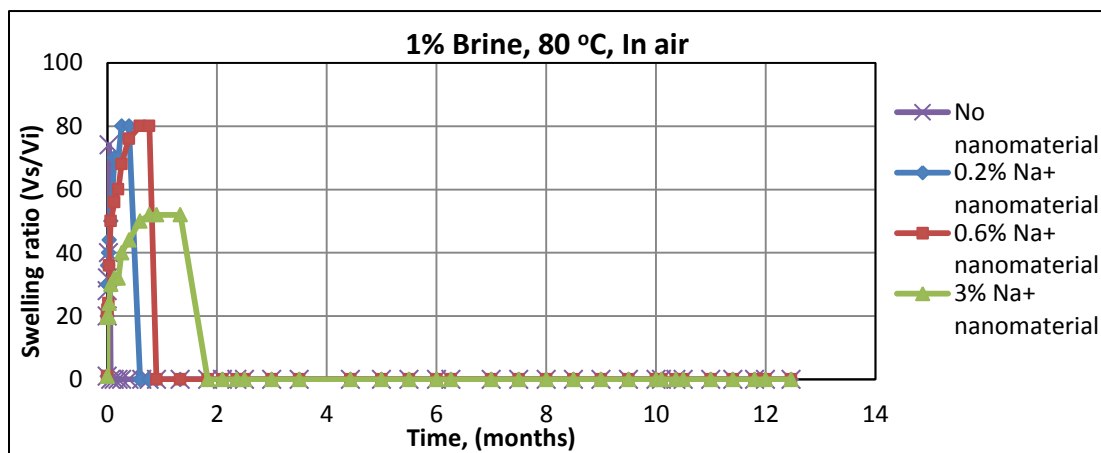
Additionally, it was observed that an increase in nanomaterial concentration led to an increase in longterm thermal resistance of hydrogels. This is as expected because increasing nanomaterial concentration leads to an increased participation of nanomaterial in the gelation process, affording a stronger gel. Such dramatic improvement in longterm thermal stability of nanocomposite hydrogels is one key reason it is believed they are potentially valuable in conformance control applications.



(a)

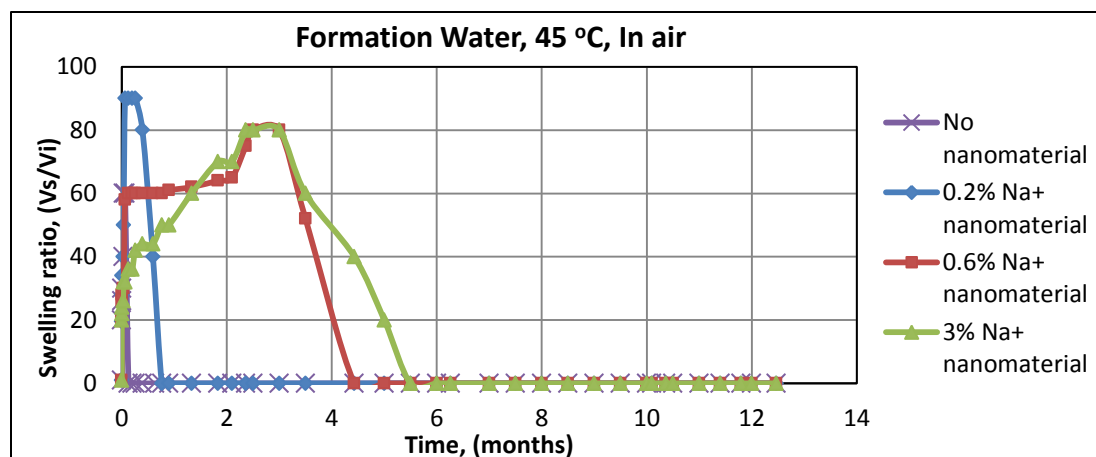


(b)

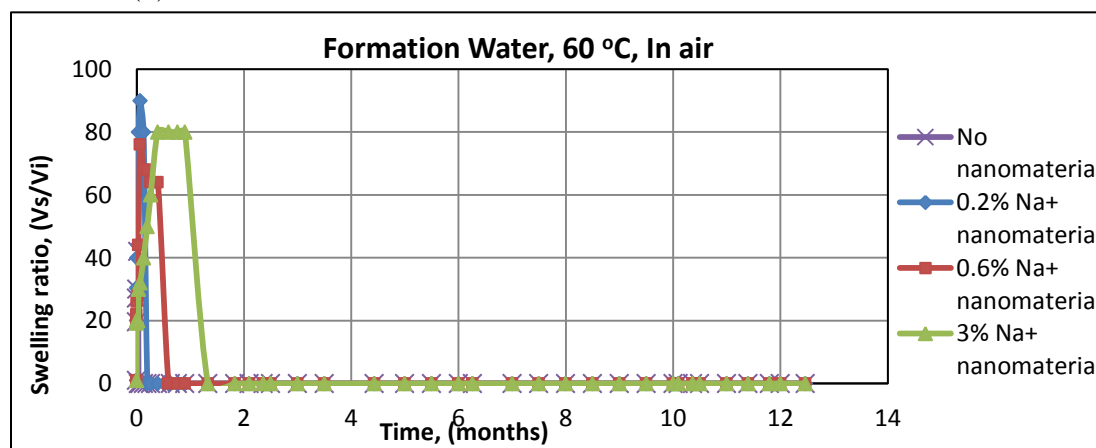


(c)

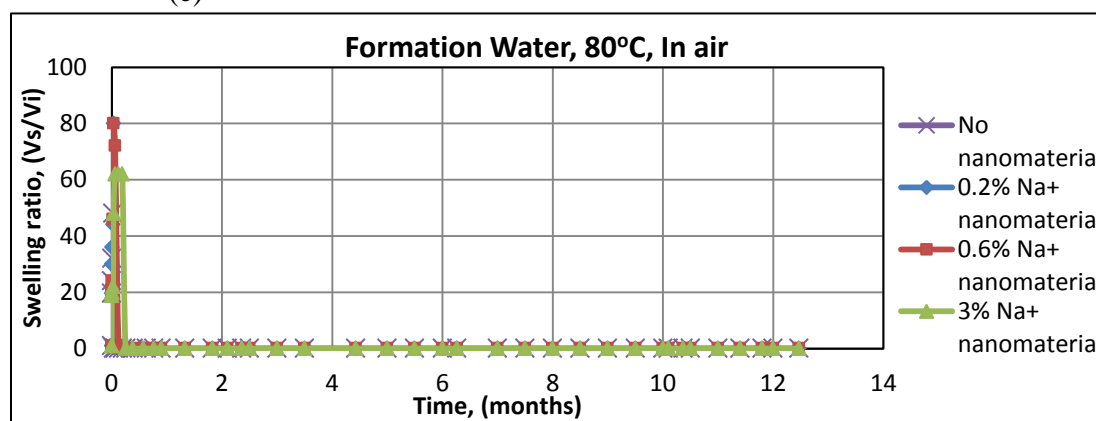
Figure 5.17. a-f: Longterm Thermal Stability of Na⁺ Nanocomposite PPG Under Aerobic Conditions and in 1% Brine Solution and Formation Water.



(d)



(e)

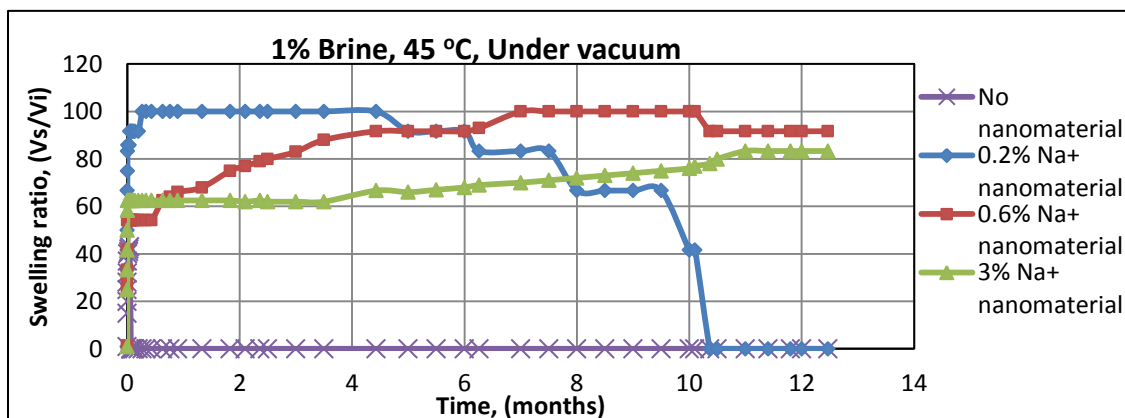


(f)

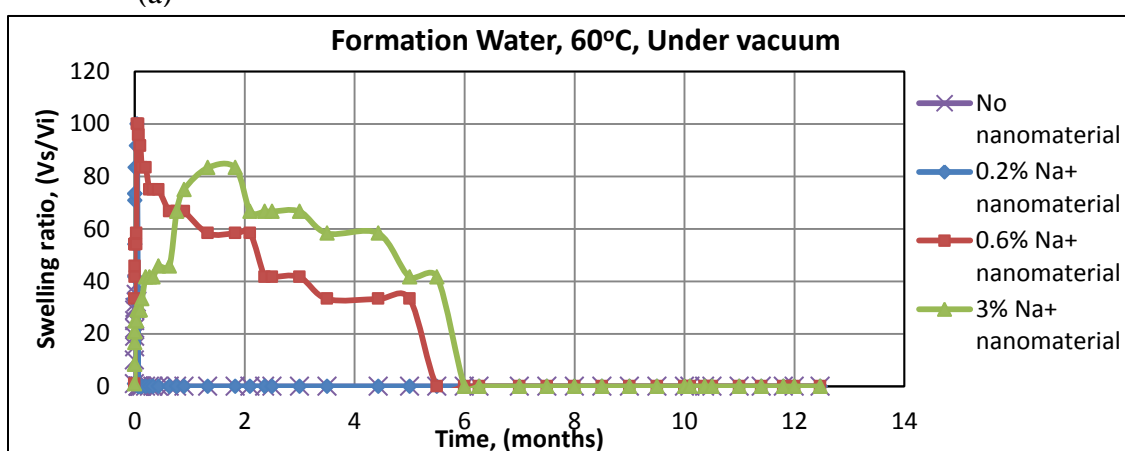
Figure 5.17. a-f: Longterm Thermal Stability of Na⁺ Nanocomposite PPG Under Aerobic Conditions and in 1% Brine Solution and Formation Water. (Cont).

(II) Swelling kinetics and thermal resistance under vacuum. Figures 5.18a-f present longterm testing of Na^+ Nanocomposite PPGs in anaerobic conditions using both 1% brine and formation water. The reason for testing gel degradation under anaerobic conditions was to simulate reservoir environment where oxygen amounts are minimal. Oxidation in presence of oxygen causes gel to degrade much faster. Therefore, it was necessary to remove every trace of oxygen in order to avoid premature gel breakdown.

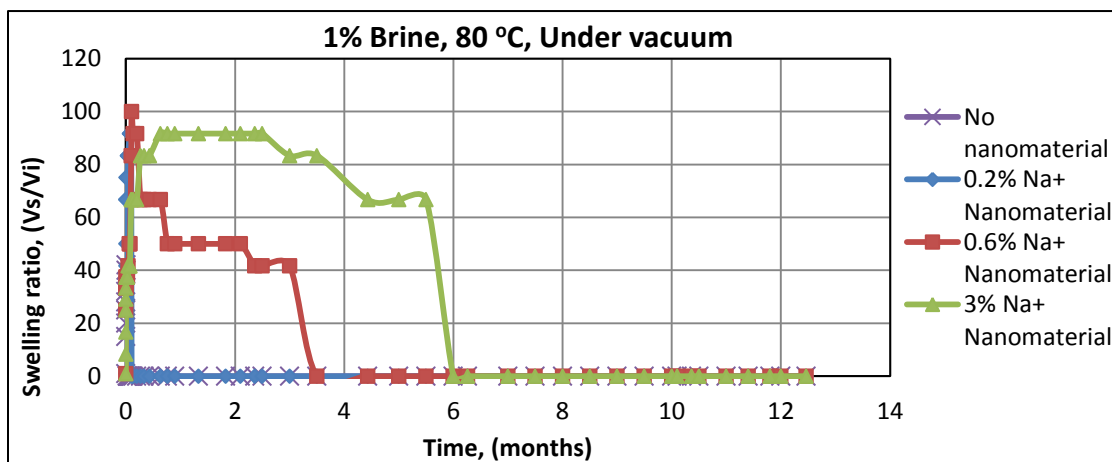
Comparing Figure 5.18 and 5.17, we observe that on average, it takes a much longer time for gels to degrade in anaerobic conditions than in aerobic conditions. For example, comparing Figure 5.17c and Figure 5.18c, in Figure 5.17c (under aerobic conditions), nanocomposite gel with 3% Ca^{2+} nanomaterial degraded under about 1.9 months. However in Figure 5.18c (under anaerobic conditions) gel degradation occurred in about 6 months. It took an additional 4 months to degrade when oxygen was removed.



(a)

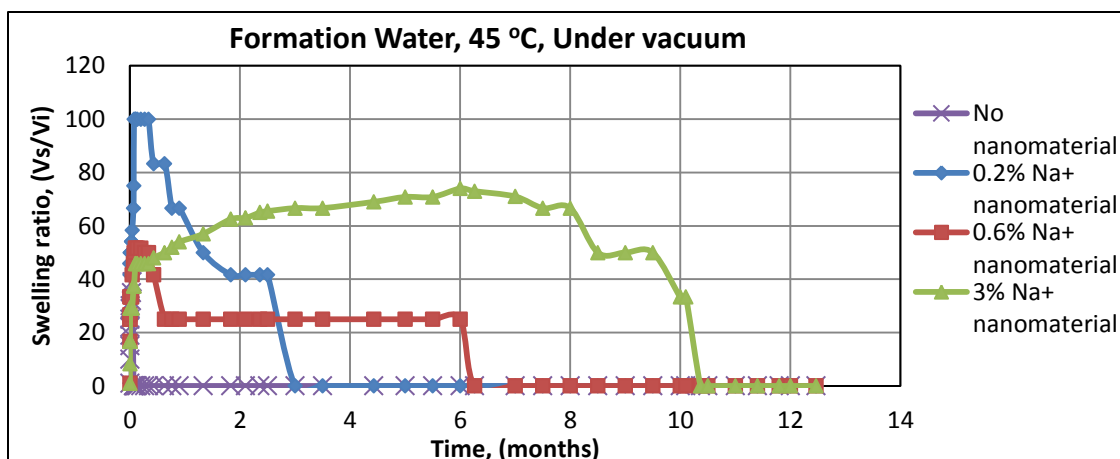


(b)

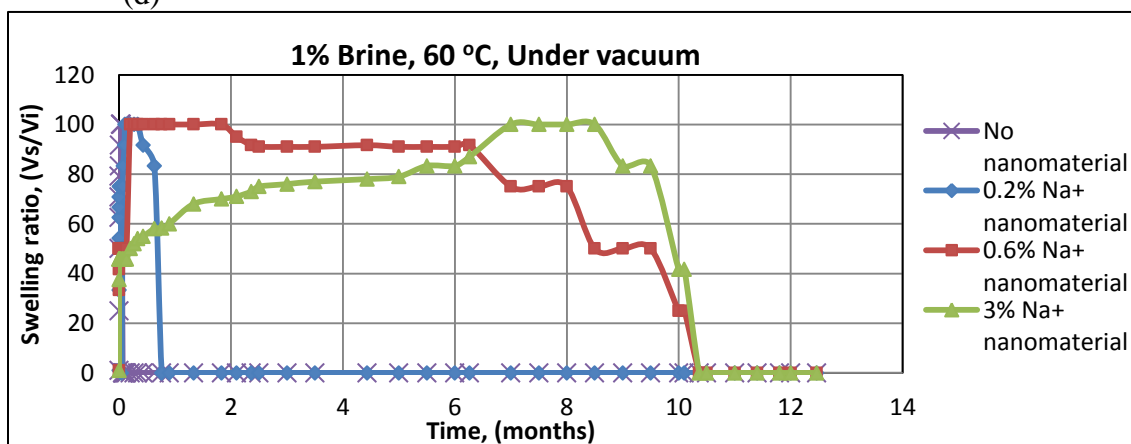


(c)

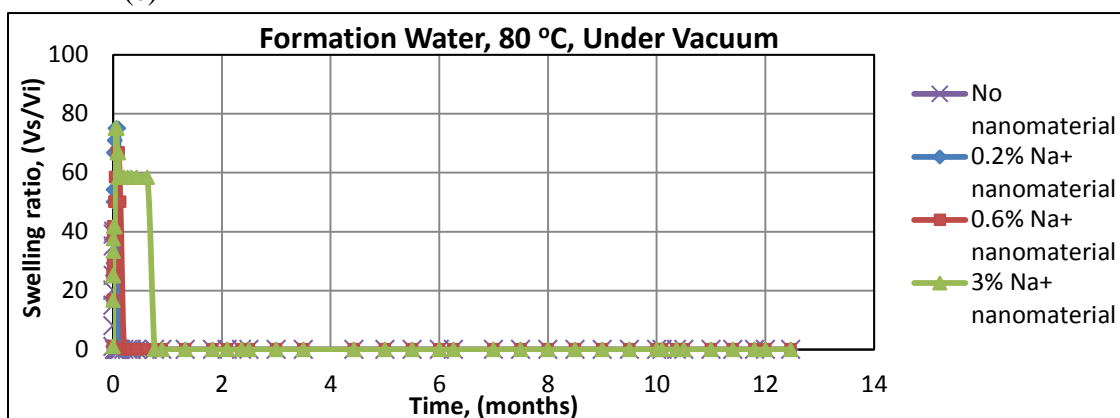
Figure 5.18. a-f: Longterm Thermal Stability of Na⁺ Nanocomposite Hydrogels Under Anaerobic Conditions and in 1% Brine Solution and Formation Water.



(d)



(e)



(f)

Figure 5.18. a-f: Longterm Thermal Stability of Na⁺ Nanocomposite Hydrogels Under Anaerobic Conditions and in 1% Brine Solution and Formation Water.(Cont).

5.3.1.3 Increased post-degradation viscosity of Na^+ nanocomposite PPG.

Similar to the viscosity measurements done for LXLG and Ca^{2+} Nanocomposite PPGs, the viscosity of degraded Na^+ Nanocomposite PPG was also measured. Figure 5.19 presents a picture of Na^+ Nanocomposite PPG both before and after their degradation in both aerobic and anaerobic environment.

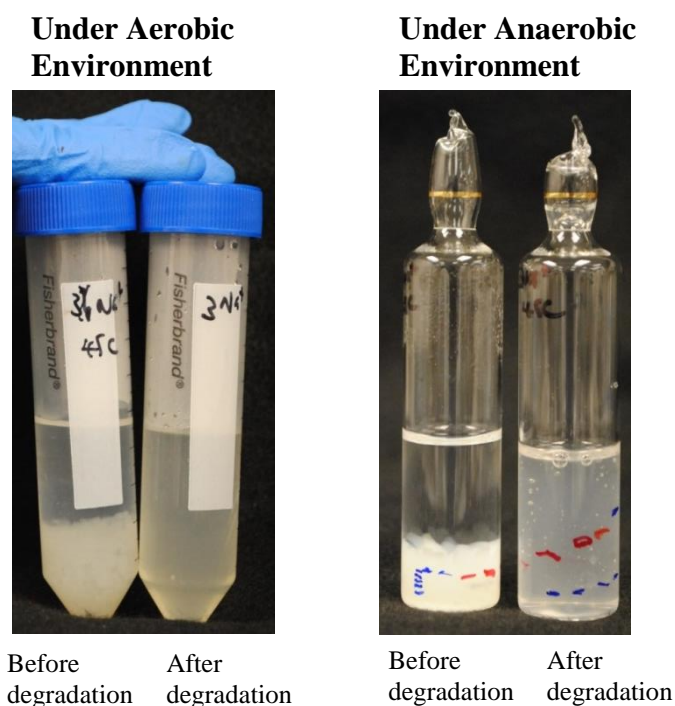


Figure 5.19. Aerobic and Anaerobic Environment of Na^+ Nanocomposite PPG Samples Tested Showing both Before and After Sample Degrades Into Polymer Solution.

The results of viscosity measurements are presented in Table 5.3. As earlier explained in Section 5.1.1.3 and Section 5.2.1.3, the nanocomposite PPG initially serves in conformance control by plugging water-thief streaks. After an extended time period however, nanocomposite PPG degrades into linear polymer solution which moves deeper into formation to enhance secondary polymer flooding.

However, it was observed that the highest viscosity of the degraded Na^+ Nanocomposite PPG (129 cp) is even less than the viscosity of the degraded hydrogel with no nanomaterial (170 cp). Therefore we suggest that Na^+ Nanocomposite PPG can only be used in plugging water-thief channels, and not in enhancing secondary polymer flooding, since its degraded viscosity is negligible.

Table 5.3. Viscosity Measurements For Pure Polymer, Pure Na^+ MMT Nanomaterial, and Degraded Na^+ Nanocomposite PPG.

| Concentration (%) | Pure Polyacrylamide Polymer (PAM) | Pure Na^+ MMT Nanomaterial | Degraded Na^+ MMT Nanocomposite PPG | | Degraded Hydrogel with No Nanomaterial |
|-------------------|-----------------------------------|-------------------------------------|--|-----------------------------|--|
| | Viscosity, (cp) | Viscosity, (cp) | Viscosity, (cp) - Aerobic | Viscosity, (cp) - Anaerobic | Viscosity, (cp) |
| 0.20% | 30.6 | 1.5 | 1.5 | 78.2 | 170 |
| 0.60% | 107.2 | 2 | 6 | 90 | |
| 1% | 353.5 | 4 | 10 | -- | |
| 3% | 6303 | 140 | 170 | 129 | |
| 5% | 48340 | 350 | 479 | -- | |

5.3.2. Evaluation of Na^+ Nanocomposite PPG Microstructure and Morphology, Before and After Degradation. Before degradation results are first presented.

5.3.2.1 Environmental scanning electron microscopy imaging of Na^+ nanocomposite PPG before its degradation. Similar to the ESEM studies conducted in Sections 5.1 and 5.2 above for LXLG and Ca^{2+} Nanocomposite PPG, a detailed microscopic study of Na^+ Nanocomposite PPG was likewise done using an Environmental Scanning Electron Microscope (ESEM), and was compared against hydrogels with no nanomaterial. Studying the network structure of hydrogel is important

because it gives us information about pore-interconnectivity. This information is useful in understanding the mechanisms of gel swelling behavior, gel strength after it swells, and perhaps even its thermal resistance ability.

Figure 5.20a presents ESEM micrographs of pure Sodium Montmorillonite nanomaterial. Figure 5.20b presents an ESEM micrograph of pure polyacrylamide (PAM) polymer. Figure 5.20c presents the 3-D bulk Micrograph of Na^+ Nanocomposite PPG. Figure 5.20d presents a micrograph of hydrogel with no nanomaterial. The micrographs of Na^+ Nanocomposite PPG swelled in 1% Brine is presented in Figure 5.20e. Figure 5.20f presents the ESEM micrographs of nanocomposite hydrogel with distilled water as the solvent. A very conspicuous porous network structure is seen.

Contrasting the hydrogel with no nanomaterial versus the hydrogel with nanomaterial, (that is Figures 5.20d versus Figures 5.20e –f), it was observed that although a porous interconnected network structure is seen in both Na^+ Nanocomposite PPG and non-nanocomposite hydrogels, in Na^+ Nanocomposite PPG however (Figures 5.20e-f), the network structure is more conspicuous, thicker, denser, and corrugated whereas in hydrogels with no nanomaterial, the network structure is finer, less dense, and smooth. Obviously, the presence of Sodium Montmorillonite nanomaterial in nanocomposite hydrogel affords this difference.

Author is also quick to point out that when brine was used as the solvent, the network structure was extremely dense (Figure 5.20e) such that the pores in the network are almost closed up. However, this phenomenon was not observed when distilled water was used as the solvent (Figure 5.20f). In distilled water, the network structure is extremely conspicuous, such that the pores are very clearly visible. In an attempt to explain this phenomenon, we could only ascribe the presence of salt ions in the brine as a reason for this occurrence.

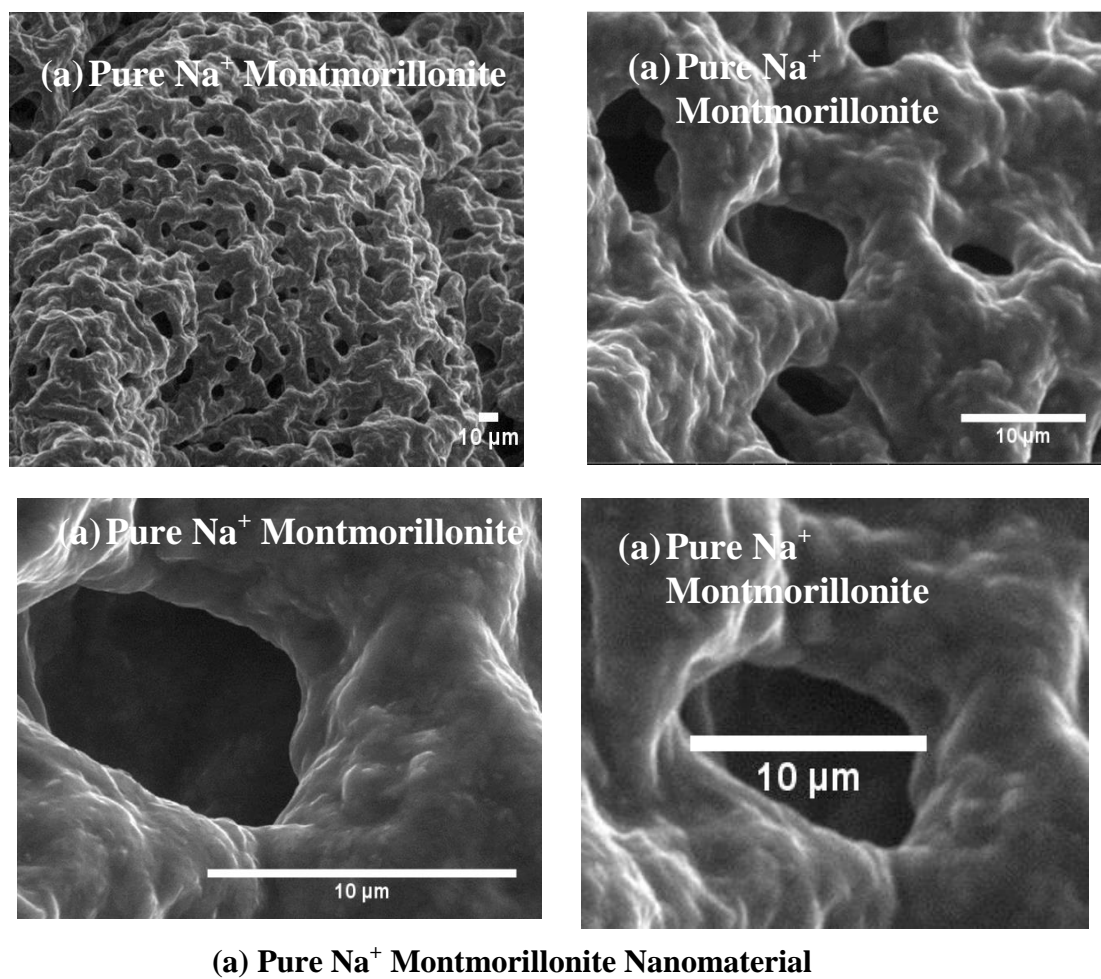
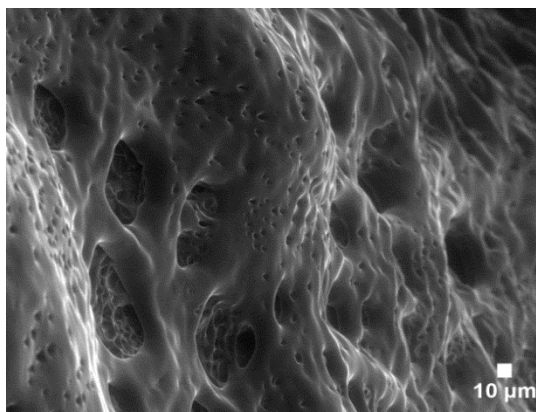
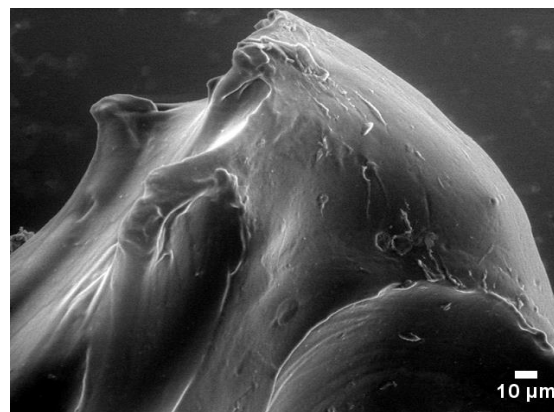


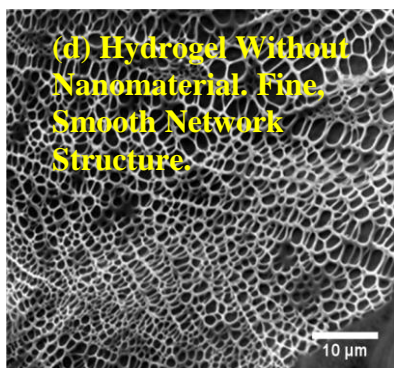
Figure 5.20. Before-degradation Environmental Scanning Electron Microscopy (ESEM) Micrographs.



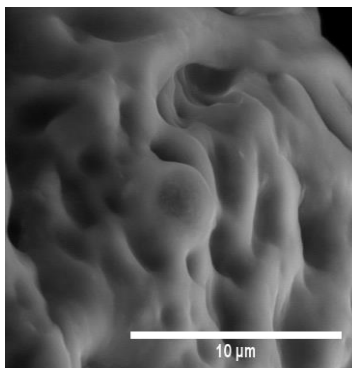
(b) Pure Polyacrylamide (PAM) Polymer Solution



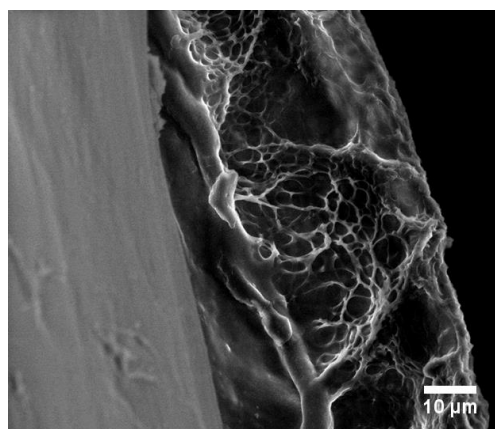
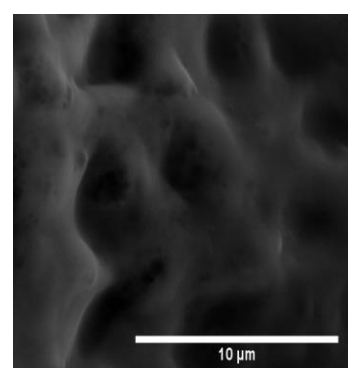
(c) 3-D bulk Micrograph of Na⁺ Nanocomposite PPG



(d) Fine, Smooth Network Structure of Hydrogel with No Nanomaterial (Jia, 2011)



(e) ESEM Micrographs of 3% Na⁺ Nanocomposite PPG Swelled in 1% Brine



(f) ESEM Micrographs of 3% Na⁺ Nanocomposite PPG Swelled in Distilled Water

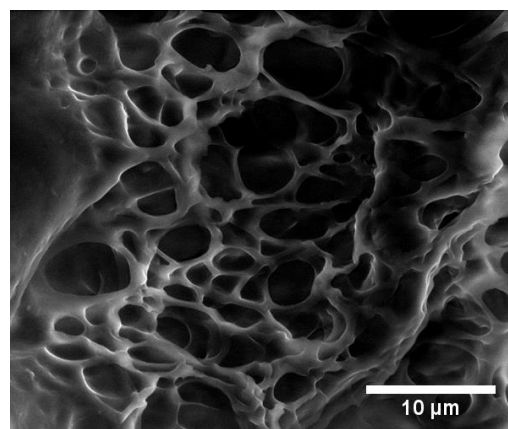
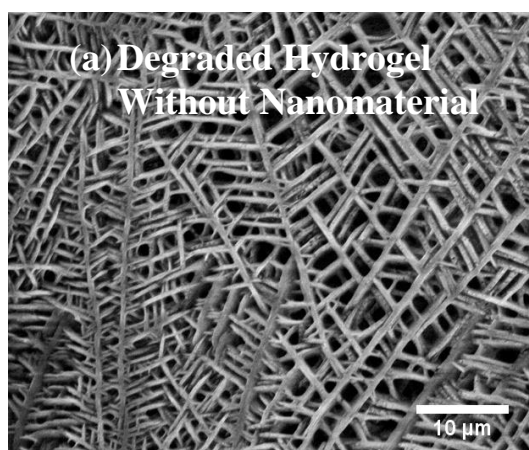
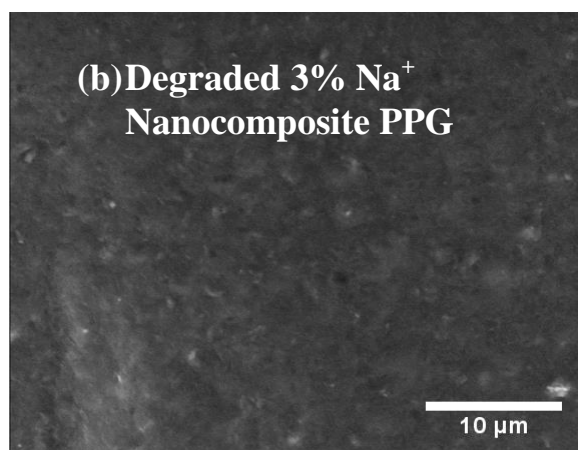


Figure 5.20. Before-degradation Environmental Scanning Electron Microscopy (ESEM) Micrographs. (Cont).

5.3.2.2 Environmental scanning electron microscopy imaging of Na⁺ nanocomposite PPG after its degradation. After the Na⁺ Nanocomposite PPG degraded, ESEM micrographs were again taken of the degraded sample. Figure 5.21a shows the micrograph of the degraded hydrogel with no nanomaterial. Figures 5.21b show the micrographs of a 3% degraded Na⁺ Nanocomposite PPG. As is clearly seen in both non-nanocomposite gel (Figure 5.21a) and Na⁺ Nanocomposite PPG (Figures 5.21b), the porous network structure that was initially observed before degradation disappears (collapses). A homogenous structure is observed in the degraded Na⁺ Nanocomposite PPG. This signifies the degradation of the gel material into a polymer solution.



(a) Degraded Hydrogel with No Nanomaterial (Jia, 2011)



(b) Degraded 3% Na⁺ Nanocomposite PPG

Figure 5.21. After-degradation Environmental Scanning Electron Microscopy (ESEM) Micrographs.

5.3.2.3 Optical microscopy imaging of Na⁺ nanocomposite PPG after degradation. After the Na⁺ Nanocomposite PPG degraded, we utilized an optical microscope to help us understand the nature of the degraded nanocomposite material. Figure 5.22 presents an optical micrograph of a 0.2% Na⁺ Nanocomposite gel after degradation. Gel composition is 23% acrylamide, 100 ppm ammonium persulfate initiator and 1500 ppm PEG crosslinker. We observed very few and tiny particles which were sparsely scattered across the entire sample and had an approximate size of about 3.8 microns (Figure 5.22). These smaller particles can travel deeper into the formation to mobilize additional oil.

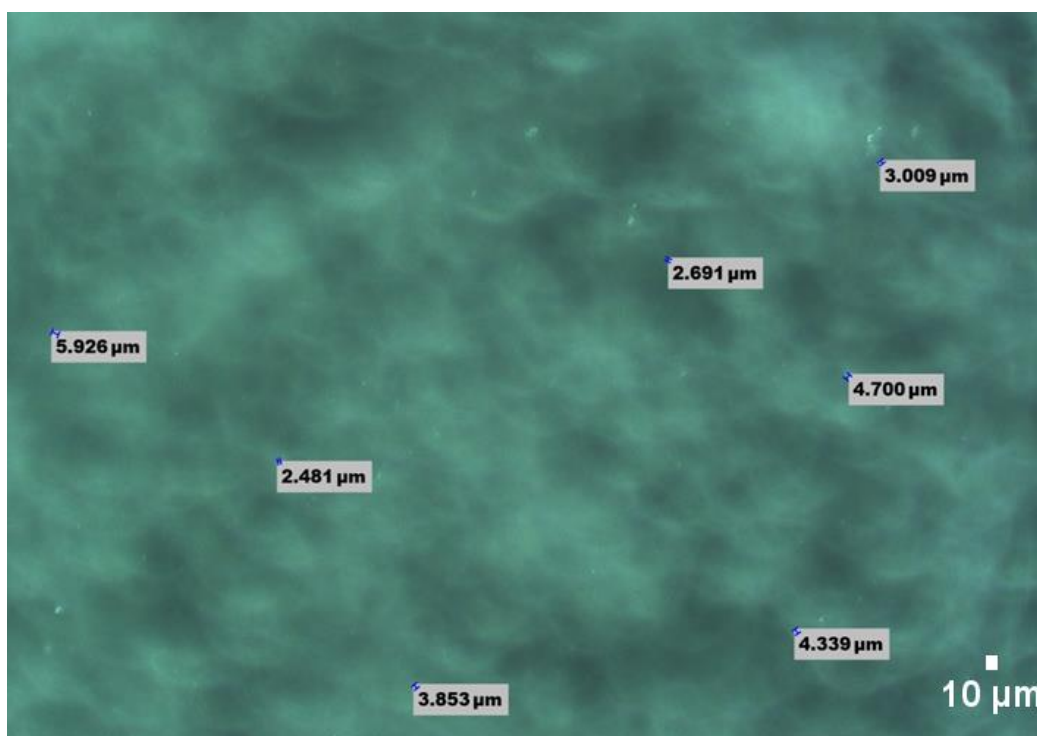


Figure 5.22. Optical Micrograph of Degraded 0.2% Na⁺ Nanocomposite PPG.

5.4. SUMMARY OF THREE TYPES OF DEGRADABLE NANOCOMPOSITE PPGs STUDIED

- Three different types of degradable nanocomposite hydrogels have been synthesized and evaluated for mobility control and fracture-plugging applications in mature reservoirs (Table 5.4).
- These three nanocomposite hydrogels were made using Laponite XLG, Calcium Montmorillonite, and Sodium Montmorillonite Nanomaterials.
- In all three nanocomposite hydrogels, it was observed that gel strength increased with increasing nanomaterial concentration.
- In all three nanocomposite hydrogels, it was also observed that longterm thermal stability of hydrogels was directly proportional to nanomaterial concentration. The higher the nanomaterial concentration, the longer the thermal stability of the hydrogels.
- It was also observed that after degradation, LXLG nanocomposite hydrogels had the highest post-degradation viscosity (4437 cp), followed by Na^+ nanocomposite hydrogels (129 cp), and lastly Ca^{2+} nanocomposite hydrogels (75.5 cp).

Thus said, the following is recommended:

- All three nanocomposite PPGs can be used for conformance control applications because they have higher strengths and longterm thermal resistance than PPGs without nanomaterial.
- For secondary polymer flooding- mobility control applications, we recommend using degradable LXLG nanocomposite hydrogels, since they have the highest post-degradation viscosity under anaerobic conditions. The post-degradation viscosities of Ca^{2+} and Na^+ nanocomposite hydrogels were negligible, thus are not suitable to enhance secondary polymer flooding. As such only LXLG nanocomposite hydrogel is recommended for secondary mobility control.
- For fracture-plugging applications, we recommend using Ca^{2+} nanocomposite PPG, since they showed the highest gel strength (17790 Pa). Next followed by Na^+ nanocomposite PPG (6363 Pa), and lastly LXLG nanocomposite PPG (4100 Pa).

Table 5.4. Summary Results of All Three Degradable Nanocomposite Hydrogels Studied.

| Conc. | Viscosity, (cp) | Viscosity, (cp) | | | Degraded Nano-PPG | | | | | | Degraded PPG without nanomaterial | Gel Strength, G' (Pa) | | | |
|-------|--------------------|-------------------|----------------------|---------------------|---------------------------|----------------------|---------------------|-----------------------------|----------------------|---------------------|-----------------------------------|-----------------------|---------------|---------------------------|--------------------------|
| | Pure Polymer (PAM) | Pure Nanomaterial | | | Viscosity, (cp) - Aerobic | | | Viscosity, (cp) - Anaerobic | | | | | | | |
| | | LXLG | Ca ²⁺ MMT | Na ⁺ MMT | LXLG | Ca ²⁺ MMT | Na ⁺ MMT | LXLG | Ca ²⁺ MMT | Na ⁺ MMT | Viscosity | No Nanomaterial | LXLG Nano-PPG | Ca ²⁺ Nano-PPG | Na ⁺ Nano-PPG |
| 0.20% | 30.6 | 2 | 2 | 1.5 | 20 | 3 | 1.5 | 1113 | 18.15 | 78.2 | 170 | 800 | 1018 | 2278 | 2100 |
| 0.60% | 107.2 | 3 | 3.5 | 2 | 39.7 | 5 | 6 | 4437 | 30 | 90 | | | 1935 | 3432 | 4170 |
| 1% | 353.5 | 3.7 | 4.5 | 4 | 612.5 | 11 | 10 | -- | -- | -- | | | -- | -- | -- |
| 3% | 6303 | 4.5 | 6 | 140 | 2190 | 13 | 170 | 7563 | 75.5 | 129 | | | 4100 | 17790 | 6363 |
| 5% | 48340 | 10 | 12 | 350 | 69820 | 17 | 479 | -- | -- | -- | | | -- | -- | -- |

6. RESULTS AND DISCUSSION: ELASTOMERIC RUBBER GEL AS PERMANENT FRACTURE-SEALING AGENT

6.1. ELASTOMERIC RUBBER GEL MADE FROM DEGRADED PPG AND NANOMATERIAL

Section six presents results of the second product: preformed gel as permanent fracture-sealing agent. In some conformance control applications, very longterm, fracture-plugging is needed.

Preformed Particle Gels are not very effective in completely sealing reservoir fractures. This is because, at higher pressures, channeling or fingering could occur through the gel plug (Figure 6.1). Thus there is a need to develop a product which overcomes this problem. This chapter presents an elastomeric rubber-like material which does not easily cause channeling and will not easily degrade under reservoir conditions.

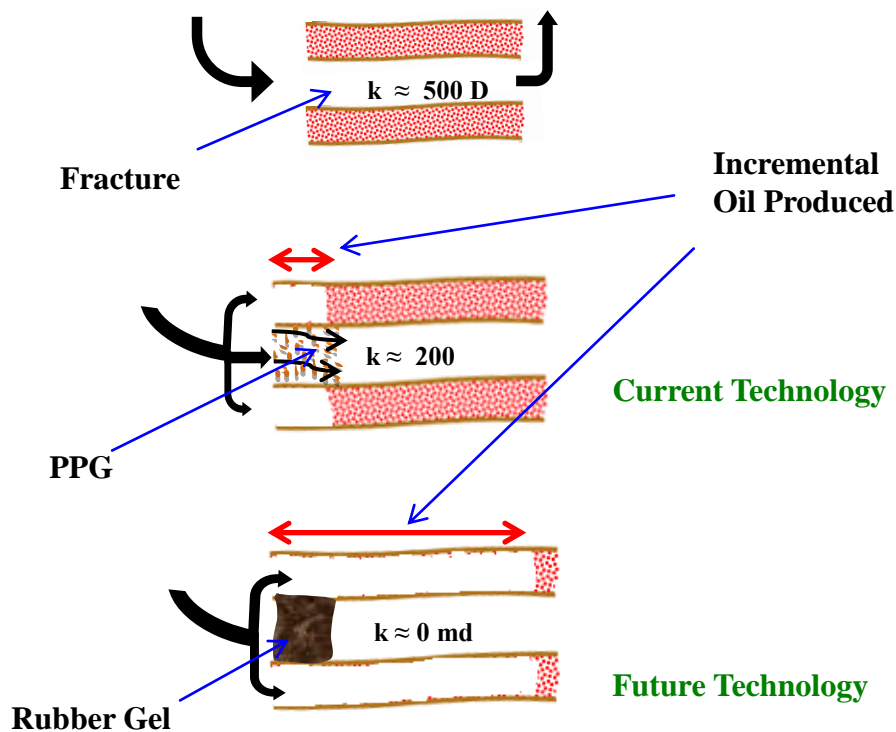


Figure 6.1. Novel Elastomeric Rubber Gel As a Fracture-Sealing Material.

6.1.1. Synthesis of Elastomeric Rubber Gel. Elastomeric rubber gel was synthesized with an organic crosslinker polyethylene glycol diacrylate (PEG-DA), then degraded on the surface into polymer solution, and degraded polymer solution was mixed with nanomaterial (natural bentonite clay) to form elastomeric rubber gel (Figure 6.2).

Rubber gel can either be coated and injected into reservoir (Once in reservoir, surface coat dissolves and PPG re-bonds together forming very strong rubber-like gel), Or, the rubber gel can be carried by a polymer solution into the formation.

The following is an example to illustrate the synthesis process for elastomeric rubber gel (Figure 6.3). First, 30 g of AM was dissolved in 100 g of distilled water in a double-necked flat-bottomed reactor equipped with inlet and outlet tubes for nitrogen gas. The mixture was stirred at room temperature for 10 minutes. Then, 1000 ppm of the crosslinker PEG-DA was added to the mixture and stirred for 10 minutes. The mixed solution was then heated to 45°C and purged with nitrogen gas for 30 minutes before 100 ppm of initiator, ammonium persulfate (APS, $(\text{NH}_4)_2\text{S}_2\text{O}_8$) was added to the solution. This resulting solution was kept for 10 hours at 45°C in a water bath to ensure complete polymerization.

The strong and elastic bulk gel formed was cut into small pieces. It was then dried in an oven at 60°C until the weight could not change any more. The dried gels were crushed into very small particle sizes, called preformed particle gels (PPGs), by blending in a blender machine (Black & Decker). PPGs with the particle size between 80-100 mesh (180µm-250µm) were selected through the standard testing sieves (Fisher Scientific Company) for further characterization and evaluation.

Then, a 5% PPG solution was prepared using 1% brine as the solvent. The PPG solution was then left to degrade in an oven (at about 80°C) into a polymer solution. The 5% degraded PPG solution was then diluted (using 1% brine) into a 0.5%, 1%, 2%, 3%, and 4% solution respectively.

Then measured amounts of bentonite clay were progressively added to these polymer solutions and mixed until rubber gel formed. The amount of clay required to form rubber gel for each concentration of degraded gel solution was recorded.

The formed elastomeric rubber gel can be transported downhole into formation using polymer solution.

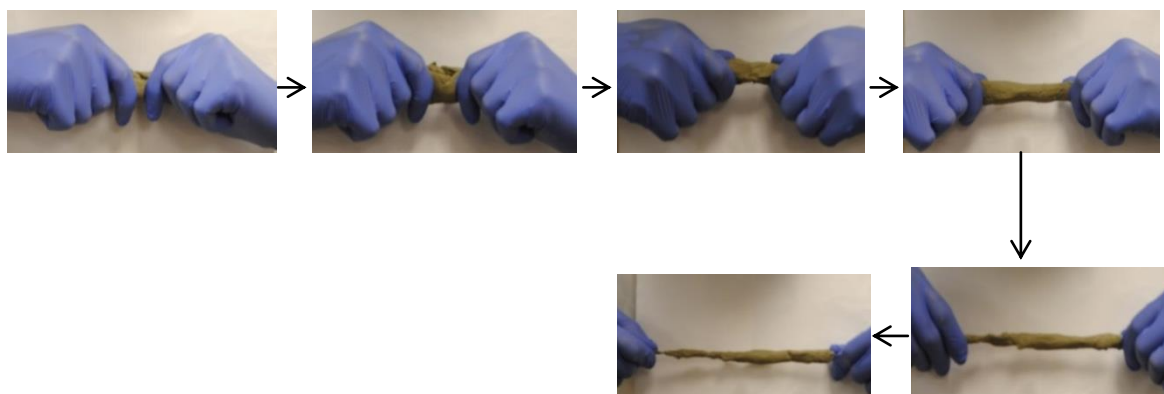


Figure 6.2. Pictorial Illustration of Elastomeric Rubber Gel.

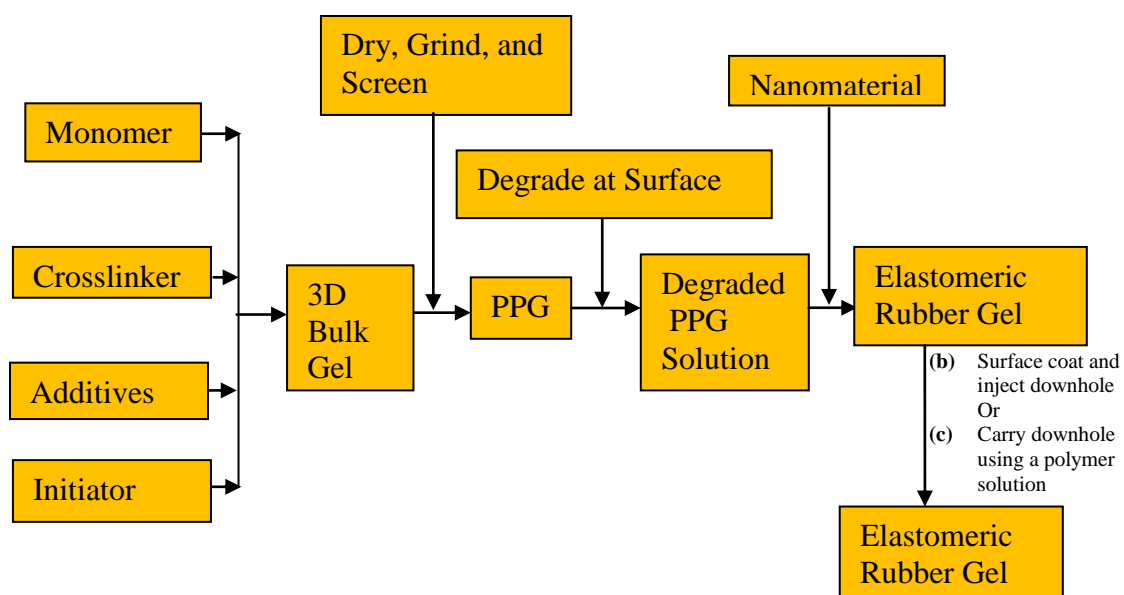


Figure 6.3. A Block Flow Diagram Illustrating the Process of Elastomeric Rubber Gel Formation.

6.1.2. Evaluation of Rubber Gel Properties. A detailed study was carried out in in order to confirm and optimize the properties of elastomeric rubber gel.

6.1.2.1 Rule out other monomer possibilities. That is, determine that rubber gel cannot be formed from other monomers besides acrylamide (AM). In order to confirm that the rubber gel will not form with other monomers, acrylic acid and 2-acrylamido-2-methylpropane sulfonic acid sodium salt monomers were utilized. The results are presented in Table 6.1.

Table 6.1. Confirming That Rubber Gel Can Only Be Formed With Acrylamide Monomer.

| Gel Name | Monomer Combinations Used (23%) | Crosslinker (1000 ppm) | Initiator (200 ppm) | Dry and grind PPG. Then degrade and mix with bentonite clay to observe if rubber gel formed. | Results |
|----------|---------------------------------|------------------------|---------------------|--|----------------------|
| TP17 | AM | PEG-200 | APS | | Rubber gel formed |
| TP18 | AM + AA | PEG-200 | APS | | No rubber gel formed |
| TP19 | AM + AMPS | PEG-200 | APS | | No rubber gel formed |
| TP20 | AA + AMPS | PEG-200 | APS | | No rubber gel formed |
| TP21 | AM + AA + AMPS | PEG-200 | APS | | No rubber gel formed |

AM: Acrylamide; AA: Acrylic Acid; AMPS: 2-acrylamido-2-methylpropane sulfonic acid sodium salt (AMPS); APS: Ammonium Persulfate.

It was observed that rubber gel was only formed with degraded AM gel. When other monomers were used (AA, AMPS, or combinations of all three) elastomeric rubber gel did not form.

6.1.2.2 Determine if elastomeric rubber gel can be formed with directly prepared polymer, without going through degraded PPG. In order to confirm that the rubber gel only forms with degraded PPG solution and not with directly prepared monomers, we directly polymerized several monomers into polymers (using initiator,

ammonium persulfate) and did not crosslink them. Then we mixed these directly prepared polymer solutions with clay and observed if rubber gels formed. The results are presented in Table 6.2.

Table 6.2. Confirming That Rubber Gel Can Only Be Formed With Degraded PPG Solution and Not With Directly Prepared Polymers.

| Sample Name | Monomer Combinations Used | Initiator | Polymer Formed | | Result |
|------------------------|------------------------------|--------------------|---------------------------|---|----------------------|
| TP27 | AM | APS | Poly AM | Mix prepared polymer with bentonite clay to observe if rubber gel formed. | Rubber gel formed |
| TP28 | AA | APS | Poly AA | | No rubber gel formed |
| TP29 | AMPS | APS | Poly AMPS | | No rubber gel formed |
| TP30 | AM + AA | APS | Co AM-AA polymer | | No rubber gel formed |
| TP31 | AM +AMPS | APS | Co AM-AMPS polymer | | No rubber gel formed |
| TP32 | AA +AMPS | APS | Co AA-AMPS polymer | | No rubber gel formed |
| TP33 | AM + AA + AMPS | APS | Co AM-AA-AMPS polymer | | No rubber gel formed |
| FLOPA AM 3230 from SNF | Low Molecular Weight HPAM | Commercial Polymer | Hydrolyzed Polyacrylamide | Mix commercial polymer with bentonite clay to observe if rubber gel formed. | No rubber gel formed |
| FLOPA AM 3430 from SNF | Medium Molecular Weight HPAM | Commercial Polymer | Hydrolyzed Polyacrylamide | | No rubber gel formed |
| FLOPA AM 3630 from SNF | High Molecular Weight HPAM | Commercial Polymer | Hydrolyzed Polyacrylamide | | No rubber gel formed |

It was observed that rubber gels did not form when directly prepared polymers were used. Rubber gels only formed when crosslinked PPG (crosslinked with PEG-DA)

was degraded into a polymer solution. Therefore, the crosslinker PEG-DA, plays a major role in rubber gel formation.

In the next section, evaluation of the properties of the gel using different molecular weights of PEG-DA will be discussed.

6.1.2.3 Effect of PEG-DA molecular weight on rubber gel properties. Since PEG-DA plays a significant role in elastomeric rubber gel formation, author conducted more experiments with different PEG-DA molecular weights to study rubber gel behavior. PEG-200-DA, PEG-400-DA, and PEG-600-DA molecular weights were studied.

6.1.2.3.1 Using PEG-200-DA. Figure 6.4 presents a phase diagram showing the amount of clay required to form elastomeric rubber when degraded PPG formed from PEG-200-DA was used. It was observed that the amount of clay needed to form rubber gel increases as degraded polymer concentration increases.

A fixed amount of degraded polymer (40 ml) was obtained, then progressive percentages of clay (of this fixed polymer volume) was added until gel formed. For instance, 5% clay is 2g, 10% clay is 4g, 50% clay is 20g etc.

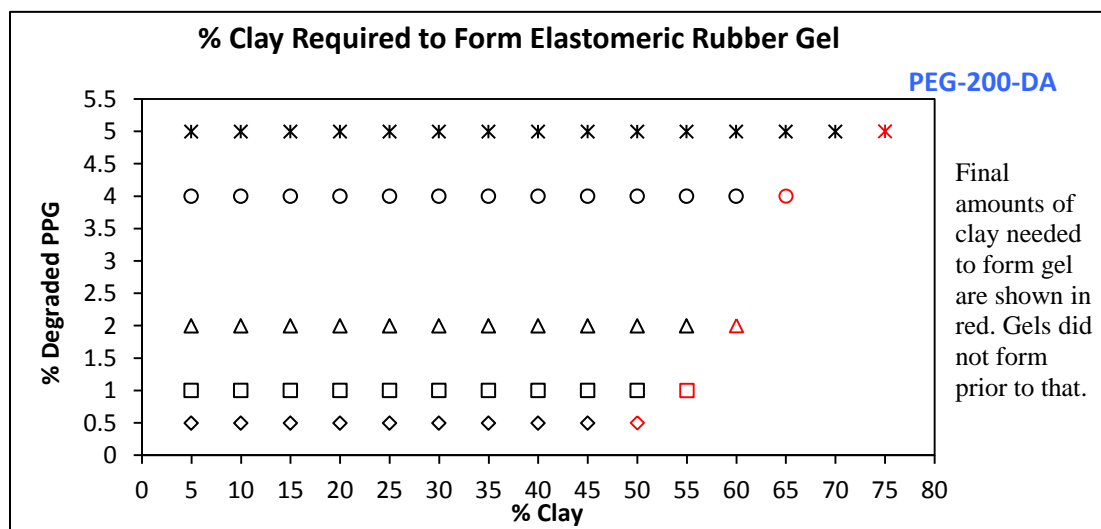


Figure 6.4. Phase Diagram Showing the Amount of Clay and Degraded PPG Required to Form Elastomeric Rubber Gel when PEG-200-DA Was Used.

Figure 6.5 show the variation of Elastomeric gel's strength with amounts of clay used for the different degraded PPG concentrations. It was observed that rubber gel's elasticity, G' decreases as clay concentration increases. It was also observed that rubber gel's elasticity decreases as degraded polymer concentration increases.

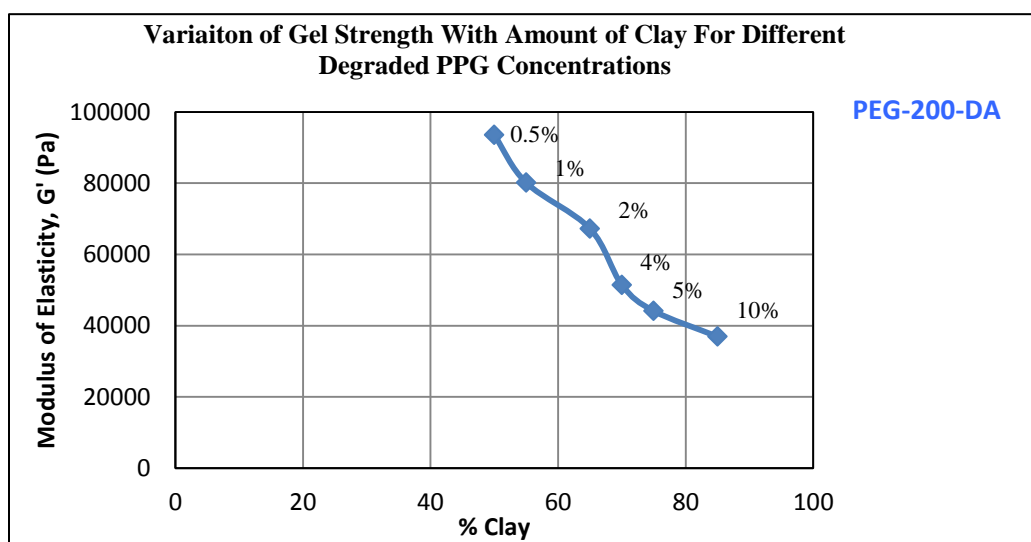


Figure 6.5. Variation of Rubber Gel's Strength (G') with Amount of Clay Used For Different Degraded PPG Concentrations.

6.1.2.3.2 Using PEG-400-DA. Figure 6.6 presents a phase diagram showing the amount of clay required to form elastomeric rubber when degraded PPG formed from PEG-400-DA was used. It was observed that the amount of clay needed to form rubber gel increases as degraded polymer concentration increases.

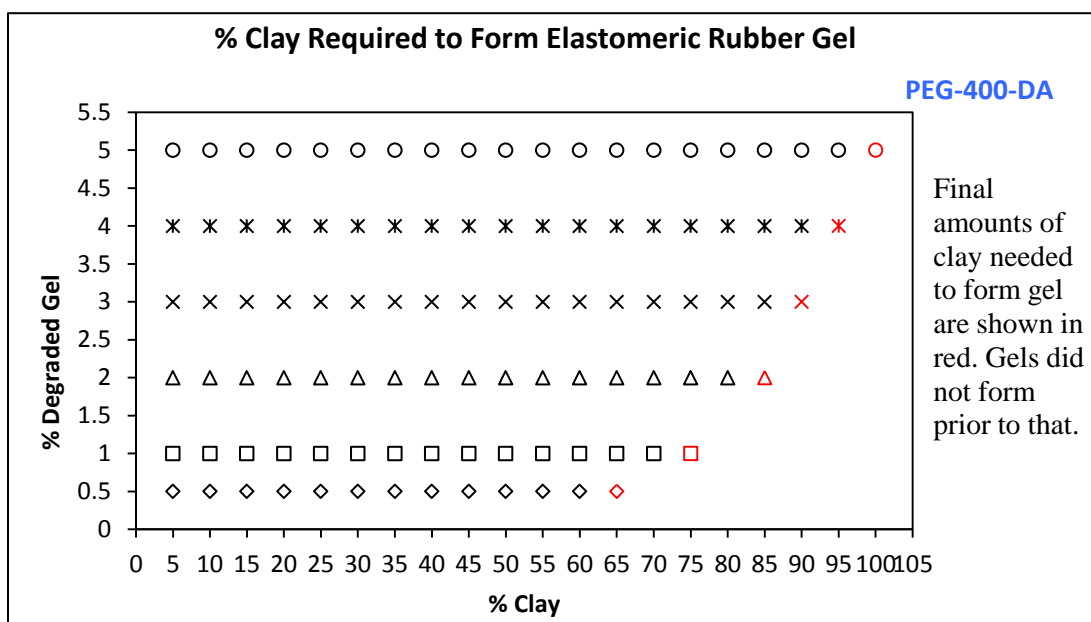


Figure 6.6. Phase Diagram Showing the Amount of Clay and Degraded PPG Required to Form Elastomeric Rubber Gel When PEG-400-DA Was Used.

Figure 6.7 show the variation of Elastomeric gel's strength with amounts of clay used for 0.5% degraded PPG. We observed that rubber gel's elasticity, G' , initially decreased, and afterwards increased as clay concentration increases. We also observed that rubber gel's elasticity initially decreased, and then gradually increased as the degraded PPG concentration increases.

Comparing Figure 6.5 (using PEG-200-DA) and Figure 6.7 (using PEG-400-DA), it was observed that when rubber gel was made using PEG-200-DA, the amount of clay needed decreased with increasing degraded PPG concentration. However, on average, when PEG-400-DA was used, the amount of clay needed to form gel increased with increasing degraded PPG concentration. This is due to the increased molecular chain length in PEG-400-DA compared to PEG-200-DA. The same phenomenon is observed with Figures 6.8 and 6.9 when PEG-600-DA was used. Thus the higher the crosslinker molecular weight, the higher the amount of clay needed.

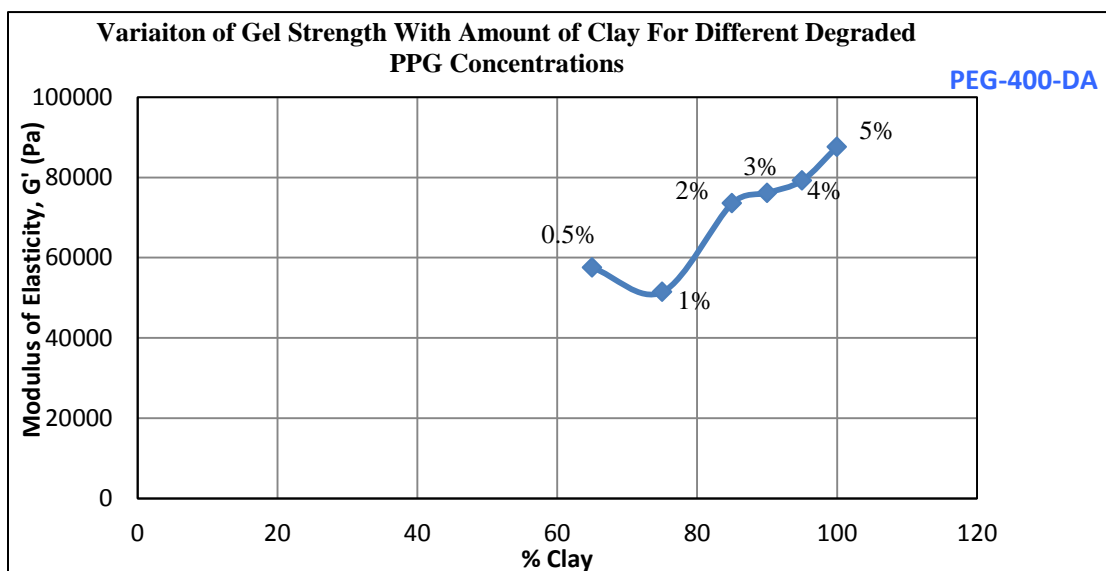


Figure 6.7. Variation of Rubber Gel's Strength (G') With Amount of Clay Used For Different Degraded PPG Concentrations.

6.1.2.3.3 Using PEG-600-DA. Figure 6.8 presents a phase diagram showing the the amount of clay required to form elastomeric rubber when degraded PPG formed from PEG-600-DA was used. It was observed that the amount of clay needed to form rubber gel increases as degraded polymer concentration increases.

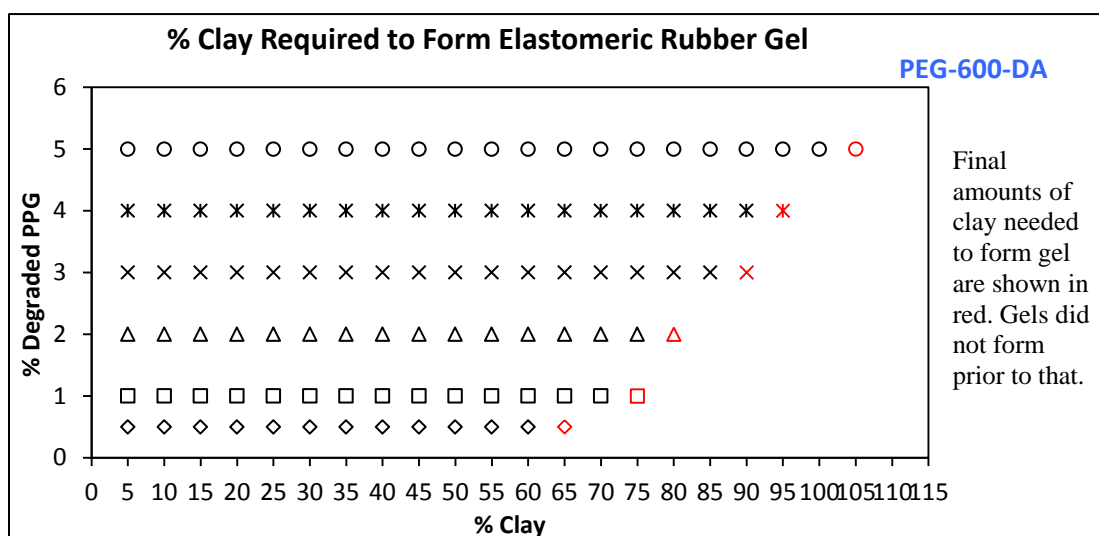


Figure 6.8. Phase Diagram Showing the Amount of Clay and Degraded PPG Required to Form Elastomeric Rubber Gel When PEG-600-DA Was Used.

Figure 6.9 show the variation of Elastomeric gel's strength with amounts of clay used. It was observed that rubber gel's elasticity, G' , increases as clay concentration increases. It was also observed that rubber gel's elasticity increases as the degraded PPG concentration increases.

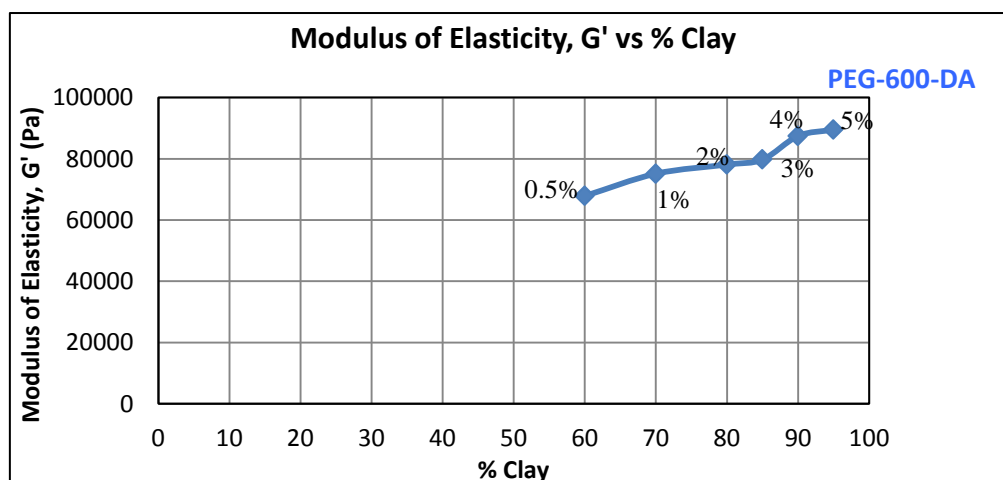


Figure 6.9. Variation of Rubber Gel's Elastic Strength (G') With Amount of Clay Used.

6.1.2.3.4 Summary of the different PEG-DA molecular weights studied.

Table 6.3 presents a summary of the results of the three different molecular weights of PEG-DA studied. Considering the fact that the cost of PEG-DA increases with increasing molecular weight, it was observed and thus concluded that elastomeric rubber gel formed using 0.5% degraded PEG-200-DA is the most economical since it contains the least amount of degraded PPG (0.5%), requires the least amount of clay (50%), and has the highest gel strength (93520 Pa).

Table 6.3. Summary of The Different PEG-DA Molecular Weights Studied.

| % Degraded Gel | PEG-200-DA | | PEG-400-DA | | PEG-600-DA | |
|----------------|------------|--------|------------|--------|------------|--------|
| | G' (Pa) | % Clay | G' (Pa) | % Clay | G' (Pa) | % Clay |
| 0.5 | 93520 | 50 | 57550 | 65 | 67850 | 65 |
| 1 | 80140 | 55 | 51430 | 75 | 75110 | 75 |
| 2 | 67270 | 60 | 73520 | 85 | 78100 | 80 |
| 3 | -- | -- | 76120 | 90 | 79740 | 90 |
| 4 | 51440 | 65 | 79220 | 95 | 87430 | 95 |
| 5 | 44120 | 75 | 87610 | 100 | 89520 | 105 |

6.1.2.4 Longterm thermal stability of rubber gel made using 0.5% degraded PPG. Since these elastomeric rubber gels are created to serve as permanent plugs, confirming their longterm stability under reservoir conditions was necessary. Once injected downhole into fractures or high permeability streaks, the longterm thermal resiliency of hydrogels to continuously seal fractures under adverse reservoir conditions is important. Longterm testing was done at 45°C, 60 °C, and 80 °C without brine solution (Figure 6.10). Results are presented in Figure 6.11 and measurements are still on-going.

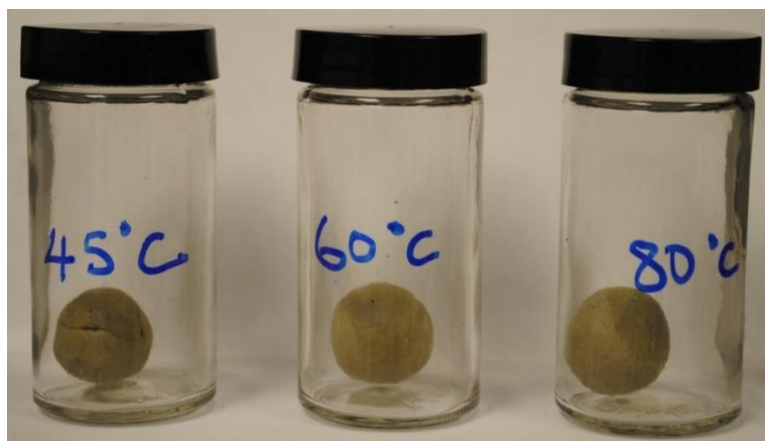


Figure 6.10. Schematic of Longterm Thermal Testing of Elastomeric Rubber Gel.

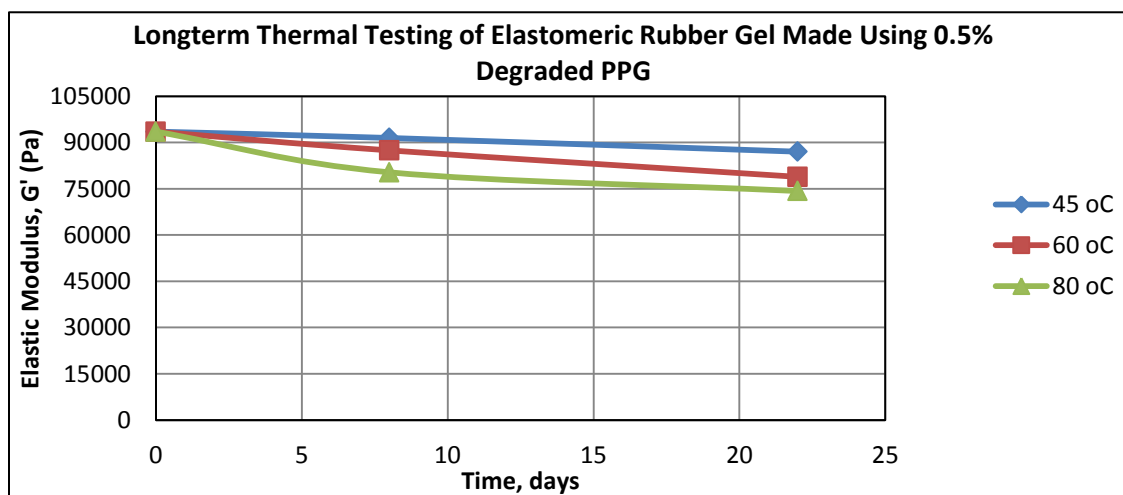


Figure 6.11. Longterm Thermal Testing of Elastomeric Rubber Gel Simulating Different Reservoir Environments of 45°C, 60 °C, and 80 °C.

6.1.2.5 Characterization of elastomeric rubber gel made from 0.5% degraded PPG using PEG-200-DA. Rubbery materials are normally characterized by one of two ways: either by using a shear or a bending geometry. In this study, shearing geometry of elastomeric material was analyzed. Additionally, in order to determine the in-service

stresses that could affect an elastomeric material, various measurements can be carried out. Some of these measurements include creep tests, recovery tests, and oscillation stress sweep tests.

A Controlled Stress (CS) Creep test is usually carried out to provide viscoelastic information of a material. In a CS Creep test, a load is applied to the sample and the elastic deformation (strain) of the sample is measured. Creep refers to the tendency of a material to undergo deformation when a mechanical stress or load is applied to it. Thus, the higher the stress applied on a material, the more likely the material would undergo deformation.

Figure 6.12 show that our elastomeric rubber gel is creep resistant, that is, it undergoes minimal deformation when mechanical stress was applied to it. It is observed from this figure that a total deformation of about 0.158 % was observed. That is, when mechanical stresses were applied to the elastomeric rubber gel, it deformed by only a negligible 0.158 %. This indicates that the material is tough and can withstand adverse stresses. In contrast, the deformation on a cellulose yarn is about 15% (De Vries, 1953) while the deformation of a pipeline steel is about 0.08% (Stijn et al., 2011).

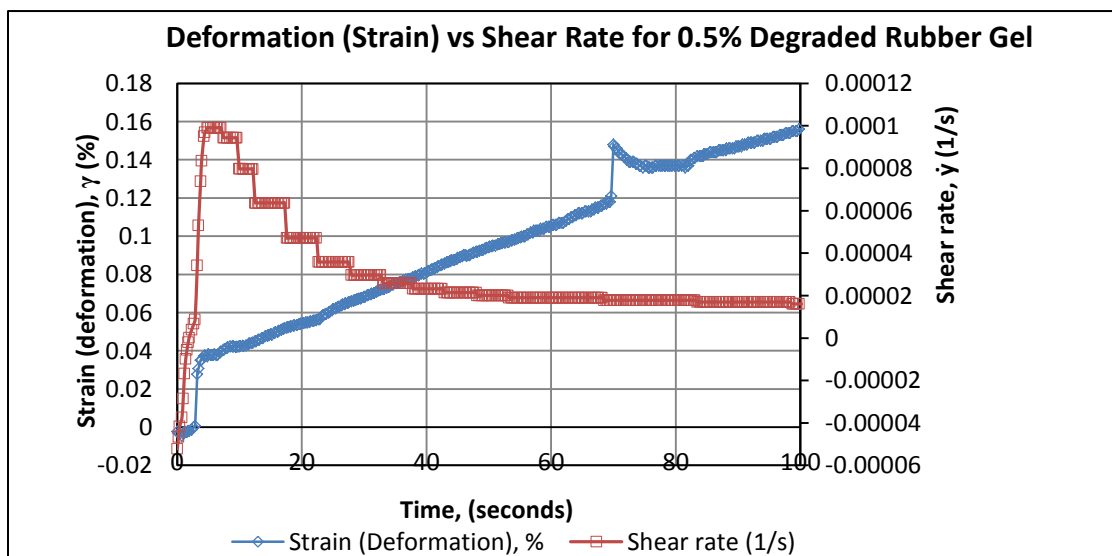


Figure 6.12. Controlled Stress Creep Measurements of 0.5% Degraded PPG Elastomeric Rubber Gel.

The deformation versus shear rate for this material is presented in Figure 6.13 below.

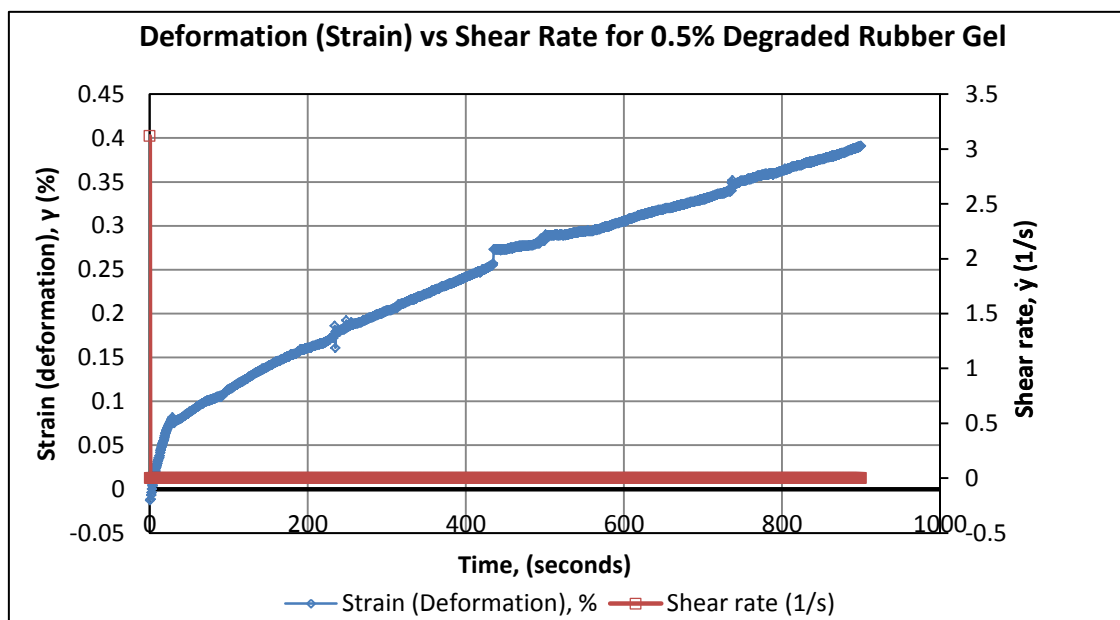


Figure 6.13. Controlled Stress (CS) Recovery Measurements of 0.5% Degraded PPG Elastomeric Rubber Gel.

Like the CS Creep test measured in Figure 6.12, Oscillation Stress Sweep measurements were also done. Oscillation Stress Sweep provides information about a material's linear visco-elastic range. It lets us understand any macro- or micro-changes that may occur in the structure of the material. This is because these micro- or macro structural changes directly affect the rheological behavior of the sample.

Figure 6.14 presents the Oscillation Stress Sweep measurements for elastomeric rubber gel. As can be seen in this figure, a relatively steady linear viscoelastic region is observed, followed by a small decrease (breakdown) in gel strength, and then a steady viscoelastic region again. These steady linear viscoelastic regions signify that the gel

sample is steady, that is, very little or negligible change in gel structure is taking place. This again confirms that our elastomeric rubber gel is stable.

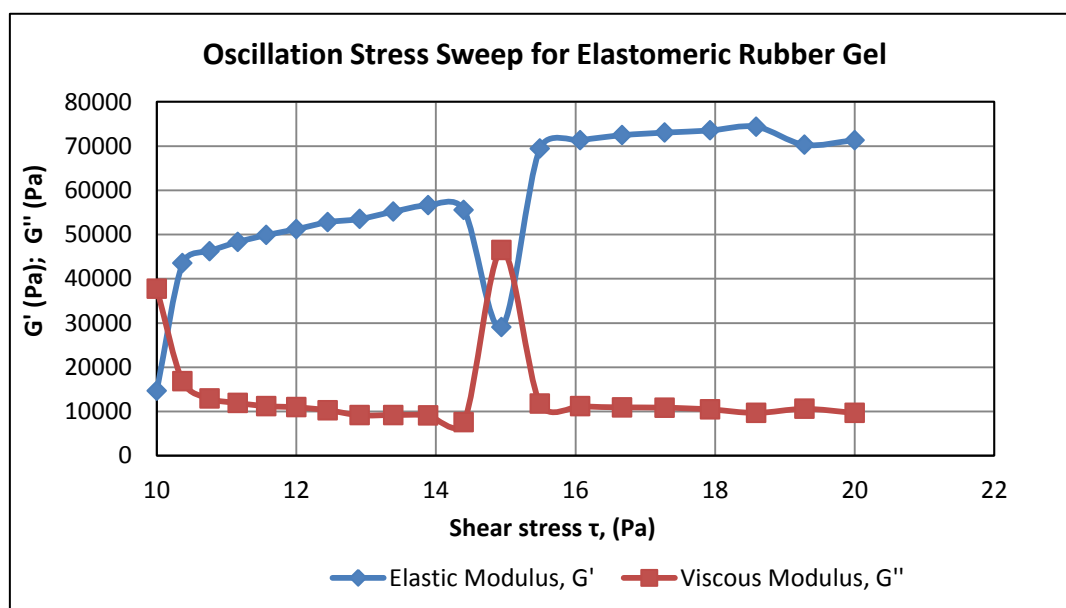


Figure 6.14. Oscillation Stress Sweep Measurements of 0.5% Degraded PPG Elastomeric Rubber Gel.

6.1.3. Summary of Elastomeric Rubber Gel Discussion. The following conclusions were derived from rubber gel discussion:

- An elastomeric rubber gel has been synthesized by mixing degraded PPG crosslinked with PEG-DA and bentonite clay.
- It was observed that rubber gel would only form with acrylamide monomer. When acrylic acid and 2-acrylamido-2-methylpropane sulfonic acid sodium salt (AMPS) monomers were used, rubber gel did not form.
- It was also observed that rubber gel did not form when directly prepared polymers were used. Rubber gel only formed when PPG was degraded into polymer solution.

- It was also observed that the amount of clay required to form rubber gel increased with increasing degraded PPG concentration.
- Elastomeric rubber gel formed using 0.5% degraded PEG-200-DA is the most economical since it contains the least amount of degraded PPG (0.5%), requires the least amount of clay (50%), and has the highest gel strength (93520 Pa).

7. CONCLUSIONS

Two products have been developed which can be potentially applied in mature fields. The first product presented was degradable nanocomposite Preformed Particle Gels for enhanced in-depth mobility control.

- This product, when injected into the reservoir, will initially act as a conformance control agent by plugging water-thief zones and channels, thereby directing injected water to sweep out oil from low permeability oil-rich zones. After a certain time period, the injected nanocomposite PPG decomposes through hydrolysis induced by heat or pH into a high viscosity linear polymer solution for the secondary polymer flooding to further enhance oil recovery.
- Three different types of degradable nanocomposite hydrogels were synthesized and evaluated for this purpose. These three nanocomposite hydrogels were made using Laponite XLG, Calcium Montmorillonite, and Sodium Montmorillonite Nanomaterials.
- In all three nanocomposite hydrogels, it was observed that gel strength increased with increasing nanomaterial concentration.
- In all three nanocomposite hydrogels, it was also observed that longterm thermal stability of hydrogels was directly proportional to nanomaterial concentration. The higher the nanomaterial concentration, the longer the thermal stability of the hydrogels.
- It was also observed that after degradation, LXLG nanocomposite hydrogels had the highest post-degradation viscosity (4437 cp), followed by Na^+ nanocomposite hydrogels (129 cp), and lastly Ca^{2+} nanocomposite hydrogels (75.5 cp). This was done at 0.6% nanocomposite PPG using 1% brine solution.
- All three nanocomposite PPGs can be used for conformance control applications because they have higher strengths and longterm thermal resistance than PPGs without nanomaterial.

- However, for secondary polymer flooding-mobility control applications, we recommend using degradable LXLG nanocomposite hydrogels, since they have the highest post-degradation viscosity under anaerobic conditions. The post-degradation viscosities of Ca^{2+} and Na^{+} nanocomposite hydrogels were less than that for degraded PPG without nanomaterial, thus are not potentially suitable to enhance secondary polymer flooding.
- For fracture-plugging applications, we recommend using Ca^{2+} nanocomposite PPG, since they showed the highest gel strength (17790 Pa). Next followed by Na^{+} nanocomposite PPG (6363 Pa), and lastly LXLG nanocomposite PPG (4100 Pa).

The second product presented was an elastomeric rubber gel as a fracture-sealing agent.

- An elastomeric rubber gel has been synthesized from degraded PPG crosslinked with PEG-DA and bentonite clay.
- It was observed that rubber gel would only form with acrylamide monomer. When acrylic acid and 2-acrylamido-2-methylpropane sulfonic acid sodium salt (AMPS) monomers were used, rubber gel did not form.
- It was also observed that rubber gel did not form when directly prepared polymers were used. Rubber gel only formed when PPG was degraded into polymer solution.
- It was also observed that the amount of clay required to form rubber gel increased with increasing degraded PPG concentration.
- Elastomeric rubber gel formed by 0.5% degraded PEG-200-DA is the most economical since it contains the least amount of degraded PPG (0.5%), requires the least amount of clay (50%), and has the highest gel strength (93520 Pa).

8. SUGGESTED FUTURE WORK

Degradable nanocomposite preformed particle gels are a novel and promising trend in EOR particle gel technology. The ability of nanocomposite PPGs to degrade into viscous polymer solution to boost in-depth secondary polymer flooding is an exciting and promising idea. This product offers superior performances compared to PPGs without nanomaterials, or better still over in-situ gelation techniques.

However, more optimization work still needs to be done. In this work, three different types of nanomaterials were studied: Laponite XLG, Calcium Montmorillonite, and Sodium Montmorillonite. However, this list is not exhaustive. Different nanomaterials such as carbon nanofibers, carbon nanotubes, polyhedral oligomeric silsesquioxanes (POSS), kaolinite, sercite, Laponite RD, Laponite RDS, Laponite EP, silica and their derivative silicates can be studied for a better post-degradation viscosity.

Additionally, further characterization still has to be done to fully understand the complex and multifaceted interactions that exist between degraded PPG and nanomaterial.

The second product is very novel and revolutionary in that it has the potentiality to overcome some of the channeling problems with PPGs. However, this product still has some limitations. More work still needs to be done on how to efficiently carry this product downhole.

BIBLIOGRAPHY

- Al-Anazi, H. A. and Sharma, M. M. Use of a pH Sensitive Polymer for Conformance Control. International Symposium and Exhibition on Formation Damage Control. Lafayette, Louisiana, 73782-MS, Society of Petroleum Engineers Inc. (2002).
- Abdel W.F.; Nasr-El-Din, H.A.; Moawad T.; Elgibaly, A. Effects of Crosslinker Type and Additives on the Performance on In-Situ Gelled Acids. SPE 112448 presented at the SPE International Symposium and Exhibition on Formation Damage Control, 13-15 February 2008, Lafayette, Louisiana, USA.
- Abdo, M.K., Chung, H.S., Phelps, C.H., 1984. Field Experience with Floodwater Diversion by Complexed Biopolymers. SPE 12642 presented at the SPErDOE Fourth Symposium on Enhanced Oil Recovery, Tulsa, OK, pp. 137–146.
- Arya, A., Hewett, T.A., Larson, R.G., Lake, L.W. Dispersion and Reservoir Heterogeneity. SPE Reservoir Engineering, SPE 14364-PA, 1988, Vol 3, 1, 139-48.
- Asghari, K., 1999. Evaluating Gel Systems for Permeability Modification Purposes in Carbon Dioxide Flooding Processes and Investigating the Fluid Flow through Hydrogels. PhD Dissertation, University of Kansas, Lawrence, KS.
- Aslam, S., Vossoughi, S., Willhite, G.P., 1986. Viscometric Measurement of Chromium _III. Polyacrylamide Gels. Chem. Eng. Commun. 48, 287–301.
- Avery, M.R., Burkholder, L.A., Gruenenfelder, M.A., 1986. Use of Crosslinked Xanthan Gels in Actual Profile Modification Field Projects. SPE 14114 presented at 1986 International Meeting on Petroleum Engineering, Beijing, China, pp. 559–568.
- Bai, B., Li, Y., Liu, X., 1999. New Development of Water Shutoff and Profile Control in Oilfields in China. Oil Drilling & Production Technology, 20, 3.
- Bai, B. 2001. Gel Treatment Technology for Fracture Reservoirs. A paper presented at the 11th Water Control Symposium of China Oilfields, Dandong, Liaoning Province, 27-31 July 2001.
- Bai, B., Huang, F., Liu, Y., Seright, R.S., Wang, Y. 2008. Case Study on Preformed Particle Gel for in-depth Fluid Diversion. SPE paper 113997 presented at the 2008 SPE/DOE Improved Oil Recovery Symposium held in Tulsa, Oklahoma, USA, 19-23 April 2008.
- Bai, B., Li, L., Liu, Y., Liu, H., Wang, Z., You, C. 2004. Preformed Particle Gel for Conformance Control: Factors Affecting its Properties and Applications. SPE paper 89389 presented at SPE/DOE at the 2004 SPE/DOE 14th Symposium on IOR held in Tulsa, OK, USA, April 17-21.

- Bai, B., Yuzhang, L., Coste, J-P., Liangxiong, L. 2004. Preformed Particle Gel for Conformance Control: Transport Mechanism through Porous Media. SPE 89468 paper presented at the 2004 SPE/DOE Fourteenth Symposium on Improved Oil Recovery held in Tulsa, Oklahoma, USA, 17-21 April 2004.
- Bai, B., Li, L., Liu, Y., Liu, H., Wang, Z., You, C. 2007a. Preformed Particle Gel for Conformance Control: Factors Affecting its Properties and Applications. SPE Reservoir Evaluation & Engineering, 10, 4, 415-422.
- Bai, B., Liu, Y., Coste, J.P., Li, L., 2007b. Preformed Particle Gel for Conformance Control: Transport Mechanism through Porous Media. SPE Reservoir Evaluation & Engineering, 10, 176.
- Bai, B., Liu, Y., Coste, J.-P. and Li, L. Preformed Particle Gel for Conformance Control: Transport Mechanism through Porous Media. SPE Reservoir Evaluation & Engineering (2007). 10(2): 176-184.
- Bai, B., Wei, M. and Liu, Y., 2013, Field and Lab Experience with a Successful Preformed Particle Gel Conformance Control Technology. Paper SPE 164511 presented at the SPE Production and Operations Symposium, Oklahoma City, Oklahoma, USA.
- Bauer, S., Gronewald, P., Hamilton, J., LaPlant, D., Mansure, A. 2005. High-Temperature Plug Formation with Silicates. SPE 92339 paper presented at the 2005 SPE International Symposium on Oilfield Chemistry held in Houston, Texas, USA, 2-4 February 2005.
- Borling, D., Chan, K., Hughes, T. and Sydansk, R. Pushing out the Oil with Conformance Control. Oilfield Review. 1994, 6(2): 44-58.
- Bruno, R., Celso, T. 2010. Brightwater® Trial in Salema Field (Campos Basin, Brazil). SPE 131299 presented at the SPE EUROPEC/EAGE Annual Conference and Exhibition held in Barcelona, Spain, 14-17 June 2010.
- Bryant, S.L., Rabaioli, M.R., Lockhart, T.P. 1996. Influence of Syneresis on Permeability Reduction by Polymer Gels. SPE 35446-PA. SPE Production & Facilities, 11, 4, 209-215.
- Chang, P.W., Goldman, I.M., Stingley, K.J., 1985. Laboratory Studies and Field Evaluation of a New Gellant for High-Temperature Profile Modification. SPE 14235 presented at the 60th Annual Technical Conference and Exhibition of the Society of Petroleum Engineers, Las Vegas, NV, Sept. 22-25, 1985.
- Chang, P.W., Gruetzmacher, G.D., Meltz, C.N., Totino, R.A., 1987. Enhanced Hydrocarbon Recovery by Permeability Modification with Phenolic Gels. U.S. Patent 4,708,974, Nov. 24.

- Chang, P.W., Philip, J.C., Burkholder, L.A., Rashan, J.M., Jr., 1988. Injector Profile Modification and Producer Treatment with Polymeric Gels, Preprint Symposia, 33, pp. 49–52, Div. Pet. Chem., American Chemical Society National Meeting, Toronto, Ontario, Canada, June 5–10, 1988.
- Chang, P.W., Gruetzmacher, G.D., Meltz, C.N., Totino, R.A., 1987. Enhanced Hydrocarbon Recovery by Permeability Modification with Phenolic Gels. U.S. Patent 4,708,974, Nov. 24, 1987.
- Chauveteau, G., Tabary, R., Renard, M., Omari, A. 1999. Controlling In-situ Gelation of Polyacrylamide by Zirconium for Water Shutoff. SPE 50752 presented at International Symposium on Oilfield Chemistry, Houston, TX, 16-19 Feb. 1999.
- Chauveteau, G., Omari, A., Tabary, R., Renard, M., Rose, J. 2000. Controlling Gelation Time and Microgel Size for Water Shutoff. SPE 59317 presented at SPE/DOE Improved Oil Recovery Symposium, Tulsa, OK, 3-5 April 2000.
- Chauveteau, G., Omari, A., Bordeaux, U., Tabary, R., Renard, M., Veerapen, J. Rose, J. 2001. New Size-Controlled Microgels for Oil Production. SPE 64988 paper presented at the 2001 International Symposium on Oilfield Chemistry, Houston, TX, 13-16 Feb. 2001.
- Chauveteau, G., Tabary, R., Lebron, C. Renard, M., Feng, Y. Omari, A. 2003. In-depth Permeability Control by Adsorption of Soft Size-Controlled Microgels. SPE 82228 presented at the SPE European Formation Damage Conference to be held in the Hague, The Netherlands, 13-14 May 2003.
- Chung Y.L.; Lai, H.M. Preparation and Properties of Biodegradable Starch Layered-Double Hydroxide-Nanocomposites. Carbohydrate Polymers 2010, 80, 525-532.
- Clampitt, R.L., Hessert, J.E., 1974. Method for Controlling Formation Permeability. U.S. Patent 3,785,437, Jan. 15, 1974
- Coste, J. P., Liu, Y., Bai, B., Y, L. I., Shen, P., Wang, Z. and Zhu, G. In-Depth Fluid Diversion by Pre-Gelled Particles. Laboratory Study and Pilot Testing. SPE/DOE Improved Oil Recovery Symposium. Tulsa, Oklahoma, Society of Petroleum Engineers Inc. (2000).
- David, Q-G., Briza, N. Z-C., Adriana, G-R., Elizabeth, P-S., Maria, G. N-A., Jose, M. C-B. 2008. Controlled Release of Model Substances from pH-Sensitive Hydrogels. J. Mex. Chem. Soc. 52, 4, 272-278.
- Darder, M.; Lopez-Blanco, M.; Aranda, P.; Leroux, F.; Ruiz-Hitzky, E. Bio-nanocomposites Based on Layered Double Hydroxides. Chemistry of Materials 2005, 17, 1969-1977

- Darder, M.; Ruiz, A. I.; Aranda, P.; Van D.H.; Ruiz, H.E. Bio-Nanohybrids Based on Layered Inorganic Solids: Gelatin Nanocomposites. *Current Nanoscience*, 2006, 2, 231-241.
- Department of Energy: "Oil Exploration & Production Program, Enhanced Oil Recovery", (June, 2005)
- De Vries H. On the elastic and optical properties of cellulose fibres, Doctoral Thesis, University of Delft, The Netherlands, 1953.
- Dinh, S.M.; DeNuzzio, J.D.; Comfort, A.R. *Intelligent Materials for Controlled Release*. ACS., New York, 1999
- Dovan, H.T., Hutchins, R.D., 1987. Development of a New Aluminum/Polymer Gel System for Permeability Adjustment. *SPE Reservoir Eng.*, 177–183.
- Erdey-Gruz, T. *Sport Phenomena in Aqueous Solutions*. John Wiley and Sons, New York City (1974) 151-63.
- Fletcher, A.J.P., Flew, S., Forsdyke, I.N., Morgan, J.C., Rogers, C., Sattles, D., 1991. Deep Diverting Gels for Very Cost Effective Waterflood Control. *Proceedings, 6th European IOR Symposium, Stavanger, Norway, May 22–23. pp. 329–335.*
- Frampton, H., Morgan, J., Cheung, S., Munson, L., Chang, K. and Williams, D., 2004, Development of a Novel Waterflood Conformance Control System. Paper SPE 89391 presented at the SPE/DOE 14th Symposium on IOR, Tulsa, OK, USA.
- Ghaddab, F., Kaddour, K., Tesconi, M., Brancolini, C., Carniani, C., Galli, G. 2010. El Borma-Bright Water®: A Tertiary Method for Enhanced Oil Recovery for a Mature Field. SPE 136140 presented at the SPE Production and Operations Conference and Exhibition held in Tunis, Tunisia, 8-10 June 2010.
- Green, D.W. & Willhite, G.P. *Enhanced Oil Recovery*, 1998, SPE Textbook Series Vol. 6, ISBN: 978-1-55563-077-5.
- Haraguchi, K. and Takeshita, T. 2002a. Nanocomposite Hydrogels: A unique Organic-Inorganic Network Structure with Extraordinary Mechanical, Optical, and Swelling/De-swelling Properties. *Adv. Mater.* 2002a, 14, 1121.
- Haraguchi, K; Takeshita, T.; Fan, S. 2002b. Effects of Clay Content on the Properties of Nanocomposite Hydrogels Composed of Poly(Nisopropylacrylamide) and Clay. *Macromolecules*; 35:10162–71.

- Heaven, W.J., Anderson G.E., Gaudet D.R., Thomas F.B., Bennion D.B.: November 8-10 1999, Resin Technology for Water Control on Production Wells”; Presented at the 5th International Conference on Water Conformance Profile- Water and Gas Shutoff in Houston.
- Hsieh, H.L., Moradi-Araghi, A., 1991. Application of water-soluble polymers to petroleum production under hostile environments. *Polym. Prepr. _Am. Chem. Soc., Div. Polym. Chem.* 32 _2, 269–270.
- Hoefner, M.R., Seetharam, R.V., Shu, P., Phelps, C.H., 1991. Selective penetration of biopolymer profile-control gels: experiment and model. *Proceedings, 6th European IOR-Symposium, Stavanger, Norway, May 22–23.* pp. 343–352.
- Huh, C., Choi, S. K. and Sharma, M. M. A Rheological Model for pH-Sensitive Ionic Polymer Solutions for Optimal Mobility-Control Applications. *SPE Annual Technical Conference and Exhibition. Dallas, Texas, Society of Petroleum Engineers.* (2005).
- Imran, A., Julio, V., Larry, E., Dwyann, D., 2008. Laboratory Evaluation of Water Swellable Materials for Fracture Shutoff. *SPE 111492.* This paper was prepared for presentation at the 2008 SPE North Africa Technical Conference and Exhibition held in Marrakech, Morocco, 12-14 March 2008.
- Jia Z. Strength Adjustable Preformed Particle Gels For Conformance Control. PhD Dissertation In Petroleum Engineering Presented At Missouri University of Science and Technology, 2011
- Jurinak, J.J., Summers, L.E., Bennett, K.E., 1989. Oilfield Application of Colloidal Silica Gel. *SPE 18505* presented at the 1989 SPE International Symposium on Oilfield Chemistry, Houston, TX, Feb. 8–10, 1989.
- Koo , J.H. and Pilato, L.A. Nanotechnology /Nanomaterials Tutorial. *International Sampe 2003 Symposium Long Beach, CA. KAI, Inc., Austin, TX 78739, USA. Pilato Consulting, Bound Brook, NJ 08805, USA*
- Kvanvik, B.A., Kolnes, J., Tyvold, T., Olafsen, K., Nilsson, S., Matre, B., and Skjellerudsveen, B.: An Evaluation of stable gel systems for deep injector treatments and high temperature producer treatments, *proceedings, 8th European Symposium on Improved Oil Recovery, Vienna, May 15-17, 1995.*
- Kytai, T. N., Jennifer L. W. 2002, Photopolymerizable Hydrogels for Tissue Engineering Applications. *Biomaterials*, 23, 4307–4314
- Lakatos, J., Lakatos-Szabo J., Tromboecky S., Munkacsi I., Kosztin B., Palasthy G., December 11, 2001: Potentials of silicates in treatment of oil producing wells. Published in *Oil and Gas Business Journal.*

- Lee, W-F., Chen, Y-C. 2004. Effect of Hydrotalcite on the Physical Properties and Drug-Release Behavior of Nanocomposite Hydrogels Based on Poly[acrylic acid-co-poly(ethylene glycol) methyl ether acrylate] Gels. *Journal of Applied Polymer Science*, 94,692-699.
- Li, A., Wang, A., Chen, J. 2004. Studies on Poly(acrylic acid)/Attapulgit Superabsorbent Composite. I. Synthesis and Characterization. *Journal of Applied Polymer Science*, 92, 1596-1603.
- Li, G. and Zhou, W. 1986. Maps of Oilfields Reservoirs in China, Vol 1&2, Petroleum Industry Press, Beijing, China.
- Li, Y., Liu, Y., Bai, B. 1999. Water Control Using Swollen Particle Gels. *Petroleum Drilling and Production Technology*. 21, 3.
- Liu, B.; Bai, B.; Li, Y. 1999. Research on Preformed Gel Grains for Water Shutoff and Profile Control. *Oil drilling and Production Technology* 21, 3.
- Liu, Y., Zhu, M., Liu, X., Zhang, W., Sun, B., Chen, Y., Hans-Juergen, P.A. 2006. High Clay Content Nanocomposite Hydrogels with Surprising Mechanical Strength and Interesting Deswelling Kinetics. *Polymer*. 47, 1-5.
- Liang, J., Lee, R.L., and Seright, R.S. Placement of Gels in Production Wells, SPE 20211 Paper Presented at the 1990 SPE/OOE Enhanced Oil Recovery Symposium, Tulsa, April 22-25.
- Lugo, N. 2010. Offshore field experience with Brightwater®. Presentation shown at the Force ART Work Shop Water based EOR Diversion techniques in Stavanger, Norway, January 20th 2010. The presentation can be found on the FORCE website at: http://www.force.org/PDW-Seminars/EOR%20Diversion_Jan_2009/Presentations/Nancy%20Lugo,%20Chevron%2020.1.2010.ppt
- Mack, J.C and Smith, J.E. 1994. In-depth Colloidal Dispersion Gels Improve Oil Recovery Efficiency. SPE/DOE 27780 paper presented at the ninth symposium in Improved Oil Recovery held in Tulsa, Oklahoma, USA, 17-20 April 1994.
- Marrocco, M.L., 1987. Gel for Retarding Water Flow. U.S. Patent 4,664,194, May 12, 1987.
- McTier, M.D. K., Ravenscroft, P. D., and Rudkin, C., Modified Methods for the Determination of Polyacrylic/Phosphinopolyacrylic Acid and Polyvinylsulfonic Acid Scale Inhibitors in Oilfield Brines. SPE 25160 presented at SPE Intern. Symp. Oilfield Chemistry, New Orleans, LA, March 2-5, 1993.

- Moradi-Araghi, A., Bjornson, G., Doe, P.H., 1989. Thermally Stable Gels for Near-Wellbore Permeability Contrast Corrections. SPE 18500 presented at the SPE International Symposium on Oilfield Chemistry, Houston, TX, February 8–10, 1989.
- Mumallah, N.A., 1987. Chromium _III. Propionate: A Crosslinking Agent for Water-Soluble Polymers in Real Oilfield Waters. SPE 15906 presented at the SPE International Symposium on Oilfield Chemistry, San Antonio, TX, Feb. 4–6, 1987.
- Needham, R.B., Threlkeld, C.B., Gall, J.W., 1974. Control of Mobility Using Polymers and Multivalent Cations. SPE 4747 presented at the SPE Improved Oil Recovery Symposium, Tulsa, OK, April 22–24, 1974.
- Nelea, M., Hoemann, C.D., Shive, M.S., Chenite, A., Buschmann, M.D. 2007. Ultrastructure of Chitosan-Glycerol Phosphate Hydrogels by ESEM. Microsc Microanal 13(Suppl). DOI: 10.1017/S1431927607073357, 472 CD-473CD
- Nelson, A. and Cosgrove, T. 2004. A Small-Angle Neutron Scattering Study of Adsorbed Poly(ethylene oxide) on Laponite. *Langmuir*, 20, 2298-2304.
- Ohms, D., McLeod, J., Graff, J.C., Frampton, H., Morgan, C.J. Cheung, S., Yancey, K., Chang, K.T. 2009. Incremental Oil Success from Waterflood Sweep Improvement in Alaska. SPE paper 121761 presented at the International Symposium on Oilfield Chemistry held in the Woodlands, Texas, USA, 20-22 April 2009.
- Okada, A., Kawasumi, M., Usuki, A., Kojima, Y., Kurauchi, T., Kamigaito, O.1990. Synthesis and Properties of nylon-6/clay hybrids. In: Schafer DW, Mark JE, editors. Polymer based molecular composites. MRS Symposium Proceedings, Pittsburg, vol. 171, 45-50.
- Okay, O.; Oppermann, W. Polyacrylamide-Clay Nanocomposite Hydrogels: Rheological and Light Scattering Characterization, *Macromolecules* 2007, 40, 3378-3387.
- Olphen, V.H. Clay Colloid Chemistry, 2nd ed.; John Wiley: New York, 1977.
- Pavlidou, S.; Papaspyrides, C. D. A Review on Poly,er-Layered Silicate Nanocomposites. *Progress in Polymer Science* 2008, 33, 1119-1198.
- Phang, I.Y.; Liu, T.; Mohamed, A.; Pramoda, K.P.; Chen, L.; Shen, L. Morphology, Thermal and Mechanical Properties of Nylon 12/Organoclay Nanocomposites Prepared by Melt Compounding. *Polym Int* 2005, Vol. 54, 456-464.
- Paul, J.M., Strom, E.T., 1987. Oil Reservoir Permeability Control Using Polymeric Gels, U.S. Patent 4,658,898, April 21, 1987.

- Parmeswar, R., Willhite, G.P., 1988. A Study of the Reduction of Brine Permeability in Berea Sandstone with the Aluminum Citrate Process. SPE Reservoir Eng., 959–966, August.
- Peppas, N.A., Bures, P.; Leobandung, W.; Ichikawa, H. 2000. Hydrogels in Pharmaceutical Formulations. Eur. J. Pharm. Biopharm. 50, 27-46.
- Pinnavaia, T. J., Beall, G. W. Polymer-Clay Nanocomposites: Chichester, 2000.
- Pritchett, J., Frampton, H., Brinkman, J., Cheung, S., Morgan, J., Chang, K.T., Williams, D., Goodgame, J. 2003. Field Application of a New In-Depth Waterflood Conformance Improvement Tool. SPE paper 84897 presented at the SPE International Improved Oil Recovery Conference in Asia Pacific held in Kuala Lumpur, Malaysia, 20-21 October 2003.
- Prud'homme, R.K. and Uhl, J.T. Kinetics of Polymer/Metal-Ion Gelation. Paper SPE 12640 presented at the 1984 SPEIDOE Enhanced Oil Recovery Symposium, Tulsa, April 15-18.
- Ray, S.S. and Okamoto, M. 2003. Polymer/layered Silicate Nanocomposites: A Review from Preparation to Processing. Progress in Polymer Science, 28, 1539-1641
- Raje, M., Asghari, K., Vossoughi, S., Green, D.W., Willhite, G.P., 1999. Gel Systems for Controlling CO₂ Mobility in Carbon Dioxide Miscible Flooding. SPE Reservoir Eval. Eng. 2_2., 205–210, April.
- Roco, M.C., Williams, R.S., Alivisatos, P. 2000. Nanotechnology Research Directions: IWGN Workshop Report, Eds., Kluwer, 2000.
- Rousseau, D., Chauveteau, G., Renard, M., Tabary, R., Zaitoun, A. Mallo, P., Braun, O., Omari, A. 2005. Rheology and Transport in Porous Media of New Water Shutoff/Conformance Control Microgels. SPE 93254 paper presented at the 2005 SPE International Symposium on Oilfield Chemistry held in Houston, Texas, USA, 2-4, Feb. 2005.
- Rouston, W.G., 1972. Method for Controlling Flow of Aqueous Fluids in Subterranean Formations. U.S. Patent 3,687,200, Aug. 29, 1972.
- Sáez, V.; Hernáez, E.; Sanz, L. Controlled Release of Drugs in Hydrogels. Rev. Iber. Polim. 2003, 4, 21-91.
- Seright, R.S., 1988. Placement of Gel to Modify Injection Profiles. SPE 17332 presented at the SPE/DOE Enhanced Oil Recovery Symposium, Tulsa, OK, pp. 137–148.
- Seright, R.S., 1989. Effect of Rheology on Gel Placement. SPE 18502 presented at the SPE International Symposium on Oilfield Chemistry, Houston, TX, pp. 389–402.

- Seright, R.S. 1991. Effect of Rheology on Gel Placement, SPE Reservoir Engineering 18502-PA
- Seright, R.S. 1990. Impact of Dispersion on Gel Placement for Profile Control, paper SPE 20127 presented at the 1990 SPE Permian Basin Oil and Gas Recovery Conference, Midland, March 8-9.
- Seright, R.S.: 1991. Impact of Dispersion on Gel Placement for Profile Control. SPE 20127-PA. SPE Reservoir Engineering, 6(3), 343-352.
- Seright, R.S. 1997. Use of Preformed Gels for Conformance Control in Fractured Systems. SPEPF 12, 1, 59-65. SPE-35351-PA. DOI: 10.2118/35351-PA.
- Seright, R.S. 1998. Gel Dehydration During Extrusion Through Fractures. SPE 39957-MS. SPE Rocky Mountain Regional/Low-Permeability Reservoirs Symposium and Exhibition held in Denver, Colorado, 5-8 April 1998.
- Seright, R.S. 1999. Polymer Gel Dehydration During Extrusion Through Fractures. SPE Prod. & Facilities, 14, (2), 110-116.
- Seright, R.S., Martin, F.D., 1991. Fluid Diversion and Sweep Improvement with Chemical Gels in Oil Recovery Processes. Annual Report, May 1, 1989–April 30, 1990, DOE/BCEr 14447-8 _DE91002232. U.S. Department of Energy, April.
- Seright, R.S. 2000. Gel Propagation through Fractures. Paper SPE 59316 presented at the 2000 SPE/DOE Improved Oil Recovery Symposium held in Tulsa, Oklahoma, 3-5 April 2000.
- Seright, R.S. 2003. Washout of Cr(III)-Acetate-HPAM Gels from Fractures. Paper SPE80200 presented at the SPE International Symposium on Oilfield Chemistry held in Houston, Texas, USA, 5-7 February 2003.
- Seright, R.S. 2004. Conformance Improvement Using Gels. Semi-Annual Technical Progress Report. US DOE award number: DE-FC26-01BC15316
- Shibayama, M., Suda, J., Karino, T., Okabe, S., Takehisa, T., Haraguchi, K. 2004. Structure and Dynamics of Poly(N-isopropylacrylamide)-Clay Nanocomposite Gels. Macromolecules, 37, 9606-9612.
- Southard, M.Z., Green, D.W., and Willhite, G.P. Kinetics of the Chromium (VI)/Thiourea Reaction in the Presence of Polyacrylamide. Paper SPE 12715 presented at the 1984 SPE/DOE Enhanced Oil Recovery Symposium, Tulsa, April 15-18.

- Southwick, J.G., Jamieson, A.M., and Blackwell, J. Conformation of Xanthan Dissolved in Aqueous Urea and Sodium Chloride Solutions. *Carbohydrate Research* (1982) 99,117-27.
- Steidtmann, J. 2008. Presentation to the Wyoming Infrastructure Authority. Enhanced Oil Recovery Institute. April 2008.
http://www.wyia.org/Docs/Presentations/2008/08_Enhanced%20Oil%20Recovery%20Institute_Jim%20Steidtmann_Laramie%20WY_April%2008,%202008.pdf
- Stijn, H., Wim, D.W., Rudi, D. 2011. A Generic Stress-Strain Model for Metallic Materials with Two-Stage Strain Hardening Behavior. *International Journal of Non-Linear Mechanics*, 46, 519-531.
- Sydansk, R. D. and Argabright, P. A. Conformance Improvement in a Subterranean Hydrocarbon-Bearing Formation Using a Polymer Gel. U.S. Patent 4,683,949 (1987).
- Sydansk, R.D., Smith, T.B., 1988. Field Testing of a New Conformance-Improvement-Treatment Chromium _III. Gel Technology. SPErDOE 17383 presented at the SPErDOE Enhanced Oil Recovery Symposium, Tulsa, OK, April 17–20, 1988.
- Sydansk, R.D., 1988. A New Conformance-Improvement-Treatment Chromium (III) Gel Technology. SPE 17329-MS paper presented at the SPE Enhanced Oil Recovery Symposium, Tulsa, OK, April 16–21.
- Sydansk, R.D., Xiong, Y., Al-Dhafeeri, A.M., Schrader, R.J., Seright, R.S. 2005. Characterization of Partially formed Polymer Gels for Application to Fractured Production Wells for Water-Shutoff Purposes. *SPE Production and Facilities*. 20, 3, 240-249
- Sydansk, R.D., Al-Dhafeeri, A.M., Xiong, Y., Seright, R.S. 2004. Polymer Gels Formulated with a Combination of High- and Low-Molecular-Weight Polymers Provide Improved Performance for Water-Shutoff Treatments of Fractured Production Wells. *SPE Production and Facilities*. 19, 4, 229-236.
- Thomas, S. Enhance oil recovery – An Overview. *Oil & Gas Science and Technology* (2008), 63(1), 9-19.
- Todd, B.J., Willhite, G.P., Green, D.W., 1991. Radial Modeling of In Situ Gelation in Porous Media. SPE 21650 presented at 1991 Production Operations Symposium, Oklahoma City, OK, April 7–9, 1991.
- Tongwa, P., Nygaard, R., Bai, B. 2013a. Evaluation of a Nanocomposite Hydrogel for Water Shut-off in Enhanced Oil Recovery Applications: Design, Synthesis, and Characterization. *Journal of Applied Polymer Science*, 128, 787-794.

- Tongwa, P., Nygaard, R., Aaron, B., Bai, B. 2013b. Evaluation of Potential Fracture-Sealing Materials for Remediating CO₂ Leakage Pathways during CO₂ Sequestration. *International Journal of Greenhouse Gas Control*, (2013), 18, 128-138.
- Vossoughi, S. 2000. Profile Modification Using in Situ Gelation Technology – A Review. *Journal of Petroleum Science and Engineering*, 26, 199-209.
- Wang, H.G., Guo, W.K., Jiang, H.F. 2001. Study and Application of Weak Gel System Prepared by Complex Polymer Used for Depth Profile Modification. Paper SPE 65379 presented at the SPE International Symposium on Oilfield Chemistry, Houston, 13-16 February. DOI: 10.2118/65379-MS.
- Wang, W., Liu, Y., Gu, Y. 2003. Application of A Novel Polymer System in Chemical Enhanced Oil Recovery (EOR). *Colloid and Polymer Science*, 281(11), 1046-1054.
- Wang, J. The Nanoporous Morphology of Photopolymerized Crosslinked Polyacrylamide Hydrogels. Chemical Engineering Department. College Station, TX, Texas A&M University. (2008). PhD dissertation: 1-135.
- Wen-Fu, L., Sung-Chuan, L. 2006. Effect of Hydrotalcite on the Swelling and Mechanical Behaviors for the Hybrid Nanocomposite Hydrogels Based on Gelatin and Hydrotalcite. *Journal of applied Polymer Science*. 100, 500-507.
- Weian Z., Wei, L., Yue, F. 2005. Synthesis and Properties of a Novel Hydrogel Nanocomposites. *Materials Letters*, 59, 2876-2880.
- Willhite, G.P., Green, D.W., Young, T.S., Thiele, J.L., Michnick, M.J., Vossoughi, S., Terry, R.E., 1986. Evaluation of Methods of Reducing Permeability in Porous Rocks by In Situ Polymer Treatment — Final Report. DOErBCr10354-16 _DE86000-264., NTIS, U.S. Department of Commerce, Springfield, VA, February.
- Xia, X., Yih, J., Nandika, A.D., Hu, Z. 2003. Swelling and Mechanical Behavior of Poly(N-isopropylacrylamide)/Na-montmorillonite Layered Silicates Composite Gels. *Polymer*, 44, 3389-3393.
- Yanez, P.A.P., Mustoni, J.L., Relling, F.M., Chang, K-T, Hopkinson, P., Frampton, H. 2007. New Attempt in Improving Sweep Efficiency at the Mature Koluel Kaike and Piedra Clavada Waterflooding Projects of the S. Jorge Basin in Argentina. SPE paper 107923 presented at the Latin American and Caribbean Petroleum Engineering Conference held in Buenos Aires, Argentina, 15-18 April 2007.

- Young, T.S., Willhite, G.P., and Green, D.W. Study of IntraMolecular Crosslinking of Polyacrylamide in Cr(III)-Polyacrylamide Gelation by Size-Exclusion Chromatography, Low-Angle Laser Light Scattering, and Viscometry. Water-Soluble Polymers for Petroleum Recovery, G.A. Stahl and D.N. Schulz (eds.), Plenum Press, New York City (1988) 329-42.
- Zaitoun, A., Tabary, R., Rousseau, D. 2007. Using Microgels to Shutoff Water in a Gas Storage Well. SPE 106042 presented at the 2007 SPE International Symposium on Oilfield Chemistry held in Houston, Texas, USA 28 February – 2 March 2007.
- Zhang, H., Bai, B. 2011. Preformed-Particle-Gel Transport through Open Fractures and Its Effect on Water Flow. SPE Journal, 16, 2, 388-400
- Zolfaghari, R.; Katbab, A.A.; Nabavizadeh, J.; Tabasi, R.J.; Nejad, M.H. Preparation and Characterization of Nanocomposite Hydrogels Based on Polyacrylamide for Enhanced Oil Recovery Applications. Journal of Applied Polymer Science 2006, 100, 2096-2103.

VITA

Paul Tongwa received a BS degree in Chemistry from the University of Buea, Cameroon in 2005 and an M.Sc degree in Chemistry from New Mexico Highlands University, Las Vegas, New Mexico in 2008. In 2010, he joined the research group of Dr Bai Baojun as a PhD student in the Petroleum Engineering Department of Missouri University of Science and Technology.

Tongwa has interdisciplinary research interests in the areas of Chemical Enhanced Oil Recovery and CO₂ sequestration. More specifically, his research interests include the various Chemistries involved in oil and gas extraction and in the sealing CO₂-induced fractures during the process of CO₂ sequestration.

Tongwa currently holds 21 peer-reviewed journal publications and 1 conference publication. He received his PhD in Petroleum Engineering from Missouri University of Science and Technology in the Spring of 2014.